University of Bath

PHD

Reactions of coordinated acetylenes

Brauers, Georg

Award date:
1995

Awarding institution:
University of Bath

Link to publication

General rights
Copyright and moral rights for the publications made accessible in the public portal are retained by the authors and/or other copyright owners and it is a condition of accessing publications that users recognise and abide by the legal requirements associated with these rights.

- Users may download and print one copy of any publication from the public portal for the purpose of private study or research.
- You may not further distribute the material or use it for any profit-making activity or commercial gain
- You may freely distribute the URL identifying the publication in the public portal ?

Take down policy
If you believe that this document breaches copyright please contact us providing details, and we will remove access to the work immediately and investigate your claim.

Download date: 13. May. 2019

Reactions of Coordinated Acetylenes

submitted by Georg Brauers

for the degree of PhD

of the University of Bath

1995

COPYRIGHT

Attention is drawn to the fact that copyright of this thesis rests with the author. This copy of the thesis has been supplied on condition that anyone who consults it is understood to recognise that copyright rests with the author and that no quotation from the thesis and no information derived from it may be published without prior written consent of the author.

This thesis may be made available for consultation within the University Library and may be photocopied or lent to other libraries for the purpose of consultation.

UMI Number: U601696

All rights reserved

INFORMATION TO ALL USERS
The quality of this reproduction is dependent upon the quality of the copy submitted.

In the unlikely event that the author did not send a complete manuscript
and there are missing pages, these will be noted. Also, if material had to be removed,
a note will indicate the deletion.

UMI U601696
Published by ProQuest LLC 2013. Copyright in the Dissertation held by the Author.
Microform Edition © ProQuest LLC.
All rights reserved. This work is protected against
unauthorized copying under Title 17, United States Code.

ProQuest LLC
789 East Eisenhower Parkway
P.O. Box 1346
Ann Arbor, MI 48106-1346

UNIVERSITY OF BATH
LIBRARY
21 23 OCT 1995
Ph D.
5095453

Memorandum

The work described in this thesis was carried out by the author between October 1993 and June 1995 within the School of Chemistry at the University of Bath, under supervision of Professor Michael Green. Unless otherwise indicated, the work is original and has not been submitted for any other degree.

Some of the results of this thesis have been published in the following papers:

- The *cis*-Insertion of Diphenylacetylene into an e*xo*-Polyhedral Boron-Hydrogen Bond of a Molybdenacarbaborane Cage; G. Brauers, S. J. Dossett, M. Green and M. F. Mahon, *J. Chem. J. Chem. Commun., Soc., Chem. Commun.* 1995, 985.
- Synthesis of a Mononuclear η^2(4e)-Bonded Phosphaalkyne Complex; Transformation into an η^4-1,3-Diphosphacyclobutadiene Complex; G. Brauers, M. Green, C. Jones, J. F. Nixon, *J. Chem. Soc., Chem. Commun.* 1995, 1125.

Acknowledgements

First and foremost, I would like to thank my supervisor Professor Michael Green, whose guidance and encouragement made this work possible.

Thanks are due to Dr Mary Mahon (Bath), Dr Peter Hitchcock (Brighton) and Dr A Guy Orpen (Bristol) for the X-ray crystallographic studies. Further thanks go to all the technical staff within the department, especially to Robert Stevens, Ahmed Sheibani and Alan Carver.

I like to thank all my laboratory colleagues for lively discussions and their help with the manuscript. I thank EPSRC(SERC) for their financial support.

Finally, I would like to thank the non-chemists Sabine Heinz and Wendy Morris for their pains to correct the manuscript.

Summary

The reaction of $[Mo(\eta^2\text{-}PhC_2Ph)\{P(OMe)_3\}_2(\eta\text{-}C_5H_5)][BF_4]$ **XI** with RMgX (R = Et, CH_2Ph) gives complexes $[Mo(\eta^2\text{-}PhC_2Ph)(R)\{P(OMe)_3\}(\eta\text{-}C_5H_5)]$ (R= Et **1**, CH_2Ph **2**). Compound **1** reacts with CO to form $[Mo\{\eta^2\text{=}C(Ph)C(Ph)C(Et)\text{-}O\}(CO)\text{-}\{P(OMe)_3\}(\eta\text{-}C_5H_5)]$ **3** containing an oxametallacycle. Heating a solution of complex **2** in presence of diphenylacetylene affords the paramagnetic 17 electron complex $[Mo(\eta^6\text{-}C_6Ph_6)(\eta\text{-}C_5H_5)]$ **4**, whose structure was determined by X-ray crystallography. For the formation of **4** a radical mechanism is proposed.

On addition of allyl magnesium bromide to **XI** a complex with a σ-bonded allyl group is formed, which could not be isolated. However, after addition of trimethylphosphite to the reaction mixture the complex $[Mo\{\eta^2\text{-}C(Ph)\text{=}C(Ph)CH_2CH\text{=}CH_2\}\{P(OMe)_3\}_2\text{-}(\eta\text{-}C_5H_5)]$ **5** is formed, the structure of which was resolved by X-ray diffraction. The mechanism of this reaction probably involves a [3,3]-sigmatropic rearrangement.

Unexpectedly, the reaction of **XI** with $CH_2(MgI)_2$ affords the zwitterionic complex $[Mo(\eta^2\text{-}PhC_2Ph)\{\eta^2\text{-}P(OMe)_2OBF_2OP(OMe)_2\}(\eta\text{-}C_5H_5)]$ **6**. The structure of **6** was established by an X-ray diffraction study. Treatment of **6** with $K[HBBu_3^s]$ yields the anionic η^2-vinyl complexes $K[Mo(\eta^2\text{=}C(Ph)C(H)Ph)\{\eta^2\text{-}P(OMe)_2OBF_2OP(OMe)_2\}\text{-}(\eta\text{-}C_5H_5)]$ **9**. Protonation of **9** generates an unsaturated *trans*-stilbene complex $[Mo(\textit{trans}\text{-}PhHC_2PhH)\{\eta^2\text{-}P(OMe)_2OBF_2OP(OMe)_2\}(\eta\text{-}C_5H_5)]$ **A**, which was treated *in situ* with CO or trimethylphosphite to give $[Mo(L)_2\{\eta^2\text{-}P(OMe)_2OBF_2OP(OMe)_2\}\text{-}(\eta\text{-}C_5H_5)]$ (L= CO **11**, $P(OMe)_3$ **12**).

Addition of phosphaalkyne to **A** affords $[Mo\{\eta^2\text{-}P(OMe)_2OBF_2OP(OMe)_2\}(\eta^2\text{-}P\equiv CBu^t)(\eta\text{-}C_5H_5)]$ **14**, the first complex in which a phosphaalkyne adopts an η^2(4e) bonding mode. **14** reacts with a second molecule of phosphaalkyne to give the diphosphacyclobutadienyl complex $[Mo\{\eta^2\text{-}P(OMe)_2OBF_2OP(OMe)_2\}\{\eta^4\text{-}P_2C_2(Bu^t)_2\}(\eta\text{-}C_5H_5)]$ **15**.

Addition of two equivalents of diphenylphosphine to $[Mo(NCMe)(\eta^2\text{-}PhC_2Ph)_2(\eta\text{-}C_5H_5)][BF_4]$ **LXIX** gives the complex $[Mo(PPh_2H)_2(\eta^2\text{-}PhC_2Ph)(\eta\text{-}C_5H_5)][BF_4]$ **16**, which can be deprotonated with $Li[N(SiMe_3)_2]$ or $K[BHBu^s{}_3]$ to afford the phosphide complex $[Mo(PPh_2)(PPh_2H)(\eta^2\text{-}PhC_2Ph)(\eta\text{-}C_5H_5)]$ **17**.

The carbaborane complexes [*closo*-3,3-$(\eta^2\text{-}PhC_2R)_2$-3-CO-3,1,2-$MoC_2B_9H_{11}$] (R= Ph **18**, R= Me **19**) were synthesised by protonation of $[NEt_4]$[*closo*-3,3-$(CO)_2$-3-$(\eta^3\text{-}C_3H_5)$-3,1,2-$MoC_2B_9H_{11}$] **XXXII** in the presence of the respective acetylene. Addition of trimethylphosphite to **18**, **19** and [*closo*-3,3-$(\eta^2\text{-}MeC_2Me)_2$-3-CO-3,1,2-$MoC_2B_9H_{11}$] **XXXIV** yields the *bis*-phosphite complexes [*closo*-3-$(\eta^2\text{-}RC_2R')$-3,3-$\{P(OMe)_3\}_2$-3,1,2-$MoC_2B_9H_{11}$] (R= R'= Ph **22**; R= Ph, R'= Me **23**; R= R'= Me **24**).

Treatment of **24** with but-2-yne at 90°C gives the complex [*closo*-3,3-$(\eta^2\text{-}MeC_2Me)_2$-3-$\{P(OMe)_3\}$-3,1,2-$MoC_2B_9H_{11}$] **26**, while treatment with diphenylacetylene yields [*closo*-3-$(\eta^2\text{-}MeC_2Me)$-3-$(\eta^2\text{-}PhC_2Ph)$-3-$\{P(OMe)_3\}$-3,1,2-$MoC_2B_9H_{11}$] **27**, which is also obtained when **22** is treated with but-2-yne. However, under the same conditions, **22** reacts with diphenylacetylene to give [*closo*-3-$(\eta^2\text{-}PhC_2Ph)$-3,3-$\{P(OMe)_3\}_2$-8-{σ-*trans*-C(Ph)=C(H)Ph}-3,1,2-$MoC_2B_9H_{10}$] **28**, whose structure was confirmed by X-ray crystallography. **28** is the product of an *exo*-polyhedral rearrangement, for which a mechanism involving two metal centres is proposed. A similar *exo*-polyhedral rearrangement reaction is observed when **18** is refluxed in acetonitrile yielding [*closo*-3,3-$(\eta^2\text{-}PhC_2Ph)_2$-3-(NCMe)-8-{σ-*trans*-C(Ph)=C(H)Ph}-3,1,2-$MoC_2B_9H_{10}$] **30**.

Protonation of **XXXII** followed by addition of $P{\equiv}CBu^t$ gives the diphosphacyclobutadienyl complex [*closo*-3,3-$(CO)_2$-3-$\{\eta^4\text{-}P_2C_2(Bu^t)_2\}$-3,1,2-$MoC_2B_9H_{11}$] **31**.

Contents

1.	**Introduction**	**1**
1.1	Alkynes in Transition Metal Chemistry.	2
1.2	The Stabilisation of Metal Fragments by Cyclopentadienyl Ligands and Carbaborane Clusters.	15
2.	**Results and Discussion**	**23**
2.1	Reaction of $[Mo(\eta^2\text{-}PhC_2Ph)\{P(OMe)_3\}_2(\eta\text{-}C_5H_5)][BF_4]$ with RMgBr (R= Et, CH_2Ph).	24
2.2	Reactivity of the Complexes $[Mo(\eta^2\text{-}PhC_2Ph)(R)\{P(OMe)_3\}(\eta\text{-}C_5H_5)]$ (R= Et **1**, CH_2Ph **2**).	27
2.3	Reaction of $[Mo(\eta^2\text{-}PhC_2Ph)\{P(OMe)_3\}_2(\eta\text{-}C_5H_5)][BF_4]$ with Allyl Magnesium Bromide.	35
2.4	Reaction of $[Mo(\eta^2\text{-}RC_2R')\{P(OMe)_3\}_2(\eta\text{-}C_5H_5)][BF_4]$ with $CH_2(MgI)_2$.	40
2.5	Preparation of the η^2-Vinyl Complexes $K[Mo\{\eta^2\text{=}C(R)C(H)Ph\}\{\eta^2\text{-}P(OMe)_2OBF_2OP(OMe)_2\}(\eta\text{-}C_5H_5)]$ (R= Ph, **9**; Me, **10**).	44
2.6	Reactivity of the η^2-Vinyl Complexes $K[Mo\{\eta^2\text{=}C(R)C(H)Ph\}\{\eta^2\text{-}P(OMe)_2OBF_2OP(OMe)_2\}(\eta\text{-}C_5H_5)]$ (R= Ph, **9**, Me, **10**).	46
2.7	Attempts to Synthesise Complexes with *tri*-Hapto and *tetra*-Hapto Boron-Bridged Phosphite Ligands.	49
2.8	Synthesis of the first mononuclear η(4e)-Bonded Phosphaalkyne Complex.	52
2.9	Reactivity of **14** - Transformation into a 1,3-Diphosphacyclobutadiene Complex	56
2.10	Investigation of Phosphide Alkyne Complexes $[Mo(PPh_2H)(PPh_2)(\eta^2\text{-}RC_2R)(\eta\text{-}C_5H_5)]$	58

2.11 Reactions of the *bis*-Alkyne(carbonyl)-Carbaborane Complexes with $P(OMe)_3$. 66

2.12 Mechanistic Investigation of the Reaction of the *bis*-Alkyne Complexes with Trimethylphophite. 71

2.13 Reaction of [*closo*-3,3-(η^2-$PhC_2Ph)_2$-3-(CO)-3,1,2-$MoC_2B_9H_{11}$] **18** with Acetonitrile. 81

2.14 Synthesis of a 1,3-Diphosphacyclobutadiene Carbaborane Complex 85

3. Experimental Section **89**

3.1 Preparation of [Mo(Et)(η^2-PhC_2Ph){$P(OMe)_3$}(η-C_5H_5)] **1.** 91

3.2 Preparation of [Mo(CH_2Ph)(η^2-PhC_2Ph){$P(OMe)_3$}(η-C_5H_5)] **2.** 91

3.3 Preparation of [Mo(η^2=C(Ph)C(Ph)C(Et)O}(CO){$P(OMe)_3$}-(η-C_5H_5)] **3.** 91

3.4 Preparation of [Mo(η-C_5H_5)(η^6-C_6Ph_6)] **4.** 92

3.5 Preparation of [Mo{$P(OMe)_3$}$_2${η^2-C(Ph)=C(Ph)CH_2CH=CH_2}-(η-C_5H_5)] **5.** 92

3.6 Preparation of [Mo(η^2-RC_2R'){η^2-$P(OMe)_2OBF_2OP(OMe)_2$}-(η-C_5H_5)] **6, 7, 8.** 93

3.7 Reaction of [Mo(η^2-RC_2R'){η^2-$P(OMe)_2OBF_2O(POMe)_2$}(η-C_5H_5)] **6, 7, 8** with K[$BHBu^s_3$]. 94

3.8 Preparation of [$Mo(CO)_2${η^2-$P(OMe)_2OBF_2OP(OMe)_2$}(η-C_5H_5)] **11.** 95

3.9 Preparation of [Mo{$P(OMe)_3$}$_2${η^2-$P(OMe)_2OBF_2OP(OMe)_2$}-(η-C_5H_5)] **12.** 95

3.10 Preparation of [Mo{$P(OMe)_3$}$_4$(η-C_5H_5)]BF_4 **13.** 96

3.11 Preparation of [Mo{η^2-$P(OMe)_2OBF_2OP(OMe)_2$}(η^2-P≡CBu^t)-(η-C_5H_5)] **14.** 96

3.12 Preparation of [Mo{η^2-$P(OMe)_2OBF_2OP(OMe)_2$}{η^4-$P_2C_2(Bu^t)_2$}-(η-C_5H_5)] **15.** 97

3.13 Synthsis of the complex $[Mo(PHPh_2)_2(\eta^2\text{-}PhC_2Ph)(\eta\text{-}C_5H_5)][BF_4]$ **16.** 97

3.14 Preparation of $[Mo(PPh_2)(PHPh_2)(\eta^2\text{-}PhC_2Ph)(\eta\text{-}C_5H_5)]$ **17.** 98

3.15 Preparation of the complexes [*closo*-3,3-$(\eta^2\text{-}RC_2R')_2$-3-(CO)-3,1,2-$MoC_2B_9H_{11}$] **18, 19.** 98

3.16 Reaction of the complexes [*closo*-3,3-$(\eta^2\text{-}RC_2R')_2$-3-(CO)-3,1,2-$MoC_2B_9H_{11}$] with $P(OMe)_3$ at room temperature. 99

3.17 Preparation of the complexes [*closo*-3-$(\eta^2\text{-}RC_2R')$-3,3-$\{P(OMe)_3\}_2$-3,1,2-$MoC_2B_9H_{11}$] **22, 23, 24.** 100

3.18 Synthesis of the complexes [*closo*-3-$(\eta^2\text{-}RC_2R)_2$-3-$(\eta^2\text{-}R'CCR')$-3-$\{P(OMe)_3\}$-3,1,2-$MoC_2B_9H_{11}$] **26, 27.** 101

3.19 Synthesis of complex [*closo*-3-$(\eta^2\text{-}PhC_2Ph)$-3,3-$\{P(OMe)_3\}$2-8-{σ-*trans*-C(Ph)=C(H)Ph}-3,1,2-$MoC_2B_9H_{10}$] **28.** 102

3.20 Reaction of **18** with acetonitrile. 103

3.21 Preparation of [*closo*-3,3-$(CO)_2$-3-$\{\eta^4\text{-}P_2C_2(Bu^t)_2\}$-3,1,2-$MoC_2B_9H_{11}$] **31.** 104

4. References **105**

5. Appendix **112**

5.1 Crystal data for **4** II

5.2 Crystal data for **5** IX

5.3 Crystal data for **6** XII

5.4 Crystal data for **28** XIV

5.5 Crystal data for **30** XXIV

5.6 Crystal data for **31** XXXIII

Abbreviations

Me	methyl
Et	ethyl
Pr	propyl
Cy	cyclohexyl
Bu^s	secondary-butyl
Bu^t	tertiary-butyl
Ph	phenyl
M	metal atom
L	trimethylphosphite
R_F	*tri*-fluoro-methyl

in diagrams:

L	$P(OMe)_3$
O	BH
●	CH, unless otherwise stated

with respect to NMR:

J	coupling constant in Hertz
N	virtual coupling constant $\lvert J + J' \rvert$ in Hertz
ppm	parts per million
Hz	Hertz
s	singlet
d	doublet
t	triplet
q	quartet
m	multiplet
br	broad
v	virtual
a	apparent

List of New Complexes

$[Mo(\eta^2\text{-}PhC_2Ph)(Et)\{P(OMe)_3\}(\eta\text{-}C_5H_5)]$	**1**
$[Mo(\eta^2\text{-}PhC_2Ph)(CH_2Ph)\{P(OMe)_3\}(\eta\text{-}C_5H_5)]$	**2**
$[Mo\{\eta^2\text{=}C(Ph)C(Ph)C(Et)O\}(CO)\{P(OMe)_3\}(\eta\text{-}C_5H_5)]$	**3**
$[Mo(\eta\text{-}C_5H_5)(\eta^6\text{-}C_6Ph_6)]$	**4**
$[Mo\{\eta^2\text{-}C(Ph)\text{=}C(Ph)CH_2CH\text{=}CH_2\}\{P(OMe)_3\}_2(\eta\text{-}C_5H_5)]$	**5**
$[Mo(\eta^2\text{-}PhC_2Ph)\{\eta^2\text{-}P(OMe)_2OBF_2OP(OMe)_2\}(\eta\text{-}C_5H_5)]$	**6**
$[Mo(\eta^2\text{-}PhC_2Me)\{\eta^2\text{-}P(OMe)_2OBF_2OP(OMe)_2\}(\eta\text{-}C_5H_5)]$	**7**
$[Mo(\eta^2\text{-}MeC_2Me)\{\eta^2\text{-}P(OMe)_2OBF_2OP(OMe)_2\}(\eta\text{-}C_5H_5)]$	**8**
$K[Mo(\eta^2\text{=}C(Ph)C(H)Ph)\{\eta^2\text{-}P(OMe)_2OBF_2OP(OMe)_2\}(\eta\text{-}C_5H_5)]$	**9**
$K[Mo(\eta^2\text{=}C(Me)C(H)Ph)\{\eta^2\text{-}P(OMe)_2OBF_2OP(OMe)_2\}(\eta\text{-}C_5H_5)]$	**10**
$[Mo(CO)_2\{\eta^2\text{-}P(OMe)_2OBF_2OP(OMe)_2\}(\eta\text{-}C_5H_5)]$	**11**
$[Mo\{P(OMe)_3\}_2\{\eta^2\text{-}P(OMe)_2OBF_2OP(OMe)_2\}(\eta\text{-}C_5H_5)]$	**12**
$[Mo\{P(OMe)_3\}_4(\eta\text{-}C_5H_5)][BF_4]$	**13**
$[Mo\{\eta^2\text{-}P(OMe)_2OBF_2OP(OMe)_2\}(\eta^2\text{-}P\equiv CBu^t)(\eta\text{-}C_5H_5)]$	**14**
$[Mo\{\eta^2\text{-}P(OMe)_2OBF_2OP(OMe)_2\}\{\eta^4\text{-}P_2C_2(Bu^t)_2\}(\eta\text{-}C_5H_5)]$	**15**
$[Mo(PHPh_2)_2(\eta^2\text{-}PhC_2Ph)_2(\eta\text{-}C_5H_5)][BF_4]$	**16**
$[Mo(PPh_2)(PHPh_2)(\eta^2\text{-}PhC_2Ph)_2(\eta\text{-}C_5H_5)]$	**17**
$[closo\text{-}3,3\text{-}(\eta^2\text{-}PhC_2Ph)_2\text{-}3\text{-}(CO)\text{-}3,1,2\text{-}MoC_2B_9H_{11}]$	**18**
$[closo\text{-}3,3\text{-}(\eta^2\text{-}PhC_2Me)_2\text{-}3\text{-}(CO)\text{-}3,1,2\text{-}MoC_2B_9H_{11}]$	**19**
$[closo\text{-}3\text{-}(\eta^2\text{-}PhC_2Ph)\text{-}3\text{-}(CO)\text{-}3\text{-}\{P(OMe)_3\}\text{-}3,1,2\text{-}MoC_2B_9H_{11}]$	**20**
$[closo\text{-}3\text{-}(\eta^2\text{-}MeC_2Me)\text{-}3\text{-}(CO)\text{-}3\text{-}\{P(OMe)_3\}\text{-}3,1,2\text{-}MoC_2B_9H_{11}]$	**21**
$[closo\text{-}3\text{-}(\eta^2\text{-}PhC_2Ph)\text{-}3,3\text{-}\{P(OMe)_3\}_2\text{-}3,1,2\text{-}MoC_2B_9H_{11}]$	**22**
$[closo\text{-}3\text{-}(\eta^2\text{-}PhC_2Me)\text{-}3,3\text{-}\{P(OMe)_3\}_2\text{-}3,1,2\text{-}MoC_2B_9H_{11}]$	**23**
$[closo\text{-}3\text{-}(\eta^2\text{-}MeC_2Me)\text{-}3,3\text{-}\{P(OMe)_3\}_2\text{-}3,1,2\text{-}MoC_2B_9H_{11}]$	**24**
$[closo\text{-}3\text{-}(CO)\text{-}3,3,3\text{-}\{P(OMe)_3\}_3\text{-}3,1,2\text{-}MoC_2B_9H_{11}]$	**25**
$[closo\text{-}3,3\text{-}(\eta^2\text{-}MeC_2Me)_2\text{-}3\text{-}\{P(OMe)_3\}\text{-}3,1,2\text{-}MoC_2B_9H_{11}]$	**26**
$[closo\text{-}3\text{-}(\eta^2\text{-}MeC_2Me)\text{-}3\text{-}(\eta^2\text{-}PhC_2Ph)\text{-}3\text{-}\{P(OMe)_3\}\text{-}3,1,2\text{-}MoC_2B_9H_{11}]$	**27**
$[closo\text{-}3\text{-}(\eta^2\text{-}PhC_2Ph)\text{-}3,3\text{-}\{P(OMe)_3\}_2\text{-}8\text{-}\{\sigma\text{-}trans\text{-}C(Ph)\text{=}C(H)Ph\}\text{-}3,1,2\text{-}MoC_2B_9H_{10}]$	**28**
$[closo\text{-}3,3\text{-}(\eta^2\text{-}PhC_2Ph)_2\text{-}3\text{-}(NCMe)\text{-}3,1,2\text{-}MoC_2B_9H_{11}]$	**29**

[*closo*-3,3-(η^2-PhC_2Ph)$_2$-3-$(NCMe)_2$-8-{σ-*trans*-C(Ph)=C(H)Ph}-3,1,2-$MoC_2B_9H_{10}$] **30**

[*closo*-3,3-$(CO)_2$-3-{η^4-$P_2C_2(Bu^t)_2$}-3,1,2-$MoC_2B_9H_{11}$] **31**

1. Introduction

1.1 Alkynes in Transition Metal Chemistry

The activation of alkynes in the coordination sphere of transition metals has attracted considerable interest, both from an industrial and an academic viewpoint. Metal alkyne complexes have been studied for polymerisation and metathesis reactions and for organic synthesis. Furthermore, rearrangement and coupling reactions have been shown to be a versatile field of research.[1]

The side-on coordination of alkynes may be conveniently described by the four orbital interactions shown in Figure 1. The extent of overlap and the difference in energy level between these interacting orbitals are important in determining the nature of the bonding. The energy levels are functions of the effective oxidation state of the metal, the nature of the auxiliary ligands and the substituents on the alkyne carbons. Calculations for metal-alkyne interactions revealed that σ-donation (a) exhibits the largest overlap. The smaller d_{π}-$\pi_{\parallel}^{*}$ (b) and d_{π}-$\pi_{\perp}$ (c) overlaps are similar, and the dδ-$\pi_{\perp}^{*}$ (d) is negligible. The interactions (a) and (b) are usually bonding and significant. It is important to note that the overlap (c) can be bonding or anti-bonding. In early tran-

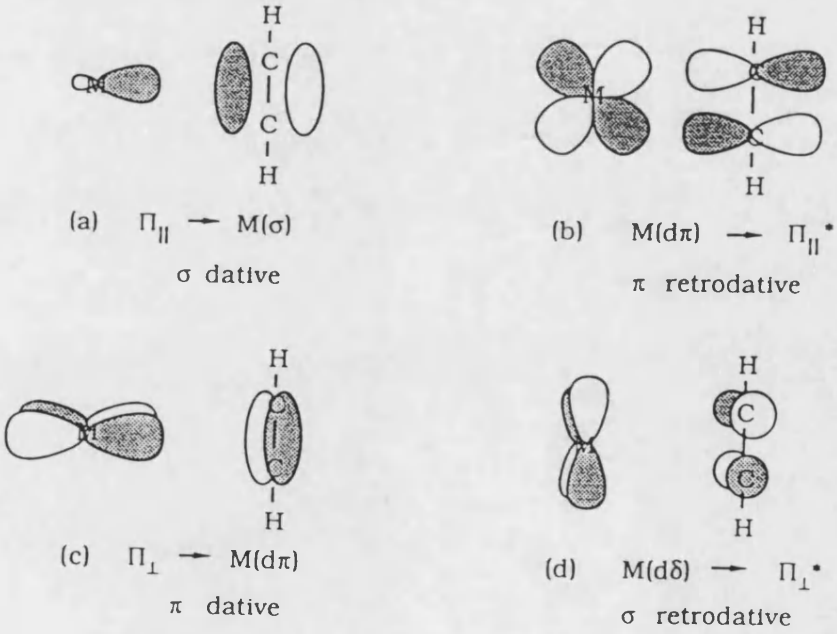

Figure 1

sition metal complexes which have vacant d_π orbitals, the interaction (c) is bonding. In later transition metal complexes, especially d^{10} complexes, the interaction should be repulsive.[2]

The availability of, respectively, filled or vacant orbitals and the energy levels of the interactions (a) to (c) determine how many electrons an alkyne formally donates to a transition metal complex. The bonding of a two-electron donor alkyne may be regarded as being analogous to the metal-olefin bonding as explained by the Dewar-Chatt-Duncanson model.[3] It is due to $\pi_\parallel$ donation from the alkyne to a vacant metal σ acceptor orbital (a) and $\pi_\parallel^*$ acceptance from a filled metal $d\pi$ orbital (b).

Alkynes are considered as being four-electron donors, when there is a donation from their filled $\pi_\perp$ orbital to an empty metal $d\pi$ orbital (c). Since there is no backbonding from the metal $d\delta$ orbital to the alkyne $\pi_\perp^*$ orbital (d), four-electron donor alkynes are always net electron donors, whereas two-electron donor alkynes can act as net electron donors or acceptors.[4]

This thesis is concerned with the synthesis and reactivity of molybdenum complexes containing four-electron donor alkynes. Hence, the spectroscopic and structural features of four-electron donor alkyne complexes will be reviewed, in addition to their reactivity.

The importance of the involvement of both of the filled alkyne π-orbitals in bonding to a single group VI metal was first recognised in the late 1960s with the description of the complex $[W(CO)(\eta^2\text{-}EtC_2Et)_3]$ by Augl *et al*[5, 6] The spectroscopic data indicated that the three alkyne ligands were equivalent, but that the two ends of every alkyne were situated in different environments. A *pseudo*-tetrahedral structure was proposed for the molecule, which was later confirmed by X-ray crystallography[7] (Figure 2).

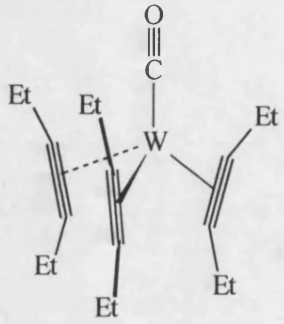

Figure 2

The assignment of every ligand as a two electron donor in this d^6 tungsten complex would give a metal electron count of 14, clearly unlikely for a centrally placed transition metal in a low oxidation state. An orbital study by King[8] showed that there is no orbital combination available by which the third alkyne can bond with both π-orbitals. It was suggested that the three alkynes are rapidly alternating in their bonding mode with two alkynes donating four electrons and one donating two. On basis of orbital theory it was also predicted that a *tris*-alkyne complex $[W(\eta^2\text{-}RC_2R)_3]$ cannot be an eighteen electron complex.

Since then, the idea that an alkyne can act as a four electron donor has been accepted and numerous compounds of this type synthesised. Alkynes in complexes where two or more alkynes are alternating in their bonding mode are given an effective number of donated electrons. This number, equal to the number of donated electrons divided by the number of alkynes, need not even be an integer number. Nevertheless, this rather formal assignment is helpful when the physical properties of complexes are being discussed.

NMR spectroscopy can be used as a diagnostic tool in determining the bonding of an alkyne and the effective number of donated electrons. It has been shown that a low field shift in the ^1H NMR spectrum for the terminal alkyne protons is dependent upon the number of donated electrons. For example, the protons of the two electron alkyne in $[Mo(\eta^2\text{-}HC_2H)(\eta\text{-}C_5H_5)_2]$ resonate at 7.7 ppm,[9] whereas the protons in the four electron alkyne in $[Mo(CO)(PPh_3)(\eta^2\text{-}HC_2H)(\eta\text{-}C_5H_5)]^+$ resonate at 12.9 and 12.0 ppm[10] respectively. The general utility of this ^1H NMR probe is, however, decreased by the scarcity of terminal alkyne complexes.

The systematic relationship between the contact carbon chemical shift in the ^{13}C NMR and the effective number of donated electrons was first noted by Templeton and Ward[11] for a series of Mo(II) and W(II) complexes. An empirical plot of alkyne ^{13}C chemical shifts, which span over 100 ppm, *versus* N, the number of electrons donated per alkyne, revealed a strong correlation (Figure 3). Signals for two, three and four electron donor alkynes fall into distinct regions, between 100 and 130 ppm, 140 and 190 ppm, and 175 and 230 ppm, respectively.[11]

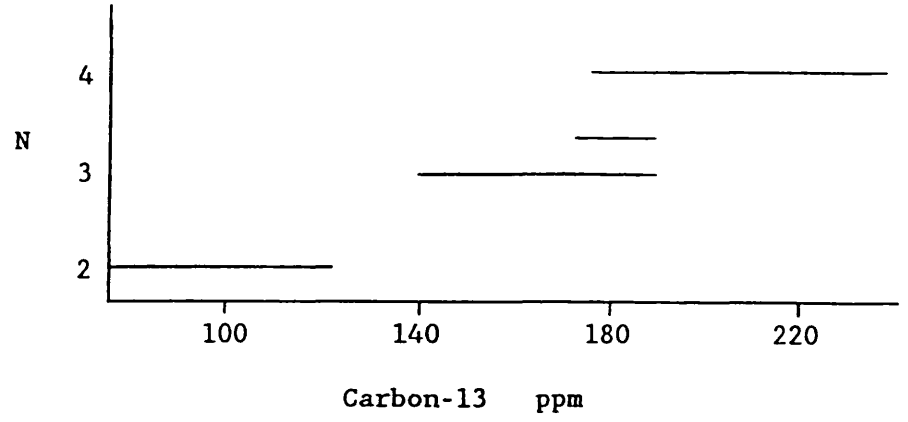

Figure 3

Variable temperature NMR spectroscopy has been used to examine alkyne rotation barriers. Activation energies for analogous molybdenum and tungsten pairs differ only slightly. The rationalisation of trends is difficult as both $\pi_{\parallel}^{*}$ acceptance and $\pi_{\perp}$ donation, as well as steric factors, influence the size of the barrier.[12] For cyclopenta-dienyl molybdenum complexes, typical rotation barriers are listed in Table 1.

Table 1

	$\Delta G_{Tc}^{\ddagger}$ / kJmol^{-1}	ref
$[MoCl(\eta^2\text{-}MeC_2Me)_2(\eta\text{-}C_5H_5)]$	38.9	13
$[MoBr(\eta^2\text{-}MeC_2Me)_2(\eta\text{-}C_5H_5)]$	60.2	13
$[Mo(\eta^2\text{-}MeC_2Me)_2(CO)(\eta\text{-}C_5H_5)][PF_6]$	81.2	14
$[Mo(\eta^2\text{-}MeC_2Me)(CO)(PEt_3)(\eta\text{-}C_5H_5)][BF_4]$	62.8	15

Cationic *bis*-alkyne complexes $[Mo(\eta^2\text{-}RC_2R')_2(CO)(\eta\text{-}C_5H_5)]^+$ exhibit relatively high rotational barriers (67 - 88 kJ/mol). Figure 4 shows the three possible isomers when

the two R-groups on the alkyne are different (i.e. R≠R'). The substituents on the alkyne can have either an adjacent (*cis*) or an opposite (*trans)* position. Both standard variable temperature NMR-techniques[16] and two dimensional methods[17] have been used to elucidate isomer interconversion schemes with two asymmetric alkynes in the coordination sphere.

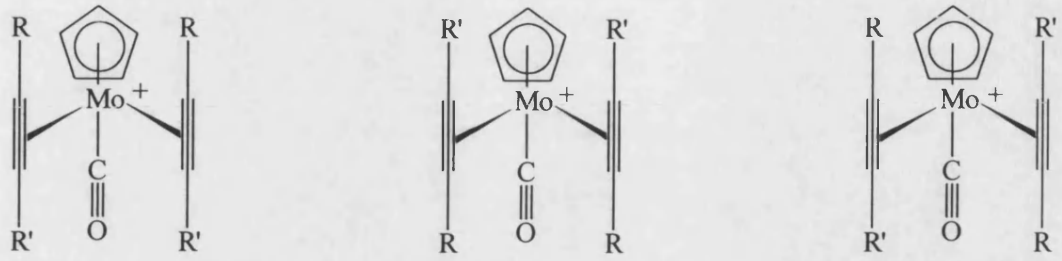

cis' *cis"* *trans*

Figure 4

Infra-red spectroscopy of alkyne complexes can give information about the metal alkyne bond. However, the alkyne absorptions υ(C≡C) ranging from 1550 to 1900 cm^{-1} are usually weak and difficult to assign. The expected trend that the number of donated electrons weakens the C≡C bond has been observed with complexes containing $MeO_2CC_2CO_2Me$ (DMAC). This diester alkyne exhibits absorptions which can be assigned to the C≡C stretching mode. The four-electron donor DMAC gives the lowest absorption at 1730 cm^{-1}, with the three-electron donor absorbing at 1790-1820 cm^{-1} and two-electron donor DMAC at 1895 cm^{-1}.[18]

Metal-alkyne interactions are reflected in metal-ligand bond lengths, ligand orientations, intra-ligand bond lengths and selected angles. Metal-carbon bond lengths are particularly useful for assessing the importance of alkyne $\pi_\perp$ donation. More than 90% of the four-electron donor alkyne ligands in Mo(II) and W(II) monomers exhibit metal-carbon bond lengths in the range 2.03 ± 0.03 Å.[12] Among the four electron donor examples, only $[Mo(CO)(SC_6H_4SPh)(\eta^2\text{-}MeC_2Me)(\eta\text{-}C_5H_5)]$[19] has a metal-carbon bond exceeding 2.06Å (at 2.03 and 2.09Å). This deviation may be accounted for by the competition of thiolate π-donation with alkyne $\pi_\perp$ donation. Given the diversity of alkynes and auxiliary ligands, the consistency of four-electron donor M-C distances is noteworthy. These distances can be compared to that of $[Mo(\eta^2\text{-}PhC_2Ph)$

$(\eta\text{-}C_5H_5)_2]$[20], a standard two electron donor monomer, with a metal-carbon distance of 2.14Å, exceeding the average four electron metal-carbon distance by around 0.10Å.

Only a small difference separates typical metal-carbon distances for N= 4 (2.03 ±0.03Å) and N=3 (2.07±0.02Å) and the two classes overlap in the long N= 4 and short N= 3 region. For example, the four electron donor alkyne complex $[Mo(CO)(PEt_3)(\eta^2\text{-}MeC_2Me)(\eta^5\text{-}C_9H_7)][BF_4]$[15] exhibits M-C bond lengths of 2.03 and 2.06Å. In the three electron donor complex $[Mo(NCMe)(\eta^2\text{-}MeC_2Me)_2(\eta\text{-}C_5H_5)][BF_4]$,[21] the distances were found to be 2.06 and 2.07Å.

Carbon-carbon bond lengths, which generally fall between 1.27 and 1.33 Å, are not adequate for probing metal-alkyne bonding.[22] Both two- and four-electron donor alkynes exhibit C≡C bond lengths at the lower end of the range (≤1.30 Å). Complexes containing diamino alkyne ligands[23] show distances of 1.35 - 1.40 Å. These longer distances may be accounted for by extensive π-delocalisation in the $R_2NC_2NR_2$-ligand system.

The structures of $[W(CO)(\eta^2\text{-}HC_2H)(\eta^2\text{-}S_2CNEt_2)_2]$[22] **I** and $[W(MA)(\eta^2\text{-}HC_2Ph)(\eta^2\text{-}S_2CNEt_2)_2]$[24] (MA= maleic anhydride) **II** reinforce the utility of the four electron donor concept (Figure 5). In both complexes, the short W-alkyne carbon bonds (2.03 and 2.01Å) indicate multiple bond character. In **I**, the alignment of the alkyne parallel to the W-C≡O axis puts $\pi_\perp$ in a position to overlap with the lone vacant metal d_π orbital, thus supporting the hypothesis that $\pi_\parallel$ and $\pi_\perp$ provide the electron density binding the acetylene to tungsten. As a result of the replacement of carbon monoxide with the single faced π-acid olefin ligand maleic anhydride **II**, the d_π ordering is shuffled and the alkyne ligand rotated by 90°. The disparity between average metal-carbon bond distances to the alkyne (2.01Å) and to the olefin (2.25Å) underlines the substantial bonding differences between these ligands.

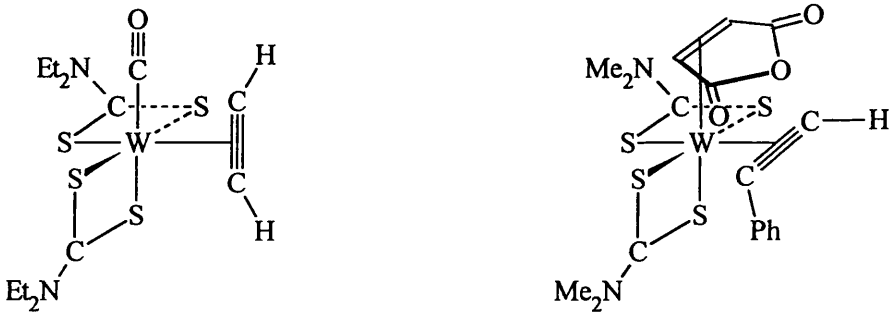

I II

Figure 5

Calculations on the octahedral model d^4-olefin-alkyne system $[W(\eta^2\text{-}H_2C_2H_2)(\eta^2\text{-}HC_2H)(\eta^2\text{-}S_2CNH_2)_2]$ showed a one to one match of all of the three metal d_π orbitals with a ligand π-function resulting in three constructive two-centre two-electron metal ligand π-bonds.[24] Extended Hückel calculations give the d_π level ordering shown in Figure 6. The first HOMO is the olefin stabilised d_{xz}, the second HOMO, d_{xy}, reflects alkyne $\pi_\parallel^*$ overlap and the LUMO consists of d_{yz} destabilised by $\pi_\perp$ donation of the four electron donor. Separate rotation of the olefin and alkyne C_2 units can be explored theoretically using EHMO methods. Overlap of the filled d_{xz} orbital with olefin π^* is eliminated as the olefin rotates 90°, creating a large barrier for olefin rotation (75 kcal/mol). On rotation, the alkyne quickly redefines the linear combinations of d_{xy} and d_{yz} which serve as d_π donor and d_π acceptor orbitals, respectively. Thus there should be a small electronic barrier to alkyne rotation (12.5 kcal/mol). These theoretical conclusions are consistent with dynamic NMR results.

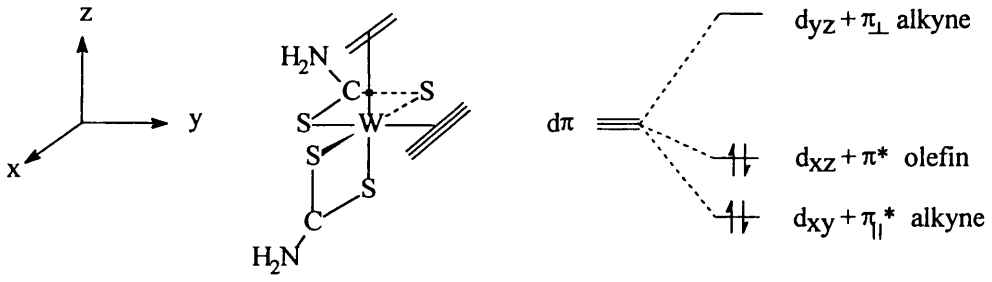

Figure 6

In cyclopentadienyl molybdenum complexes, the alkyne orientation depends on the two *cis*-ligands. A comparative structural study of $[Mo(CO)(SC_6F_5)(\eta^2\text{-}CF_3C_2CF_3)(\eta\text{-}C_5H_5)]$ **III** and $[Mo(O)(SC_6F_5)(\eta^2\text{-}CF_3C_2CF_3)(\eta\text{-}C_5H_5)]$ **IV** revealed alkyne orien-

tations differing by 90° for the d^4 and d^2 configurations (Figure 7). The rotational preferences of the alkyne in this example are clearly dictated by electronic factors.[25]

III **IV**

Figure 7

The structure of $[WCl(CF_3C_2CF_3)_2(\eta\text{-}C_5H_5)]$,[26] shown in Figure 8, exhibits the key geometric features assumed to characterise all d^4-*bis*-alkyne complexes. The two *cis*-alkynes lie approximately parallel to the adjacent M-L axis, here W-Cl. The *pseudo*-tetrahedral description with parallel *cis*-alkynes accurately describes $[Mo(L)(\eta^2\text{-}MeC_2Me)_2(\eta\text{-}C_5H_5)]$ for both L= CO **V** and L= MeCN **VI**. However, a significant difference is found in the Mo-C(alkyne) distances adjacent to L, which average 2.06 Å for L= MeCN and 2.13 Å for L=CO.[21]

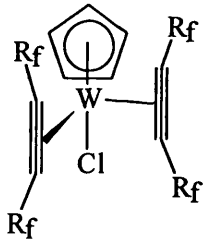

Figure 8

The reactivity of alkyne complexes towards nucleophiles is particularly noteworthy. The nucleophilic addition of an H^- nucleophile at a two electron donating alkyne in the saturated iron-complex $[Fe(CO)(PPh_3)(\eta^2\text{-}MeC_2Me)(\eta\text{-}C_5H_5)][BF_4]$ **VII** generates the compound $[Fe(CO)(PPh_3)(\sigma\text{-}CMe{=}CHMe)(\eta\text{-}C_5H_5)]$ **VIII** containing an η^1-vinyl group.[27]

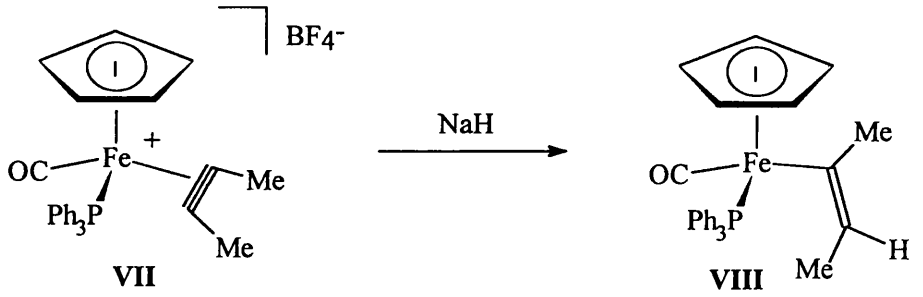

Scheme 1

Consideration of the electronic configuration around the metal leads one to expect that η^1-vinyl complexes could not be the stable product of a similar reaction with a four electron donor alkyne. However, the sixteen electron η^1-vinyl species which inevitably results can be stabilised by addition of a two electron donor ligand to the metal centre. This is illustrated in Scheme 2 by the reaction of $[Mo\{P(OMe)_3\}_2(\eta^2\text{-}Bu^tC_2H)(\eta^5\text{-}C_9H_7)][BF_4]$ **IX** with $NaBH_4$ in the presence of $P(OMe)_3$. The stable 18 electron η^1-vinyl complex $[Mo\{P(OMe)_3\}_3(\sigma\text{-}CH{=}CHBu^t)(\eta^5\text{-}C_9H_7)]$ **X** can be isolated.[28]

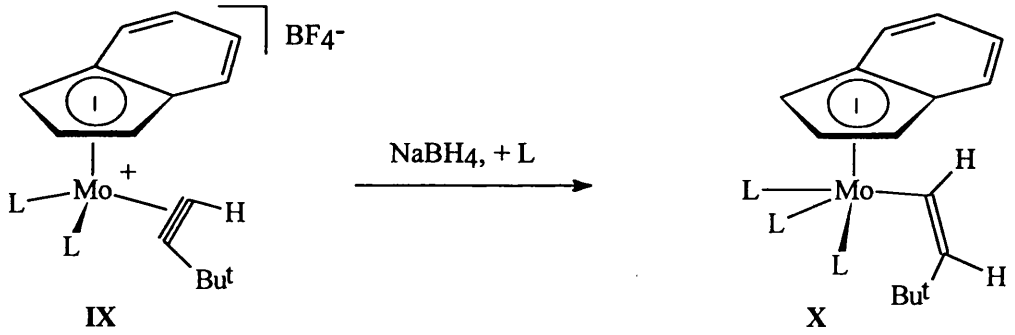

Scheme 2, L= $P(OMe)_3$

More interesting, however, is that the reaction of $[Mo(\eta^2\text{-}RC_2R')\{P(OMe)_3\}_2(\eta\text{-}C_5H_5)][BF_4]$ (R= R'= Ph) **XI** with $K[HBBu^s_3]$ produces the stable products $[Mo(\eta^2{=}CRC(H)R')\{P(OMe)_3\}_2(\eta\text{-}C_5H_5)]$[29, 30] **XII**. The product contains a three electron donor unit which may be described as an η^2-vinyl ligand, metallocyclopropene or cyclic alkylidene.

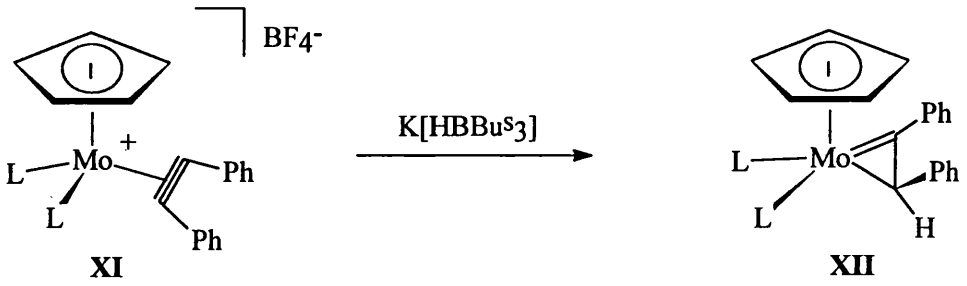

Scheme 3, L= $P(OMe)_3$

Similar metallacyclopropene systems were obtained when the starting complex had substituents like Bu^t, Tol or Ph on the alkyne or when different nucleophiles were employed.[30] However, when at least one of the alkyne substituents in the analogous complexes $[Mo(\eta^2\text{-}RC_2R')\{P(OMe)_3\}_2(\eta\text{-}C_5H_5)][BF_4]$ were Me or H, nucleophilic addition reaction gave η^3-allyl **XIII** for (R= R'= Me)[31] and carbyne complexes **XIV** for (R= Bu^t, R= H).[28] As is shown in Scheme 4, it is believed that the initial product in every case is an η^2-vinyl complex, which then rearranges.

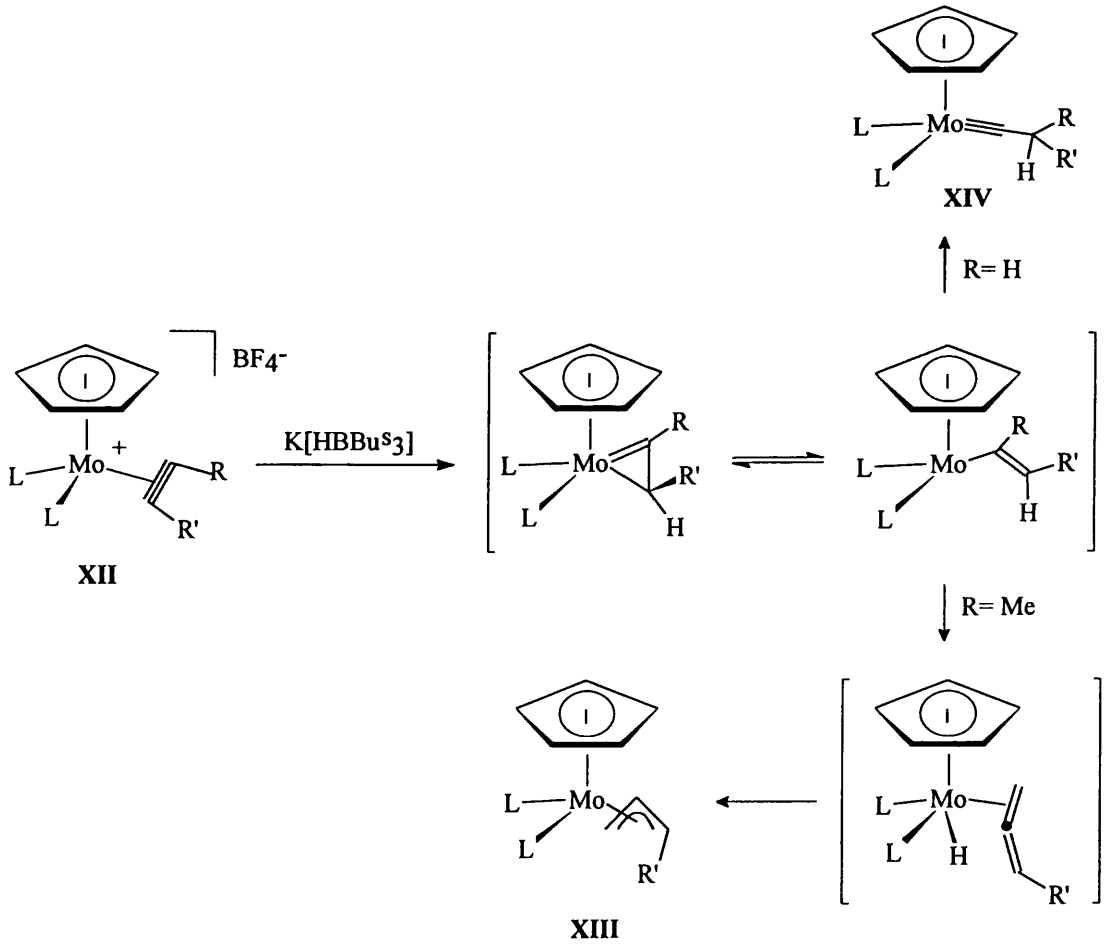

Scheme 4, L= $P(OMe)_3$

Isolation and characterisation of η^2-vinyl complexes has important mechanistic implications since it infers the possible stabilisation of unsaturated intermediates with vinyl ligands *via* η^1(1e) to η^2(3e) transformation. The salient structural features of η^2-vinyl complexes of the type $[Mo\{\eta^2{=}CRC(H)R'\}(L)_2(\eta\text{-}C_5H_5)]$ include the orientation of the two C_β substituents roughly orthogonal to the $MC_\alpha C_\beta$ plane (Figure 9). This is opposite to the location of C_β substituents of η^1-vinyl ligands which lie in the $MC_\alpha C_\beta$ plane.[32] The short M-C_α distances (1.94 - 1.96 Å) are appropriate for a molydenum-carbon double bond and the M-C_β distances (2.25 - 2.30 Å) are in the single bond range whereas the C_α-C_β bond lengths (1.43- 1.46 Å) indicate some double bond character. The C_α-C_β vector lies parallel to one of the Mo-L bonds, a feature reminiscent of alkyne complexes of the type $[Mo(\eta^2\text{-}RC_2R)(L)_2(\eta\text{-}C_5H_5)]$.

Unambiguous identification of η^2-vinyl ligands is often possible based on ^{13}C NMR spectra. The carbenoid character of C_α is reflected in low-field chemical shifts of 230-290 ppm, while the C_β signal appears at much higher field, typically near 20 - 30 ppm.[30]

The fluxionality of η^2-vinyl ligands, where it can be observed, parallels that of alkynes. On the basis of orbital calculations it was suggested that a 'windscreen wiper' motion of 90° occurs, as is shown in Figure 9. A full rotation (180°) of the η^2-moiety would have a far higher barrier to rotation.[30]

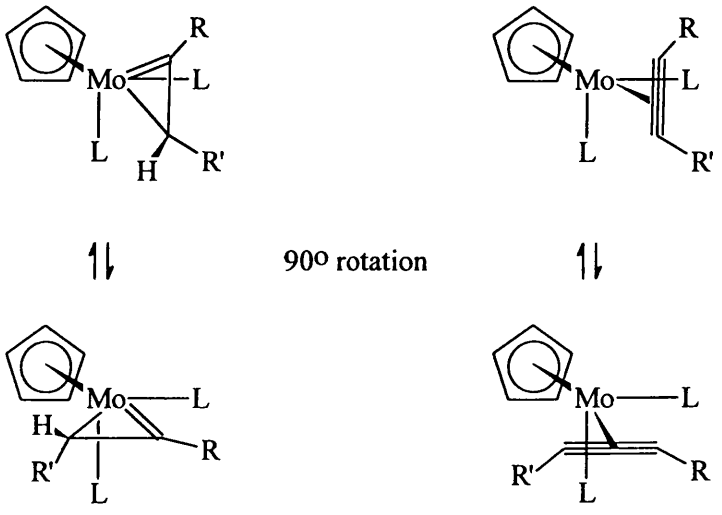

Figure 9, L= $P(OMe)_3$

The bonding of an η^2-vinyl fragment has been extensively studied by Green and co-workers.[30] In a fragment molecular orbital analysis, the frontier orbitals of the $[MoL_2(\eta\text{-}C_5H_5)]^+$, HC_2H and $CHCH_2^-$ moieties were calculated (Figure 10). The main conclusion was that the η^2-vinyl fragment interacts with the metal *via* the same combination of orbitals as a four electron donor alkyne, leading to electron donation from the vinyl σ and $\pi_\perp$ orbitals and back donation to the $\pi_\parallel^*$ orbital. The major difference between the alkyne and η^2-$C_2H_3^-$ frontier orbitals lies in the energy and spatial nature of the $\pi_\perp$ orbital. In the vinyl ligand, this orbital is essentially pure $C_\alpha(p)$ in character, and is therefore both asymmetric with respect to the two contact

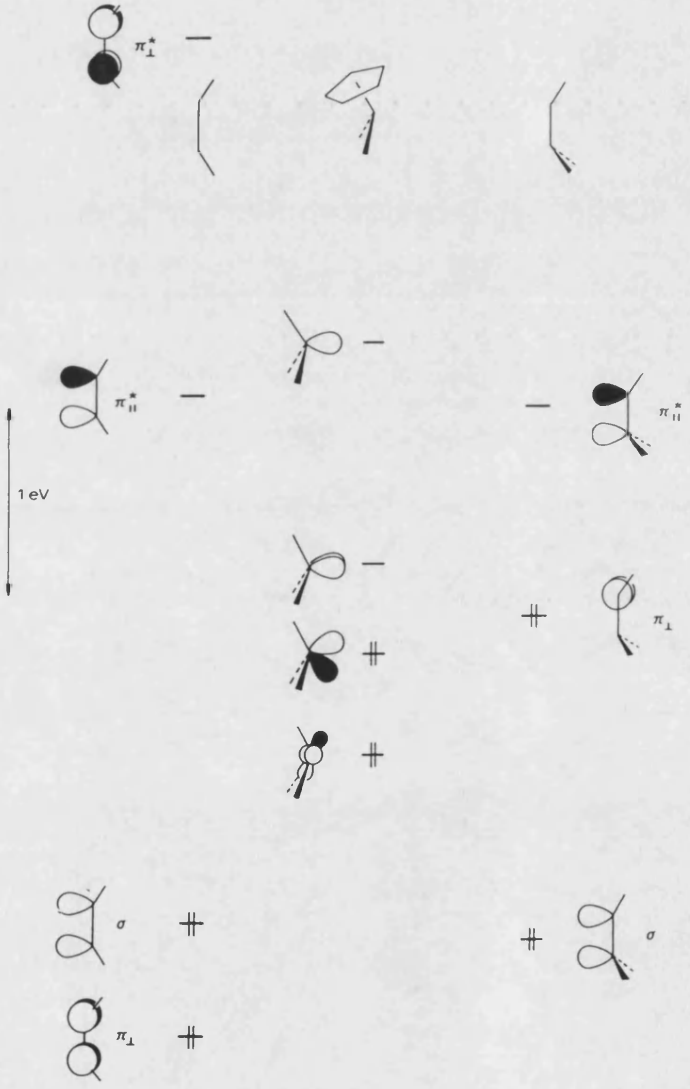

Figure 10, Frontier molecular orbitals of the fragments η^2-HC_2H, $[Mo\{P(OH)_3\}_2(\eta\text{-}C_5H_5)]$ and η^2-$C_2H_3^-$.

carbons and at a higher energy than the $\pi_{\perp}$ orbital of the alkyne. Hence, on energetic grounds, it can be concluded that the η^2-$C_2H_3^-$ fragment is a better donor than C_2H_2, and that the M-C_α double bond is localised.

1.2 The Stabilisation of Metal Fragments by Cyclopentadienyl Ligands and Carbaborane Clusters

The systematic nomenclature of metallacarbaboranes that is applied throughout this thesis depends upon the principle that they are *hetero*-atomic analogues of polyhedral boranes.[33] However, when parallels between carbaborane- and cyclopentadienyl metal chemistry are drawn, it seems useful to view the anion $[nido\text{-}C_2B_9H_{11}]^{2-}$ as a metal bound η^5-ligand.

This analogy becomes apparent when the synthesis of some cyclopentadienyl and carbaborane complexes are reviewed. The reaction of the cyclopentadienyl anion $[C_5H_5]^-$ with $FeCl_3$ leading to the discovery of ferrocene is today considered as the birthmark of modern organometallic chemistry. The highly thermostable ferrocene molecule was the first sandwich complex to be prepared and its structural characterisation was a milestone in the development of the concept of metal-carbon π-bonds.[34]

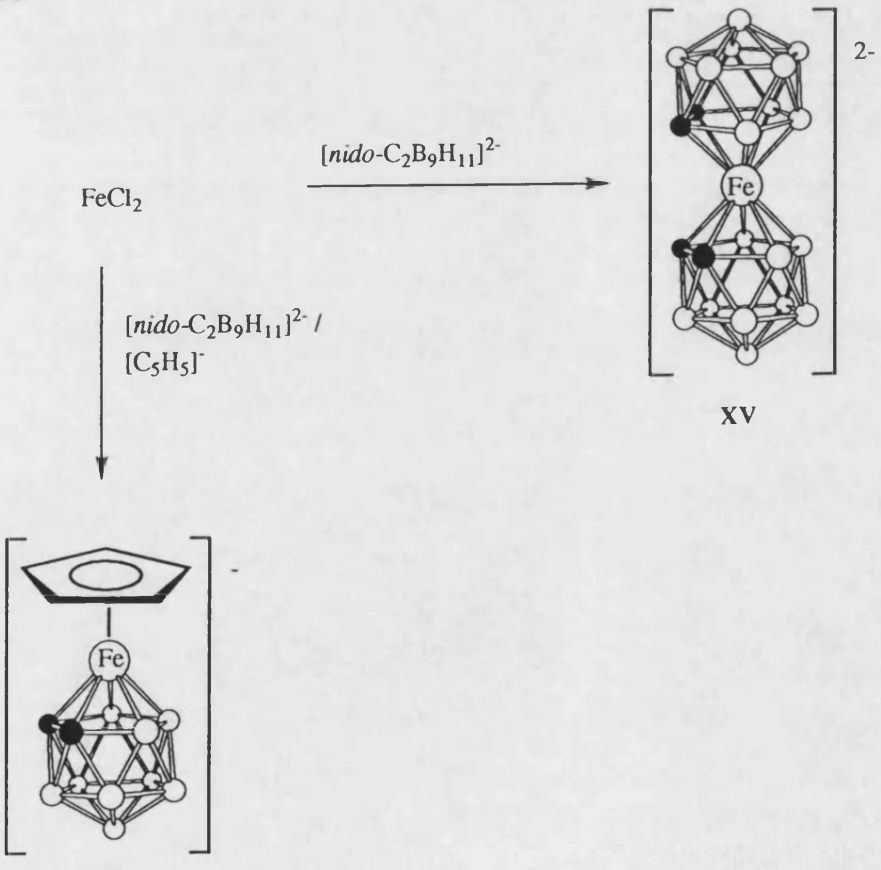

XV

XVI

Scheme 5, O = BH, ● = CH

Similarly, the reaction of $FeCl_2$ with the dianion $[nido\text{-}C_2B_9H_{11}]^{2-}$ gives the sandwich complex $[3,3'\text{-}(closo\text{-}3,1,2\text{-}FeC_2B_9H_{11})_2]^{2-}$ **XV** (Scheme 5).[35] The mixed sandwich complex $[closo\text{-}3\text{-}(\eta\text{-}C_5H_5)\text{-}3,1,2\text{-}FeC_2B_9H_{11})]^-$ **XVI** was synthesised by reacting $FeCl_2$ with a 1:1 mixture of the $[nido\text{-}C_2B_9H_{11}]^{2-}$ dianion and the cyclopentadienyl anion.[36]

The reaction of $[Mo(CO)_6]$ with $[C_5H_5]^-$ generates the anionic complex $[Mo(CO)_3(\eta\text{-}C_5H_5)]^-$ **XVII**.[37] After methylation with MeI the neutral complex $[Mo(Me)(CO)_3(\eta\text{-}C_5H_5)]$ **XVIII** can be isolated.[38] Similarly, $[nido\text{-}C_2B_9H_{11}]^{2-}$ reacts with $[Mo(CO)_6]$ to yield the dianionic complex $[closo\text{-}3,3,3\text{-}(CO)_3\text{-}3,1,2\text{-}MoC_2B_9H_{11}]^{2-}$ **XIX**, which may be isolated as its tetraethylammonium salt. Methylation followed by addition of $[Et_4N]Cl$ yields the complex $[NEt_4][closo\text{-}3\text{-}(Me)\text{-}3,3,3\text{-}(CO)_3\text{-}3,1,2\text{-}MoC_2B_9H_{11}]$ **XX**.[39] As with the cyclopentadienyl ligand, sandwich and half-sandwich complexes of $[nido\text{-}C_2B_9H_{11}]^{2-}$ have been prepared with most transition metals.[40]

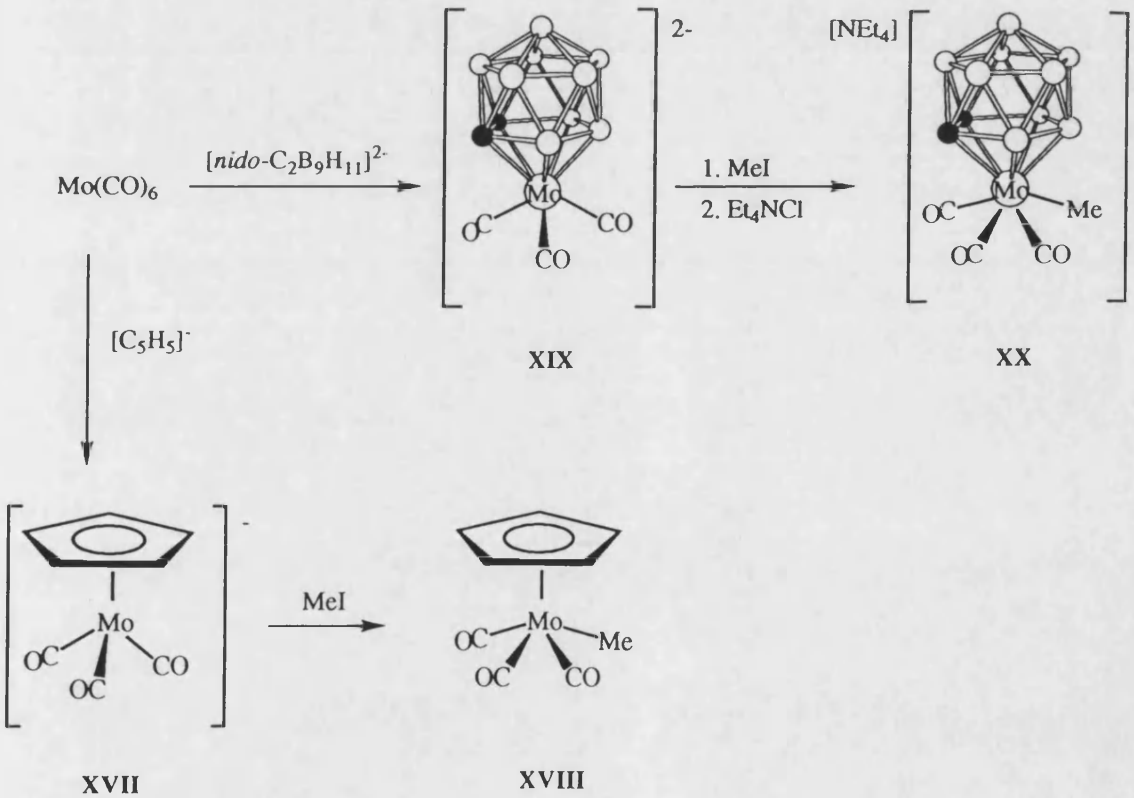

Scheme 6, ○ = BH, ● = CH

The structural characterisation of these metallacarbaboranes added experimental support to the theoretical calculations of Lipscomb, who had suggested that the bonding orbitals in $[nido\text{-}C_2B_9H_{11}]^{2-}$ are similar to those of the cyclopentadienyl anion.[41] More recent work by Hanusa suggests that a better analogy exists between $[nido\text{-}C_2B_9H_{11}]^{2-}$ and the pentamethylcyclopentadienyl anion.[42]

A cyclopentadienyl ligand has five molecular orbitals available for interaction with metal orbitals of suitable symmetry (Figure 11). Similarily, the open pentagonal face of $[nido\text{-}C_2B_9H_{11}]^{2-}$ exhibits five orbitals which are directed towards the empty icosahedral vertex.[43]

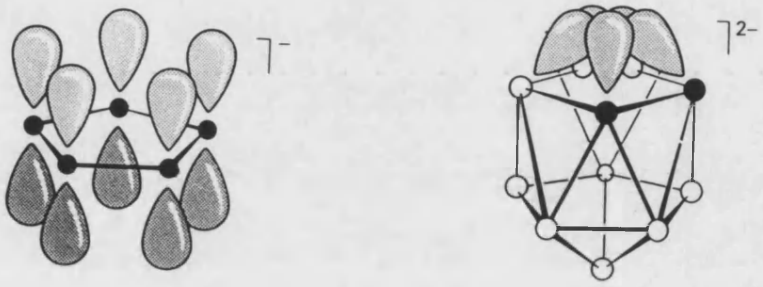

Figure 11, O = BH, ● = CH

Although the electron donating abilities are comparable, differences arise from the greater steric requirements of the carbaborane ligand and the fact that analogous complexes are differently charged. One example of the increased stability of a metallacarbaborane complex is that the formally 15-electron complex [3,3'-(*closo*-3,1,2-$CrC_2B_9H_{11})_2]^-$ **XXI** may be crystallised from water as a caesium salt, and is

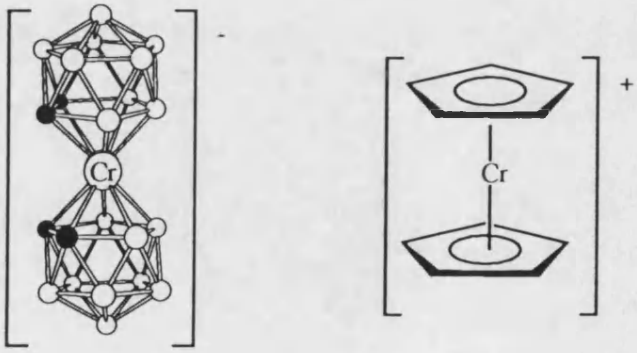

XXI **XXII**

Figure 12, O = BH, ● = CH

stable to molecular oxygen and concentrated sulphuric acid.[44] In contrast, the cationic $[Cr(\eta\text{-}C_5H_5)_2]^+$ **XXII** is readily hydrolysed and air sensitive.[45] However, metallacarbaborane complexes with a half-sandwich structure often show no greater stability towards hydrolysis or oxidation than their cyclopentadienyl analogues.[42]

Another important difference between the cyclopentadienyl ligand and the [*nido*-$C_2B_9H_{11}]^{2-}$ 'ligand' is observed for transition metals with an electronic configuration of greater than d^6. Viewed as a metallacarbaborane cluster, these complexes contain an excess of 26 skeletal electrons. While with d^0 to d^6 metals *closo*-icosahedral structures are adopted, higher electron numbers give rise to 'slip-distorted' structures. The metal atom is laterally shifted (by 0.1 - 0.3 Å) from the centre of the C_2B_3 bonding face of the $[C_2B_9H_{11}]^{2-}$ ligand, usually such that the metal-boron distances are shorter than the metal-carbon vectors.[46]

Calculations by Mingos and co-workers show that the distortions are a consequence of the interactions between the e-symmetry π-bonding molecular orbitals of the [*nido*-$C_2B_9H_{11}]^{2-}$ ligand and the essentially d_{xy} and d_{xz} metal orbitals.[47] Thus, the metallacarbaborane adopts a more open geometry as the electron configuration number and the effective electron density at the metal increases. This is illustrated by the two examples shown in Figure 13 and Figure 14. It was shown by Warren and Hawthorne[48] that the d^6-nickel complex [3,3'-(*closo*-3,1,2-$NiC_2B_9H_{11})_2$] **XXIII** has an icosahedral structure, whereas the d^8-nickel complex [3,3'-(*closo*-3,1,2-$NiC_2B_9H_{11})_2]^{2-}$ **XXIV** shows a 'slip-distortion' of both cages from an η^5-bonding mode to an η^3-linkage.

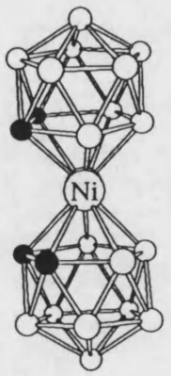

XXIII

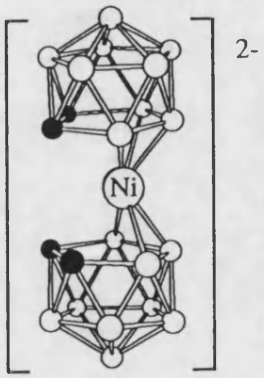

XXIV

Figure 13, ○ = BH, ● = CH

Wallbridge *et al*[49] illustrated the influence of the electron density for the pair of palladium compounds [*closo*-3-{$Me_2N(CH_2)_2NMe_2$}-3,1,2-$PdC_2B_9H_{11}$] **XXV** and [*closo*-3,3-$(PMe_3)_2$-3,1,2-$PdC_2B_9H_{11}$] **XXVI** with the same electron configuration. The degree of 'slippage' is greater when the metal is ligated by the σ-donor ligand Me_2N-$(CH_2)_2NMe_2$. The metal-cage antibonding interaction is reduced by the delocalisation of electron density onto the π-acceptor ligand PMe_3.

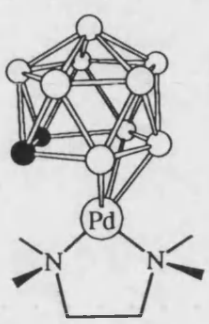

XXV

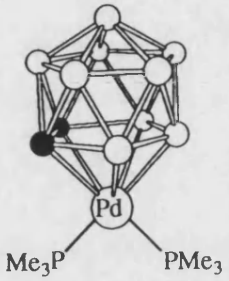

XXVI

Figure 14, ○ = BH, ● = CH

Major contributions to the molybdena- and tungstena-carbaborane chemistry have come from Stone and his coworkers.[50, 51] Because of the link to the chemistry described in this thesis, their work will be briefly discussed. The carbaborane alkylidyne complexes of molybdenum or tungsten [A][*closo*-3,3-$(CO)_2$-3-(≡CR)-3,1,2-$MC_2B_9H_{11}$] {A= NEt_4, $N(PPh_3)_2$, PPh_4} **XXVII**[52, 53, 54] are synthesised by reacting the respective alkylidyne halide compounds with [*nido*-$C_2B_9H_{11}$]$^{2-}$ at - 40°C followed by treatment of the mixtures with a salt [A][Cl].

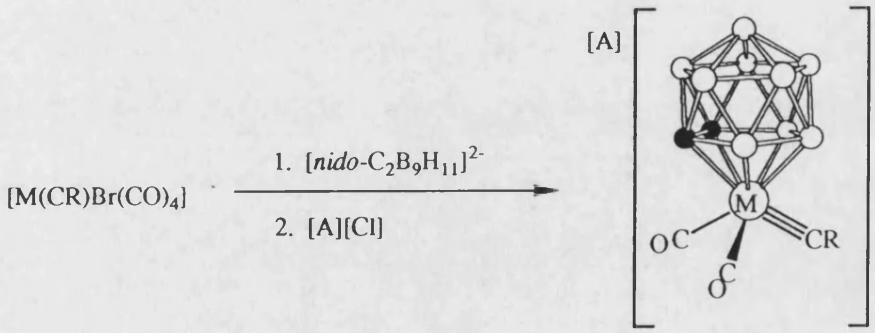

XXVII

Scheme 7, ○ = BH, ● = CH

The alkylidyne complexes **XXVII** were used as building blocks for the synthesis of multinuclear metal species and clusters. It was shown that the metal carbon triple bond can function like an alkyne, coordinating to metal fragments *via* its π-system. For example, the reaction of [AuCl(PPh_3)] with one of the complexes [A][*closo*-3,3-$(CO)_2$-3-(≡CR)-3,1,2-$MC_2B_9H_{11}$] **XXVII** in thf in the presence of $TlPF_6$, to remove chloride as insoluble TlCl, affords the tungsten-gold complex [*closo*-3,3-$(CO)_2$-3-{Au(PPh_3)-(μ-CR)}-3,1,2-$MC_2B_9H_{11}$] **XXVIII**.[52]

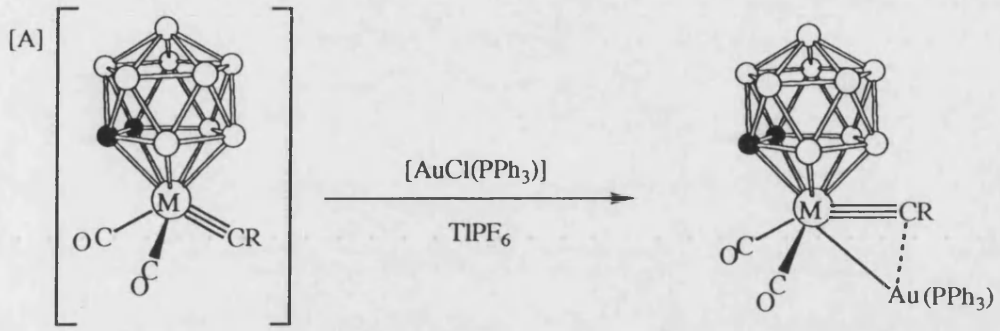

XXVII **XXVIII**

Scheme 8, ○ = BH, ● = CH

More interesting, however, was the observation that the carbaborane ligand is not always a spectator ligand, unlike the cyclopentadienyl ligand. Treatment of [A][*closo*-3,3-$(CO)_2$-3-(≡CR)-3,1,2-$WC_2B_9H_{11}$] **XXVII** with [Ru(CO)$(NCMe)_2$(η-C_5H_5)][BF_4] **XXIX** in CH_2Cl_2 affords the dimetal complex [*closo*-3,3-$(CO)_2$-3-{Ru(μ-CR)(CO)(η-C_5H_5)}-3,1,2-$WC_2B_9H_{11}$] **XXX** in which the carbaborane moiety forms an *exo*-polyhedral B-H→Ru bond (Scheme 9).[55] Treatment of this dimeric complex with a base followed by addition of [$N(PPh_3)_2$]Cl yields the species [$N(PPh_3)_2$][*closo*-3,3-$(CO)_2$-3,8-{Ru(μ-CR)(CO)(η-C_5H_5)}-3,1,2-$WC_2B_9H_{11}$] **XXXI** containing a two center B-Ru σ bond.

Stone *et al* showed that a great number of neutral carbaborane molybdenum or tungsten complexes can be prepared *via* protonation with $HBF_4.Et_2O$ of the anionic complexes [NEt_4][*closo*-3,3-$(CO)_2$-3-(η^3-C_3H_5)-3,1,2-$MC_2B_9H_{11}$][56, 57] **XXXII** in the presence of donor ligands (Scheme 10). Complexes of the type [*closo*-3,3-$(L)_2$-3,3-$(CO)_2$-3,1,2-$MC_2B_9H_{11}$] **XXXIII** with L_2= $(CO)_2$, $(PPh_3)_2$, or (butadiene), and the *bis*-alkyne complex [*closo*-3,3-(η^2-$MeC_2Me)_2$-3-CO-3,1,2-$MoC_2B_9H_{11}$][56] **XXXIV** have been synthesised.

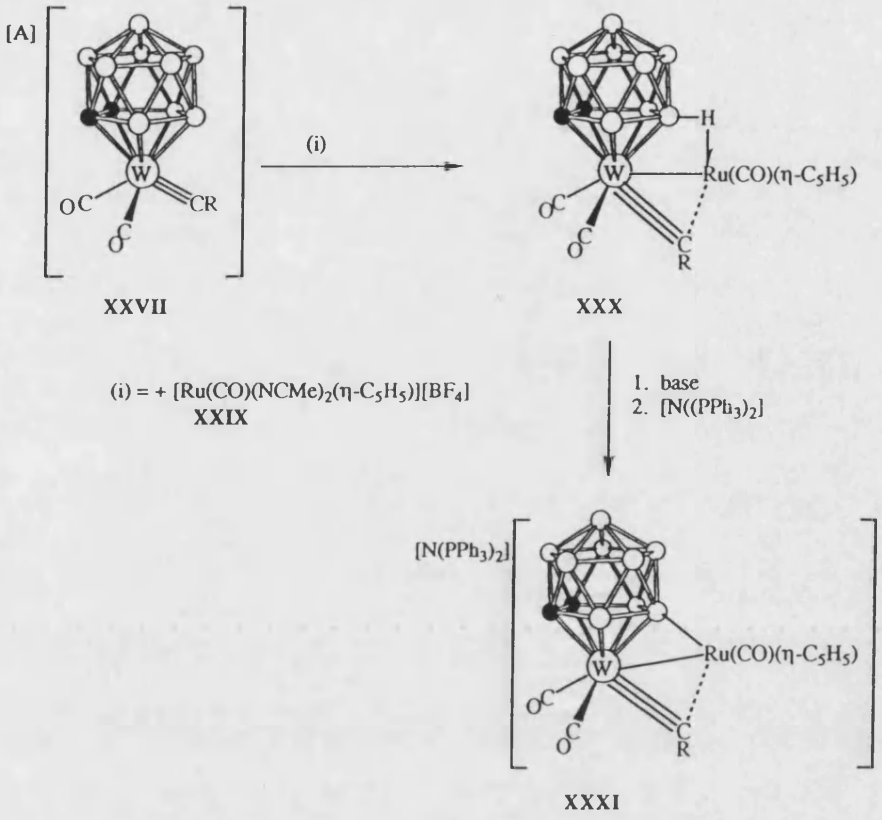

Scheme 9, ○ = BH, ● = CH

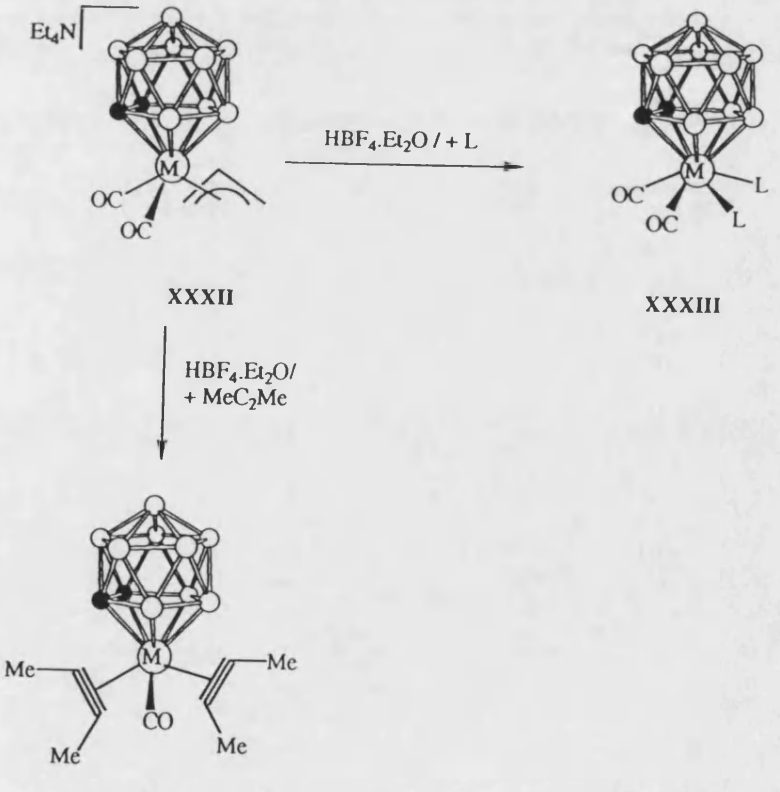

Scheme 10, ○ = BH, ● = CH

On protonation of the anionic allyl complex $[N(PPh_3)_2][closo\text{-}1,2\text{-}Me_2\text{-}3,3\text{-}(CO)_2\text{-}3\text{-}(\eta^3\text{-}C_3H_5)\text{-}3,1,2\text{-}MoC_2B_9H_9]$ **XXXV** with HI in presence of CO the I^- acts as nucleophile and the anionic *tris*-carbonyl(iodo)complex $[N(PPh_3)_2][closo\text{-}1,2\text{-}Me_2\text{-}3\text{-}I\text{-}3,3,3\text{-}(CO)_3\text{-}3,1,2\text{-}MC_2B_9H_9]$ **XXXVI** is obtained.[58]

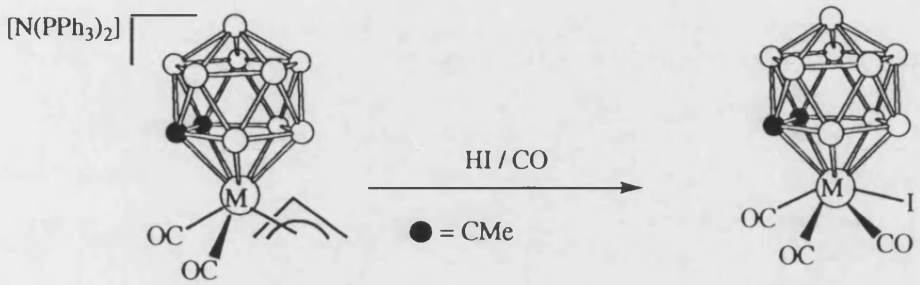

XXXV **XXXVI**

Scheme 11, ○ = BH, ● = CMe

This introduction can only give a short overview and specific examples will be discussed together with the results when appropriate.

2. Results and Discussion

2.1. Reaction of $[Mo(\eta^2\text{-}PhC_2Ph)\{P(OMe)_3\}_2(\eta\text{-}C_5H_5)][BF_4]$ XI with RMgBr (R= Et, CH_2Ph).

Earlier work in our group has shown that the reaction of the cationic complex $[Mo(\eta^2\text{-}PhC_2Ph)\{P(OMe)_3\}_2(\eta\text{-}C_5H_5)][BF_4]$ **XI** with nucleophiles can result in two different types of products. The first possible product is a complex containing an η^2-vinyl group, as was shown in the introduction. Thus, when complex **XI** is treated with $K[HBBu^s{}_3]$ the product $[Mo\{\eta^2\text{=}CPhC(H)Ph\}\{P(OMe)_3\}_2(\eta\text{-}C_5H_5)]$ **XII** is formed.[29, 30] The second type of product can be obtained from the reaction of compound **XI** with the Grignard reagent MeMgI. In this reaction, one phosphite molecule has been replaced by the nucleophilic methyl group to give the complex $[Mo(\eta^2\text{-}PhC_2Ph)(Me)\{P(OMe)_3\}(\eta\text{-}C_5H_5)]$[59] **XXXVII**. However, the reaction of compound **XI** with methyl lithium cuprate yields both types of product.[30] It is also important to note that the addition of trimethylphosphite to **XXXVII** does not give **XXXVIII**. These findings are illustrated in Scheme 12.

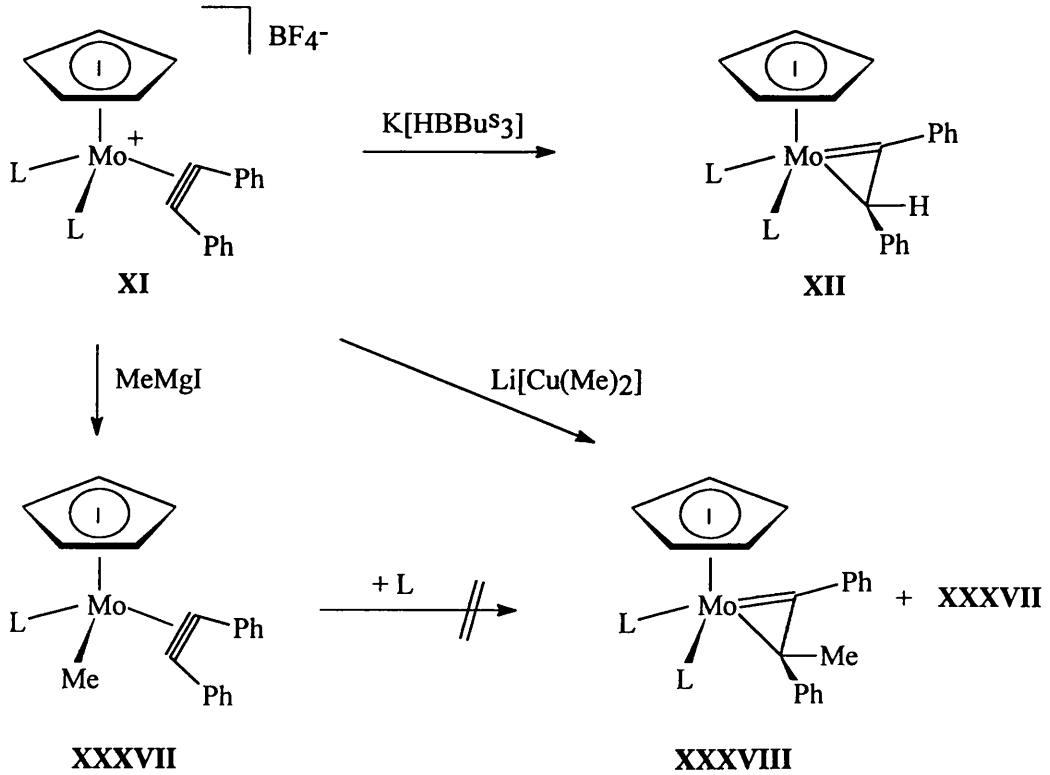

Scheme 12, L= $P(OMe)_3$

Only a few compounds of the second type had been prepared before this work and their reactivity displayed a great degree of variety. These results encouraged us to investigate further reactions of cationic complexes of the type $[Mo(\eta^2\text{-}RC_2R')\text{-}\{P(OMe)_3\}_2(\eta\text{-}C_5H_5)]^+$ towards Grignard reagents and possible rearrangement reactions of the products.

A suspension of the violet complex $[Mo(\eta^2\text{-}PhC_2Ph)\{P(OMe)_3\}_2(\eta\text{-}C_5H_5)][BF_4]$ **XI** in thf was reacted with EtMgBr at 0°C. The colour changed immediately to dark green. Column chromatography on alumina with CH_2Cl_2/hexane gave a green fraction, which after recrystallisation from hexane afforded green needles of the neutral complex $[Mo(\eta^2\text{-}PhC_2Ph)(Et)\{P(OMe)_3\}(\eta\text{-}C_5H_5)]$ **1**. In an analogous way, complex **XI** was treated with $PhCH_2MgBr$ to yield the benzyl substituted complex $[Mo(\eta^2\text{-}PhC_2Ph)(CH_2Ph)\{P(OMe)_3\}(\eta\text{-}C_5H_5)]$ **2**.

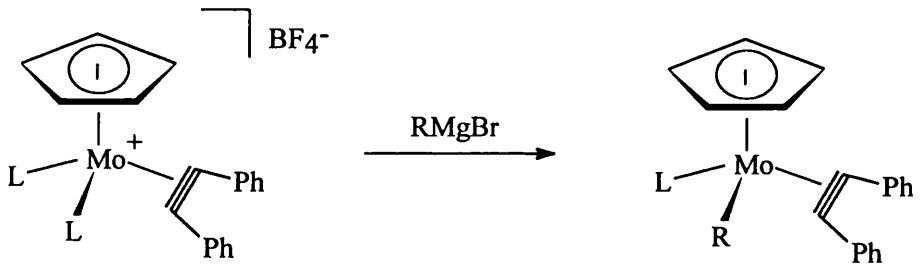

XI

R=CH_2CH_3 **1**

CH_2Ph **2**

Scheme 13, L= $P(OMe)_3$

Both compounds **1** and **2** are very soluble in the common polar and nonpolar solvents and quite air sensitive. This corresponds with observations made earlier that the complex $[Mo(\eta^2\text{-}PhC_2Ph)(Me)\{P(OMe)_3\}(\eta\text{-}C_5H_5)]$ **XXXVII** reacts with air resulting in replacement of the phosphite ligand by an oxygen atom to give the molydenum(IV) complex $[Mo(O)(\eta^2\text{-}PhC_2Ph)(Me)(\eta\text{-}C_5H_5)]$.[30]

In the proton NMR spectrum of **2**, the two diastereotopic benzyl protons show chemical shifts of 2.92 and 2.53 ppm, respectively, with a geminal coupling of 11.4 Hz and a coupling to the phosphorus nucleus of 6.6 and 6.0 Hz. However, the couplings of the methylene protons in complex **1** are obscured, because all five protons of the ethyl

group appear as one multiplet between 1.52 - 1.73 ppm. The contact carbon atoms of the acetylene ligand in complex **1** show a singlet at 202.8 ppm and a doublet at 201.3 ppm [*J*(PC) 10.6 Hz]. From the two different shifts it can be concluded that the alkyne is not fluxional. The singlet can be assigned to the carbon *cisoid* to the phosphorus, and the doublet to the transoid bonded carbon. The acetylene ligand in **2** exhibits very similar data with a singlet at 204.1 and a doublet at 201.1 ppm [*J*(PC) 10.8 Hz]. Hence, in both complexes, the alkyne acts as a four electron donor.

2.2. Reactivity of the Complexes [Mo(η^2-PhC$_2$Ph)(R){P(OMe)$_3$}(η-C$_5$H$_5$)] (R= Et 1, CH$_2$Ph 2).

As discussed in the previous chapter, one reason for investigating compounds of the type [Mo(η^2-PhC$_2$Ph)(R){P(OMe)$_3$}(η-C$_5$H$_5$)] is their ability to rearrange and their involvement in coupling reactions. The earlier mentioned complex [Mo(η^2-PhC$_2$Ph)-(Me){P(OMe)$_3$}(η-C$_5$H$_5$)][59] **XXXVII** showed an interesting rearrangement reaction, which is illustrated in Scheme 14. On heating complex **XXXVII** for 12 hours with an excess of diphenylacetylene, the new complex [Mo(H){P(OMe)$_3$}(η^4-C$_5$Ph$_4$H$_2$)(η-C$_5$H$_5$)] **XXXIX** is obtained, which contains an η^4-tetraphenylcyclopentadiene ligand. The mechanism is believed to involve an α-hydrogen elimination from the σ-bonded methyl group.

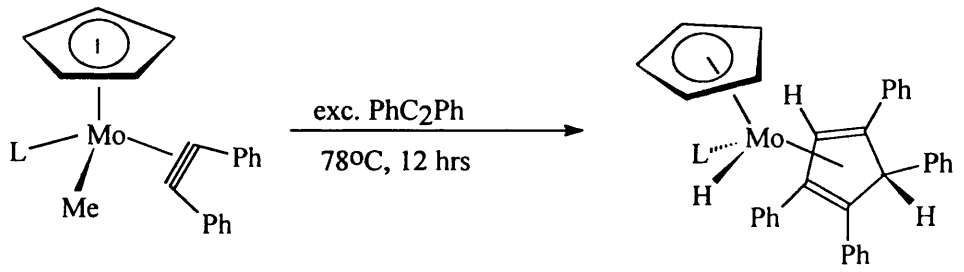

XXXVII **XXXIX**

Scheme 14, L= P(OMe)$_3$

The reaction of the cation [Mo(η^2-PhC$_2$Ph){P(OMe)$_3$}$_2$(η-C$_5$H$_5$)][BF$_4$] **XI** with the vinyl Grignard reagent CH$_2$=CHMgBr probably initially leads to the expected compound with a σ-bonded vinyl group **A** (Scheme 15). However, this intermediate then

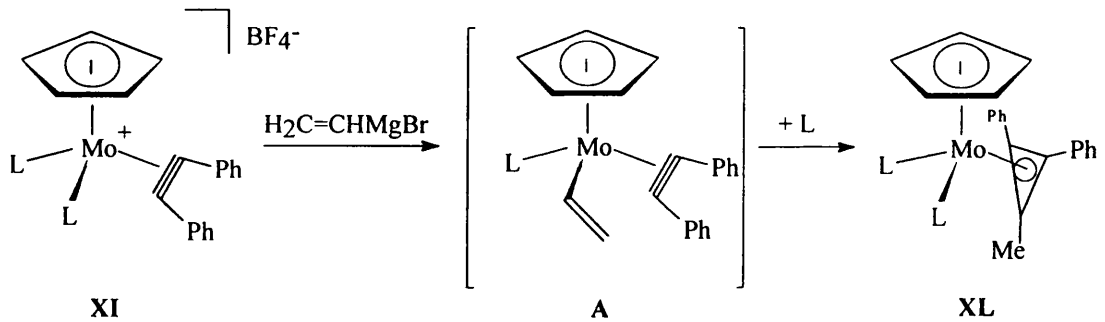

XI **A** **XL**

Scheme 15, L= P(OMe)$_3$

rearranges *via* migration of the α-hydrogen and coupling with the alkyne, so that the complex [Mo(η^3-C_3(Me)Ph_2){P(OMe)$_3$}$_2$(η-C_5H_5)] **XL** containing an η^3-cyclopropenyl ligand is isolated.[59]

The reactivity of the compounds **1** and **2** was, therefore, thoroughly investigated. CO was bubbled through a solution of complex **1** in toluene resulting in an immediate colour change from green to red. After removing the solvent and recrystallisation from toluene/hexane, the compound [Mo{η^2=C(Ph)C(Ph)C(Et)-O}(CO){P(OMe)$_3$}(η-C_5H_5)] **3** was obtained in the form of a red powder. Treatment of complex **2** with CO, however, did not lead to a product that could be isolated.

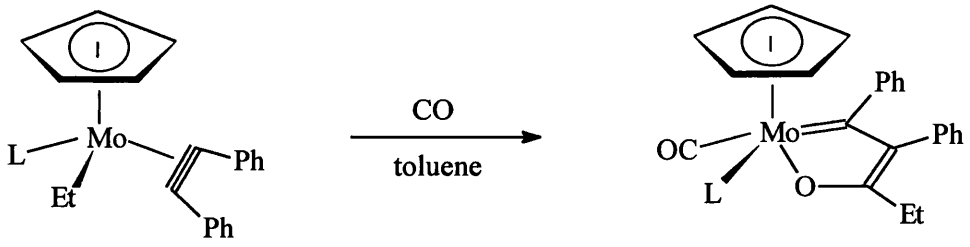

1 **3**

Scheme 16, L= P(OMe)$_3$

Compound **3** is soluble in aromatic and polar solvents, but not in aliphatic hydrocarbons. The NMR spectra exhibit one set of signals indicating that only one isomer is formed. The ^{1}H NMR spectrum shows the presence of two phenyl groups (m, 7.44-6.95 ppm), one cyclopentadienyl ligand (s, 5.07 ppm), one phosphite moiety [d, 3.54 ppm, *J*(PH) 13.0 Hz], and an ethyl group [m, 2.84-2.73 ppm, 2 H and t, 1.23 ppm, *J*(PH) 7 Hz, 3 H]. It is the carbon NMR spectrum, however, that reveals the structure of the ring system, with a chemical shift of 250.6 ppm for the molybdenum bonded carbon C_α, 196.3 ppm [*J*(PC) 8.1 Hz] for the carbon bonded to the oxygen atom and a singlet at 156.3 ppm for the β-carbon of the metallacycle. The relatively large coupling constant [*J*(PC) 25 Hz] for C_α suggests that the phosphite moiety is situated in a *trans*-position as illustrated in Scheme 16. The ^{31}P-{^{1}H} NMR spectrum of **3** shows one signal at 194.7 ppm and in the IR spectrum one prominent carbonyl absorption at 1859 cm^{-1} was found.

Consideration of the two canonical forms **A** and **B**, as shown in Figure 15, explains the quality of bonding within the five-membered metallacycle. The form **A** can be described as an oxametallacyclopentadiene, whereas in form **B** a propenonyl ligand is found.

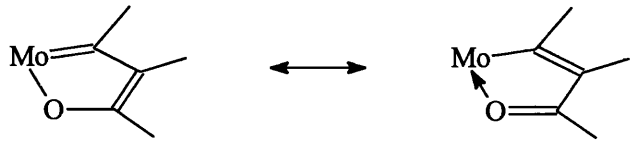

A **B**

Figure 15

The ^{13}C NMR shifts of **3** are very similar to those found earlier for the compound $[Mo\{\eta^2=C(Me)C(Me)C(CH=CH_2)\text{-}O\}(CO)_2(\eta\text{-}C_5H_5)]$[60] **XLI** or more recently, for the analogous metallacycle in the tantalum complex $[Ta\{\eta^2=C(Ph)C(Ph)C(Me)\text{-}O\}(Me)\{\eta\text{-}C_5(Me)_5\}]$[61] **XLII**. However, these two compounds have been structurally characterised and they show distinct differences, as shown in Figure 16. While the oxametallacyclic fragments in both compounds exhibit a pronounced single-double-single bond alternation, the molybdenum system is best represented as a propenone complex and the tantalum complex as a cyclopentadiene. As a result the tantalacycle is folded (124° along the C_1-O axis), whereas the molybdenacycle is nearly planar. Detailed orbital considerations revealed that electron rich metals donate into the π_3^*-orbital of the butadiene-like C_3O unit, while the C_1-C_2 and the C_3-O bonds display single bond character.[61] However, the carbon NMR data of these compounds do not seem to reflect these differences (C_1: 261.8 ppm, molybdenum

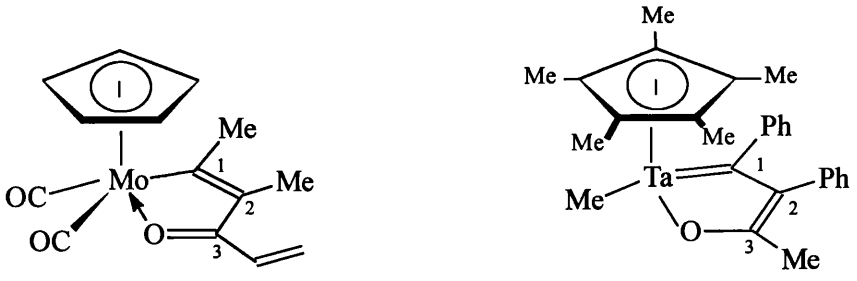

XLI **XLII**

Figure 16

complex; 224.5 ppm, tantalum complex) and, therefore, the secondary structural features of compound **3** remain unknown.

It can be assumed that the first step of the reaction of **1** with CO involves an addition of CO to the complex **1** *via* a switch of the bonding mode of the alkyne from a four electron donor to a two electron donor in **A** (Scheme 17). The next step would be the insertion of CO into the metal carbon bond to give **B**. After addition of a second molecule of CO leading to the formation of **C**, coupling between the propionyl moiety and the two electron donor acetylene ligand follows to yield **3**.

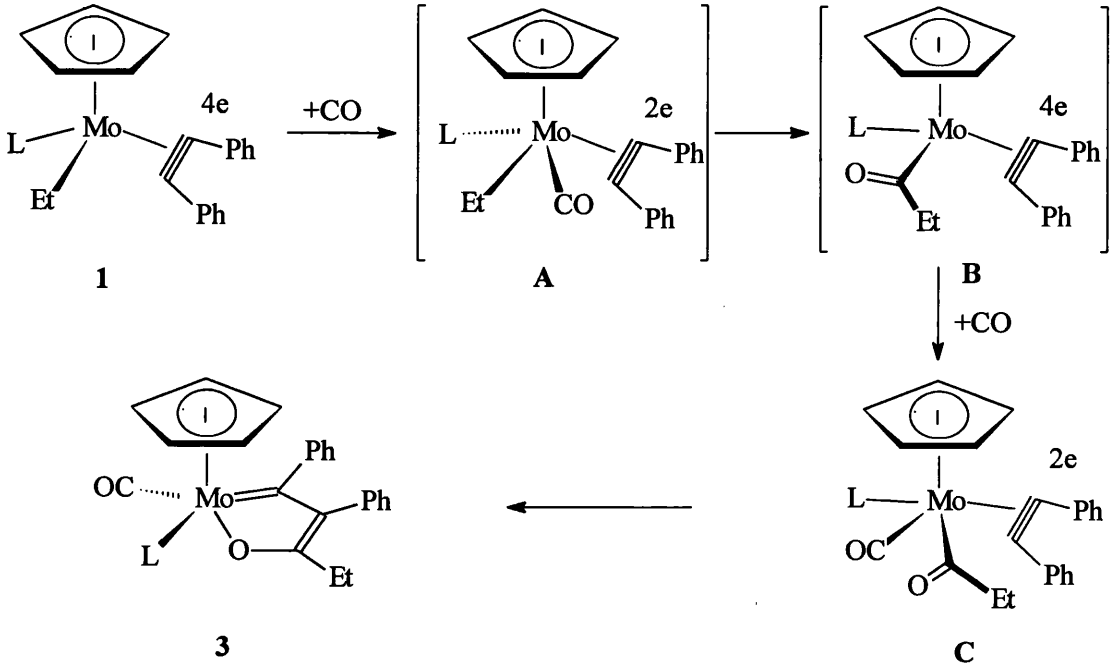

Scheme 17, L= $P(OMe)_3$

Solutions of complexes **1** and **2** in toluene were heated in the presence of diphenyl-acetylene at different temperatures. Up to 70°C compound **1** appears to be stable, above that temperature only decomposition was observed. However, on heating to 100°C with an excess of diphenylacetylene, complex **2** reacts cleanly to give the yellow 17-electron complex $[Mo(\eta^6\text{-}C_6Ph_6)(\eta\text{-}C_5H_5)]$ **4** (Scheme 18).

The paramagnetism of **4** causes the proton and carbon NMR spectra to show broad signals, which were not sufficient to identify the product. Hence, the molecular structure has been determined by X-ray crystallography, which unveiled an unit cell

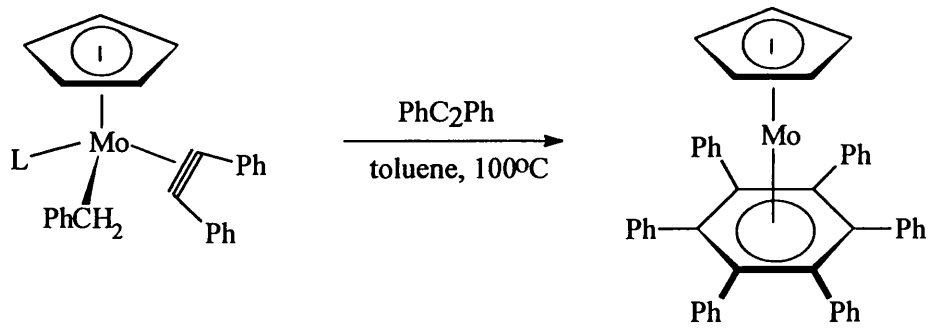

2 4

Scheme 18, L= $P(OMe)_3$

with two independent molecules having essentially the same geometry. The diffraction study also showed that **4** crystallises with toluene in a one to one ratio. Two ORTEP drawings of **4** are shown in Figure 17. In a) one molecule of **4** is plotted with the phenyl ring atoms and in b) **4** these are omitted for clarity .The bond lengths between molybdenum and the ring carbon atoms for one of the molecules in the unit cell are listed in Table 2.

Table 2: Selected bond lengths (Å) of **4**.

C(1)-Mo	2.326(6)	C(2)-Mo	2.321(6)	C(3)-Mo	2.316(7)	C(4)-Mo	2.318(7)
C(5)-Mo	2.323(7)	C(6)-Mo	2.252(8)	C(7)-Mo	2.247(7)	C(8)-Mo	2.246(7)
C(9)-Mo	2.230(8)	C(10)-Mo	2.249(8)	C(11)-Mo	2.246(8)		

As expected in this sandwich complex the two planes created by the cyclopentadienyl ligand and hexaphenylbenzene ligand are parallel. The carbon atoms of the benzene ligand are closer to the central metal (average distance 2.249 Å) than the carbon atoms of the cyclopentadienyl ligand (average distance 2.320 Å) The phenyl moieties are fixed in a staggered position, which they presumably also adopt in solution.

In this reaction molybdenum is converted from the formal oxidation state +II in **2** to +I in **4**. This one electron reduction step clearly suggests that a radical mechanism is involved in the transformation. The initial step could be the homolytic cleavage of the metal benzyl bond leading to the formation of the relatively stable benzyl radical and an unsaturated 17 electron molybdenum species **A** (Scheme 19). This species could

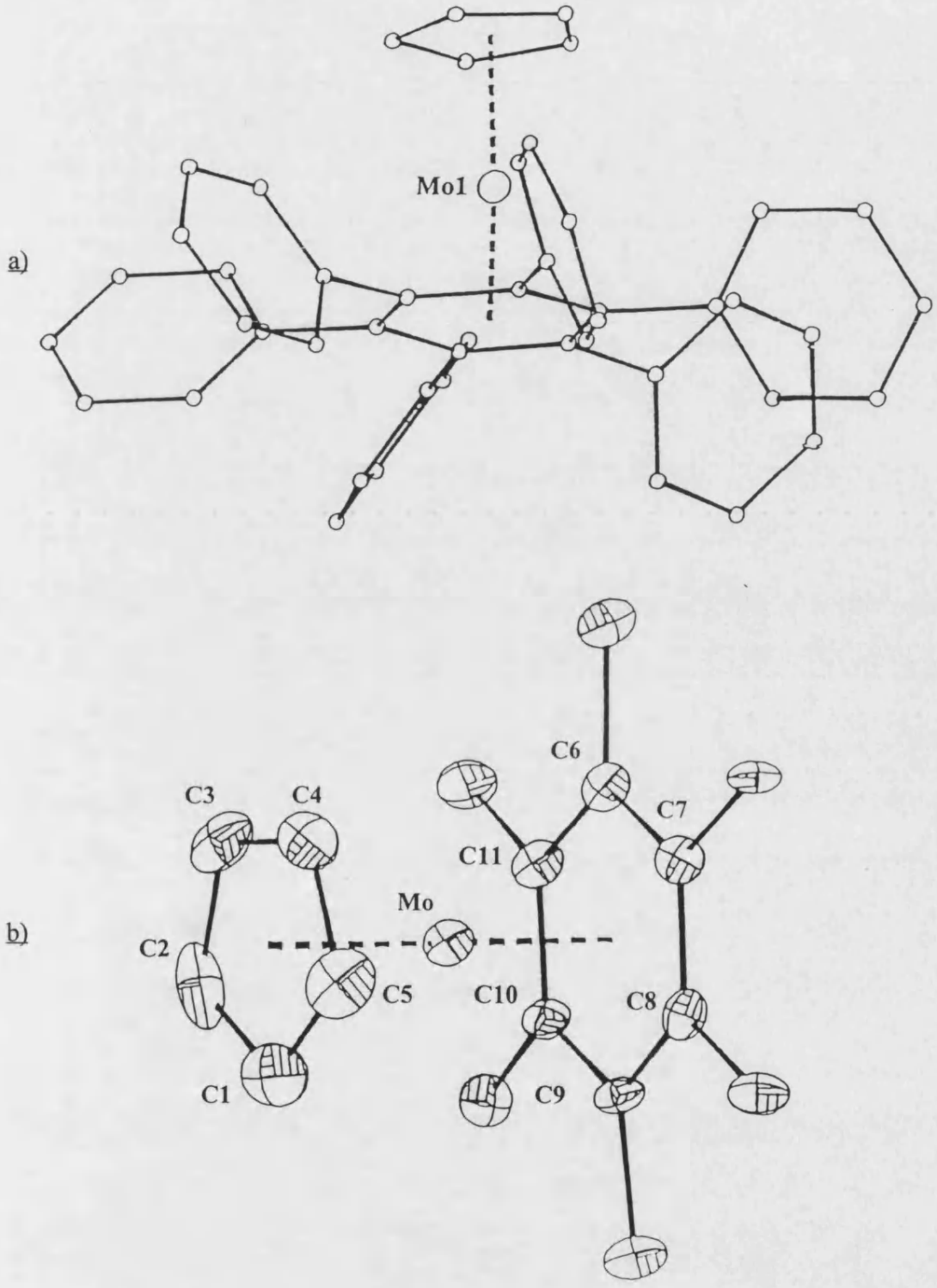

Figure 17, ORTEP drawing of **4**.

incorporate a diphenylacetylene unit to give **B**. The two coordinated alkynes then couple to form the metallacyclopentadiene in **C**. After coordination of a third diphenylacetylene molecule to yield **D** and coupling to the molybdenacycloheptatriene complex **E**, the phosphite moiety is expelled and complex **4** formed. It is interesting to note that the 18 electron *bis*-alkyne(phosphite)carbaborane complexes **26** and **27** (section 2.12), which are reminiscent of intermediate **B**, are stable under the conditions employed in the generation of **4**.

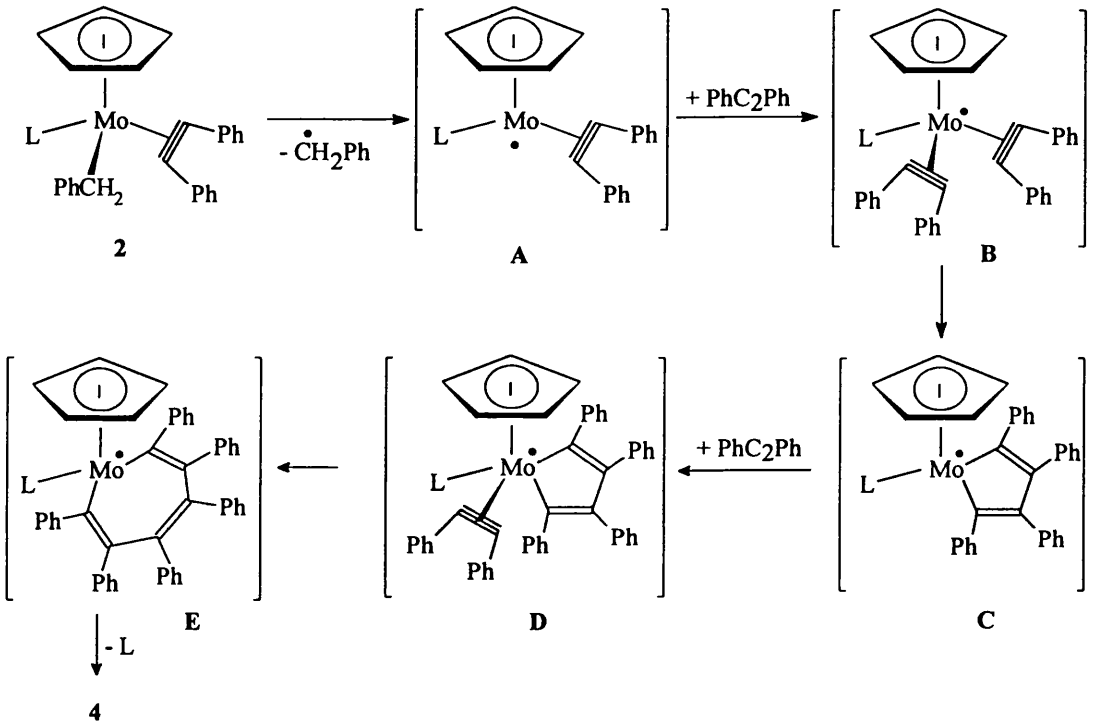

Scheme 19, L= $P(OMe)_3$

The transition metal catalysed trimerisation of acetylenes has long been known. Nickel in particular has been shown to be a very active catalyst,[62] while palladium complexes have been used to study the mechanism of this type of coupling reaction.[63] The mechanism suggested all involve the formation of metallacyclopentadiene and metallacycloheptatriene as intermediates. Although the trimerisation of diphenylacetylene to hexaphenyl benzene has been observed, no hexaphenyl arene metal complex has been isolated. For example, the reaction of $PdCl_2$ with an excess diphenylacetylene yielded hexaphenylbenzene, but the palladium complex which was isolated was the cyclobutadienyl compound $[PdCl_2(\eta^4\text{-}C_4Ph_4)]$[64] **XLIII** (Scheme 20).

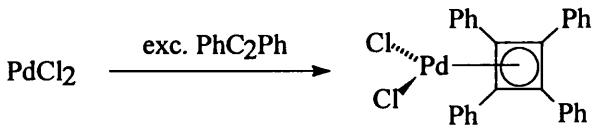

XLIII

Scheme 20

It seemed feasible that the 17 electron complex **4** could be reduced and then reacted with an electrophile to yield an 18 electron complex. On treatment of a solution of **4** in thf with one equivalent of sodium naphthalide at -78°C the colour changed immediately from yellow to red indicating a reaction. However, addition of methyl iodide did not lead to the desired product [Mo(Me)(η^6-C_6Ph_6)(η-C_5H_5)], but regenerated the starting material **4**, which was quantitatively recovered.

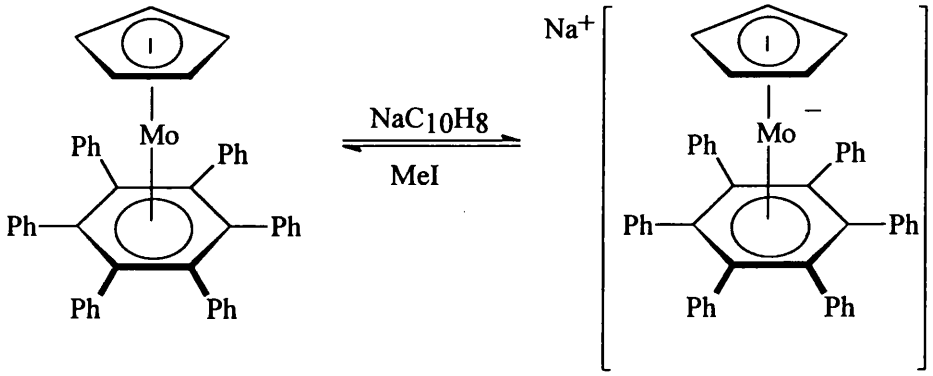

4 **A**

Scheme 21.

Presumably, the reduction with sodium occurs generating the 18 electron anion **A** (Scheme 21), as indicated by the colour change, but the hexaphenylbenzene ligand is sterically too demanding to allow the methyl iodide to react with the molybdenum centre.

2.3. Reaction of $[Mo(\eta^2\text{-}PhC_2Ph)\{P(OMe)_3\}_2(\eta\text{-}C_5H_5)][BF_4]$ XI with Allyl Magnesium Bromide

It was expected that the reaction of $[Mo(\eta^2\text{-}PhC_2Ph)\{P(OMe)_3\}_2(\eta\text{-}C_5H_5)][BF_4]$ **XI** with allyl magnesium bromide would cause the replacement of a phosphite ligand and lead to a complex containing a metal bonded η^1-allyl ligand **A** (Scheme 22). Indeed, after addition of the Grignard reagent at low temperature the colour of the reaction mixture turned green, which is indicative for this type of compound, e.g. **1** and **2**. However, at room temperature the colour changed to orange before a dark colour indicated decomposition of the product. Hence, the apparent rearrangement of the initial product **A** seems to generate an unsaturated species.

The reaction was repeated and after the colour had turned to green one equivalent of trimethylphosphite was added. On warming to room temperature a yellow reaction mixture was obtained. Column chromatography with Et_2O/hexane (1:1) using Al_2O_3 as solid support yielded $[Mo\{\eta^2\text{-}C(Ph)=C(Ph)CH_2CH=CH_2\}\{P(OMe)_3\}_2(\eta\text{-}C_5H_5)]$ **5** in moderate yield.

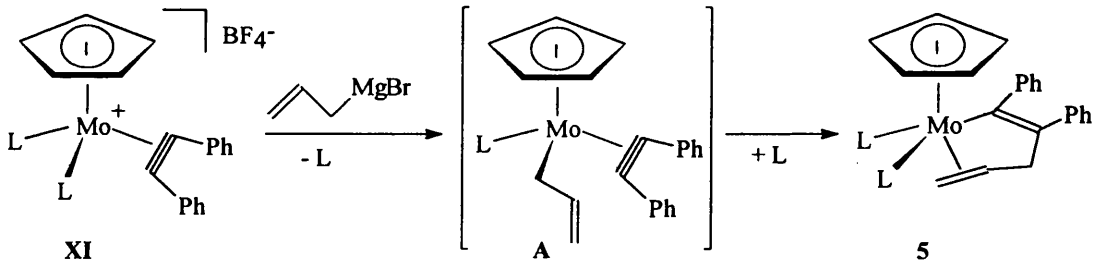

Scheme 22, L= $P(OMe)_3$

The ^1H NMR spectrum of **5** shows a multiplet for the ten phenyl protons between 7.31 and 6.96 ppm and a doublet for the five cyclopentadienyl protons at 5.03 ppm [*J*(PH) 3.1 Hz]. Two doublets, at 3.29 ppm [*J*(PH) 10.3 Hz] and 3.24 ppm [*J*(PH) 9.5 Hz], were assigned to the phosphite moieties. The methylene resonances appeared as a multiplet between 2.49 and 2.19 ppm. The signals for the $CH=CH_2$ group were obscured by other signals and therefore could not be assigned. The $^{31}P\text{-}\{^1H\}$ NMR spectrum displays an AB system for the two non-equivalent phosphorus nuclei with shifts of 194.3 and 183.3 ppm, respectively, and a coupling constant of 70.5 Hz. Due to the thermal instability of **5** in solution no ^{13}C NMR spectrum could be obtained.

Because only incomplete NMR data were obtained an X-ray diffraction study was performed on single crystals of **5** which were obtained by slowly cooling a saturated solution of **5** in Et_2O/hexane. The established structure (Figure 18) displays a molecule with a four-legged piano-stool geometry, the molybdenum being bonded to two trimethylphosphite ligands, an η^5-C_5H_5 ligand and, *via* one σ- and one π-bond, to a pentadienyl ligand. This pentadienyl ligand exhibits pronounced single and double bonds. The Mo-C(11) distance of 2.319(4) Å is in the dimension of a single bond while the C(10)-C(11) distance of 1.338(5) Å is characteristic for carbon-carbon double bonds.[65] The coordinated olefin C(7)-C(8) lies parallel to the Mo-P(2) vector, a feature which has been observed for π-ligands in *bis*-phosphite complexes.[31]

Table 3: Selected bond lengths (Å) and angles (°) of **5**

Mo-P(1)	2.437(2)	Mo-P(2)	2.422(1)	Mo-C(7)	2.286(5)	Mo-C(8)	2.235(4)
Mo-C(11)	2.319(4)	C(7)-C(8)	1.410(7)	C(8)-C(9)	1.502(7)	C(9)-C(10)	1.515(7)
C(10)-C(11)	1.338(5)	C(10)-C(21)	1.503(6)	C(11)-C(31)	1.500(6)		

P(1)-Mo-P(2)	88.3(1)	P(1)-Mo-C(7)	74.6(1)	P(2)-Mo-C(7)	85.9(1)
P(1)-Mo-C(8)	85.9(1)	P(2)-Mo-C(8)	121.0(1)	C(7)-Mo-C(8)	36.3(2)
Mo-C(7)-C(8)	69.9(3)	Mo-C(11)-C(10)	115.0(3)	Mo-C(11)-C(31)	126.8(3)
P(1)-Mo-C(11)	149.4(1)	P(2)-Mo-C(11)	83.5(1)	C(7)-Mo-C(11)	75.4(2)
C(8)-Mo-C(11)	73.4(2)				

It was mentioned in section 2.1 that addition of trimethylphoshite to the complex [Mo(η^2-PhC_2Ph)(Me){$P(OMe)_3$}(η-C_5H_5)] **XXXVII** does not initiate a migration of the σ-bonded methyl group onto the coordinated alkyne to yield the stable η^2-vinyl complex [Mo{η^2=CPhC(Me)Ph}{$P(OMe)_3$}$_2$(η-C_5H_5)] **XXXVIII**, which was synthesised by a different method. It is, therefore, unlikely that a simple migration of the allyl group is involved in the formation of **5**. A radical mechanism, as described in section 2.2, does not seem feasible since the rearrangement of the σ-bonded allyl group occurs at ambient temperatures.

The initial step of the reaction presumably is the addition of a phosphite unit to the intermediate **A** to give a species **B** (Scheme 23). On the basis of the isolobal concept,[66] which relates transition metal complexes to organic molecules, it can be

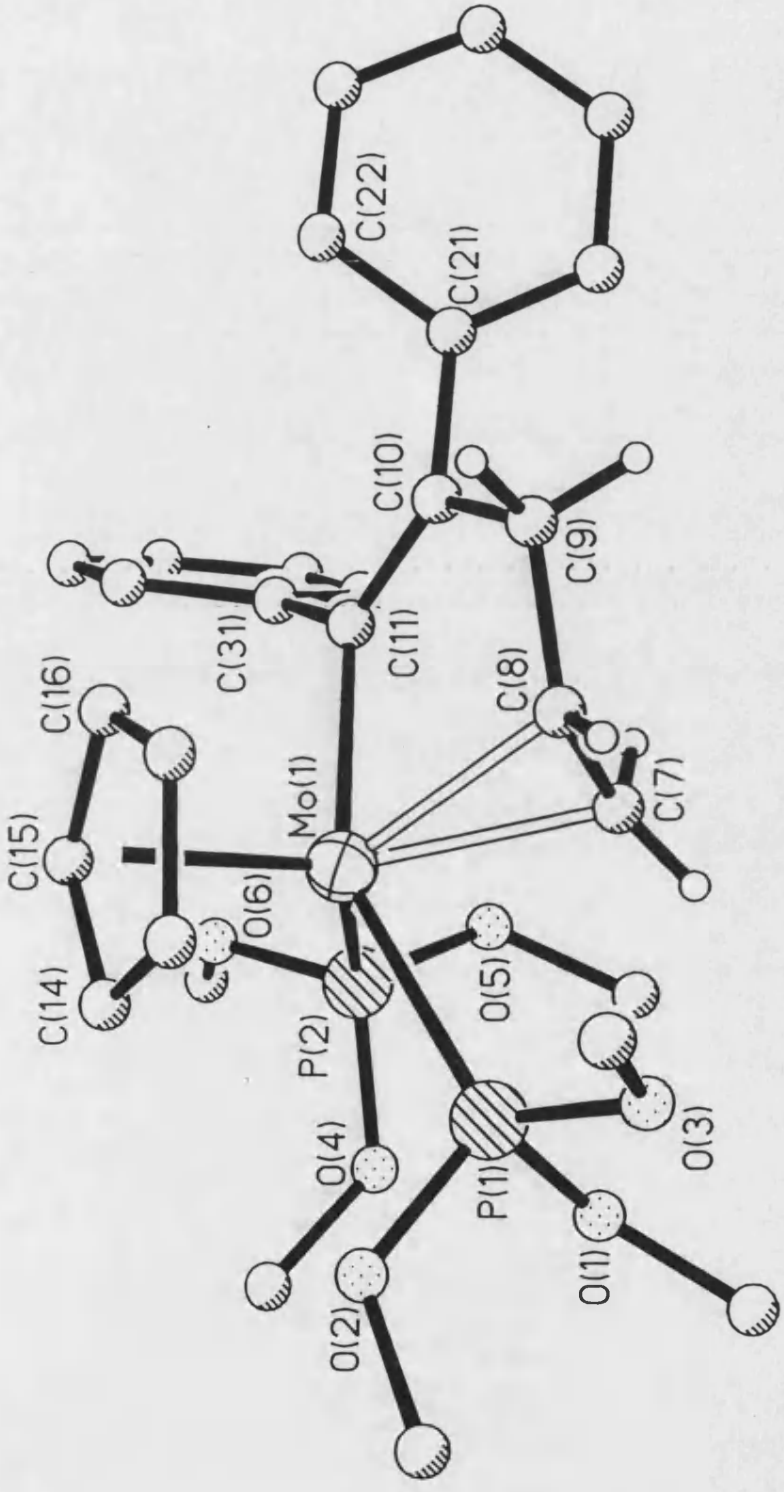

Figure 18: ORTEP drawing of **5**

shown that a d^6ML_5 fragment like $[Mo\{P(OMe)_3\}_2(\eta\text{-}C_5H_5)]$ is isolobal to CH and the species **B** can, therefore, be viewed as a 1,5-diene system.

It is well know that organic 1,5-diene systems can undergo [3,3]-sigmatropic re-arrangement reactions facilated by an aromatic 3 electron pair transition state. As a consequence of orbital symmetry relationships a chair like transition state is favoured for this type of reaction.[67] However, 1,2-divinylcyclopropanes, which can react only in the boat form, give this rearrangement so rapidly that they generally cannot be isolated at room temperature.[68] Thus, the species **B** could adopt a boat configuration and undergo a [3,3]-sigmatropic rearrangement to generate **C** containing an η^2-vinyl ligand. This metallacyclopropene could irreversibly open to an η^1-vinyl system for the metal in the final product **5** to accommodate the olefin function.

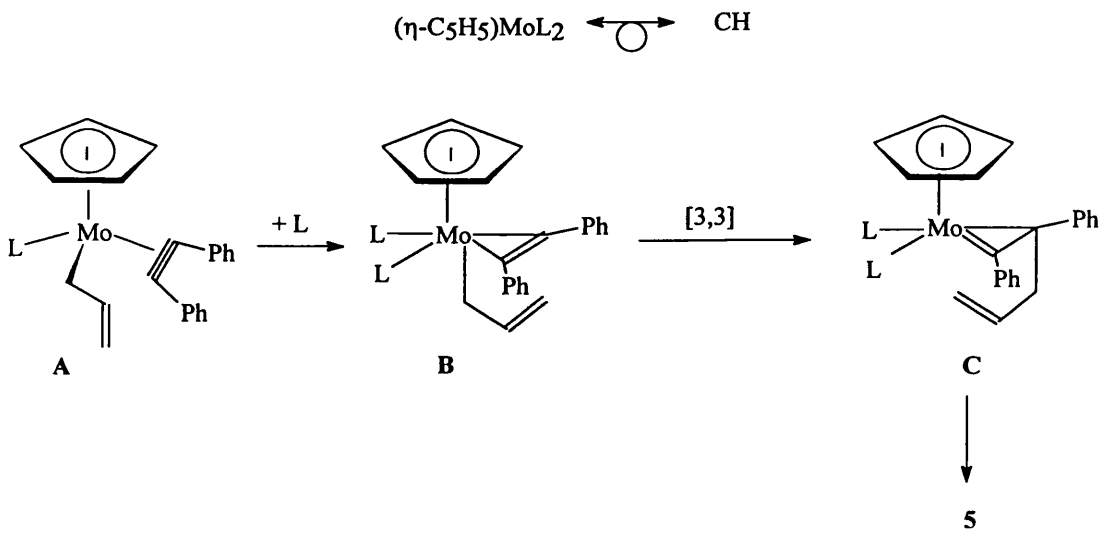

Scheme 23, L= $P(OMe)_3$

The η^2(4e)-niobium complex $[Tp^*NbCl_2(\eta^2\text{-}PhC_2Ph)]$ {Tp*= hydridotris(3,5-dimethylpyrazolyl)borate} **XLIV** reacts with one equivalent of allyl magnesium chloride to initially form $[Tp^*NbCl(\eta^1\text{-}CH_2CH{=}CH_2)(\eta^2\text{-}PhC_2Ph)]$ **A** containing a σ-bonded allyl group.[69] Here, the alkyne and the allyl moieties couple to form the η^4-butadienyl ligand present in $[Tp^*NbCl(\eta^4\text{-}CPh{=}CPhCH{=}CHMe)]$ **XLV** (Scheme 24). The mechanism is believed to involve the migration of the allyl group onto the alkyne. In this context it is interesting to note that, unlike the cyclopentadienyl molybdenum system discussed in this section, on heating to 100°C the complex $[Tp^*NbCl(Et)(\eta^2\text{-}$

PrC_2Ph)] **XLVI** undergoes a reversible rearrangement reaction, exchanging the propyl and the ethyl group to yield [Tp*NbCl(Pr)(η^2-EtC_2Ph)][70] **XLVII**.

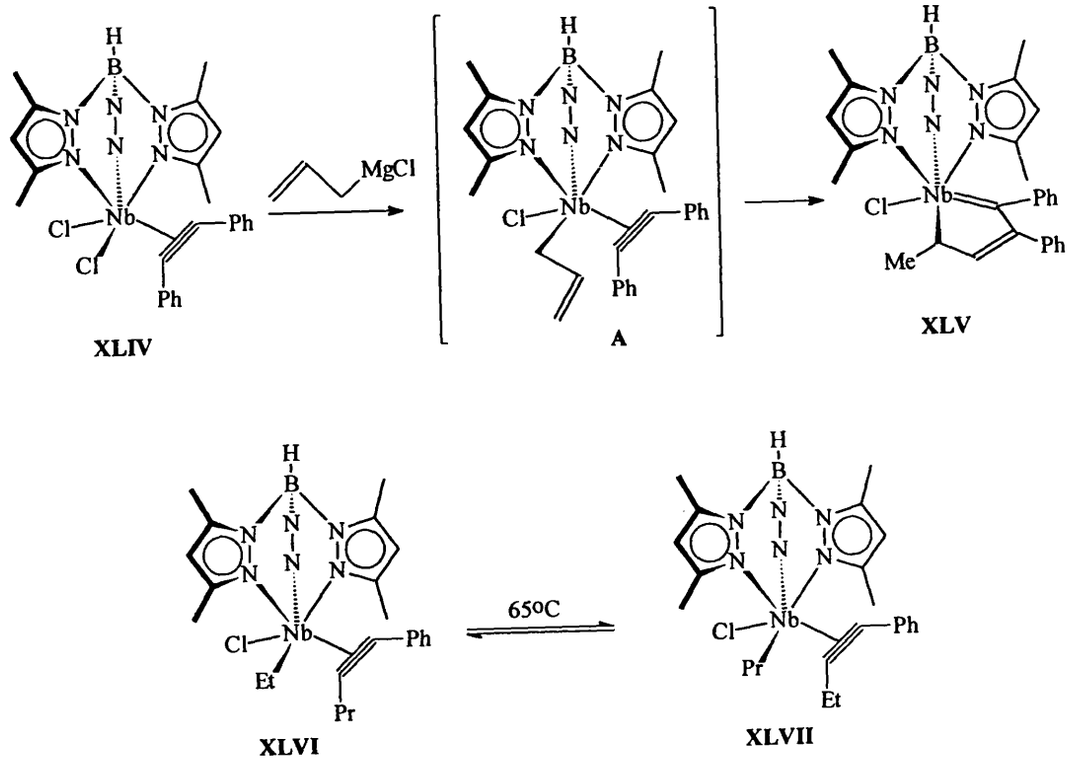

Scheme 24

2.4. Reaction of $[Mo(\eta^2\text{-}RC_2R')\{P(OMe)_3\}_2(\eta\text{-}C_5H_5)][BF_4]$ with $CH_2(MgI)_2$.

It was expected that in analogy to the aforementioned reactions with Grignard reagents, the reaction of $[Mo(\eta^2\text{-}PhC_2Ph)\{P(OMe)_3\}_2(\eta\text{-}C_5H_5)][BF_4]$ **XI** with 1,1-di-Grignard reagents would result in replacement of one phosphite ligand to give either carbene complexes or dimeric complexes.

We chose $CH_2(MgI)_2$[71] for our reaction, as it is the only readily available 1,1-di-Grignard reagent.[72] Surprisingly, addition of $CH_2(MgI)_2$ to a suspension of complex **XI** does not result in an immediate colour change, but a white precipitate is formed. After stirring the reaction mixture overnight, a green solution was observed. Workup, involving column chromatography and recrystallisation from dichloromethane and hexane, afforded the blue zwitterionic complex $[Mo(\eta^2\text{-}PhC_2Ph)\{\eta^2\text{-}P(OMe)_2OBF_2O\text{-}P(OMe)_2\}(\eta\text{-}C_5H_5)]$ **6** in a good yield. The molecular structure has been confirmed by X-ray diffraction and will be discussed later in this section. In order to generalise this synthesis of the anionic phosphite ligand the two complexes $[Mo(\eta^2\text{-}RC_2R')\text{-}\{P(OMe)_3\}_2(\eta\text{-}C_5H_5)][BF_4]$ (R, R'= Ph, Me) were reacted with $CH_2(MgI)_2$. The analogous compounds $[Mo(\eta^2\text{-}PhC_2Me)\{\eta^2\text{-}P(OMe)_2OBF_2OP(OMe)_2\}(\eta\text{-}C_5H_5)]$ **7** and $[Mo(\eta^2\text{-}MeC_2Me)\{\eta^2\text{-}P(OMe)_2OBF_2OP(OMe)_2\}(\eta\text{-}C_5H_5)]$ **8** were obtained.

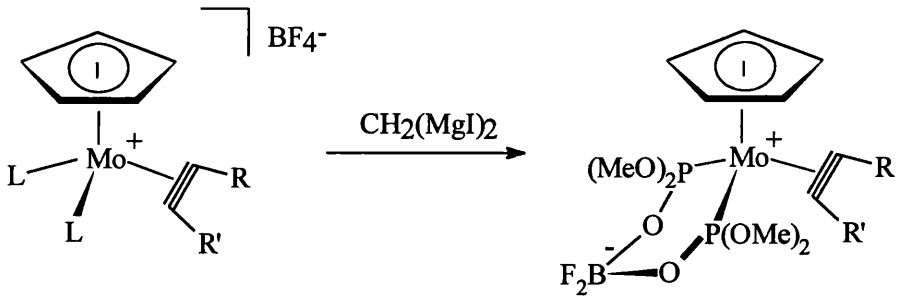

R= R'= Ph **6**
R= Ph, R'= Me **7**
R= R'= Me **8**

Scheme 25, L= $P(OMe)_3$

Compounds **6** - **8** are soluble in polar solvents such as thf and CH_2Cl_2 and insoluble in hexane. The solubility in toluene decreases depending on the substituents, from **6** to **8**. While **6** is quite soluble, **8** is almost insoluble in toluene.

The ^{1}H NMR spectrum of **6** shows (apart from the signals for the phenyl and the cyclopentadienyl ligand) two virtual triplets at 3.54 and 2.93 ppm [*N*(PH) 11.0, 12.6 Hz, respectively], which integrate to six protons each. These two signals were assigned to the methoxy groups on the *bis*-phosphite ligand with the two *exo*-groups being equivalent as well as the two *endo*-groups. Virtual couplings can be observed in AXX' systems, when the coupling constant *J*(XX') is greater than *J*(AX'). The virtual coupling constant *N*(AX) is defined as the sum of *J*(AX) and *J*(AX').[73] In complex **6** the two phosphorus atoms are magnetically equivalent (one singlet at 158.0 ppm was observed in the ^{31}P-{^{1}H} NMR spectrum), nevertheless their coupling constant *J*(PP') is greater than the proton phosphorus coupling *J*(PH). In this case *N*(PH) equals the separation of the outer lines of the virtual triplet.

The ^{19}F NMR spectrum consists of two multiplets between -135.93 to -135.54 ppm and -140.96 to -140.71 ppm and the ^{11}B NMR spectrum shows one broad singlet at 1.95 ppm. In the ^{13}C-{^{1}H} NMR spectrum it can be seen that the diphenylacetylene acts as a four electron donor, as the quarternary carbon atoms resonate at 214.4 ppm. The NMR data for the compounds **7** and **8** are very similar to those of **6** and are listed in the experimental section.

Using a different route this anionic BF_2-bridged phosphite ligand has previously been prepared with nickel as the coordination sphere. Werner and coworkers reacted the cationic complex [Ni{P(OH)(OMe)$_2$}{P(O)(OMe)$_2$}(η-C_5H_5)] **XLVIII** with $HBF_4.Et_2O$ and obtained the compound [Ni{η^2-P(OMe)$_2$OBF$_2$OP(OMe)$_2$}(η-C_5H_5)] **XLIX** containing the boron-bridged dipod ligand (Scheme 26).[74] The analogous palladium compound [Pd{η^2-P(OMe)$_2$OBF$_2$OP(OMe)$_2$}(η-C_5H_5)] **L** was prepared by

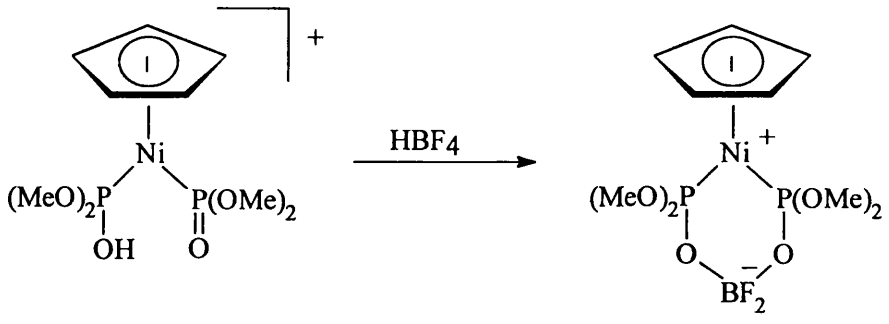

XLVIII **XLIX**

Scheme 26

the same route.[75] These compounds were fully characterised spectroscopically, but no molecular structure has been confirmed.

Since there were no crystal data known on metal complexes with this type of *bis*-phosphite ligand, an X-ray diffraction study of **6** was undertaken. Suitable crystals for the analysis were obtained by slowly cooling a solution of **6** in thf. Selected bond lengths and angles are listed in Table 4. An ORTEP drawing of **6** is shown in Figure 19.

The structure shows that the molybdenum, two P-O units, and a boron atom are connected in a six membered ring, which in the solid state takes a chair-like conformation. The zwitterionic character of **6** can be deduced from the tetrahedral coordination of four substituents around a negatively charged boron atom. However, since **6** is a neutral and diamagnetic complex, simple electron count reveals the necessity of a positive charge at the molybdenum atom. The P-O distances in the ring system [P(1)-O(4) 1.539(2) and P(2)-O(1) 1.553(2) Å] are considerably shorter than the *exo*-cyclic P-O distances with an average length of 1.585 Å. This suggests that there is partial conjugation throughout the ring system.

Table 4: Selected bond lengths (Å) and angles (°) for **6**

Mo-P(1)	2.397(1)	Mo-P(2)	2.375(1)	Mo-C(1)	2.325(3)	Mo-C(2)	2.341(3)
Mo-C(3)	2.326(3)	Mo-C(4)	2.304(3)	Mo-C(5)	2.297(3)	Mo-C(6)	2.013(2)
Mo-C(7)	2.050(3)	P(1)-O(4)	1.539(2)	P(1)-O(5)	1.581(3)	P(1)-O(6)	1.590(2)
P(2)-O(1)	1.553(2)	P(2)-O(2)	1.587(2)	P(2)-O(3)	1.592(2)	O(1)-B	1.471(4)
O(4)-B	1.471(3)	O(2)-C(21)	1.412(3)	O(3)-C(20)	1.421(3)	O(5)-C(23	1.443(5)
O(6)-C(22)	1.419(4)	C(6)-C(7)	1.310(3)	C(7)-C(14)	1.458(4)		

P(1)-Mo-P(2)	83.5(1)	P(1)-Mo-C(6)	101.6(1)	P(1)-Mo-C(7)	88.9(1)
P(2)-Mo-C(6)	118.4(1)	P(2)-Mo-C(7)	82.0(1)	Mo-P(1)-O(4)	119.2(1)
Mo-P(2)-O(1)	121.5(1)	Mo-P(1)-O(4)	119.2(1)	P(2)-O(1)-B	129.5(2)
Mo-C(7)-C(14)	155.3(2)	C(14)-C(7)-C(6)	135.0(2)	O(1)-B-F(2)	109.9(2)
Mo-C(6)-C(8)	148.0(2)	O(1)-B-F(1)	107.7(3)	O(2)-P(2)-O(3)	104.1(1)
F(1)-B-F(2)	111.0(2)	C(6)-Mo-C(7)	37.6(1)	P(1)-O(4)-B	132.2(2)
Mo-C(7)-C(6)	69.7(2)	C(7)-C(6)-C(8)	139.3(2)	O(1)-B-O(4)	111.2(2)
Mo-C(6)-C(7)	72.7(1)	O(4)-B-F(1)	106.8(2)	O(4)-B-F(2)	110.2(3)

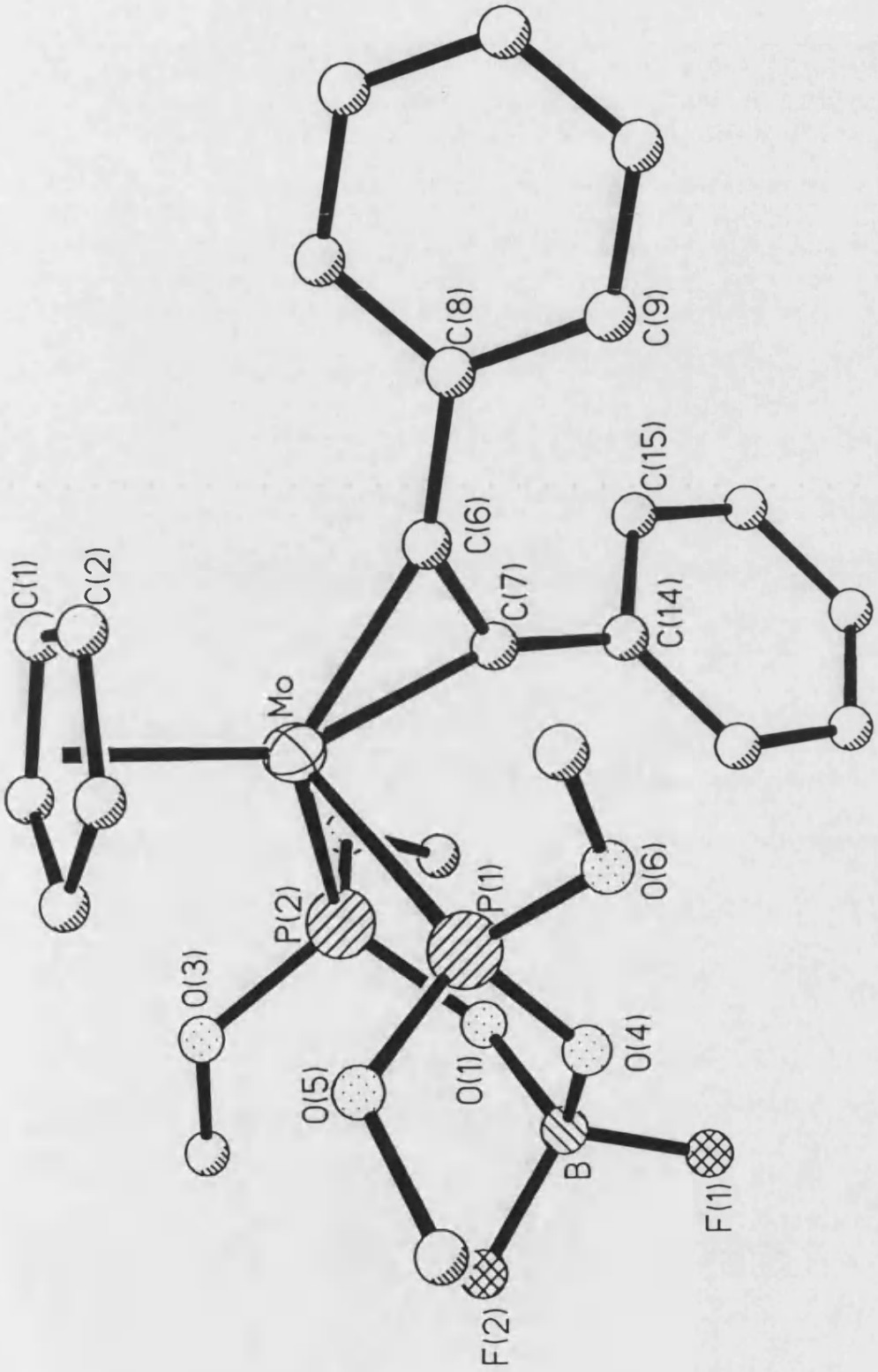

Figure 19: ORTEP drawing of **6**

2.5. Preparation of the η^2-Vinyl Complexes $K[Mo(\eta^2=C(R)C(H)Ph)\{\eta^2-P(OMe)_2OBF_2OP(OMe)_2\}(\eta-C_5H_5)]$ (R= Ph 9, Me 10)

As discussed in the introduction treatment of alkyne complexes with nucleophiles can lead to the formation of η^2-vinyl complexes. Studies carried out on the neutral η^2-vinyl complexes $[Mo\{\eta^2=C(Me)CR'R\}\{P(OMe)_3\}_2(\eta-C_5H_5)]$ (R, R'= Ph, Me) also showed that the metallacyclopropene initially formed can rearrange to give the corresponding η^3-allyl system.[31]

Solutions of the complexes $[Mo(\eta^2-PhC_2R)\{\eta^2-P(OMe)_2OBF_2OP(OMe)_2\}(\eta-C_5H_5)]$ (R= Ph **6**, Me **7**) in thf were reacted with $K[HBBu^s_3]$ and after recrystallisation from thf/toluene/hexane green-yellow powders were isolated. The products were characterised, using multinuclear NMR techniques, as the η^2-vinyl complexes $K[Mo(\eta^2=C(R)C(H)Ph)\{\eta^2-P(OMe)_2OBF_2OP(OMe)_2\}(\eta-C_5H_5)]$ (R= Ph **9**, Me **10**). However, as a result of the extreme air sensitivity of **9** and **10**, exact microanalyses could not be obtained.

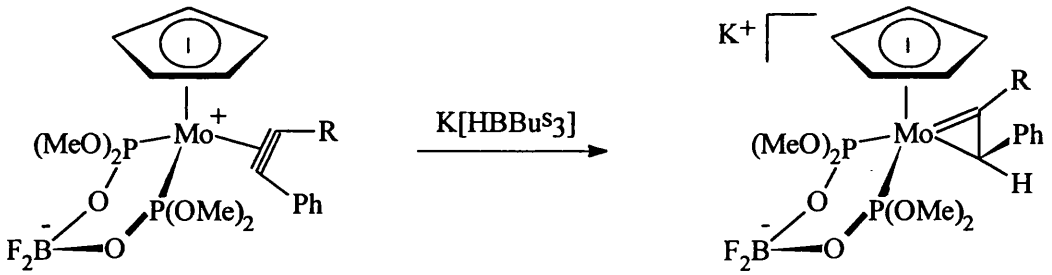

R= Ph **6**
R= Me **7**

9
10

Scheme 27

The complexes **9** and **10** are soluble in thf and CH_2Cl_2, but in the later solvent they slowly decompose. Both are moderately soluble in toluene, but insoluble in alkanes. The proton NMR spectrum of **9** shows four doublets between 3.44 and 3.30 ppm for the phosphorus bound methoxy groups and the proton on the η^2-vinyl ligand resonates as a multiplet at 3.42-3.35 ppm. In the spectrum of **10** these signals are indistinguishable and appear as one multiplet between 3.55 and 3.27 ppm. The carbon NMR spectrum reveals the carbenoid character of the α-carbon of the η^2-vinyl group with

resonances at 240.8 ppm (**9**) and 242.3 ppm (**10**). The inequivalence of the phosphorus nuclei in **9** and **10** give rise to an AB pattern in the $^{31}P-\{^{1}H\}$ NMR spectrum.

The reaction of the di-methyl substituted complex **8** with $K[HBBu^{s}_{3}]$ also affords a yellow powder. On account of its very poor solubility in other solvents, NMR spectra had to be run in CD_2Cl_2, in which the compound evidently decomposes. Hence, only proton and phosphorus NMR experiments were carried out. These suggest that the product is an anionic allyl complex, presumably $K[Mo\{\eta^3\text{-}C(Me)C(H)CH_2\}\{\eta^2\text{-}P(OMe)_2OBF_2OP(OMe)_2\}(\eta\text{-}C_5H_5)]$. The formation of an η^3-allyl-ligand parallels the reactivity of the analogous *bis*-phosphite but-2-yne complex $[Mo(\eta^2\text{-}MeC_2Me)\text{-}\{P(OMe)_3\}_2(\eta\text{-}C_5H_5)][BF_4]$, which was discussed in the introduction (1.1).

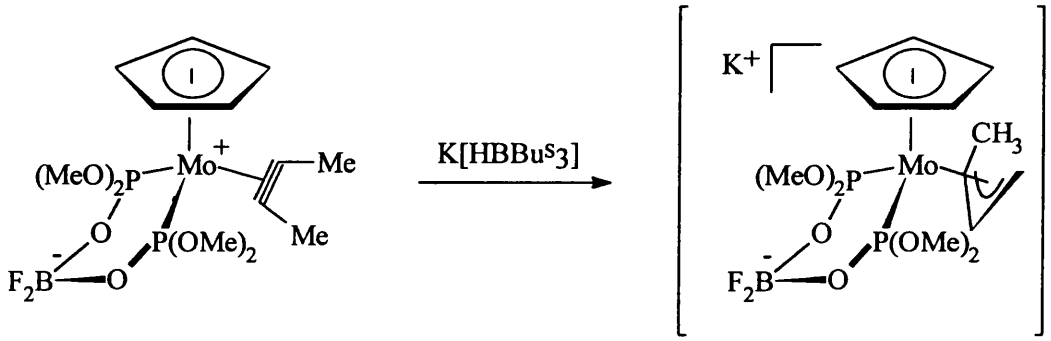

8

Scheme 28

The proton and phosphorus NMR spectra of this product show significant differences to those of **9** and **10**, indicating that there is no η^2-vinyl ligand present. Two virtual triplets for the methoxy groups are found in the ^{1}H NMR spectrum, which are similar to those observed for symmetrically substituted complexes such as the starting complex **6**. Also, only one broad signal at 201 ppm is found in the $^{31}P-\{^{1}H\}$ NMR spectrum. Broad multiplets between 1.35-1.50 ppm and 2.05-2.16 ppm in the proton NMR spectrum show a typical pattern for allyl systems. However, since low temperature NMR experiments did not give better resolved signals and $^{13}C-\{^{1}H\}$ NMR experiments could not be carried out, the description of this product must remain uncertain.

2.6. Reactivity of the η^2-Vinyl Complexes K[Mo{η^2=C(R)C(H)Ph}{η^2-P(OMe)$_2$OBF$_2$OP(OMe)$_2$}(η-C$_5$H$_5$)] (R= Ph 9, Me 10)

Protonation of η^2-vinyl metal complexes could in principle occur at all three atoms of the metallacyclopropene. Templeton and co-worker[76] showed that the η^2-vinyl group in [Tp*W{η^2=C(Ph)C(H)Me}(CO)$_2$] {Tp*= hydridotris(3,5-dimethylpyrazolyl)-borate} **LI** is protonated at the formally sp^3 hybridised carbon. They isolated the cationic 16 electron carbene complex [Tp*W{=C(Ph)C(H)$_2$Me}(CO)$_2$]$^+$ **LII** which is stabilised by an agostic interaction between the metal and a hydrogen on the β-carbon of the carbene ligand.

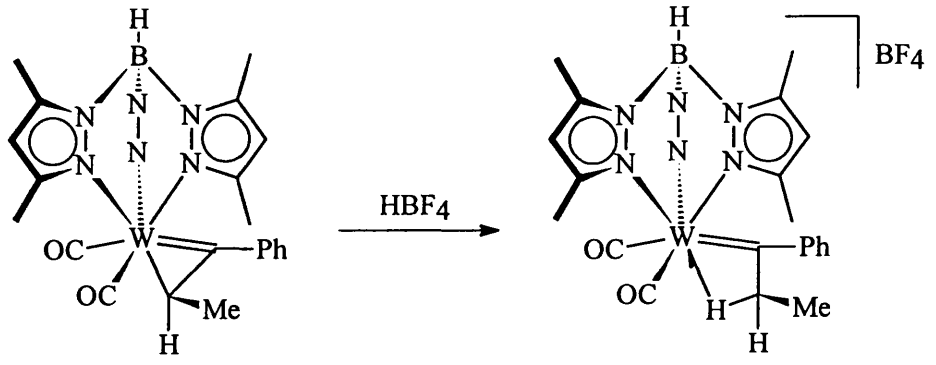

LI **LII**

Scheme 29

The η^2-vinyl complex K[Mo{η^2=C(R)C(H)Ph}{η^2-P(OMe)$_2$OBF$_2$OP(OMe)$_2$}(η-C$_5$H$_5$)] **9** was treated with one equivalent of HBF$_4$ whereupon the colour immediately changed from yellow to red. The reaction mixture was filtered through alumina and a red solution of **A** (Scheme 30) was obtained. The proton NMR spectrum showed several singlets with different intensities in the region in which the resonance of the cyclopentadienyl protons is expected (4.5-6.0ppm). Since a separation of so many different products or isomers did not seem feasible, CO was bubbled through the NMR sample resulting in a colour change to yellow. The NMR spectrum of the reaction mixture revealed that all products or isomers **A** from the protonation reaction react with CO to give one metal complex, as there was only one signal found in the proton NMR spectrum which could be assigned to cyclopentadienyl protons. The molybdenum complex was precipitated and characterised as the *bis*-carbonyl complex [Mo(CO)$_2${η^2-P(OMe)$_2$OBF$_2$OP(OMe)$_2$}(η-C$_5$H$_5$)] **11**. The supernatant solution was

analysed; exclusively *trans*-stilbene and no *cis*-stilbene, was identified. The reaction of **10** with HBF_4, followed by treatment with CO is very similar and also gives complex **11**. However, here no organic by-product was identified. Addition of diphenylacetylene to the intermediate **A** gave the complex **6**.

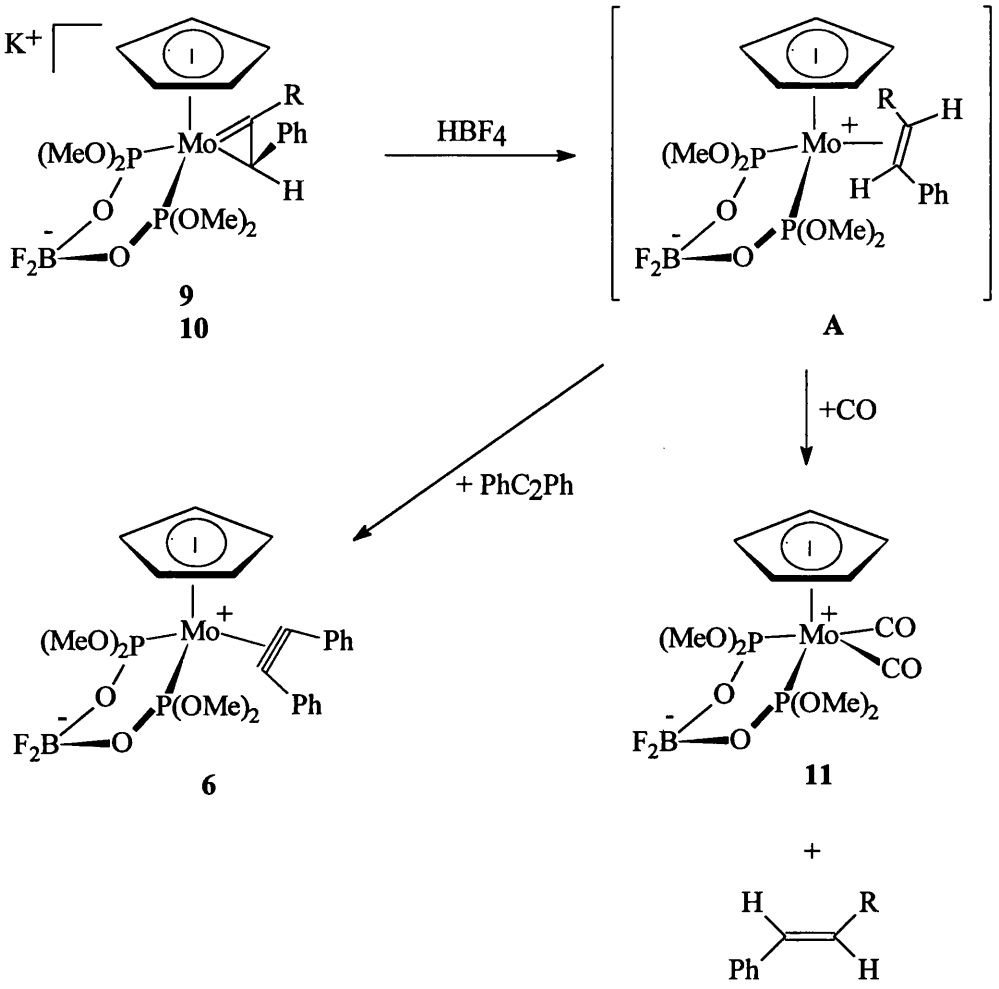

Scheme 30

The red complex **11** is soluble in the common aromatic and chlorinated solvents, but not in alkanes. The proton NMR spectrum shows a singlet for the cyclopentadienyl ligand at 5.00 ppm and two virtual triplets, characteristic for the *bis*-phosphite ligand, at 3.48 and 3.46 ppm. The carbonyl ligands are identified by two strong infra red absorption bands at 1992 and 1923 cm^{-1} and a resonance at 237.5 ppm in the carbon NMR spectrum.

It can be assumed that the product **A** is a mixture of different isomers of a formally 16 electron stilbene complex, possible bonding modes of which are shown in Figure 20. The isomer **A** may be stabilised by an agostic interaction (**B**) or by bonding of one arene double bond to the metal, forming a butadienyl ligand (**C**). Attempts to obtain single crystals of **A** for X-ray diffraction have not been successful.

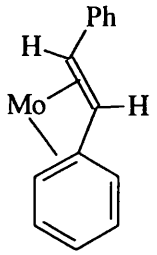

B

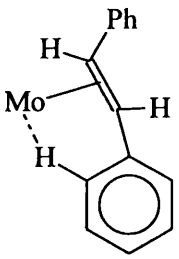

C

Figure 20, Possible bonding modes for *trans*-stilbene in **A**

2.7 Attempts to Synthesise Complexes with *tri*-Hapto and *tetra*-Hapto Boron-Bridged Phosphite Ligands

Recently, there has been considerable interest in new tripodal ligands for transition metal complexes, in particular in hard ligand systems such as the hydridotris(3,5-dimethylpyrazolyl)borato anion or tris-amido ligands.[77] Last year Kläuli *et al* published a synthesis for an anionic phosphite ligand, which was generated within the coordination sphere of ruthenium. The complex $[Ru\{P(OH)(OMe)_2\}_2\{P(O)(OMe)_2\}(\eta\text{-}C_5Me_5)]$ **LIII** was reacted with $PhBCl_2$ in presence of a base to yield $[Ru\{\eta^3\text{-}(P(OMe)_2O\}_3BPh\}(\eta\text{-}C_5Me_5)]$ **LIV**, the structure of which was characterised by X-ray analysis.[78]

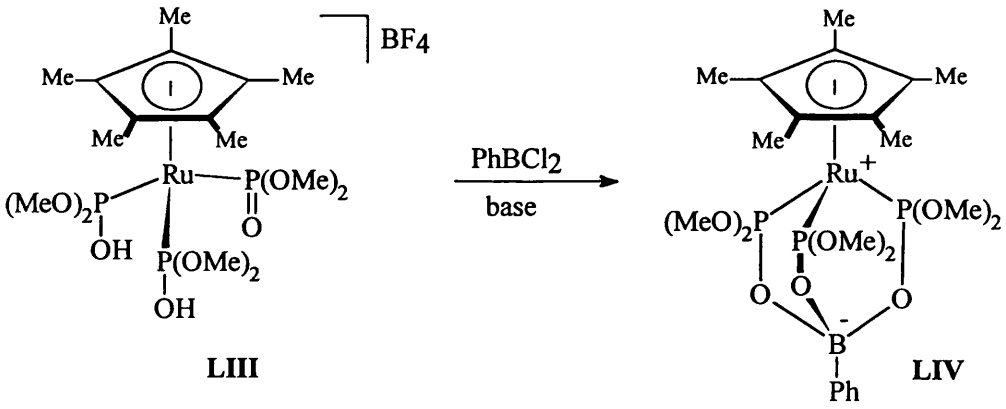

LIII **LIV**

Scheme 31

In section 2.3 it was shown that the reagent $CH_2(MgI)_2$ promotes a linkage of two adjacent phosphite moieties with a boron atom. It was therefore feasible that three phosphite ligands could also be linked together with the same reagent, if a starting complex is used which has more than two phosphite molecules on a cyclopentadienyl molybdenum fragment. Therefore, suitable starting complexes were synthesised.

Firstly, the same method as used for the synthesis of the di-carbonyl complex **10** in section 2.6 was applied. Protonation of the anionic η^2-vinyl complexes $K[Mo\{\eta^2\text{=}C(R)C(H)Ph\}\{\eta^2\text{-}P(OMe)_2OBF_2OP(OMe)_2\}(\eta\text{-}C_5H_5)]$ **9** or **10** in the presence of two equivalents of trimethylphosphite gave the bright yellow compound $[Mo\{P(OMe)_3\}_2\{\eta^2\text{-}P(OMe)_2OBF_2OP(OMe)_2\}(\eta\text{-}C_5H_5)]$ **12** in good yield (Scheme 32).

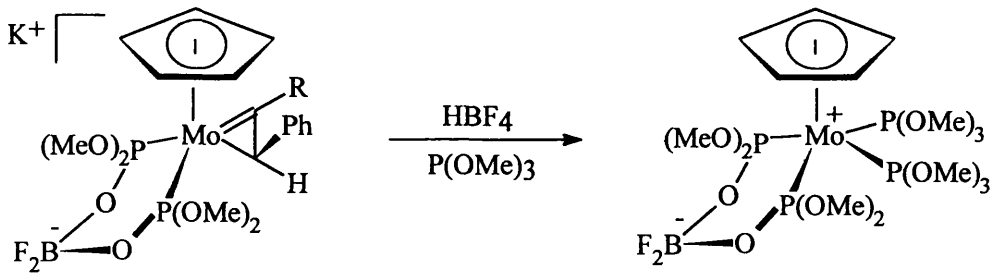

9
10

12

Scheme 32

The proton NMR shows three virtual triplets at 3.74, 3.70, and 3.42 ppm with relative intensities 1:1:3. The first two resonances can be assigned to the chelating *bis*-phosphite ligand and the last to the two phosphite ligands. In the ^{31}P-{^{1}H} NMR spectrum, the expected AA'XX' pattern appears between 196.5-195.0 and 173.9-172.7 ppm. However, due to broadening of the XX' part of the spectrum, not all of the signals necessary to determine the underlying coupling constants could be found.

Secondly, in order to obtain a cationic starting material, the *bis*-phosphite π-allyl complex [Mo(η^3-C_3H_4Me){$P(OMe)_3$}$_2$(η-C_5H_5)][31] **XIII** was protonated with HBF_4 in the presence of trimethylphosphite and the cationic *tetrakis*-phosphite compound [Mo{$P(OMe)_3$}$_4$(η-C_5H_5)][BF_4] **13** was obtained.

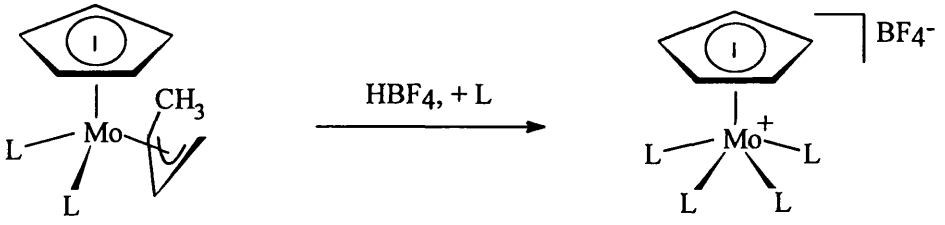

XIII

13

Scheme 33, L= $P(OMe)_3$

The bright yellow highly air sensitive complex **13** is soluble in chlorinated solvents and thf, while almost insoluble in less polar solvents. The ^{1}H NMR spectrum of **13** shows a singlet for the cyclopentadienyl ligand and one virtual quintet for all phosphite protons. The equivalence of the phosphite moieties is also reflected in the ^{31}P-{^{1}H} NMR featuring one singlet at 190.9 ppm. The ^{13}C-{^{1}H} NMR spectrum exhibits

a resonance at 84.7 ppm for the η-C_5H_5 ligand and a singlet for the phosphite carbons at 52.7 ppm.

Both compounds **12** and **13** were reacted with $CH_2(MgI)_2$, but no reaction was observed.

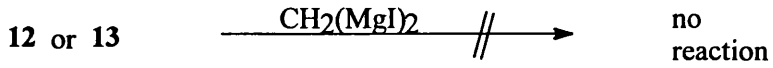

Scheme 34

This could indicate that the alkyne ligand in the compound $[Mo(\eta^2\text{-}PhC_2Ph)\text{-}\{P(OMe)_3\}_2(\eta\text{-}C_5H_5)][BF_4]$ **XI** plays an important role in the reaction with $CH_2(MgI)_2$. Presumably it opens a reaction site at the metal by switching from a four electron donor to a two electron donor. Steric reasons might also be responsible for the decreased reactivity of **12** and **13** compared to complex **XI**.

2.8 Synthesis of the First Mononuclear η(4e)-Bonded Phosphaalkyne Complex

Since the first preparation of stable phosphaalkynes in 1981[79] there has been considerable interest in its coordination chemistry. Several transition metal complexes containing phosphaalkynes have been prepared,[80, 81, 82] but so far no stable mononuclear complex containing an η^2(4e)-phosphaalkyne ligand has been synthesised. It is interesting to note, however, that it has been reported that treatment of the complex $[Ti(PMe_3)(\eta^2\text{-}Bu^tCP)(\eta\text{-}C_5H_5)_2]$ **LVI** with BEt_3 leads to loss of PMe_3 as the adduct Me_3PBEt_3 and formation of an equilibrium mixture, which is thought to contain $[Ti(\eta^2\text{-}Bu^tCP)(\eta\text{-}C_5H_5)_2]$ **LVII** and the corresponding phosphorus-bridged dimer **LVIII**. However, from this mixture, only the dimeric complex **LVIII** was isolated.[83]

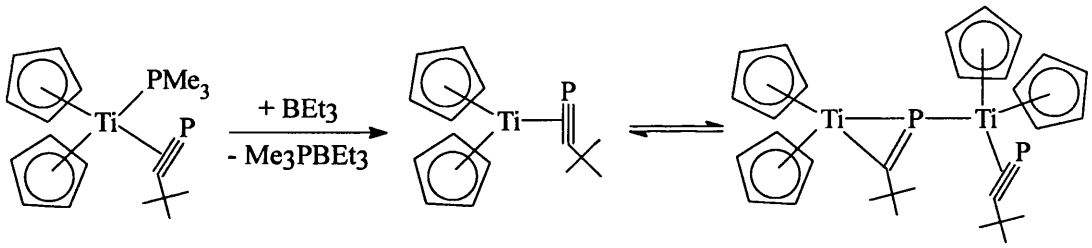

LVI **LVII** **LVIII**

Scheme 35

As was shown in section 2.6, the protonation of the anionic complexes **9** or **10** in the presence of donor ligands yields neutral zwitterionic complexes. In particular, it was shown that this reactivity can be used to introduce 4(e)-donor alkynes into the complex. It therefore, seemed feasible that phosphaalkyne could be coordinated to this metal fragment and thus be forced into an 4(e)-donating bonding mode.

Complex **9** was treated with one equivalent of $HBF_4.Et_2O$ to generate the intermediate $[Mo(\textit{trans}\text{-}PhHC{=}CHPh)\{\eta^2\text{-}P(OMe)_2OBF_2OP(OMe)_2\}(\eta\text{-}C_5H_5)]$ **A** *in situ*, as was shown in the previous chapter. When the yellow reaction mixture was cooled to -78°C, and one molar equivalent of $Bu^tC{\equiv}P$ was added, there was an immediate change of colour to deep green. Workup by removal of the solvent *in vacuo*, extraction with toluene, followed by addition of hexane and cooling (-20°C) afforded a low melting complex $[Mo\{\eta^2\text{-}P(OMe)_2OBF_2OP(OMe)_2\}(\eta^2\text{-}P{\equiv}CBu^t)(\eta\text{-}C_5H_5)]$ **14** (Scheme 36). The highly air sensitive green complex **14** consists of the zwitterionic

metal fragment [Mo{η^2-P(OMe)$_2$OBF$_2$OP(OMe)$_2$}(η-C$_5$H$_5$)] and one phosphaalkyne moiety, which - as has been deduced from electron count and NMR evidence - acts as a four electron donor.

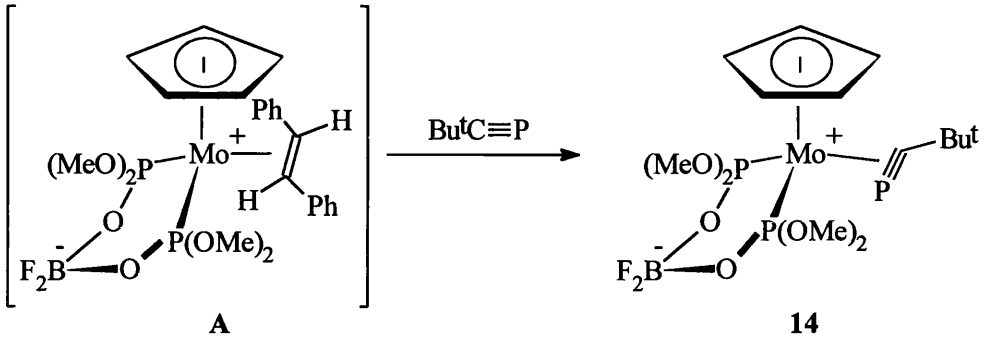

A **14**

Scheme 36

Compound **14** was fully characterised by its analytical and spectroscopic data. The NMR spectra show the features expected for the metal fragment [Mo{η^2-P(OMe)$_2$O-BF$_2$OP(OMe)$_2$}(η-C$_5$H$_5$)], which was discussed in detail in 2.4. Hence, in the ^{1}H NMR spectrum, a triplet at 5.43 ppm [*J*(PH) 1.4 Hz] was attributed to the cyclopentadienyl ligand and two virtual triplets at 3.52 [*N*(PH) 11.2 Hz] and 3.31 ppm [*N*(PH) 11.5 Hz] were assigned to the methoxy groups on the phosphite ligand. Correspondingly, in the ^{13}C-{^{1}H} NMR spectrum two virtual triplets were seen for these methoxy groups and a singlet at 93.8 ppm which is attributable to the cyclopentadienyl ligand. The appearance in the ^{31}P-{^{1}H} NMR spectrum of a singlet resonance at 157.3 ppm due to the bidentate ligand [(MeO)$_2$POBF$_2$OP(OMe)$_2$], confirms that in solution on the NMR timescale the phosphaalkyne, in a similar way to alkynes, undergoes a facile windscreen wiper motion (Scheme 37). The ^{31}P-{^{1}H} NMR spectrum is invariant in the temperature range +25°→ -80°C.

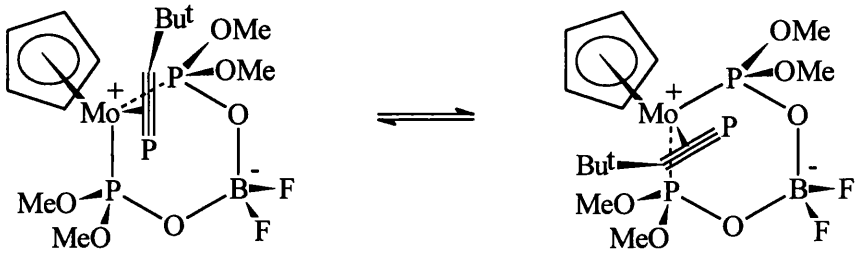

Scheme 37

More interesting are the features displayed by the phosphaalkyne ligand. The integration of the singlet for the *tert*-butyl group at 1.52 ppm clearly shows that only one alkyne molecule has been incorporated into the complex. In the $^{31}P-\{^{1}H\}$ NMR spectrum, a low field signal at 467.8 ppm is assigned to the phosphorus of the η^2(4e)-bonded $Bu^tC{\equiv}P$. This resonance is highly deshielded compared to the shifts exhibited by the η^2(2e)-bonded $Bu^tC{\equiv}P$ ligands present in the platinum complexes $[Pt(\eta^2\text{-}Bu^tCP)(PPh_3)_2]$ (84.1 ppm),[84] $[Pt(\eta^2\text{-}Bu^tCP)(diphos)]$ (87.7 ppm)[85] and $[Pt(\eta^2\text{-}Bu^tCP)(\eta^2\text{-}Ph_2PCH_2CMe(CH_2PPh_2)CH_2PPh_2]$ (82.3 ppm).[86] Interestingly, the aforementioned mixture containing $[Ti(\eta^2\text{-}Bu^tCP)(\eta\text{-}C_5H_5)_2]$ **LVII**[83] shows a low field signal at 431.6 ppm in the $^{31}P-\{^{1}H\}$ NMR spectrum (d^8-thf, -40°C). This signal, however, was very broad ($h_{1/2}\approx$ 970 Hz).

Support for the assignment of the low field ^{31}P NMR shift is also provided by the recent[87] report that the $^{31}P-\{^{1}H\}$ NMR spectrum of the aromatic phosphirenylium cation $[PhCC(Bu^t)P][B(OSO_2CF_3)_4]$ **LIX** shows a resonance at 309.7 ppm deshielded by 313 ppm from $PhC{=}C(Bu^t)POSO_2CF_3$ **LX**. Thus, on account of the isolobal relationship between $MoL_2(\eta\text{-}C_5H_5)$ and CR (Figure 21), a similar low field resonance would be expected in the $^{31}P-\{^{1}H\}$ NMR spectrum of **14** and it is reasonable to assume that the signature of a η^2(4e)-bonded phosphaalkyne is a ^{31}P NMR resonance in the region of 450 ppm.

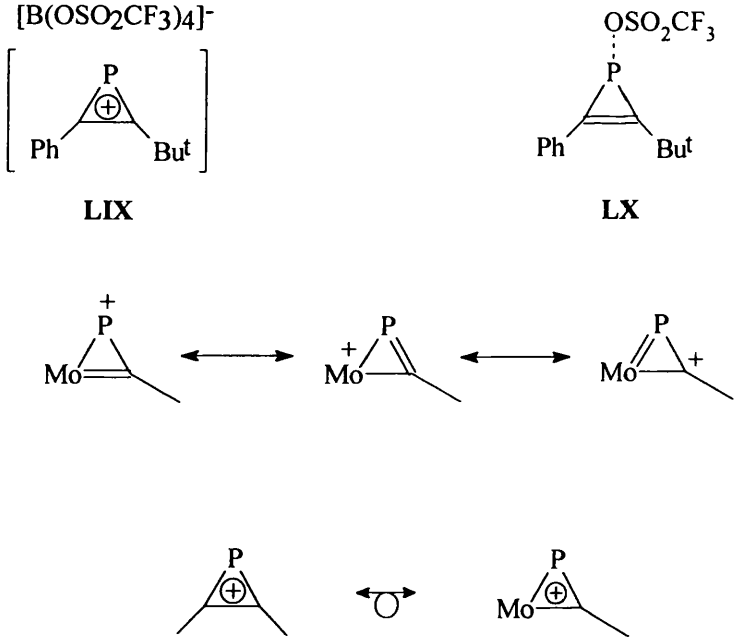

Figure 21

The ^{13}C-{^{1}H} NMR spectrum of **14** shows a doublet of triplets as low field as 328.5 ppm [^{1}J(PC) 114.4 Hz, ^{3}J(PC) 6.6 Hz]. As mentioned earlier, with mononuclear transition metal alkyne complexes, there is a correlation between the contact ^{13}C chemical shifts and the effective number of electrons donated to the metal, and it is clearly important to consider whether a similar correlation exists for phosphaalkyne complexes. On comparison with the ^{13}C shifts observed for uncoordinated $Bu^{t}C{\equiv}P$ [184.3 ppm, d, J(PC) 38.6 Hz], and for the presumed η^2(2e)-bonded phosphaalkyne complex [$Pt(\eta^2$-$Bu^{t}CP)(PPh_3)_2$] [242.0 - 239.5 ppm, m] the corresponding shift of **14** appears at very low field, suggesting that such a correlation does indeed exist. In this context it is interesting to note that the complex [$WCl(\eta^2$-$MeCN)(PMe_3)_2(bipy)$] [PF_6],[88] which contains a η^2(4e)-bonded nitrile, shows a low field contact ^{13}C resonance at 235 ppm [t, J(PC) 52.8 Hz], which is shifted 135 ppm to low field of uncoordinated methylcyanide.

However, it has been reported that the η^2(2e)-complex [$Ti(\eta^2$-$Bu^{t}CP)(PMe_3)(\eta$-$C_5H_5)_2$] **LVI**[83] shows a phosphaalkyne contact carbon resonance at 298.6 ppm, suggesting that although the ^{13}C shift observed for **14** is consistent with an η^2(4e)-bonding mode, the distinction between η^2(4e)- and η^2(2e)-bonding for a phospha-alkyne as observed by contact carbon shifts is less pronounced than with alkynes.

Thus, to summarise the NMR data, it is the ^{31}P chemical shift which clearly suggests that the phosphaalkyne ligand present in **14** acts as a four electron donor and is therefore able to act simultaneously as a single-faced π-acid (through $\pi_{\parallel}^{*}$) and as a single-faced π-base (through $\pi_{\perp}$).

2.9 Reactivity of 14 - Transformation into a 1,3-Diphosphacyclobutadiene Complex

Complexes containing η^2(4e)-bonded phosphaalkyne ligands are also interesting in the context of reactivity. Treatment of a toluene solution of **14** with one molar equivalent of $Bu^tC{\equiv}P$ resulted in a colour change over a period of three days from green to yellow. Column chromatography of the reaction mixture on alumina and elution with dichloromethane afforded a single yellow band, which on recrystallisation from CH_2Cl_2/hexane produced yellow crystals (48% yield) of the 1,3-diphosphacyclobutadiene complex $[Mo\{\eta^2\text{-}P(OMe)_2OBF_2OP(OMe)_2\}\{\eta^4\text{-}P_2C_2(Bu^t)_2\}(\eta\text{-}C_5H_5)]$ **15**.

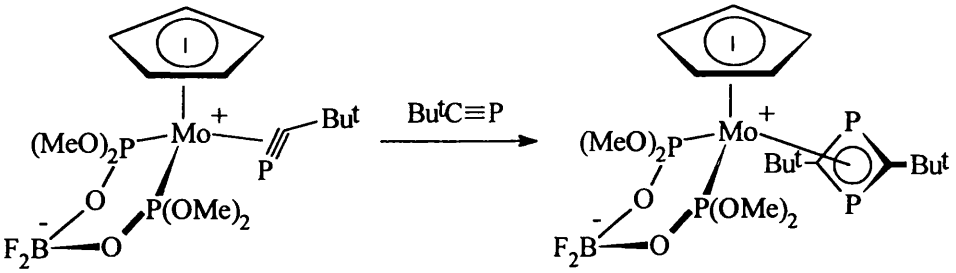

14 **15**

Scheme 38

The characterisation of compound **15** was accomplished by ^1H, ^{13}C, and ^{31}P NMR spectroscopy. In the ^1H NMR spectrum the signals for the metal fragment $[Mo\{\eta^2\text{-}P(OMe)_2OBF_2OP(OMe)_2\}(\eta\text{-}C_5H_5)]$ in compounds **15** and **14** are very similar. The important difference is, however, that in the spectrum of **15** the integration of the singlet at 0.90 ppm, which is attributable to *tert*-butyl groups, represents 18 protons. The $^{31}P\text{-}\{^1H\}$ NMR spectrum shows two singlets for the diphosphacyclobutadiene ligand at 56.5 and 51.1 ppm and a singlet for the two phosphite phosphorus nuclei at 151.7 ppm. The NMR data, two magnetically equivalent *tert*-butyl groups and two different phosphorus nuclei in the cyclobutadienyl ligand, suggest that the four membered ring is not rotating and that the two carbon atom in the ring together with the two phosphite phosphorus span a plane.

The stepwise nature of the formation of η^4-1,3-diphosphacyclobutadienes has, prior to this work, not been demonstrated, despite frequent reports of the formation of this ligand on reaction of metal complexes with phosphaalkynes.[80, 82] However, Binger

and coworkers have reported[89] that the dimeric cobalt compound $[Co_2(\mu\text{-}Me_3Si\text{-}C_2SiMe_3)(\eta\text{-}C_5H_5)_2]$ **LXI** reacts with a mixture of $Bu^tC{\equiv}P$ and $Me_3SiC_2SiMe_3$ to give the monomeric η^4-cyclobutadienyl complexes **LXII - LXIV**, as is shown in Scheme 39.

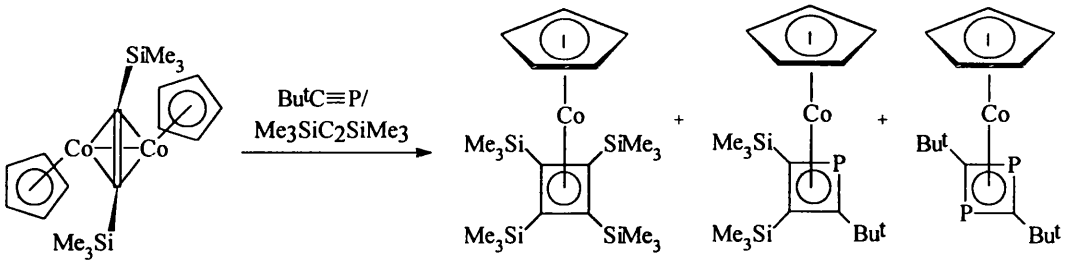

LXI **LXII** **LXIII** **LXIV**

Scheme 39

It is suggested that the transformation **14**→ **15** involves a switch $[\eta^2(4e) \rightarrow \eta^2(2e)]$ in the bonding mode of the coordinated $Bu^tC{\equiv}P$ ligand, which is present in **14**, so as to accommodate a second $\eta^2(2e)$-bonded phosphaalkyne prior to its head to tail coupling to form the possible precursors **A** and **B** (Figure 22) of the 1,3-diphosphacyclo-butadiene ring.

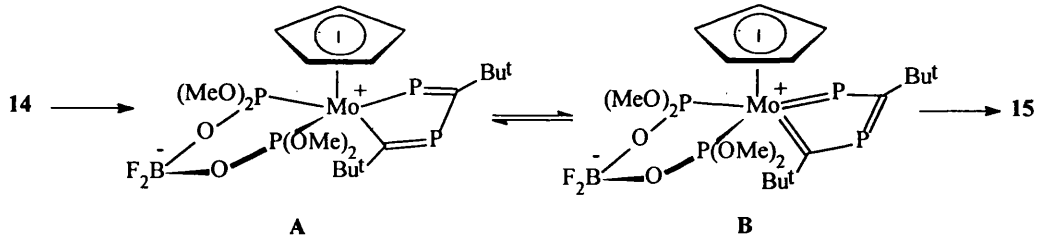

A **B**

Figure 22

2.10. Investigation of Phosphide Alkyne Complexes $[Mo(PPh_2H)(PPh_2)(\eta^2\text{-}RC_2R)(\eta\text{-}C_5H_5)]$

The elements comprising an alkyne transition metal bond have been discussed in detail in the introduction (1.1). In particular, this focused on the ability of alkynes to act as two or as four electron donor ligands. Their reactivity towards nucleophiles was another characteristic mentioned therein.

Similarly, the phosphide ligand (PR_2) can coordinate to a transition metal with two different bonding modes, as illustrated in Figure 23. Firstly, it can act as a one electron donor with a σ-bond between the phosphorus and the metal. The phosphorus in this so-called phosphido-group is sp^3-hybridised and a *pseudo*-tetrahedral conformation is found. The lone pair of the phosphorus is localised and does not contribute to the M-P bond.[4]

Secondly, the phosphide ligand can donate three electrons to the metal, an arrangement which is also called a phosphenium complex. Here the phosphorus is sp^2-hybridised and its three substituents are in one plane. Between metal and phosphorus there is a double bond, which can formally be described as one σ- and one dative bond stemming from the free electron pair at the phosphorus.[4]

phosphido phosphenium

Figure 23

Examples of complexes with one electron donor phosphide ligands are $[Mo(CO)_2(PMe_3)(PPh_2)(\eta\text{-}C_5H_5)]$ **LXV**[90] and $[Re(NO)(PPh_3)(PPh_2)(\eta\text{-}C_5H_5)]$ **LXVI**.[91] X-ray diffraction studies on the rhenium complex showed that the sum of the three bond angles about the phosphorus is 323.0° and, therefore, close to 328.5° for an idealised tetrahedral atom.

When two phosphide ligands contribute a total number of four electrons to the metal complex they can donate one and three electrons respectively, as was found for the

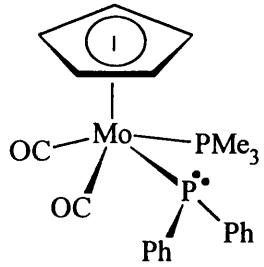

LXV

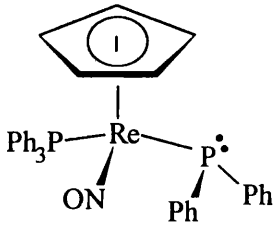

LXVI

Figure 24

metallocene hafnium complex $[Hf(PEt_2)_2(\eta\text{-}C_5H_5)_2]$ **LXVII**.[92] Here one phosphorus is in a *pseudo*-tetrahedral, and the other in a planar, coordination sphere. Alternatively, both phosphide ligands donate two electrons each resulting in a P-M bond order of 1.5. This was observed in the tungsten complex $[W(H)(PMe_3)(PPh_2)_2(\eta\text{-}C_5H_5)]$ **LXVIII**[93] where the two *transoid* phosphide ligands together with the metal adopt a *pseudo*-allylic bond. However, for both complexes only one resonance in their ^{31}P NMR spectra was found indicating that in solution they are fluxional.

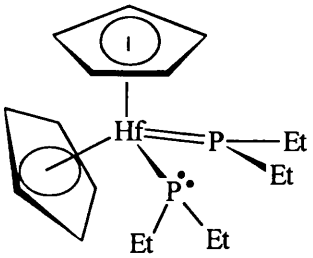

LXVII

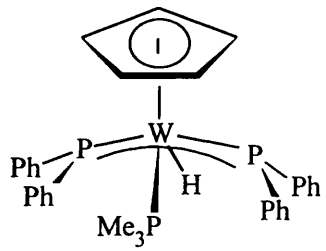

LXVIII

Figure 25

Three reaction types, which have been used to synthesise neutral transition metal phosphide complexes, are shown in Figure 26. These are: transmetallation with sodium phosphide and a transition metal halide (**A**), the HX elimination from halogeno secondary phosphine metal complexes (**B**) and the HX elimination from cationic secondary phosphine metal complexes (**C**). It is noteworthy that for 18 electron complexes the paths **A** and **C** lead to one electron donor phosphides, whereas path **B** leads to three electron donor phosphides.[94]

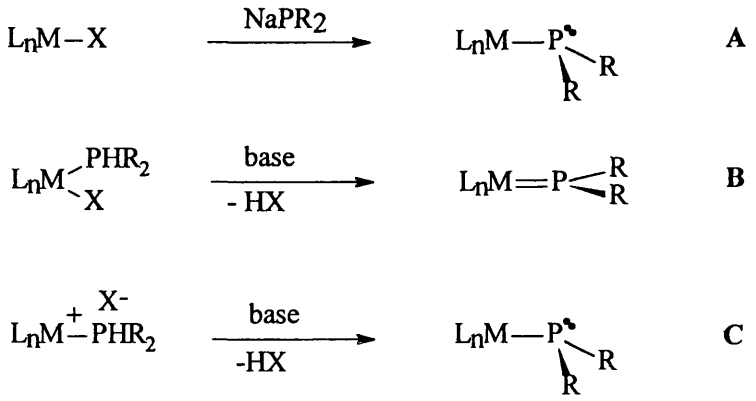

Figure 26

It seemed interesting to synthesise model complexes containing two ambivalent ligands, an alkyne and a phosphide. With these complexes it should be possible to quantify the relative donor ability of alkynes *versus* phosphides.

Since the complexes with tertiary phosphines $[Mo(PR_3)_2(\eta^2\text{-}R'C_2R')(\eta\text{-}C_5H_5)][BF_4]$ (R= Me, Et, Ph; R'= Me, Ph, 4-tolyl)[15] are readily accessible, it was anticipated that the analogous complexes with secondary phosphines $[Mo(PR_2H)_2(\eta^2\text{-}R'C_2R')(\eta\text{-}C_5H_5)][BF_4]$ can be prepared by the same route. Abstraction of HBF_4 (path **C**) would generate a compound $[Mo(PR_2)(PR_2H)(\eta^2\text{-}R'C_2R')(\eta\text{-}C_5H_5)]$ accommodating a phosphide and an alkyne ligand. An electron count reveals that the alkyne and the phosphide ligand together have to deliver five electrons to the metal in order to fulfil the 18 electron rule. Thus, it was anticipated that there would be the desired competition between the two ligands.

As expected, addition of two equivalents of diphenylphosphine to the *bis*-alkyne acetonitrile complex $[Mo(NCMe)(\eta^2\text{-}PhC_2Ph)_2(\eta\text{-}C_5H_5)][BF_4]$ **LXIX**[15] gives the *bis*-phosphine complex $[Mo(PPh_2H)_2(\eta^2\text{-}PhC_2Ph)(\eta\text{-}C_5H_5)][BF_4]$ **16**. This cationic complex was purified by repeated recrystallisation from CH_2Cl_2/hexane until it was obtained in the form of a green powder (Scheme 40).

The proton NMR spectrum of **16** shows a triplet at 5.44 ppm for the cyclopentadienyl ligand with a phosphorus coupling of 1.4 Hz and the 30 phenyl protons can be seen as a multiplet between 7.51 and 6.91 ppm. The two protons bonded to the phosphorus are detected as a doublet centred at 7.15 ppm with a phosphorus coupling of 379 Hz. This coupling is also found in the proton coupled ^{31}P NMR spectrum which shows a

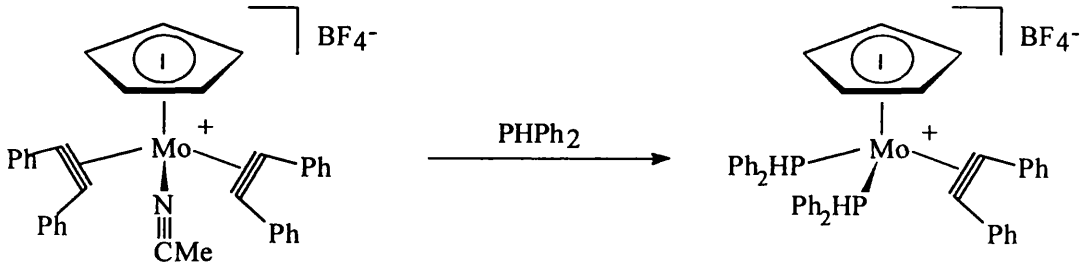

LXIX 16

Scheme 40

doublet at 39.1 ppm. The $^{13}C-\{^1H\}$ NMR spectrum of **16** displays, in addition to a signal for the η-C_5H_5 ligand at 96.5 ppm and several signals for the phenyl carbons between 138.3 and 127.5 ppm, a singlet for the contact carbons of the alkyne moiety at 222.6 ppm, a shift which is characteristic for a four electron donor.

Complex **16** was treated with one equivalent of the amide base $Li[N(SiMe_3)_2]$ in thf at -78°C. On warming to room temperature the colour of the solution turned from green to red. After all volatiles were removed, the product was extracted with toluene and recrystallised from toluene/hexane to give high yields of the dark red compound $[Mo(PPh_2)(PPh_2H)(\eta^2\text{-}PhC_2Ph)(\eta\text{-}C_5H_5)]$ **17**. Protonation of **17** with $HBF_4.Et_2O$ regenerated quantitatively the starting complex **16**.

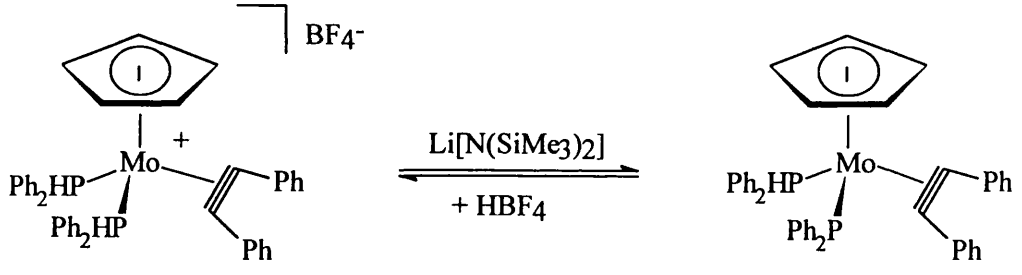

16 17

Scheme 41

The air sensitive complex **17** is soluble in all common solvents except hydrocarbons However, slow decomposition of **17** occurs in chlorinated solvents, a point discussed later in this section. Single crystals which were obtained from toluene/hexane using the layering technique were twinned and, therefore, not suitable for an X-ray diffraction study.

The ^{1}H NMR spectrum reveals the presence of 30 phenyl protons (8.05-6.92 ppm, multiplet) and a cyclopentadienyl ligand [4.95 ppm, doublet, *J*(PH) 1.1 Hz]. A doublet of doublets at 7.70 ppm [^{1}J(PH) 345 Hz, ^{3}J(PH) 3.0 Hz] is attributable to a hydrogen bonded to a phosphorus. The splitting and the coupling constants show that the hydrogen is bonded to only one phosphorus and does not adopt a bridging position between the two phosphorus atoms or exchanges between the two. Accordingly, the ^{31}P-{^{1}H} NMR spectrum shows two signals at 63.0 and 53.7 ppm, of which the latter is split into a doublet of 345 Hz in the proton coupled spectrum. The signal at 63.0 ppm was, therefore, assigned to the phosphorus nucleus of the phosphide ligand. A singlet at 151.7 ppm in the ^{13}C-{^{1}H} NMR spectrum was attributed to the alkyne contact carbons, this shift being consistent with the alkyne groups acting as three electron donors.

As no X-ray diffraction study on complex **17** could be accomplished, the competition in donor ability of the alkyne and the phosphide ligand must be solely discussed on the basis of NMR evidence. The relationship between the number of donated electrons of a coordinated alkyne and the shift in the ^{13}C NMR has been mentioned earlier (1.1). Similarly, ^{31}P-{^{1}H} NMR spectroscopy is a useful tool for analysing the ambivalent bonding modes of phosphide ligands. One electron donating phosphides generally show an upfield shift; e. g. the aforementioned rhenium complex [Re(NO)-(PPh_3)(PPh_2)(η-C_5H_5)] **LXVI**[91] resonates at -48.3 ppm, or the molybdenum complex [Mo(CO)$_2$(PMe_3)(PPh_2)(η-C_5H_5)]**LXV**[90] at -31.9 ppm. The resonances for phosphides, which formally donate two electrons, are found at higher chemical shift values; e.g. [Hf(PR_2)$_2$(η-C_5H_5)$_2$]**LXVII**[92] (R = Et, Cy, Ph) 100 - 160 ppm, [W(H)-(PMe_3)(PPh_2)$_2$(η-C_5H_5)]**LXVIII**[93] 98.8 ppm. A characteristic lowfield shift of three electron donors can be exemplified with the complexes [Mo(PMe_3)($PHPh_2$)(PPh_2)(η-C_5Me_5)][93] (177.1 ppm for PPh_2) and [Mo(PMe_3)$_2$(PPh_2)(η-C_5H_5)][95] (224.4 ppm for PPh_2). On the basis of these examples it seems reasonable to view the phosphide ligand in complex **17** formally as a two electron donor.

In summary, for the complex **17** it was shown that both ambivalent ligands adopt a bonding mode somewhere between the maximum and minimum number of electrons they are able to contribute to a metal centre.

It is also noteworthy that experiments to vary the substituents on the relevant ligands failed. The reaction of the but-2-yne complex $[Mo(PPh_2H)_2(\eta^2\text{-}MeC_2Me)(\eta\text{-}C_5H_5)]\text{-}[BF_4]$ with $Li[N(SiMe_3)_2]$ did not give any stable product.

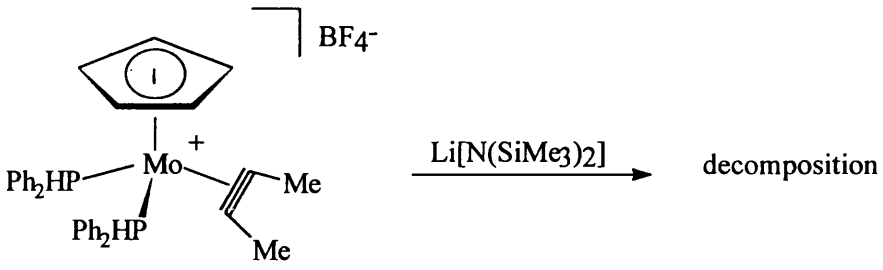

LXIX

Scheme 42

The reaction of **16** with a hydride source could, as with other cationic cyclopentadienyl molybdenum complexes, lead to a nucleophilic attack at the alkyne and the formation of an η^2-vinyl complex. However, the reaction of **16** with $K[BHBu^s_3]$ generates compound **17**, showing that the phosphines in complex **16** have considerable acidity and thus the hydride acts as a base.

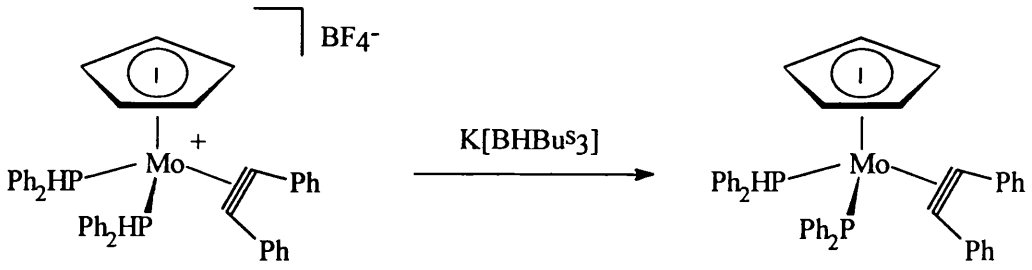

16 **17**

Scheme 43

An attempt was made to deprotonate complex **17** in order to obtain an anionic diphosphido complex. However, on addition of one equivalent of $Li[N(SiMe_3)_2]$ to a solution of **17** in thf no reaction was observed. On using the far stronger base $LiBu^t$ for this reaction complete decomposition occurs (Scheme 44).

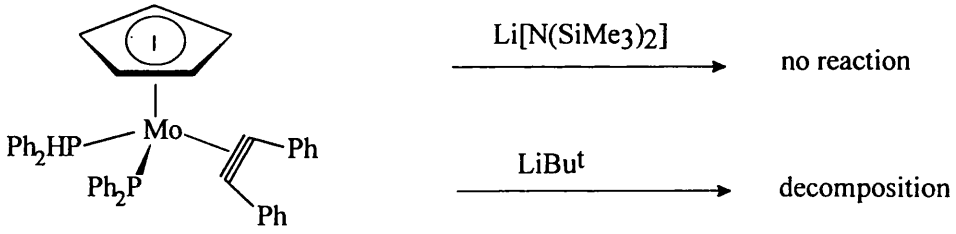

17

Scheme 44

It is known that phosphido complexes can act as nucleophiles, even with not very reactive substrates such as CH_2Cl_2. Gladysz *et al* [91] reported that on dissolving the aforementioned rhenium complex $[Re(NO)(PPh_3)(PPh_2)(\eta\text{-}C_5H_5)]$ **LXVI** in CH_2Cl_2 the cationic compound $[Re(NO)(PPh_3)\{P(CH_2Cl)Ph_2\}(\eta\text{-}C_5H_5)]Cl$ **LXX** is formed.

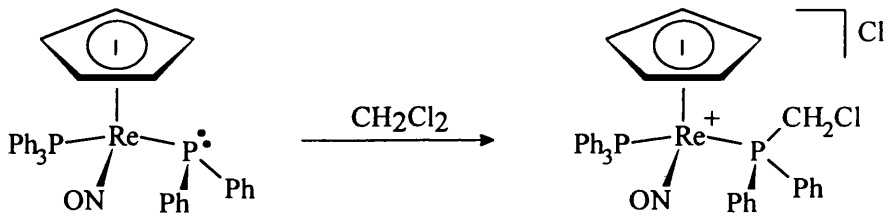

LXVI **LXX**

Scheme 45

An investigation of the reactivity of **17** towards electrophiles was carried out. One equivalent of either CH_2Cl_2, CH_2I_2 or BCl_3 was added to a solution of **17** in thf. After 5 hours a reaction was observed with CH_2Cl_2 and CH_2I_2, while with BCl_3 an immediate colour change occurred. However, in neither case could a stable product be isolated. It can be assumed that after initial formation of the desired product an intramolecular oxidation of the molybdenum occurs leading to decomposition.

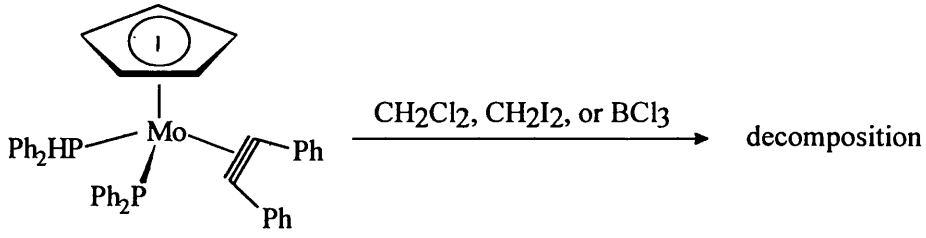

17

Scheme 46

2.11. Reactions of the *bis*-Alkyne(carbonyl)-Carbaborane Complexes with $P(OMe)_3$

The isolobal relationship between $[nido\text{-}C_2B_9H_{11}]^{2-}$ and $[C_5H_5]^-$ has already been elaborated upon (section 1.2). It was therefore expected that the chemistry of *bis*-alkyne complexes [*closo*-3,3-(η^2-$RC_2R)_2$-3-CO-3,1,2-$MoC_2B_9H_{11}$] (R= alkyl, aryl) would parallel that of the cationic cyclopentadienyl analogues [Mo(η^2-$RC_2R)_2$(CO)(η-C_5H_5)][BF_4]. The cyclopentadienyl complexes [Mo(η^2-$RC_2R)_2$(CO)(η-C_5H_5)]-[BF_4] react with trimethylphosphite to yield exclusively the *bis*-phosphite complexes [Mo(η^2-RC_2R){$P(OMe)_3$}$_2$(η-C_5H_5)][BF_4], a type of compound which has played a pivotal role in studies of the chemistry of η^2(4e)-bonded alkyne ligands.[96, 97] In this chapter, the reactivity of the carbaborane complexes [*closo*-3,3-(η^2-$RC_2R)_2$-3-CO-3,1,2-$MoC_2B_9H_{11}$] towards $P(OMe)_3$ will be described.

It has been shown by Stone and coworkers that a great number of neutral carbaborane-molybdenum complexes can be prepared *via* protonation of the anionic complex [NEt_4][*closo*-3,3-$(CO)_2$-3-(η^3-C_3H_5)-3,1,2-$MoC_2B_9H_{11}$] **XXXII**[56, 57] in the presence of donor ligands. This route also provided access to the *bis*-alkyne complex [*closo*-3,3-(η^2-$MeC_2Me)_2$-3-CO-3,1,2-$MoC_2B_9H_{11}$] **XXXIV**[57] which was obtained in a good yield (Scheme 47).

In order to put our investigations on a broad basis it seemed desirable to synthesise analogous complexes. Protonation of **XXXII** in the presence of diphenylacetylene or methyl phenylacetylene afforded, after column chromatography and recrystallisation from CH_2Cl_2/hexane, the complexes **18** and **19**, respectively.

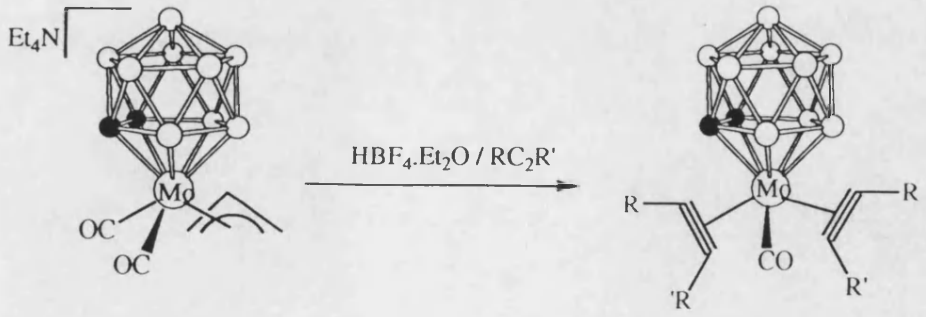

XXXII

R	R'	
Me	Me	**XXXIV**
Ph	Ph	**18**
Me	Ph	**19**

Scheme 47, O = BH, ● = CH

The spectroscopic properties of the bright yellow compounds **18** and **19** are very similar to those of complex **XXXIV** but they will be briefly discussed for the sake of completeness. The ^{1}H NMR spectrum of **18** shows a multiplet between 7.60 and 7.29 ppm for the phenyl protons and a broad singlet for the two cage-CH nuclei. The $^{13}C-\{^{1}H\}$ NMR spectrum exhibits a resonance for the CO group at 222.1 ppm and a broad signal for the cage carbon atoms. The appearance of two resonances (at 168.8 and 152.9 ppm), attributable to the alkyne contact carbons, suggests that the alkynes are not rotating on the NMR timescale. The IR spectrum of **18** shows a strong carbonyl absorption at 2062 cm^{-1}.

The NMR spectra of compound **19** shows two sets of peaks due to two isomers, while the IR spectrum displays only one absorption (at 2049 cm^{-1}). This is a common feature for non-symmetrically substituted *bis*-alkyne complexes and has, for example, been observed for the cyclopentadienyl complex $[Mo(\eta^2\text{-}RC_2R')(CO)(\eta\text{-}C_5H_5)][BF_4]$ (section 1.1). From the three possible isomers (Figure 27), only the presence of the non-symmetrically substituted complex **C** can be ascertained. This isomer exhibits two different methyl resonances and the lack of a C_2-axis gives rise to two resonances for the cage-CH groups in the ^{1}H and ^{13}C NMR spectra. However, not all the peaks could be unambiguously assigned and a distinction between an isomer **A** or **B** was not possible. The alkyne contact carbon resonances between 177.0 and 150.4 ppm all fall in the area expected for a three electron donor.

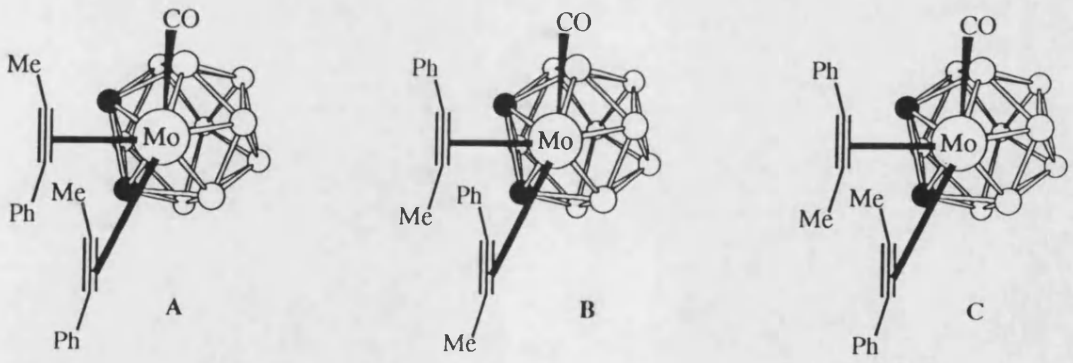

Figure 27, O = BH, ● = CH

In contrast to the analogous cyclopentadienyl complexes, the reaction of the *bis*-alkyne carbonyl complexes **XXXIV**, **18**, and **19** with trimethyl phosphite occurs slowly. Hence, the stepwise nature of the reaction could be investigated thoroughly. After stirring a mixture of compound **18** in CH_2Cl_2 with 2.5 equivalents of $P(OMe)_3$ at room temperature, the IR spectrum of the mixture showed that most of the starting complex had been consumed and one new carbonyl containing product had been formed. Separation of the reaction mixture by column chromatography (CH_2Cl_2/ hexane) yielded the *mono*-phosphite carbonyl complex **20** as the main product. Also isolated were small amounts of starting material (first fraction) and the *bis*-phosphite complex **22** (third fraction). Similarly, compound **XXXIV** reacts with $P(OMe)_3$ to give mainly the *mono*-phosphite complex **21** and small amounts of the *bis*-phosphite complex **24**.

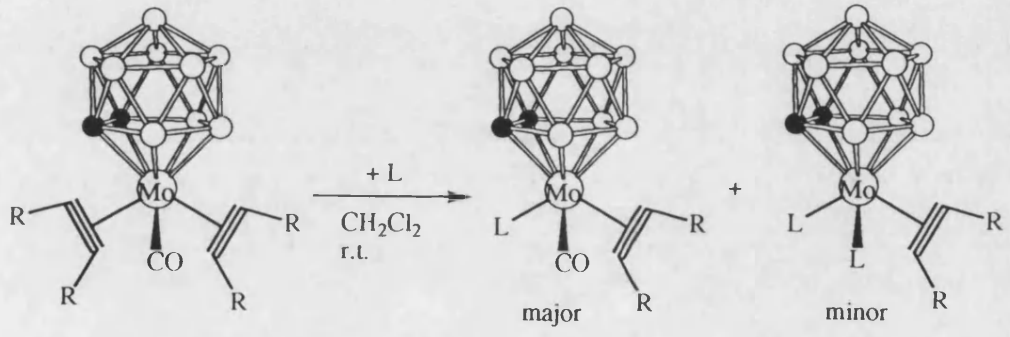

R = Ph **18**
R = Me **XXXIV**

R = Ph **20**
R = Me **21**

R = Ph **22**
R = Me **24**

Scheme 48, ○ = BH, ● = CH, L= $P(OMe)_3$

The blue *mono*-phosphite compounds **20** and **21** are soluble in CH_2Cl_2 and thf, fairly soluble in toluene and insoluble in hexane. Characterisation of **20** and **21** was performed by analytical and spectroscopic methods. The IR spectrum of **20** shows one strong absorption at 1977 cm^{-1} for the carbonyl group, which is also represented as a doublet at 234.2 ppm [J(PH) 19.2 Hz] in the carbon NMR spectrum. In the ^1H NMR spectrum of **20** there are two resonances for the non-equivalent cage C-H atoms at 4.12 and 3.52 ppm, and correspondingly in the ^{13}C-{^1H} NMR spectrum there are two peaks for the carbon atoms of these moieties at 51.1 and 43.9 ppm. A doublet at 3.52 ppm [J(PH) 11.5 Hz] in the proton NMR and a singlet resonance at 162.1 ppm in the ^{31}P-{^1H} NMR spectrum is attributable to the phosphite ligand. Also noteworthy is

that the alkyne ligand seems to be rotating about the metal bonding axis, giving rise to a broad signal at 213.1 ppm in the ^{13}C-{^{1}H} NMR spectrum.

The ^{1}H NMR spectrum of **21** features two broad signals for the cage-CH groups at 3.72 and 2.59 ppm and a doublet for the phosphite protons at 3.49 ppm [*J*(PH) 10.9 Hz]. One singlet for the alkyne methyl groups at 3.20 ppm suggests that the alkyne is rotating. Further support for alkyne rotation is found in the ^{13}C-{^{1}H} NMR spectrum. The alkyne contact carbons show only one resonance at 212.0 ppm and the methyl groups resonate at 19.9 ppm. The ^{31}P-{^{1}H} NMR spectrum exhibits one singlet at 166.3 ppm and in the IR spectrum a carbonyl absorption at 1965 cm^{-1} is found. The ^{11}B NMR spectra of **20** and **21** show broad signals between -3.0 and - 19.9 ppm, an area where resonances for BH groups of metallacarbaboranes are expected.[51]

In order to synthesise the desired *bis*-phosphite complexes mentioned above, the compound **18** was refluxed in CH_2Cl_2 with 2.5 equivalents of $P(OMe)_3$ for 12 hrs, after which the reaction mixture was separated by column chromatography. The major product was the *bis*-phosphite complex **22** and only traces of the *mono*- phosphite complex **20** were found. Accordingly, the analogous *bis*-phosphite complexes **23** and **24** were synthesised in good yields.

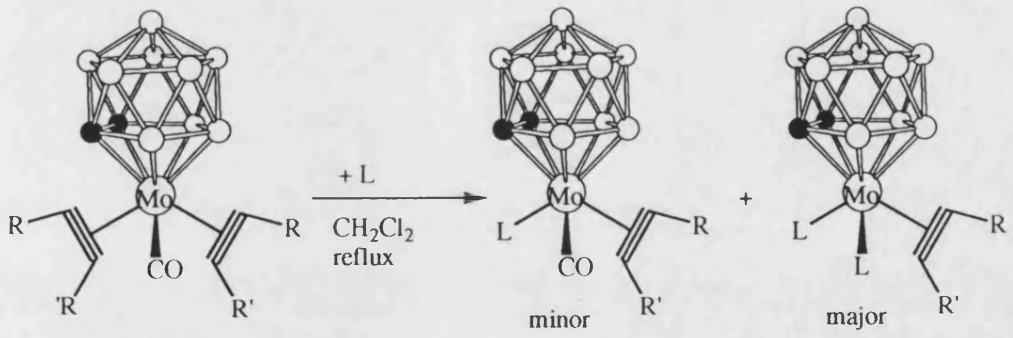

R = R' = Ph **18**
R = Ph, R' = Me **19**
R= R' = Me **XXXIV**

R = R' = Ph **20**
R = R' = Me **21**

R = R' = Ph **22**
R = Ph, R' = Me **23**
R = R' = Me **24**

Scheme 49, ○ = BH, ● = CH, L= $P(OMe)_3$

The green compounds **22** and **23** and the blue compound **24** were readily characterised by elemental analysis and spectroscopy. The NMR spectra of the three complexes

show common features, such as a virtual triplet for 18 phosphite protons in the ^{1}H NMR spectrum at 3.54, 3.59, and 3.52 ppm, respectively, and a broad singlet at 3.13, 3.13, and 2.79 ppm for the two cage C-H groups. The ^{11}B spectra display resonances between -0.7 and -22.5 ppm, characteristic of carbaborane B-H groups,[51] and in the $^{31}P-\{^{1}H\}$ NMR spectra, there is one singlet for the equivalent phosphite moieties found at 174.7, 181.4, and 180.6 ppm, respectively. In the $^{13}C-\{^{1}H\}$ NMR spectra, the alkyne contact carbons in **22, 23** and **24** resonate at low field, thereby confirming that the alkynes act as 4 electron donors. Complex **22** shows a triplet at 220.7 ppm [*J*(PC) 16.3 Hz] indicating that the alkyne is rotating. Compound **23** displays two triplets at 220.7 [*J*(PC) 10.8 Hz] and 217.4 ppm [*J*(PC) 24.4 Hz] due to the asymmetry of the alkyne. For the alkyne contact carbons in **24** a broad singlet was found at 222.0 ppm. However, the methyl groups of the alkyne appear to be equivalent and therefore freely rotating since they give rise to only one singlet at 21.3 ppm in the $^{13}C-\{^{1}H\}$ NMR and one triplet at 3.05 ppm [*J*(PH) 1.3 Hz] in the ^{1}H NMR spectrum.

To shorten the reaction time, the *bis*-alkyne complexes **18** and **XXXIV** were refluxed with $P(OMe)_3$ in toluene. After only 15 minutes the IR spectrum of the reaction mixture showed no peak due to a carbonyl containing product. The main products were the *bis*-phosphite compounds **22** and **24**, respectively, but these reactions led to by-products, which lowered their yield. Consequently, the temperature desired for the preparation of complexes **22** and **24** is no higher than in refluxing CH_2Cl_2. Characterisation of the by-products, which are described in chapter 2.12 gave unexpected insight into the reaction mechanism.

2.12 Mechanistic Investigation of the Reaction of the *bis*-Alkyne Complexes XXXIV and 18 with Trimethylphosphite.

As mentioned in chapter 2.11 and shown in Scheme 50, the reactions of the *bis*-alkyne carbonyl complexes **XXXIV** and **18** with $P(OMe)_3$ in boiling toluene gave the by-products [*closo*-3-(CO)-3,3,3-{$P(OMe)_3$}$_3$-3,1,2-$MoC_2B_9H_{11}$] **25** and [*closo*-3-(η^2-PhC_2Ph)-3,3-{$P(OMe)_3$}$_2$-8-{σ-*trans*-C(Ph)=C(H)Ph}-3,1,2-$MoC_2B_9H_{11}$] **28**, respectively. In this chapter these products will be described, followed by a discussion of a proposed mechanism.

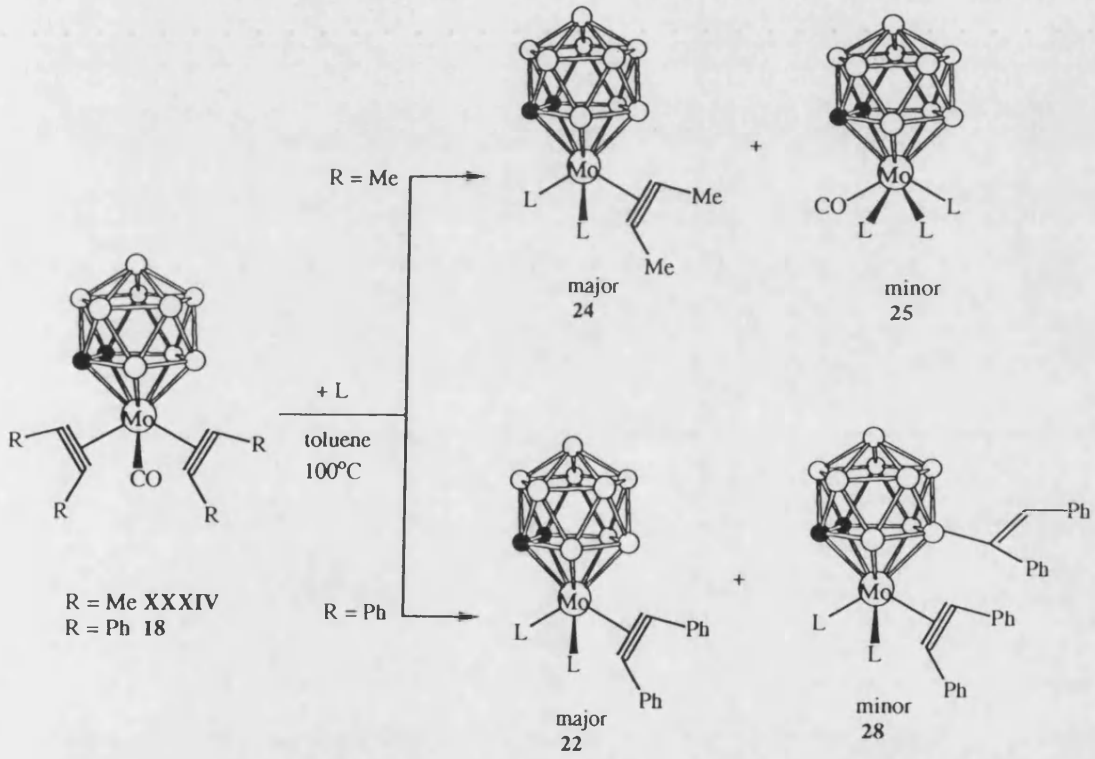

Scheme 50, O = BH, ● = CH, L= $P(OMe)_3$

The complex **25** obtained in *ca* 10 % yield was characterised by elemental analysis and spectroscopy as a molybdenacarbaborane cage with three phosphites and a carbonyl ligand attached to the molybdenum. The ^1H NMR spectrum of **25** displays a multiplet between 3.75 - 3.68 ppm, which integrates to 27 protons and which is apparently a doublet for 9 protons overlapping a virtual triplet for 18 protons. In addition, one broad singlet at 3.06 ppm was found for the two C-H nuclei of the cage vertices.

The ^{31}P-{^{1}H} NMR spectrum is in agreement with the formulation of **25** showing a doublet at 178.1 ppm representing two phosphorus atoms and a triplet at 167.4 ppm representing one phosphorus atom with a coupling constant [*J*(PP)] of 40.8 Hz. The carbonyl ligand is established by its multiplet resonance in the ^{13}C-{^{1}H} NMR spectrum at 249.3 ppm and its absorption at 1878 cm^{-1} in the IR spectrum.

The green complex **28** was isolated from the reaction of **18** with trimethylphosphite in *ca* 15% yield. The structural identity of **28** was not readily discernible from the spectroscopic data and hence a single crystal X-ray diffraction study was undertaken. As is shown in Figure 28, the complex contains a 3,1,2-$MoC_2B_9H_{11}$ cage, in which there are two trimethylphosphite ligands and one diphenylacetylene molecule coordinated to the molybdenum centre. The alkyne, which is η^2(4e)-bonded, is orientated in the solid state such that the C-C bond lies parallel to one of the Mo-P linkages. Importantly, a second diphenylacetylene molecule has undergone a formal *cis*-insertion into an *exo*-polyhedral B-H bond, thus forming an 8-substituted *cis*-BC(Ph)=C(Ph)H group.

The NMR spectra of **28** are similar to those of **22** except for the resonances of the vinyl group present in **28**. In the ^{1}H NMR spectrum the singlet for the vinyl proton can be seen at 5.88 ppm and the integration over the region between 7.50 and 6.06 ppm reveals that there are 20 phenyl protons present. The two vinyl carbon nuclei were not detected in the ^{13}C-{^{1}H} NMR, which is probably due to broadening of the signals through the quadropolar effect of the adjacent ^{11}B nucleus. In the ^{11}B NMR spectrum the characteristic resonance for the boron atom attached to the *exo*-polyhedral organic group is seen at 14.9 ppm.[51] This is also the only signal which does not split into a doublet in the proton coupled spectrum.

Complexes **25** and **28** are such different compounds that it seemed interesting to question the mechanism of their generation. Hence, a series of experiments were carried out, using different alkynes; the results of which are shown in Scheme 51.

Table 5: Selected bond lengths (Å) and angles (°) for **28**

P(1)-Mo	2.427(4)	P(2)-Mo	2.398(4)	B(1)-Mo	2.380(8)	B(2)-Mo	2.441(8)
B(3)-Mo	2.464(9)	C(7)-Mo	2.046(8)	C(8)-Mo	2.026(8)	C(7)-C(8)	1.333(9)
C(35)-Mo	2.407(8)	C(36)-Mo	2.466(8)	B(1)-B(2)	1.825(11)	B(2)-B(3)	1.802(11)
B(1)-C(35)	1.688(11)	B(3)-C(36)	1.662(11)	C(35)-C(36)	1.593(10)	B(2)-C(21)	1.582(10)
C(21)-C(22)	1.362(9)	C(21)-C(23)	1.495(9)	C(22)-C(29)	1.474(9)		

P(1)-Mo-P(2)	84.3(2)	P(1)-Mo-C(7)	91.9(3)	P(1)-Mo-C(8)	93.2(3)
P(2)-Mo-C(7)	76.1(3)	P(2)-Mo-C(8)	114.3(3)	C(7)-C(8)-C(9)	136.4(5)
C(7)-C(8)-C(15)	132.9(5)	B(2)-C(21)-C(22)	118.7(6)	C(21)-C(22)-C(29)	133.2(6)

Complex **22** was heated to 100°C in toluene in the presence of diphenylacetylene and after 30 minutes most of **22** had been converted to **28** (Scheme 51). This reaction proved to be a convenient synthesis of **28**, the yield exceeding 70%. However, in a similar experiment, **22** was heated in the presence of but-2-yne and, surprisingly, the bright yellow complex [*closo*-3-(η^2-MeC_2Me)-3-(η^2-PhC_2Ph)-3-{$P(OMe)_3$}-3,1,2-$MoC_2B_9H_{11}$] **27**, with no *exo*-polyhedral vinyl group, was obtained in almost quantitative yield. Interestingly, **27** contains two different alkynes, a feature which would be difficult to synthesise by another route.

Compound **27** was characterised by elemental analysis and NMR spectroscopy. The ^1H NMR shows, in addition to a multiplet for 10 phenyl protons between 7.47 - 6.89 ppm and two broad singlets for the non-equivalent cage C-H atoms at 3.10 and 2.17 ppm, a broad singlet due to the 6 methyl protons of the but-2-yne at 2.85 ppm. In the ^{31}P-{^1H} NMR there is, as expected for **27**, one singlet at 160.6 ppm. In the ^{11}B spectrum were several resonances found between -2.0 and -20.6 ppm. All signals split into doublets in a proton coupled spectrum, thus showing that there is no organic fragment attached to a boron. The ^{13}C-{^1H} NMR spectrum of **27** shows three resonances for alkyne contact carbons acting as three electron donors. The doublets at 166.7 ppm [*J*(PC) 8.1 Hz] and 146.7 ppm [*J*(PC) 27.1 Hz] were assigned to the diphenylacetylene moiety, assuming the alkyne is not rotating. A doublet at 141.0 ppm [*J*(PC) 10.8 Hz] was attributed to the quaternary carbons of the but-2-yne, which is rotating round the metal alkyne bond. Additional support for this assignment is provided by the observation that only one singlet at 19.1 ppm for the methyl groups of the but-2-yne was found.

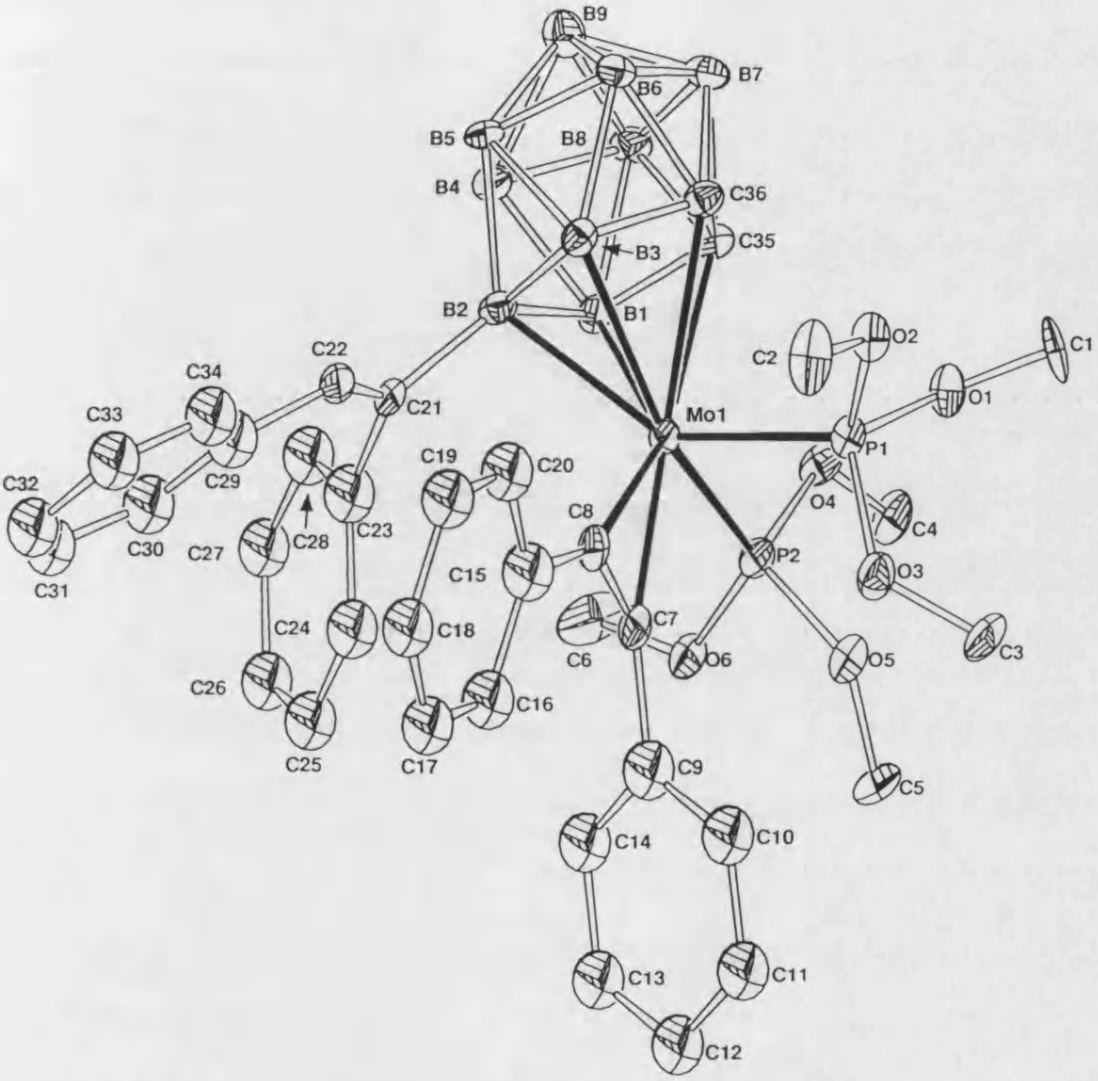

Figure 28: ORTEP drawing of **28**

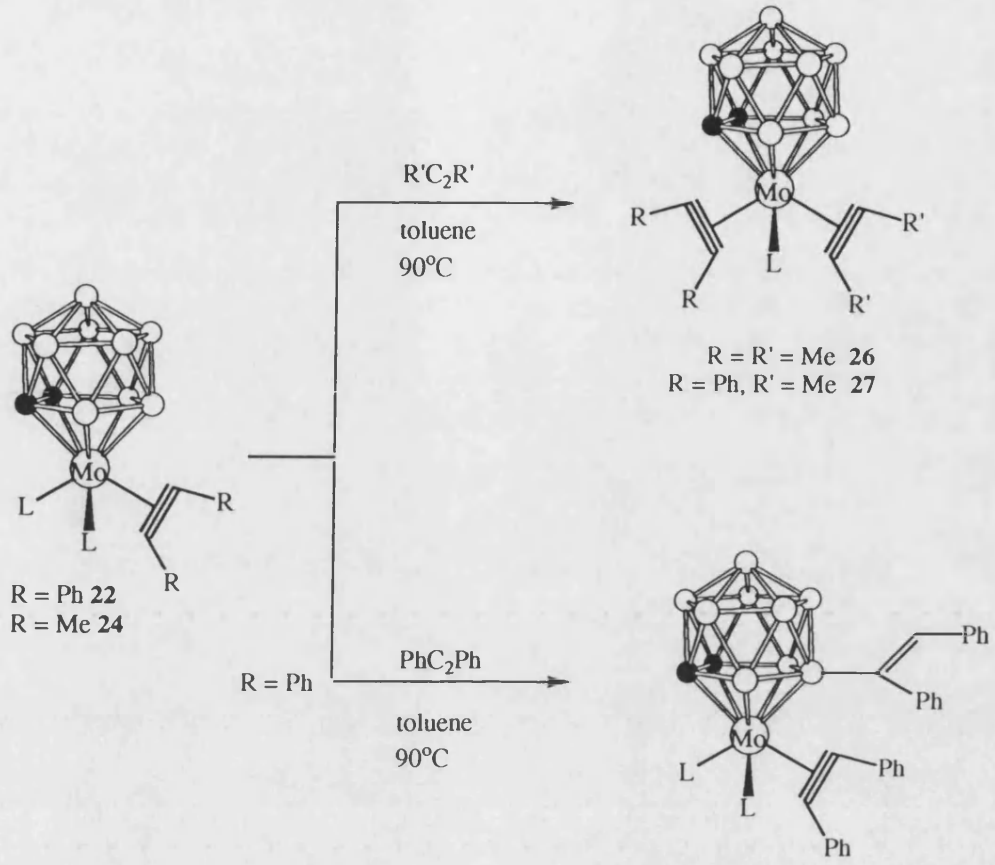

Scheme 51, ○ = BH, ● = CH, L= $P(OMe)_3$

In a complimentary experiment the but-2-yne complex **24** was treated with diphenyl-acetylene in toluene at 100°C. Again, the mixed alkyne complex **27** was generated, but the reaction was considerably slower and not as clean as the earlier experiment. It is important to note, however, that ^{11}B NMR spectroscopy did not indicate any product with an organic fragment attached to a boron atom. In another experiment, **24** was heated to 100°C in the presence of but-2-yne. Within 10 minutes one phosphite ligand had been replaced, giving rise to an almost quantitative yield of the *bis*-but-2-yne *mono*-phosphite complex [*closo*-3,3-(η^2-$MeC_2Me)_2$-3-{$P(OMe)_3$}-3,1,2-$MoC_2B_9H_{11}$] **26**. Also, in this experiment no product with an *exo*-polyhedral group was generated, as evidenced by ^{11}B NMR spectroscopy.

Compound **26** was characterised by its elemental analysis and NMR data. The ^1H NMR spectrum shows a doublet at 4.36 ppm [*J*(PH) 10.4 Hz] for the 9 phosphite

protons and a broad singlet at 2.40 ppm for the two cage C-H groups. The methyl groups give rise to two singlets, at 3.30 and 2.86 ppm, indicating that the but-2-yne ligands are not rotating. This can also be concluded from the ^{13}C-{^{1}H} NMR spectrum, which shows two signals for the methyl groups, i.e. a doublet at 16.6 ppm [*J*(PC) 6.1 Hz] and a singlet at 17.1 ppm. The alkyne contact carbons resonate as doublets at 180.7 ppm [*J*(PC) 8.1 Hz] and 154.1 ppm [*J*(PC) 29.8 Hz], an area characteristic for alkynes donating three electrons to a transition metal. In the ^{31}P-{^{1}H} NMR spectrum, one singlet was observed at 167.6 ppm. The ^{11}B NMR spectrum shows only signals between -2.2 and -21.4 ppm, characteristic for carbaborane B-H groups.[51]

The experiments described in this chapter and shown in Scheme 50 and Scheme 51 can be summarised as follows. In the *mono*-phosphite carbonyl alkyne complex **21** the carbonyl as well as the alkyne moiety can be replaced by trimethylphosphite. In the *bis*-phosphite alkyne complexes **22** and **24** one phosphite ligand is easily replaced by but-2-yne. However, replacement of a phosphite moiety by diphenylacetylene in complex **24** occurs slowly, whereas in complex **22** no phosphite ligand is replaced, but a diphenylacetylene molecule inserts into an *exo*-polyhedral B-H bond to give **28**.

Although there are a number of reported examples[50, 51] of alkylidene and alkylidyne ligands formally 'inserting' into an *exo*-polyhedral B-H bond of a metallacarbaborane there are only two examples of the 'insertion' of an alkyne. Firstly, it has been reported[57] that the complex [*closo*-1,2-Me_2-3-(η^2-PhC_2Ph)-3-(CO)-3-(PPh_3)-3,1,2-$MoC_2B_9H_9$] **LXXI** decomposes in solution to give an inseparable mixture of [*closo*-1,2-Me_2-3,3,3-$(CO)_3$-3-(PPh_3)-3,1,2-$MoC_2B_9H_9$] **LXXII** and [*closo*-1,2-Me_2-3,3-

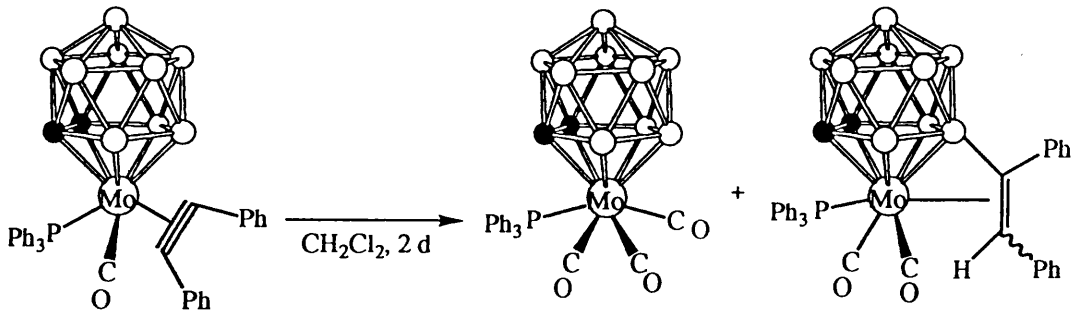

LXXI **LXXII** **LXXIII**

Scheme 52, O = BH, ● = CMe

$(CO)_2$-3-(PPh_3)-8,3-{σ:η^2-C(Ph)=CHPh}-3,1,2-$MoC_2B_9H_8$] **LXXIII**, where the stereochemistry of the B-vinyl group was not defined (Scheme 52).

Secondly, the insertion of a silyl-substituted alkyne has been observed in the rearrangement of [*closo*-1,2-Me_2-3,3-(η^2-$Me_3SiC_2H)_2$-3-(CO)-3,1,2-$MoC_2B_9H_9$] **LXXIV** into the *trans*-vinyl substituted cage [*closo*-1,2-Me_2-3,3-(η^2-Me_3SiC_2H)-3-(CO)-8,3-{σ:η^2-*trans*-CH=C($SiMe_3$)H}-3,1,2-$MoC_2B_9H_8$] **LXXV**.[57] However, this reaction has been shown to involve the initial rearrangement of an η^2-bonded Me_3SiC_2H into the vinylidene Mo=C=C($SiMe_3$)H, and can therefore be viewed as a further example of the insertion of an alkylidene into a B-H bond.

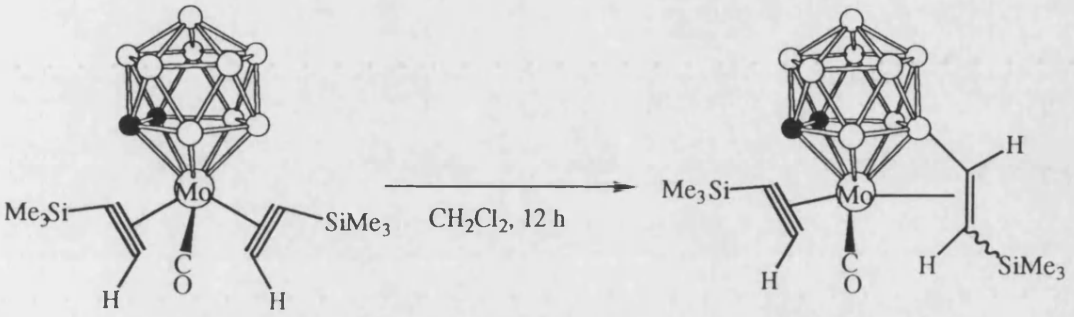

LXXIV **LXXV**

Scheme 53, O = BH, ● = CMe

Clearly, the formation of the complex **28** is unlikely to involve an analogous phenyl migration to give Mo=C=CPh_2, and even if this was the case it would then be difficult to explain the regio-selective formation of a *cis*-BC(Ph)=C(Ph)H group.

The studies discussed earlier in this section have shown that the phosphite ligands in the *bis*-phosphite complexes are labile and it is, therefore, likely that an initial step in the generation of **28** is the dissociation of a phosphite ligand from **22**. It has been shown by Stone[50, 51] and coworkers that unsaturated carbaborane species can be stabilised by dimerisation. One example is illustrated in Scheme 54. Protonation of the tungsten alkylidyne complex [A][*closo*-3,3-$(CO)_2$-3-(≡CR)-3,1,2-$WC_2B_9H_{11}$] {A= NEt_4, $N(PPh_3)_2$, PPh_4} **XXVII** with 0.5 equivalents of $HBF_4.Et_2O$ generates an unsaturated carbene species, which then is stabilised by formation of the dimeric complex **LXXVI**.[98]

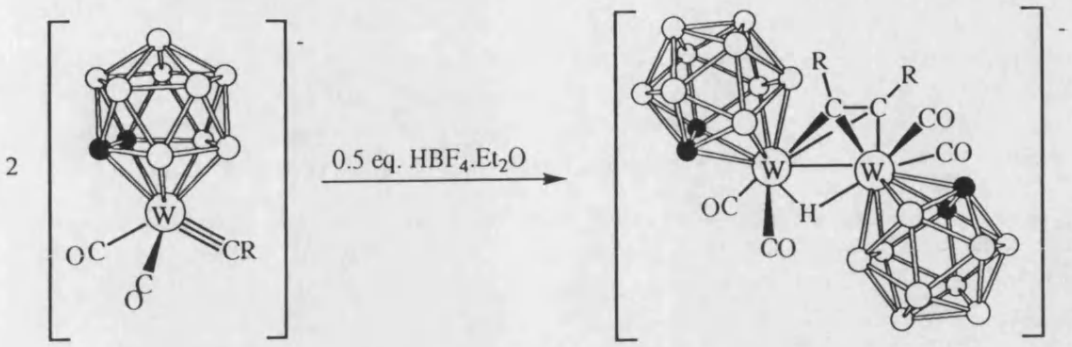

XXVII **LXXVI**

Scheme 54, ○ = BH, ● = CH

An alternative way in which a coordinatively unsaturated metal species can be stabilised has been demonstrated by Hawthorne and co-workers[99] for the rhodium carbaborane species [*closo*-3,3-$(PPh_3)_2$-3-H-3,1,2-$RhC_2B_9H_{11}$]. This involves a *closo*/*exo-nido* equilibrium process (Scheme 55). However, this process is favoured for metals with a configuration higher than d^6 (section 1.2).

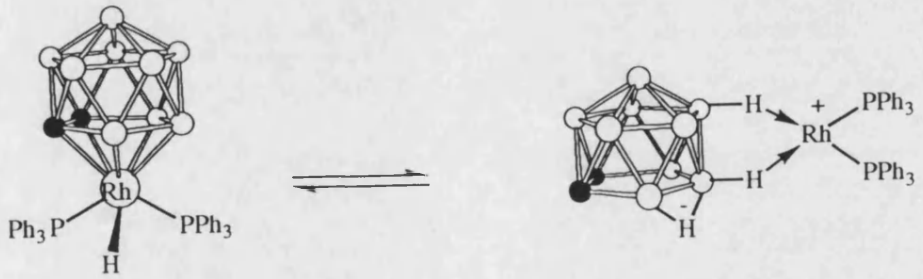

closo *exo-nido*

Scheme 55, ○ = BH, ● = CH

It is reasonable, therefore, to suggest that the formation of **28** requires the involvement of two metal centres. Thus, it is proposed that in solution at 90°C the complex **22** is in equilibrium with free $P(OMe)_3$ and the 16e species [*closo*-3-(η^2-PhC_2Ph)-3-{$P(OMe)_3$}-3,1,2-$MoC_2B_9H_{11}$], which is stabilised by dimerisation assisted by the establishment of an agostic B(μ-H)Mo interaction. As is shown in Scheme 56 the resulting dimer **A** contains two diphenylacetylene ligands, η^2(4e)- and η^2(2e)-bonded to adjacent molybdenum centres. Complete transfer of the hydrogen, which is involved in the original agostic interaction to the second metal centre, then affords

intermediate **B**, in which there is an η^2(2e) bonded alkyne adjacent to a Mo-H bond. Coordination of trimethylphosphite to this metal centre would then be expected to promote migration (**B**→**C**) of the hydrogen from the metal to the coordinated alkyne thus generating **C**, in which there are now boron-molybdenum and *cis*-MoC(Ph)= C(Ph)H fragments in a *cis*-configuration relative to each other. The boron-vinyl moiety present in the final product **28** can then be generated by a reductive elimination step (**C**→**D**), which is followed by disproportionation of **D** in the presence of

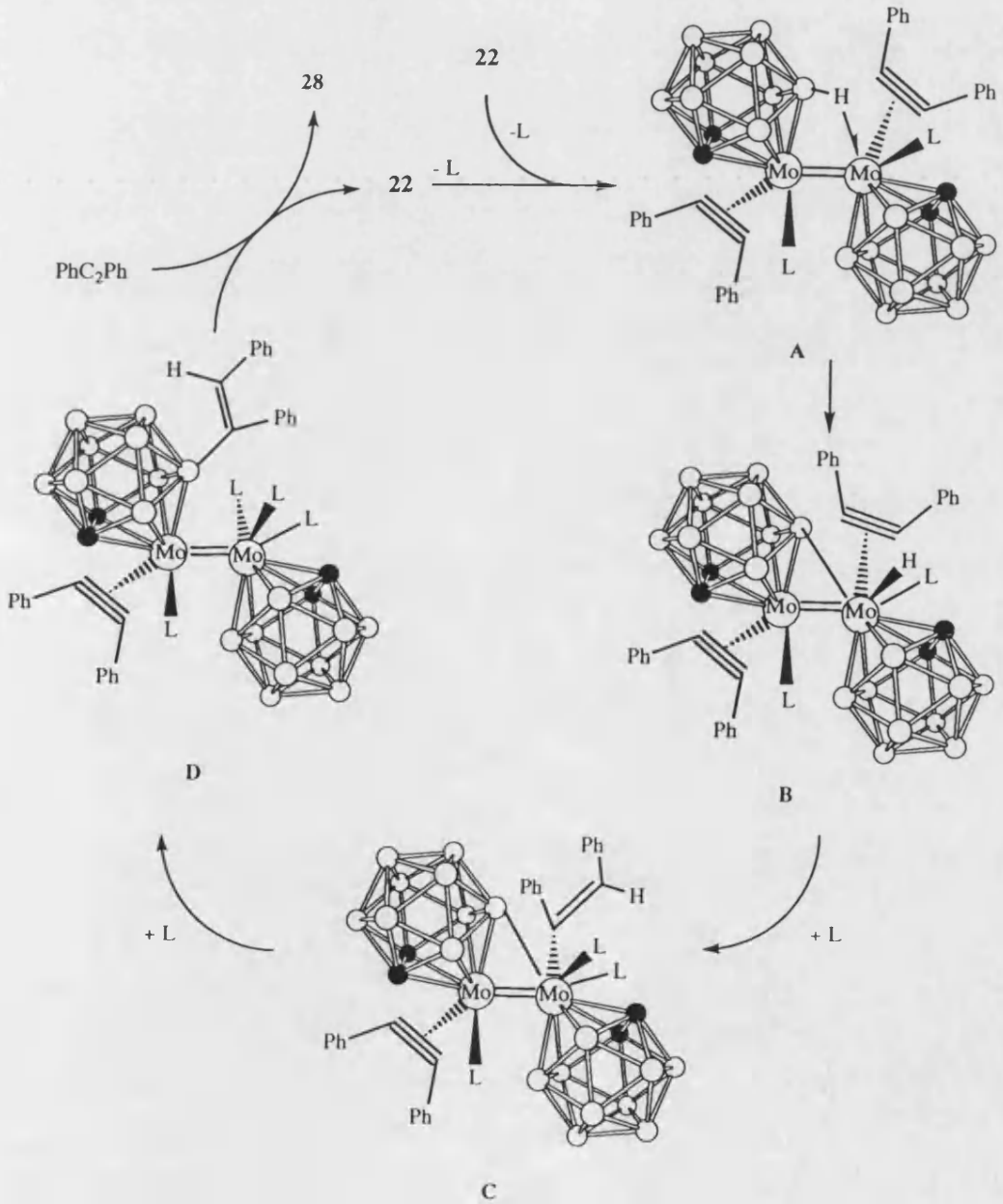

Scheme 56, ○ = BH, ● = CH, L= $P(OMe)_3$

diphenylacetylene to give **18** and **28**. In this way all of complex **18** is converted into **28** *via* a reaction sequence which involves the interplay of two metal centres, and where the *cis*-vinyl group is created at one centre before transfer to a cage boron. Thus, the overall effect is to achieve a formal hydroboration of an alkyne.

With this insight it may be suggested that related dinuclear pathways are also involved in the reactions observed by Stone and coworkers where there is an apparent 'insertion' of alkylidene, alkylidyne[50, 51] and also norbornadiene[100] into an *exo*-BH bond of a variety of metallacarbaboranes.

2.13 Reaction of [*closo*-3,3-(η^2-$PhC_2Ph)_2$-3-(CO)-3,1,2-$MoC_2B_9H_{11}$] 18 with Acetonitrile.

In cyclopentadienyl molybdenum chemistry the reaction of the *bis*-alkyne carbonyl cation $[Mo(CO)(\eta^2\text{-}RC_2R')_2(\eta\text{-}C_5H_5)][BF_4]$ with acetonitrile yields the corresponding acetonitrile complex $[Mo(NCMe)(\eta^2\text{-}RC_2R')_2(\eta\text{-}C_5H_5)][BF_4]$.[15] It was, therefore, expected that the reaction of [*closo*-3,3-(η^2-$PhC_2Ph)_2$-3-(CO)-3,1,2-$MoC_2B_9H_{11}$] **18** with acetonitrile would give the analogous carbaborane complex, which could be a valuable starting material for the preparation of anionic *bis*-alkyne halogeno complexes.

Complex **18** was refluxed in acetonitrile for 12 hours whereupon the colour had changed from yellow to green. The reaction mixture was cooled to room temperature and after 24 hours a yellow precipitate had formed. The supernatant solution was decanted, the residue dissolved in CH_2Cl_2 and carefully columned on alumina with CH_2Cl_2/hexane to give two fractions with similar properties. The first contained the expected acetonitrile complex [*closo*-3,3-(η^2-$PhC_2Ph)_2$-3-(NCMe)-3,1,2-$MoC_2B_9H_{11}$] **29** (9%), while the second fraction gave [*closo*-3,3-(η^2-$PhC_2Ph)_2$-3-$(NCMe)_2$-8-{σ-*trans*-C(Ph)=C(H)Ph}-3,1,2-$MoC_2B_9H_{10}$] **30** (25%) with an *exo*-polyhedral vinyl group (Scheme 57). The complex **30** can be prepared in good yields by refluxing **18** with an excess of diphenylacetylene in acetonitrile. In this preparation the compound **29** is formed in minor quantities.

The complexes **29** and **30** were characterised by their spectroscopic and analytical data. The NMR data for both compounds show similarities. For example, the two cage C-H groups resonate as one broad singlet at 2.74 ppm in **29** and 2.70 ppm in **30**. A singlet for the acetonitrile ligand is found at 2.01 ppm in **29** and at 1.71 ppm in **30**. Also, both compounds exhibit only one alkyne contact carbon resonance in the $^{13}C\text{-}\{^1H\}$ NMR spectrum (at 180.2 and 178.5 ppm, respectively), a shift which is attributable to alkynes donating three electrons to a complex. Differences in the NMR spectra arise from the *exo*-polyhedral vinyl group in **30**. In the ^1H NMR spectrum the signal for the vinyl proton is seen at 6.50 ppm and the integration of the multiplet between 7.45 and 6.74 ppm shows that 30 phenyl protons are present in **30**. No signals due to the vinyl group were found in the $^{13}C\text{-}\{^1H\}$ NMR spectrum, probably

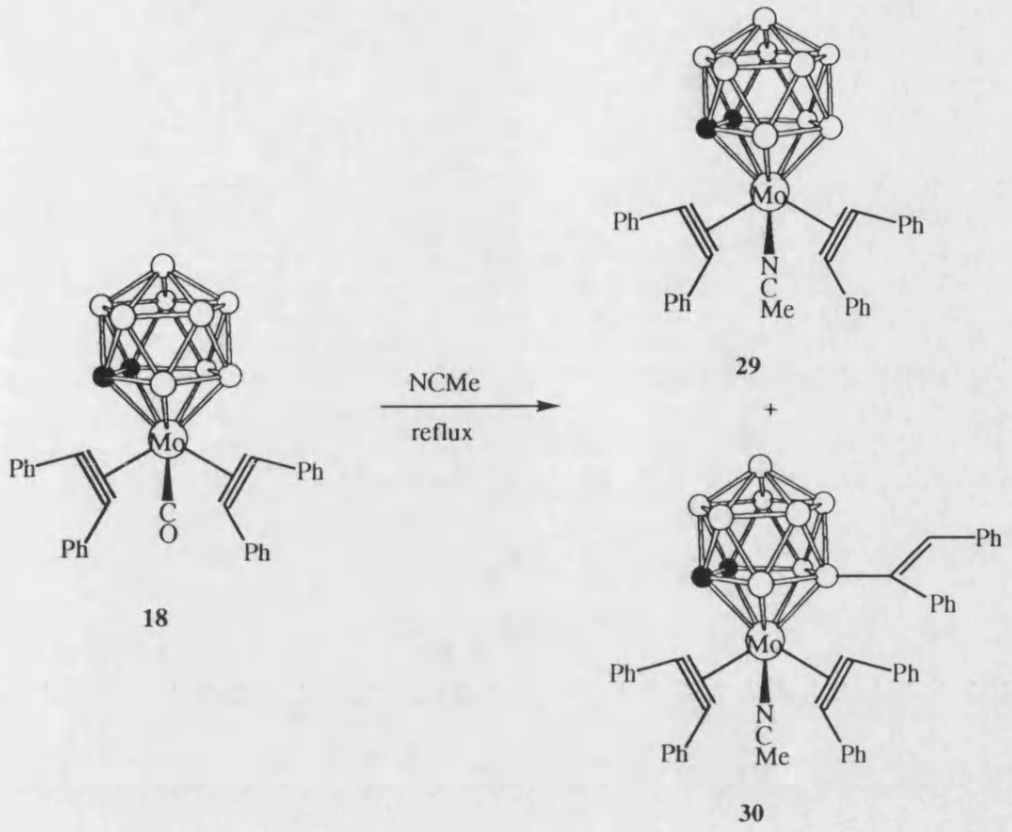

Scheme 57, ○ = BH, ● = CH

because of the quadrupolar effect of the adjacent boron atom. In the boron spectrum a resonance at 8.7 ppm characteristic for a boron nucleus attached to an organic fragment is found.[51]

Compound **30** was also subjected to an X-ray diffraction study, which confirmed that, like in complex **28**, a formal *cis*-hydroboration had occurred leading to an *exo*-polyhedral vinyl group. Figure 29 shows an ORTEP plot of **28** and Table 6 lists selected bond lengths and angles. Although metal alkyne and *intra*-alkyne bond lengths are not an adequate probe for the type of bonding, there is a significant difference in bond length of the alkynes. One alkyne shows a distance typical for a two electron donor [Mo-C(1), 2.10(1); Mo-C(2), 2.12(1) Å], while the other alkyne exhibits distances which are characteristic for a four electron donor alkyne [Mo-C(3), 2.02(1); Mo-C(4), 2.01(2) Å]. However, this feature has little effect on the alkyne C-C-distances [C(1)-C(2), 1.28(2); C(3)-C(4), 1.26(2)]. Also, both alkyne ligands lie approximately parallel to the Mo-N vector, a characteristic, which was discussed in the introduction for the analogous complex $[Mo(L)(\eta^2\text{-}MeC_2Me)_2(\eta\text{-}C_5H_5)]^+$.

It seems reasonable to believe that the observations and assumptions made in the last section concerning the formation of an *exo*-polyhedral vinyl group also apply for the generation of **30**. It is, therefore, likely that the mechanism involves a dimeric species, in which a diphenylacetylene unit is transferred from one metal center to the adjacent carbaborane cage.

Table 6: Selected bond lengths (Å) and angles (°) for **30**.

Mo-N	2.13(1)	N-C(8)	1.11(2)	Mo-C(1)	2.10(1)	Mo-C(2)	2.12(1)
Mo-C(3)	2.02(1)	Mo-C(4)	2.01(2)	Mo-C(1')	2.46(2)	Mo-C(2')	2.49(2)
Mo-B(6)	2.46(1)	Mo-B(7)	2.44(2)	Mo-B(8)	2.44(1)	C(1)-C(2)	1.28(2)
C(3)-C(4)	1.26(2)	B(8)-C(5)	1.57(3)	C(5)-C(6)	1.37(2)		

N-Mo-C(1)	112.5(5)	N-Mo-C(2)	78.8(5)	N-Mo-C(3)	114.1(6)
N-Mo-C(4)	77.6(6)	B(8)-C(5)-C(6)	119.5(14)	C(5)-C(6)-C(39)	130.2(13)
C(1)-Mo-C(3)	88.1(6)	C(2)-Mo-C(4)	105.0(6)		

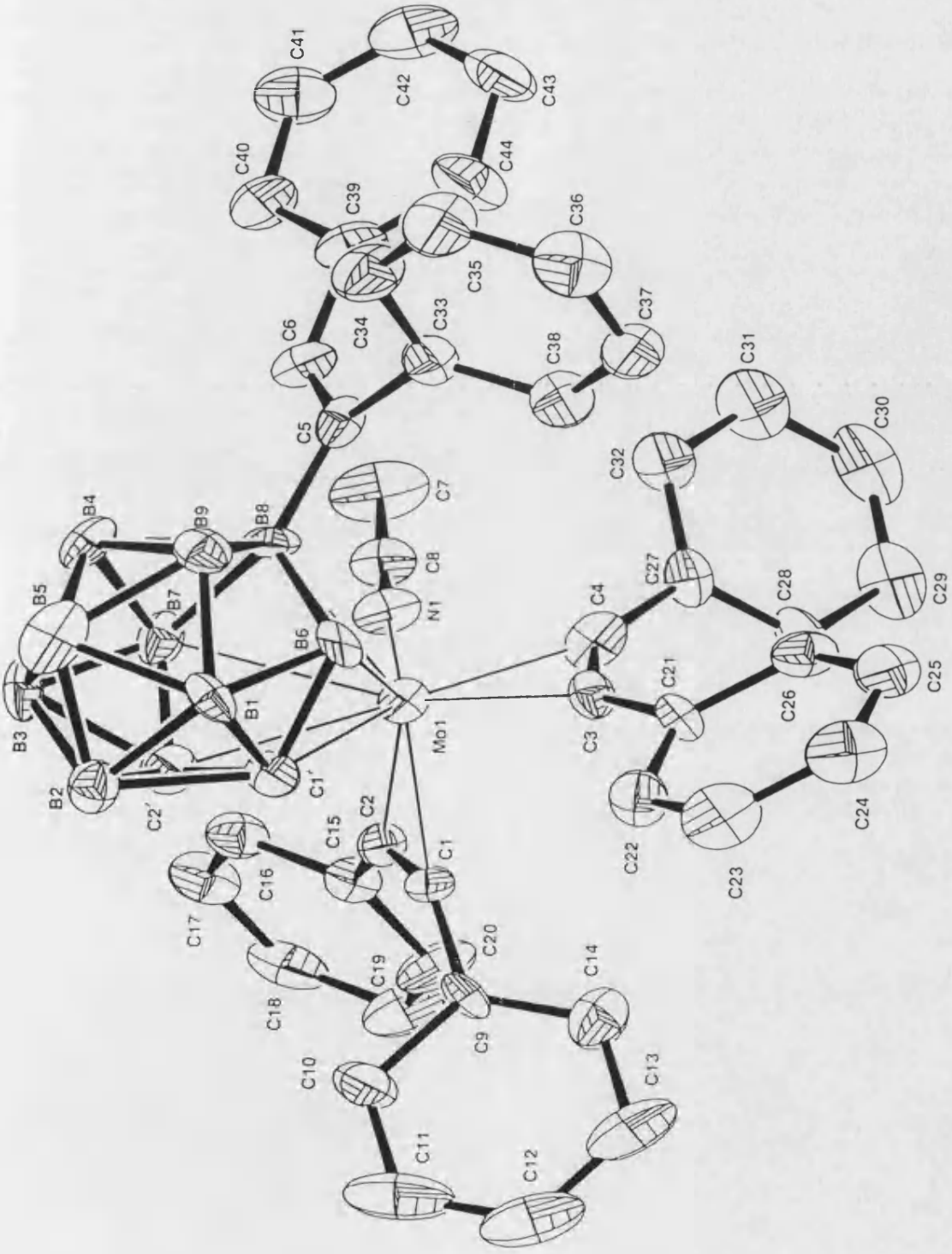

Figure 29: ORTEP drawing of **30**.

2.14 Synthesis of a 1,3-Diphosphacyclobutadiene Carbaborane Complex

The interest in complexes containing phosphaalkynes donating more than two electrons was mentioned earlier and a successful synthetic approach was presented in section 2.8. However, an attempt to access complexes of this type had focused on the reaction of $Bu^tC{\equiv}P$ with *cis*-$[Mo(NCMe)_2(CO)_2(\eta^5\text{-}C_9H_7)][BF_4]$ **LXXVII** in the expectation of obtaining the cation $[Mo(\eta^2\text{-}Bu^tCP)_2(CO)(\eta^5\text{-}C_9H_7)][BF_4]$ **LXXVIII**. As has been reported by Nixon *et al*[101] a facile cyclodimerisation reaction occurs leading to the formation of $[Mo\{\eta^3\text{-}(Bu^tCPC(Bu^t)PFBF_3\}(CO)_2(\eta^5\text{-}C_9H_7)]$.

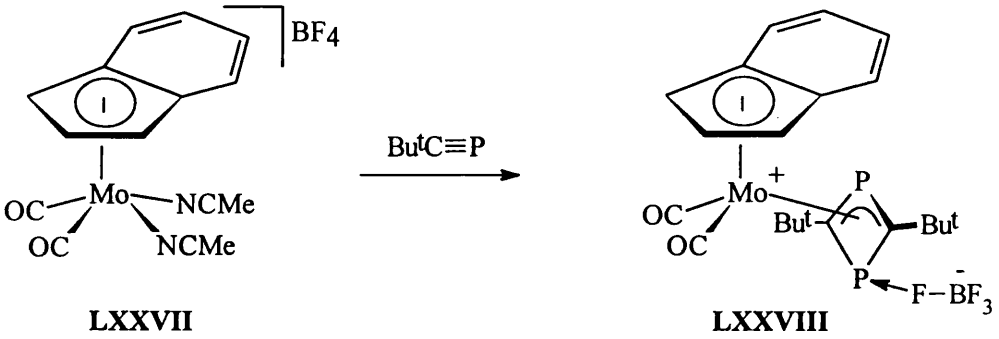

LXXVII **LXXVIII**

Scheme 58

In section 2.11 the preparation of alkyne molybdenacarbaborane complexes *via* protonation of the anionic allyl complex **XXXII** in presence of an alkyne was described. In light of this it was felt that the carbaborane complex containing two η^2(3e) phosphaalkyne units may be synthesised by this route. An advantage could be that the product is neutral and unlike the aforementioned indenyl analogue no interference of a counter anion was anticipated.

The anionic complex **XXXII** in CH_2Cl_2 was treated with one equivalent $HBF_4.Et_2O$. Once the protonation became apparent, two equivalents of phosphaalkyne were added. Following an immediate colour change to bright yellow an IR spectrum was recorded. This showed two carbonyl absorptions at 2049 and 2012 cm^{-1}. From the reaction mixture, the complex [*closo*-3,3-$(CO)_2$-3-$\{\eta^4\text{-}P_2C_2(Bu^t)_2\}$-3,1,2-$MoC_2B_9H_{11}$] **31** was isolated as a bright yellow air stable powder.

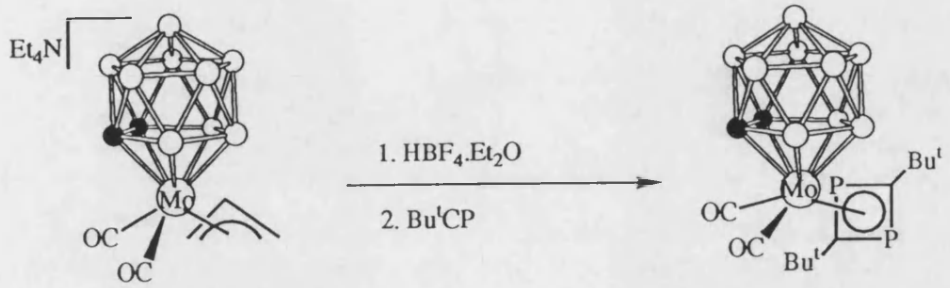

XXXII **31**

Scheme 59, ○ = BH, ● = CH

The nature of compound **31** did not become apparent until an X-ray diffraction study was carried out. Single crystals suitable for X-ray diffraction were obtained by slowly cooling a saturated solution of **31** in CH_2Cl_2/toluene (1:1).

Once the structure of **31** had been established, the spectroscopic data could be readily interpreted. For example, the ^1H NMR spectrum shows a broad singlet at 3.70 ppm due to the two cage C-H protons and a singlet for the 18 protons of the *tert*-butyl groups. In the ^{13}C-{^1H} NMR spectrum, the two carbonyl ligands resonate at 217.4 ppm and the signal for the cage carbons is found at 42.7 ppm. Triplets due to the *di*-phosphacyclobutadienyl ligand are found in the ^{13}C-{^1H} NMR spectrum at 110.3 ppm (55.1 Hz), at 37.1 ppm (7.1 Hz), and 33.2 ppm (5.6 Hz). The first signal can be assigned to the ring carbons, the second to the quaternary carbon of the *tert*-butyl group and the last to the methyl groups. The observed couplings are clearly derived from the two phosphorus nuclei. However, no peak was found in the ^{31}P-{^1H} NMR between -500 and +500 ppm even when the spectra were recorded at temperatures as low as -80°C. The reason why no phosphorus resonance can be detected is as yet unknown.

The X-ray diffraction study unveiled a unit cell with two independent molecules having essentially the same geometry. Hence, only the data of one molecule will be discussed. The molybdenum is η^4-coordinated by the butadienyl ring and η^5-coordinated by the icosahedral [*nido*-$C_2B_2H_{11}$] fragment. The dihedral angle between the diphosphacyclobutadiene plane (P1, P2, C3, C4) and the carbaborane plane (C13, C14, B1, B2, B3) is 34.68° allowing two CO molecules to be coordinated to the

molybdenum. In the diphosphacyclobutadienyl ring the P-C distances are closely similar, averaging 1.785Å. These distances reflect partial double bond character of these bonds in the four membered ring.

This attempt to access complexes containing phosphaalkyne ligands donating more than two electrons to a transition metal centre has failed due to the well documented tendency of phosphaalkynes to dimerise. There are several diphosphacyclobutadienyl complexes known, some of which have been characterised by X-ray diffraction studies.[102] Stone and coworkers reported in 1990 that the reaction of the carbaborane anion [*closo*-3,3-$(PPh_3)_2$-3,1,2-$RhC_2B_9H_{11}$]$^-$ **LXXIX** with $Bu^tC{\equiv}P$ leads to the formation of a diphosphacyclobutadienyl ligand in the coordination sphere of the rhodium atom and the formation of [*closo*-3-{η^4-$P_2C_2(Bu^t)_2$}-3,1,2-$RhC_2B_9H_{11}$]$^-$ **LXXX**.[103]

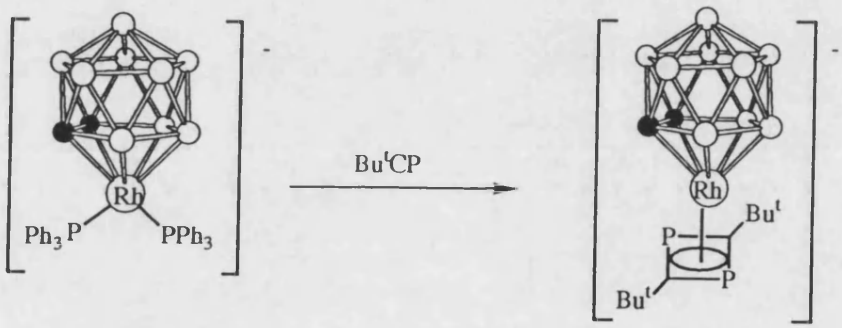

LXXIX **LXXX**

Scheme 60, ○ = BH, ● = CH

Table 7: Selected bond lengths (Å) and angles (°) for **31**.

Mo-P(1)	2.565(2)	Mo-P(2)	2.529(2)	Mo-C(1)	1.995(7)	Mo-C(2)	1.994(8)
Mo-C(3)	2.355(6)	Mo-C(4)	2.366(7)	Mo-C(13)	2.393(7)	Mo-C(14)	2.406(7)
Mo-B(1)	2.403(8)	Mo-B(2)	2.381(8)	Mo-B(3)	2.395(8)	P(1)-C(3)	1.769(7)
P(1)-C(4)	1.761(6)	P(2)-C(3)	1.805(6)	P(2)-C(4)	1.806(7)	C(3)-C(5)	1.517(9)
C(4)-C(9)	1.520(10)	C(13)-C(14)	1.629(9)	C(13)-B(3)	1.684(12)	C(13)-B(6)	1.736(11)
C(14)-B(1)	1.677(11)	B(1)-B(2)	1.838(13)	B(2)-B(3)	1.855(11)		

P(1)-C(3)-P(2)	95.5(3)	P(1)-C(4)-P(2)	95.7(3)	P(1)-C(3)-C(5)	126.9(5)
P(2)-C(3)-C(5)	131.0(5)	P(1)-C(4)-C(9)	127.2(5)	P(2)-C(4)-C(9)	130.4(5)
C(1)-Mo-C(2)	81.1(3)	C(1)-Mo-cB[a)]	108.0(2)	C2-Mo-cB	108.3(2)
cB-Mo-cP[a)]	141.7(3)				

a) cB and cP are the centroids of the C_2B_3 face of the carborane and the P_2C_2 ring respectively.

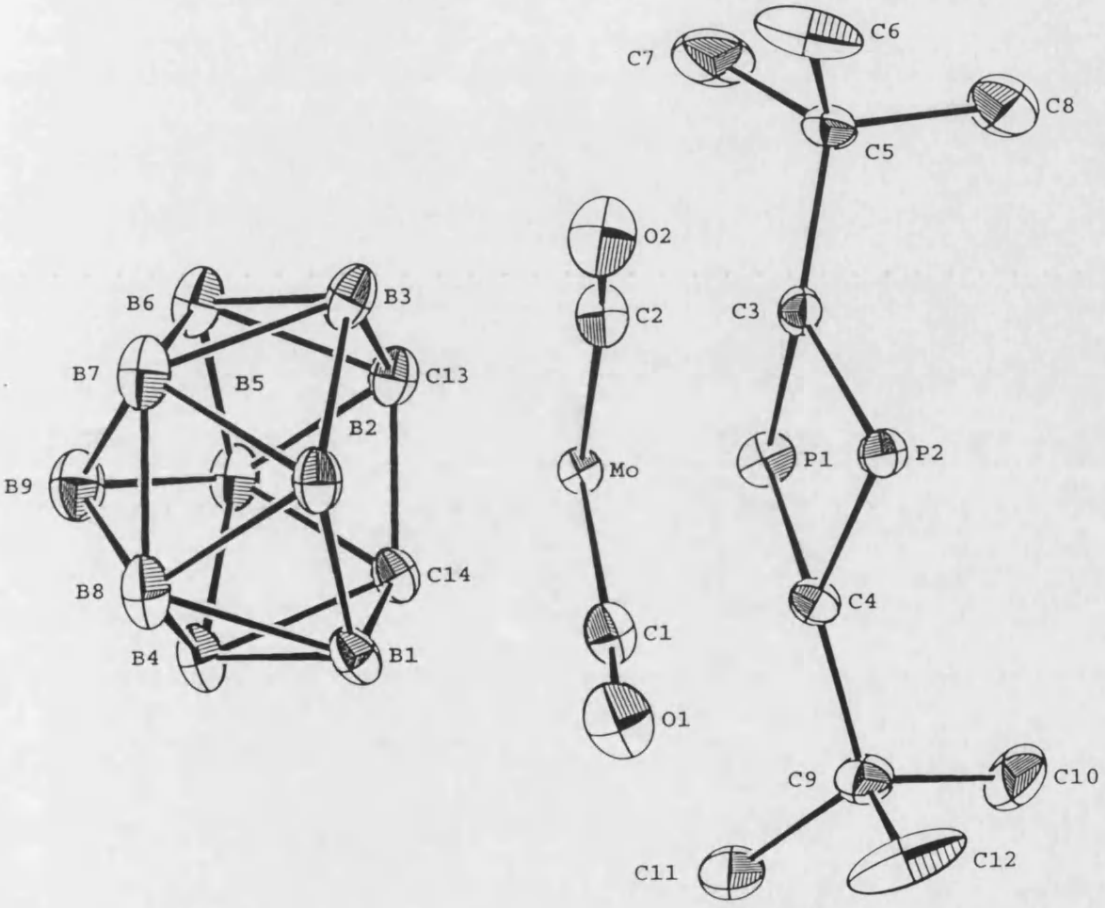

Figure 30: ORTEP drawing of **31**.

3. Experimental Section

General Experimental Procedures

All reactions were carried out under an atmosphere of dry, oxygen-free nitrogen, using standard Schlenk techniques. All solvents used were deoxygenated and dried by standard literature methods.[104]

NMR spectra were recorded on Jeol JNM GX270 (270 MHz) or Jeol EX400 (400MHz) Fourier transform spectrometers. NMR spectra are referenced to the following standards: ^{1}H Me_4Si; ^{13}C Me_4Si; ^{31}P 85% H_3PO_4; ^{11}B, $BF_3.Et_2O$; ^{19}F, $CFCl_3$.
Infrared spectra were recorded on a Nicolet 510P FT-IR spectrometer. The samples were dissolved in the stated solvents and the absorption recorded using sodium chloride cells.
Microanalyses were determined in School of Chemistry, University of Bath.

Preparation of Starting Materials

The following compounds were prepared according to the published literature procedures:
$[Mo(\eta^2\text{-}PhC_2Ph)\{P(OMe)_3\}_2(\eta\text{-}C_5H_5)][BF_4]$ **XI** [15]
$[Mo(NCMe)(\eta^2\text{-}PhC_2Ph)_2(\eta\text{-}C_5H_5)][BF_4]$ **LXIX** [15]
$CH_2(MgI)_2$ [71]
$[Mo(\eta^3\text{-}C_3H_4Me)\{P(OMe)_3\}_2(\eta\text{-}C_5H_5)]$ **XIII** [30]
$[NEt_4][closo\text{-}3,3\text{-}(CO)_2\text{-}3\text{-}(\eta^3\text{-}C_3H_5)\text{-}3,1,2\text{-}MoC_2B_9H_{11}]$ **XXXII** [56]
$[closo\text{-}3,3\text{-}(\eta^2\text{-}MeC_2Me)_2\text{-}3\text{-}CO\text{-}3,1,2\text{-}MoC_2B_9H_{11}]$ **XXXIV** [57]
$Bu^tC{\equiv}P$ was kindly donated by Professor J. F. Nixon (University of Sussex).

All other compounds and reagents were obtained from comercial sources and were used as received unless otherwise indicated. Chromatography was carried out on Aldrich Alumina (Brockman III).

3.1 Preparation of [Mo(η^2-PhC_2Ph)(Et){$P(OMe)_3$} (η-C_5H_5)] 1.

A solution of EtMgBr (0.7ml, 1M in Et_2O) was added at 0°C to a stirred suspension of [Mo(η^2-PhC_2Ph){$P(OMe)_3$}$_2$(η-C_5H_5)][BF_4] **XI** (0.237ml , 0.35mmol) in 10 ml thf. The colour changed immediately to dark green. After stirring the suspension for 5 min. at room temperature it was filtered through alumina and the solvent was removed *in vacuo*. The residue was dissolved in toluene and columned on alumina (10 cm) with toluene/hexane (1:1) to give one green band which afforded dark green crystals of **1** from pentane at -30°C (0.117g, 68%). Anal: Found: C, 58.3; H, 5.98; $C_{24}H_{29}MoO_3P$ requires C, 58.5; H, 5.94%.
NMR: ^{1}H (C_6D_6): δ 7.91-7.09 (m, 10 H, Ph), 5.08 (s, 5 H, C_5H_5), [3.26 d, *J*(PH) 10.8, 9 H, POMe], 1.52-1.73 (m, 5 H, Et); ^{13}C-{^{1}H} (C_6D_6): δ 202.8 (s, *C*≡C), 201.3 [d, *J*(PC) 10.6, C≡*C*], 139.5-125.5 (s, Ph), 90.9 (s, C_5H_5), 51.9 [d, *J*(PC) 5.5, POMe], 27.3 [d, *J*(PC) 5.5, Me], 9.6 [d, *J*(PC) 13.6, CH_2]; ^{31}P-{^{1}H} (C_6D_6): δ 191.7 (s).

3.2 Preparation of [Mo(η^2-PhC_2Ph)(CH_2Ph){$P(OMe)_3$}(η-C_5H_5)] 2.

A similar reaction between $PhCH_2MgBr$ (2ml, 0.6M in thf) and [Mo{$P(OMe)_3$}$_2$(η^2-PhC_2Ph)(η-C_5H_5)][BF_4] **XI** (0.400g 0.593mmol) afforded, after recrystallisation from hexane, dark green crystals of **2** (0.194g, 59%). Anal: Found: C 62.8; H, 5.75; $C_{29}H_{31}MoO_3P$ requires C, 62.8; H, 5.64%.
NMR: ^{1}H (C_6D_6): δ 7.81 -6.92 (m, 15 H, Ph), 4.95 (s, 5 H, C_5H_5), 3.26 [d, *J*(PH) 10.8, 9 H, POMe], 2.92 [dd, ^{2}*J*(HH) 11.4, *J*(PH) 6.6, 1 H, CH_2], 2.53 [dd, *J*(PH) 6.0, 1 H, CH_2]; ^{13}C-{^{1}H} (C_6D_6): δ 201.1 [d, *J*(PC) 10.8, *C*≡C], 204.1 (s, C≡*C*), 160.1-121.6 (s, Ph), 92.4 (s, C_5H_5), 51.7 [d, *J*(PC) 5.4, POMe], 21.8 [d, *J*(PC) 13.6, CH_2]; ^{31}P-{^{1}H} (C_6D_6): δ 190.3 (s).

3.3 Preparation of [Mo{η^2=C(Ph)C(Ph)C(Et)O}(CO){$P(OMe)_3$}(η-C_5H_5)] 3.

A stream of CO was bubbled through a solution of **1** (65mg, 0.132mmol) in toluene (3ml) causing a colour change from green to red. The solvent was reduced *in vacuo* to *ca.* 0.5ml and hexane added to give a red powder, which was recrystallised from

toluene/hexane affording **3** (0.062g, 86%). Anal: Found: C 57.0; H, 5.35; $C_{26}H_{29}MoO_5P$, requires C, 56.9; H, 5.33%.
NMR: ^1H (C_6D_6): δ 7.44 -6.95 (m, 10 H, Ph), 5.07 (s, 5 H, C_5H_5), 3.53 [d, *J*(PH) 13.0, 9 H, POMe], 2.84-2.73 (m, 2 H, CH_2), 1.23 [t, ^3J(HH) 7.0, 3 H, Me]; ^{13}C-{^1H} (C_6D_6): δ 272.0 (s, CO), 250.6 [d, *J*(PH) 26.5, Mo=C], 196.3 [d, *J*(PH) 8.1, =C-O], 156.3 (s, C=*C*-C=Mo), 141.4-124.7 (s, Ph), 93.3 (s, C_5H_5), 52.3 (s, POMe), 31.0 (s, CH_2), 11.6 (s, Me); ^{31}P-{^1H} (C_6D_6): δ 194.7 (s).

3.4 Preparation of [Mo(η-C_5H_5)(η^6-C_6Ph_6)] 4.

To a green solution of **2** (0.18g, 0.32mmol) in benzene (10ml) was added PhC_2Ph (0.43g, 2.4mmol) and the mixture heated at 100°C for 17hrs in a closed Young's tube. After reduction of the solvent volume to 2ml, pentane (10ml) was added.The resulting yellow solid was washed with pentane and then crystallised from thf at -30°C to afford **4** as a bright yellow, extremely air sensitive solid (0.11g, 50%). No satisfactory analysis was found.
NMR: ^1H (CD_2Cl_2): δ 11.40 (br s), 10.35 (br s), 8.84 (br s), 7.84 (br s); ^{13}C-{^1H} (CD_2Cl_2): δ 134.8 (br s), 132.4 (br s), 130.9 (br s), 117.6 (br s).

3.5 Preparation of [Mo{P(OMe)$_3$}$_2${η^2-C(Ph)=C(Ph)CH_2CH=CH_2}(η-C_5H_5)] 5

To a suspension of [Mo(η^2-PhC_2Ph){P(OMe)$_3$}$_2$(η-C_5H_5)][BF_4] **XI** (0.228g, 0.338mmol) in 10ml thf was added a solution of C_3H_5MgBr (0.68ml, 1M in Et_2O). After stirring for five minutes at room temperature $P(OMe)_3$ (0.060ml, 0.5mmol) was added and the solution filtered through alumina. The solvent was removed *in vacuo*, the residue dissolved in Et_2O and columned on alumina (10 cm) with Et_2O/hexane (1:1) to give one yellow band which afforded **5** as a yellow powder (0.264g, 42%).
NMR: ^1H (C_6D_6): δ 7.31-6.96 (m, 10 H, Ph), 5.03 [d, *J*(PH) 3.1, 5 H, C_5H_5], 4.33-4.42 [m, 1 H, =C(H)], 3.29 [d, *J*(PH) 10.3, 9 H, POMe], 3.24 [d, *J*(PH) 9.5, 9 H, POMe], 2.49-2.19 (m, 2 H, CH_2), the signals for the $CH=CH_2$ group protons were obscured by other signals and, therefore, could not be assigned; ^{31}P-{^1H} (C_6D_6): δ 194.3 [d, *J*(AB) 70.5), 183.3(d).

3.6 Preparation of $[Mo(\eta^2\text{-}RC_2R')\{\eta^2\text{-}P(OMe)_2OBF_2OP(OMe)_2\}(\eta\text{-}C_5H_5)]$ 6, 7, 8.

a) R= R'= Ph; $CH_2(MgI)_2$ (0.363mmol) in toluene/diethylether (1:1) was added dropwise to a stirred suspension of $[Mo(\eta^2\text{-}PhC_2Ph)\{P(OMe)_3\}_2(\eta\text{-}C_5H_5)][BF_4]$ **XI** (0.433g, 0.642mmol) in thf (20ml). Immediately a white precipitate was formed, whereas the suspended complex only gradually dissolved. After stirring overnight a green solution was observed, which was filtered through alumina. The solvent was removed *in vacuo*, the residue dissolved in 1ml CH_2Cl_2 and columned on alumina with CH_2Cl_2/Et_2O (3:1). The blue fraction was collected reduced to *ca.* 5ml *in vacuo*. 20ml pentane was added, and the solution cooled to -25°C to give blue crystals of **6** (0.175g, 45%). Anal: Found: C 45.7; H, 4.31; $C_{23}H_{27}BF_2MoO_6P_2$, requires C, 45.6; H, 4.50%.
NMR: ^1H (C_6D_6): δ 7.63-7.09 (m, 10 H, Ph), 5.31 [t, *J*(PH) 1.3, 5 H, C_5H_5], 3.54 [vt, *N*(PH) 11.0 Hz, 6 H, POMe], 2.93 [vt, *N*(PH) 12.2, 6 H, POMe]; $^{13}C\text{-}\{^1H\}$ (C_6D_6): δ 214.4 (bs, C≡C), 142.1-128.5 (Ph), 95.8 (s,C_5H_5), 52.6 (s, POMe), 52.1 (s, POMe); $^{31}P\text{-}\{^1H\}$ (C_6D_6): δ 158.0 (s); $^{11}B\text{-}\{^1H\}$(C_6D_6): δ 1.95 (s); ^{19}F(C_6D_6): δ -135.93- -135.54 (m), -140.96- -140.71 (m).

b) R= Ph, R'= Me; A similar reaction between $[Mo(\eta^2\text{-}PhC_2Me)\{P(OMe)_3\}_2(\eta\text{-}C_5H_5)][BF_4]$ (2.50g, 4.08mmol) and $CH_2(MgI)_2$ (2.04mmol) afforded after workup blue crystalline powder of **7** (1.177g, 53%). Anal. Found: C, 39.4; H 4.61; $C_{18}H_{25}BF_2MoO_6P_2$ requires C, 39.7; H, 4.64%.
NMR: ^1H (CD_2Cl_2): δ 7.56-7.42 (m, 5 H, Ph), 5.63 [t, *J*(PH) 1.2, 5 H, C_5H_5], 3.60 [vt, *N*(PH) 11.0, 6 H, POMe], 3.17 [t, *J*(PH) 1.2, 3 H, ≡C-Me], 2.98 [vt, *N*(PH) 13.0, 6 H, POMe]; $^{11}B\text{-}\{^1H\}$ (CD_2Cl_2): δ -2.90 (s); $^{13}C\text{-}\{^1H\}$ (CD_2Cl_2): δ 212.4 and 208.9 (s, C≡C), 138.9-128.6 (Ph), 95.0 (s, C_5H_5), 51.5 (s, POMe), 50.9 (s, POMe), 21.5 (s, C-*Me*); ^{19}F (CD_2Cl_2): δ -137.56- -137.84 (m), -142.19- -142.41 (m); $^{31}P\text{-}\{^1H\}$ (CD_2Cl_2): δ 164.5 (s).

c) R= R'= Me; an analogous reaction between a suspension of $[Mo(\eta^2\text{-}MeC_2Me)\{P(OMe)_3\}_2(\eta\text{-}C_5H_5)][BF_4]$ (0.639g; 1.16mmol) in 20 ml in thf and $CH_2(MgI)_2$ (0.656mmol) in toluene/diethyl ether yielded blue crystals of **8** (0.324, 58%). Anal. Found: C, 32.5; H, 4.83. $C_{13}H_{23}BF_2MoO_6P_2$ requires C, 32.4; H, 4.82%.

NMR: ^{1}H (CD_2Cl_2): δ 5.52 [t, *J*(PH) 1.1, 5 H, C_5H_5], 3.56 [vt, *N*(PH) 11.0, 6 H, POMe], 2.96 [vt, *N*(PH) 13.0, 6 H, POMe], 2.87 [t, *J*(PH) 1.0, 6 H, C-Me]; ^{13}C-{^{1}H} (CD_2Cl_2): δ 206.5 (br s, C≡C), 95.1 (s, C_5H_5), 50.8 (s, POMe), 50.6 (s, POMe), 21.0 (s, Me): ^{11}B-{^{1}H} (CD_2Cl_2): δ -2.95 (s); ^{19}F (CD_2Cl_2): δ -137.50- -137.78 (m, 1 F), -142.08- -142.32 (m, 1 F); ^{31}P-{^{1}H} (CD_2Cl_2): δ 166.4 (s).

3.7 Reaction of [Mo(η^2-RC$_2$R'){η^2-P(OMe)$_2$OBF$_2$O(POMe)$_2$}(η-C$_5$H$_5$)] 6, 7, 8 with K[BHBu$^s_3$].

a) R= R'= Ph; a solution of **6** (0.160g, 0.264mmol) in 10ml of toluene was cooled to -78°C, and one equivalent of K[$BHBu^s_3$] (0.264ml, 1M in thf) was added with stirring. The reaction mixture was allowed to warm to room temperature, and the solvent reduced to 1ml *in vacuo*. Adding 10ml of hexane afforded bright green powder, which was recrystallised from Et_2O/hexane to give bright green powder of **9** (0.153g, 90%).
NMR: ^{1}H (CD_2Cl_2): δ 7.35-6.68 (m, 10 H, Ph), 5.11 (s, 5 H, C_5H_5), 3.44 [d, *J*(PH) 10.5, 3 H, POMe], 3.42-3.35 (m, overlapping, 1 H, C-H), 3.40 [d, *J*(PH) 9.9, 3 H, POMe], 3.3 [d, *J*(PH) 13.2, 3 H, POMe], 3.09 [d, *J*(PH) 12.8, 3 H, POMe]; ^{13}C-{^{1}H} (CD_2Cl_2): δ 240.8 (bs, Mo=C), 157.9-121.1 (Ph), 91.0 (s, C_5H_5), 50.3, 49.5, 49.1, 49.0 (all s, POMe), 31.0 [d, *J*(PH) 10.8, Mo-C-H]; ^{11}B-{^{1}H} (CD_2Cl_2): δ -3.0 (s); ^{31}P-{^{1}H} (CD_2Cl_2): δ 192.6 [d, *J*(AB) 80.5], 190.0 (d).

b) R= Ph, R'= Me; a similar reaction between compound **7** (0.300g, 0.549mmol) in 20ml of thf and K[$BHBu^s_3$] (0.549 ml, 1M in thf) at -78°C afforded **10** as a pale green powder (0.254g, 85%).
NMR: ^{1}H (CD_2Cl_2): δ 7.01-6.56 (m, 5 H, Ph), 4.78 (s, 5 H, C_5H_5), 3.55-3.27 [m, 13 H, Mo-CH and P(OMe)], 2.58 (s, 3 H, Me); ^{13}C-{^{1}H} (d^8-thf): δ 242.3 [dd, *J*(PC) 20.2, *J*(P'C) 33.3, Mo=C], 162.9 (s, *ipso*-Ph), 128.3-120.2 (Ph), 91.1 (s, C_5H_5), 50.4 (s, POMe), 50.0 (s, POMe), 49.4 [t, *J*(PC) = *J*(P'C) 8.1, Mo-C], 30.5 [d, *J*(PC) 16.3, Mo=C-*Me*]; ^{31}P-{^{1}H} (CD_2Cl_2): δ 196.5 [d, *J*(AB) 72.1], 194.5 (d).

c) K[$BHBu_3{}^s$] (0.213ml, 1M in thf) was added dropwise to a strirred solution of compound **8** in 10ml toluene at -78°C. The reaction mixture was allowed to warm to

room temperature, and the colour changed from blue to brown-yellow. After removing the solvents *in vacuo*, the remaining brown oil was dissolved in 0.5ml toluene. Adding 10ml of pentane afforded a yellow powder, which was washed several times with pentane. Recrystallisation from Et_2O/pentane yielded a pale yellow powder (0.089g, 87%).

3.8 Preparation of $[Mo(CO)_2\{\eta^2\text{-}P(OMe)_2OBF_2OP(OMe)_2\}(\eta\text{-}C_5H_5)]$ 11.

A solution of **9** (0.105g, 0.162mmol) in 10ml of toluene was cooled to -78°C and one equivalent of $HBF_4.Et_2O$ (0.023 ml, 0.162mmol) added. The reaction mixture was allowed to warm to room temperature and filtered through Al_2O_3 (5cm). A stream of CO was bubbled through the filtrate, causing a change of colour from red to yellow. The solvent was reduced *in vacuo* to 0.5ml. Addition of hexane afforded a yellow powder, which was recrystallised from Et_2O/hexane yielding **11** as yellow crystals (0.064g, 82%). The supernatant was reduced to 0.5 ml *in vacuo* and columned on Al_2O_3 with hexane. The first fraction was identified as *trans*-stilbene by comparison of its NMR-data to that of a pure sample. Anal. Found: C, 27.4; H, 3.61: $C_{11}H_{17}BF_2MoO_8P_2$ requires C, 27.3; H, 3.55%.
NMR: ^1H (C_6D_6): δ 5.00 (s, 5 H, C_5H_5), 3.48 [vt, *N*(PH) 6.1, POMe], 3.46 [vt, *N*(PH) 5.7, POMe]; $^{13}C\text{-}\{^1H\}$ (C_6D_6): δ 237.5 (s, CO), 92.8 (s, C_5H_5) 53.2 (s, POMe); $^{31}P\text{-}\{^1H\}$ (C_6D_6): δ 153.4 (s). IR (CH_2Cl_2): 1992.7, 1923.3 cm^{-1}.

3.9 Preparation of $[Mo\{P(OMe)_3\}_2\{\eta^2\text{-}P(OMe)_2OBF_2OP(OMe)_2\}(\eta\text{-}C_5H_5)]$ 12.

$HBF_4.Et_2O$ (0.112ml, 0.800mmol) and $P(OMe)_3$ (0.230 ml, 2.00mmol) were added to a stirred solution of **9** (0.455g, 0.704mmol) in thf (20ml). The reaction mixture was allowed to warm to room temperature, and the solvent reduced to 2ml *in vacuo*. 5ml of hexane were added, and the yellow solution quickly filtered through cotton wool. The solution was cooled to -28°C overnight affording yellow crystals, which were recrystallised from thf/hexane to give **12** (0.328g, 69%). Anal. Found: C, 26.4; H, 5.20; $C_{15}H_{35}BF_2MoO_{12}P_4$, requires C, 26.6; H, 5.23%.

NMR: ^{1}H (C_6D_6): δ 5.28 (s, 5 H, C_5H_5), 3.74 [vt, *N*(PH) 11.4, 6 H, $P(OMe)_2$], 3.70 [vt, *N*(PH) 10.6, 6 H, $P(OMe)_2$], 3.42 [vt, *N*(PH) 5.4, 18 H, $P(OMe)_3$]; ^{13}C-{^{1}H} (C_6D_6): δ 92.7 (s, C_5H_5), 52.5 [vt, *N*(PC) 4, 6 C, $P(OMe)_3$], 52.2 [vt, *N*(PC) 4.8, 2 C, $P(OMe)_2$], 51.9 [vt, *N*(PC) 5.5, 2 C, $P(OMe)_2$]; ^{31}P-{^{1}H} (C_6D_6): δ 195.8 (A part of AA'XX' system), 173.3 (br, X part of AA'XX' system).

3.10 Preparation of $[Mo\{P(OMe)_3\}_4(\eta\text{-}C_5H_5)][BF_4]$ 13.

A solution of $[Mo(\eta^3\text{-}C_3H_4Me)\{P(OMe)_3\}_2(\eta\text{-}C_5H_5)]$ **XIII** (0.489g, 0.756mmol) in thf (20ml) was cooled to -78°C and 2.2 equivalents of $P(OMe)_3$ (0.180ml, 1.520mmol) were added. After injecting $HBF_4.Et_2O$ (0.105ml, 0.756mmol) the reaction mixture was warmed to room temperature. The bright yellow solution was stirred for further 10 minutes after which the solvents were reduced *in vacuo*. The remaining oil was dissolved in 5ml CH_2Cl_2, filtered through cotton wool and the volume of the solution was reduced to *ca.* 1ml. Slow addition of thf afforded bright yellow, very air sensitive crystals, which were washed with hexane and dried *in vacuo* to give **13** (0.383g, 68%).
NMR: ^{1}H (C_6D_6): δ 5.07 (s, 5 H, C_5H_5), 3.61 [v quintet, *N*(PH) 21.2, 36 H, POMe]; ^{13}C-{^{1}H} (C_6D_6): δ 84.7 (s, C_5H_5), 52.7 (s, POMe); ^{31}P-{^{1}H} (C_6D_6): δ 190.9 (s).

3.11 Preparation of $[Mo\{\eta^2\text{-}P(OMe)_2OBF_2OP(OMe)_2\}(\eta^2\text{-}P{\equiv}CBu^t)(\eta\text{-}C_5H_5)]$ 14.

To a blue solution of **6** (158mg, 0.309mmol) in thf (8ml) at -78°C was added $K[BHBu^s_3]$ (0.309ml, 1M in thf). On warming to room temperature the colour changed to a pale yellow-green. After 5 min stirring the reaction mixture was cooled to -78°C and $HBF_4.Et_2O$ (0.050ml , 0.309mmol) was added. The mixture was left to warm up to room temperature, before the black solution was again cooled to -78°C and $P{\equiv}CBu^t$ (0.050ml, 0.310mmol) was added. The colour changed immediately to deep green. After stirring for 10 min at room temperature the volatiles were removed *in vacuo*, the remaining oil dissolved in toluene and filtered through cotton wool. Addition of hexane afforded a green oil of **14** (0.108g, 65%).

NMR $^1H(C_6D_6)$: δ 5.43 [t, *J*(PH) 1.4, 5 H, C_5H_5), 3.52 [vt, *N*(PH) 11.2, 6 H, POMe], 3.31 [vt, N(PH) 11.5 Hz, 6 H, POMe], 1.52 (s, 9 H, Bu^t); $^{13}C-\{^1H\}(C_6D_6)$: δ 328.5 [d t, ^1J(PC) 114.4, ^2J(PC) 6.6, P≡*C*], 93.8 (s, C_5H_5), 52.0 [vt, *N*(PH) 8.5, POMe], 51.5 [vt, *N*(PH) 6.1, POMe], 34.0 (s, C*Me*$_3$), 30.1 (s, *C*Me$_3$); $^{31}P-\{^1H\}(C_6D_6)$: δ 467.8 (s, P ≡C), 157.3 (s, POMe).

3.12 Preparation of [Mo{η^2-P(OMe)$_2$OBF$_2$OP(OMe)$_2$}{η^4-P$_2$C$_2$(Bu^t)$_2$}(η-C$_5$H$_5$)] 15.

To a solution of **14** (0.108g, 0.201mmol) in toluene (2ml) was added $Bu^tC{\equiv}P$ (0.048ml, 0.30mmol) and the mixture was stirred at ambient temperature for three days. The mixture was transferred onto the top of a column (Al_2O_3, 5 cm) and elution with CH_2Cl_2 gave one yellow fraction. The volume of the solution was reduced *in vacuo* to a minimum and on addition of hexane a pale yellow powder of **15** was obtained (0.061g, 48%).
NMR: $^1H(CDCl_3)$: δ 5.56-5.54 (m, 5 H, C_5H_5), 3.68 [vt, *N*(PH) 11.5, 6 H, POMe], 3.62 [vt, 6 H, *N*(PH) 10.9, POMe], 0.90 (s, 18 H, Bu^t); $^{13}C-\{^1H\}$ ($CDCl_3$): 128.6-128.2 (m, C=P), 93.8 (s, C_5H_5), 52.7 [vt, *N*(PH) 10.8, POMe], 34.8 -34.6 (m, C*Me*$_3$), 33.7-33.6 (m, *C*Me); $^{31}P-\{^1H\}$ ($CDCl_3$): 151.7 (s, POMe), 56.5 (s, P=C), 51.1 (s, P=C).

3.13 Synthesis of the Complex [Mo(PHPh$_2$)$_2$(η^2-PhC$_2$Ph)(η-C$_5$H$_5$)][BF$_4$] 16.

$PHPh_2$ (0.488ml, 2.80mol) was added to a solution of [Mo(NCMe)(η^2-$PhC_2Ph)_2$(η-C_5H_5)][BF_4] **LXIX** (0.900g, 1.31mmol) in CH_2Cl_2 (20ml) and the mixture was stirred at room temperature for one hour. After removing the volatiles *in vacuo* the remaining green oil was in several cycles dissolved in CH_2Cl_2, precipitated with Et_2O and the supernatant solution decanted. These cycles were continued until a green powder precipitated, which was dried *in vacuo* to give **16** (0.966g, 92%). Anal. Found: C, 64.4; H, 4.70; $C_{43}H_{37}BF_4MoP_2$, requires C, 64.4; H, 4.66%.

NMR: ^{1}H (C_6D_6): δ 7.51-6.91 (m, 30 H, Ph), 7.15 [d, *J*(PH) 379, 2 H, PH], 5.44 [t, *J*(PH) 1.4, 5 H, C_5H_5); ^{13}C-{^{1}H} (C_6D_6): δ 222.6 (s, C≡C), 138.3-127.5 (Ph), 96.5 (s, C_5H_5); ^{31}P (C_6D_6): δ 39.1 [d, *J*(HP) 372].

3.14 Preparation of [Mo(PPh$_2$)(PHPh$_2$)(η^2-PhC$_2$Ph)(η-C$_5$H$_5$)] 17.

a) A suspension of **16** (0.221g, 0.277mmol) in thf was cooled to -78°C and Li[N(SiMe$_3$)$_2$] (0.275ml, 1M in thf) was added. The mixture was warmed to room temperature and stirred for 10 minutes before the volatiles were removed *in vacuo*. The residue was dissolved in toluene, filtered through cotton wool and a red powder was precipitated by adding hexane to the filtrate. Recrystallisation from toluene/hexane afforded **17** in the form of a red powder (0.150g, 76%). Anal. Found: C, 72.4; H, 5.11; $C_{43}H_{36}MoP_2$, requires C, 72.7; H, 5.07%.
NMR: ^{1}H (C_6D_6): δ 8.05-6.92 (m, 30 H, Ph), 7.70 [dd, ^{1}J(PH) 345, ^{3}J(PH) 3, 1 H, PH], 4.96 [d, *J*(PH) 1.1, 5 H, C_5H_5]; ^{13}C-{^{1}H} (C_6D_6): δ 151.7 (s, C≡C), 137.8-125.2 (Ph), 96.5 (s, C_5H_5); ^{31}P (C_6D_6): δ 63.0 (s, PPh$_2$), 53.7 [d, *J*(HP) 345, PHPh$_2$].

b) In an analogous reaction **16** (0.113g, 0.142mmol) was treated with K[BHBu$^{s}_3$] (0.142ml, 1M in thf). After workup as described in a) **17** was obtained (0.062g, 61%).

3.15 Preparation of the Complexes [*closo*-3,3-(η^2-RC$_2$R')$_2$-3-(CO)-3,1,2-MoC$_2$B$_9$H$_{11}$] 18, 19.

a) R= R'= Ph; HBF$_4$.Et$_2$O (0.372ml, 2.28mmol) was added to a solution of [NEt$_4$][*closo*-3,3-(CO)$_2$-3-(η^3-C$_3$H$_5$)-3,1,2-MoC$_2$B$_9$H$_{11}$] **XXXII** (1.04g, 2.28mmol) and diphenylacetylene (1.96g, 11.0mmol) in CH_2Cl_2 (50ml). After the mixture was stirred for 5 hrs, the solvent was removed *in vacuo*. The residue was chromatographed on alumina with the same solvent to give a yellow fraction. Removal of the solvent *in vacuo* and crystallisation from CH_2Cl_2/hexane afforded a bright yellow powder of **18** (1.01g, 72%). Anal. Found: C, 60.7; H, 5.1. $C_{31}H_{31}B_9MoO$ requires C, 60.8; H, 5.1%.

NMR: $^{1}H(CD_2Cl_2)$: δ 7.60-7.29 (m, 20 H, Ph), 3.31 (br s, 2 H, cage-CH); $^{11}B-\{^{1}H\}$ (CD_2Cl_2): δ -3.5 (s, 1B), -5.8 (s, 2B), -6.9 (s, 1B), -11.5 (s, 2B), -16.2 (s, 3B); $^{13}C-\{^{1}H\}$ (CD_2Cl_2): δ 222.1 (s, CO), 168.8 (s, ≡*C*-Ph), 152.9 (s, ≡*C*-Ph), 134.9-127.4 (Ph), 51.6 (br s, cage-C). IR(CH_2Cl_2): 2062 cm^{-1}.

b) R= Ph, R'= Me, in an analogous reaction $HBF_4.Et_2O$ (0.508ml, 3.11mmol) was added to a solution of $[NEt_4][closo\text{-}3,3\text{-}(CO)_2\text{-}3\text{-}(\eta^3\text{-}C_3H_5)\text{-}3,1,2\text{-}MoC_2B_9H_{11}]$ **XXXII** (1.419g, 3.114mmol) and PhC_2Me (1.56ml, 12.5mmol) in CH_2Cl_2 (50ml). Workup as described in a) afforded **19** (1.14g, 75%). Anal. Found: C, 51.7; H, 5.66. $C_{21}H_{27}B_9MoO$ requires C, 51.6; H, 5.57%.
NMR: the NMR spectra of compound **19** show two sets of peaks due to two isomers, which cannot unambiguously be assigned. $^{1}H(CD_2Cl_2)$: δ 7.57-7.26 (m, 10 H, Ph), 3.65, 3.07, 2.49 (all br s, 2 H, cage-CH), 3.23, 3.12, 3.05 (all s, 6 H, Me); $^{11}B-\{^{1}H\}$ (CD_2Cl_2): δ -3.9 (s, 1 B), -6.1 (s, 2 B), -7.7 (s, 1 B), -10.5 (s, 1 B), -12.1 (s, 1 B), -13.6 (s, 1 B), -17.2 (s, 2 B); $^{13}C-\{^{1}H\}$ (CD_2Cl_2): δ 224.0, 223.0 (all s, CO), 177.0, 173.7, 161.5, 157.0, 154.8, 150.4 (all s, C≡C), 142.1-127.7 (Ph), 54.1, 50.9, 48.0 (all br s, cage-C), 18.8, 17.5, 16.8 (all s, Me). IR(CH_2Cl_2): 2049 cm^{-1}.

3.16 Preparation of the Complexes $[closo\text{-}3\text{-}(\eta^2\text{-}RC_2R)\text{-}3\text{-}(CO)\text{-}3\text{-}\{P(OMe)_3\}\text{-}3,1,2\text{-}MoC_2B_9H_{11}]$ 20,21.

a) R= Ph; to a solution of **18** (0.310g, 0.601mmol) in CH_2Cl_2 (20ml) $P(OMe)_3$ (0.213ml, 1.80mmol) was added and the mixture stirred at ambient temperature for 5 hrs. The solvent was reduced *in vacuo*, the oily residue dissolved in 1ml CH_2Cl_2 and columned on silica with toluene. The first fraction yielded starting material (*ca.* 0.30g, 10%), and the second blue fraction gave, after removing the solvents *in vacuo* and recrystallisation from CH_2Cl_2/hexane, **20** (0.133g, 51%) in the form of a blue powder. From the third green fraction **22** (0.102g, 26%), whose preparation and properties are described in 3.17, was isolated.
20. Anal. Found: C, 43.0; H, 5.5. $C_{20}H_{30}B_9MoO_4P$ requires C, 43.0; H, 5.4%.
NMR: $^{1}H(CD_2Cl_2)$: δ 7.68-7.49 (m, 10 H, Ph), 4.12 (br s, 1 H, cage-CH), 3.52 [d, 9 H, *J*(PH) 11.5, POMe], 2.91 (br s, 1 H, cage-CH); $^{11}B-\{^{1}H\}$ (CD_2Cl_2): δ -2.1 (s, 1B), -5.3 (s, 1 B), -7.1 (s, 2 B), -8.3 (s, 1 B), -12.2 (s, 1 B), -16.2 (s, 1 B), -18.5 (s, 2 B); $^{13}C-$

{^{1}H} (CD_2Cl_2): δ 234.2 [d, *J*(PC) 19.2, CO], 213.0 [d, *J*(PC) 16.4, *C*=C], 213.1 (s, *C*=C), 137.3-128.8 (s, Ph), 53.9 (s, POMe), 51.1 (br s, cage-C), 43.9 (br s, cage-C); ^{31}P-{^{1}H} (CD_2Cl_2): δ 162.1 (s). IR (CH_2Cl_2): 1977 cm^{-1}.

b) R= Me, in a similar reaction [*closo*-3,3-(η^2-$MeC_2Me)_2$-3-(CO)-3,1,2-$MoC_2B_9H_{11}$] **XXXIV** (0.560g, 1.539mmol) and $P(OMe)_3$ (0.454ml, 3.85mmol) was stirred in CH_2Cl_2 (15ml) for 5 hrs. After workup as described in a) three fractions were obtained, of which the first contained starting material (*ca.* 0.056g, 10%). From the second fraction the solvent was removed *in vacuo*, and the residue recrystallised from CH_2Cl_2/hexane to yield a yellow powder of **21** (0.384g, 60 %). The third fraction yielded **24** (0.114g, 15%), a compound which is described in detail in 3.17.
21: Anal. Found: C, 27.7; H, 6.2. $C_{10}H_{26}B_9MoO_4P$ requires C, 27.6; H, 6.0%.
NMR: ^{1}H(CD_2Cl_2): δ 3.72 (br s, 1 H, cage-CH), 3.49 [d, *J*(PH) 10.9, 9 H, POMe], 3.20 (s, 6 H, Me), 2.59 (br s, 1 H, cage-CH); ^{11}B-{^{1}H} (CD_2Cl_2): δ -3.0 (s, 1 B),-5.8 (s, 1 B), -6.2 (s, 2 B), -8.9 (s, 1 B), -13.3 (s, 2 B), -18.6 (s, 1 B), -19.9 (s, 1 B); ^{13}C-{^{1}H} (CD_2Cl_2): δ 233.2 [d, *J*(CP) 22.0, CO], 212.0 (br s, *C*Me), 53.6 (s, POMe), 49.5 (s, cage-C), 44.1 (s, cage-C), 19.9 (s, C*Me*); ^{31}P-{^{1}H} (CD_2Cl_2): δ 166.3 (s). IR (CH_2Cl_2): 1965 cm^{-1}.

3.17 Preparation of the Complexes [*closo*-3-(η^2-RC_2R')-3,3-{$P(OMe)_3$}$_2$-3,1,2-$MoC_2B_9H_{11}$] 22, 23, 24.

a) R=Ph; $P(OMe)_3$ (0.213ml, 1.80mmol) was added to a CH_2Cl_2 solution (10ml) of compound **18** (0.310g, 0.601mmol) and the mixture was refluxed for 12 hrs, during which its colour turned to green. The solvent was removed *in vacuo*. The residue was dissolved in CH_2Cl_2/hexane (5:1, 2ml), and chromatographed on alumina with the same solvent mixture. The blue fraction was collected which, after removal of the solvent *in vacuo* and crystallisation from CH_2Cl_2/hexane, gave **22** in the form of green *microcrystals* (0.456g, 58%). Anal. Found: C, 39.9; H, 6,1. $C_{22}H_{39}B_9MoO_6P_2$ requires C, 40,4; H, 6.0%.
NMR: ^{1}H (CD_2Cl_2): δ 7.45-7.29 (m, 10 H, Ph), 3.54 [vt, *N*(PH) 10.6, 18 H, POMe], 3.13 (br s, 2 H, cage-CH); ^{11}B-{^{1}H} (CD_2Cl_2): δ -1.2 (s, 1 B), -8.7 (s, 3 B), -11.3 (s, 2

B), -18.1 (s, 2 B), -22.5 (s, 1 B); ^{13}C-{^{1}H} (CD_2Cl_2): δ 220.7 [t, *J*(PC) 16.3, *C*≡C], 142.0-124.6 (Ph), 53.7 (s, POMe), 47.9 (br s, cage-C); ^{31}P-{^{1}H} (CD_2Cl_2): δ 174.7 (s).

b) R= Ph, R'= Me; similarly, a mixture of **19** (0.75g, 1.54mmol) and $P(OMe)_3$ (0.453ml, 3.84mmol) was refluxed for 12hrs. As was described in a) **23** (0.606g, 71%) was isolated from the reaction mixture. Anal. Found: C, 31.9; H, 5.95. $C_{17}H_{37}B_9MoO_6P_2.CH_2Cl_2$ requires C, 31.9; H, 5.80%.
NMR: ^{1}H ($CDCl_3$): δ 7.53-7.29 (m, 5 H, Ph), 3.59 [vt, *N*(PH) 10.6, 18 H, POMe], 3.23 [t, *J*(PH) 3.1, 3 H, Me], 3.13 (br s, 2 H, cage-CH); ^{11}B-{^{1}H} ($CDCl_3$): δ -3.0 (s, 1 B), -8.7 (s, 3 B), -11.2 (s, 2 B), -18.2 (s, 2 B), -21.9 (s, 1 B); ^{13}C-{^{1}H} ($CDCl_3$): δ 220.7 [tr, *J*(PC) 10.8, *C*≡C], 217.4 [t, *J*(PC) 24.4, C≡*C*], 139.7-127.1 (Ph), 53.3 (s, POMe), 46.6 (br s, cage-C), 22.6 (s, Me); ^{31}P-{^{1}H} ($CDCl_3$): δ 181.4 (s).

c) R= R'= Me; in an analogous reaction [*closo*-3,3-(η^2-MeC_2Me)-3-(CO)-3,1,2-$MoC_2B_9H_{11}$] **XXXIV** (0.415g, 1.139mmol) and $P(OMe)_3$ (0.336ml, 2.85mmol) were refluxed for 24 hrs in CH_2Cl_2 to give a green solution. Workup as described in a) gave **24** (0.502g, 83%) in the form of blue *microcrystals*. Anal. Found: C, 27.1; H, 6,7. $C_{12}H_{35}B_9MoO_6P_2$ requires C, 27.2; H, 6.7%.
NMR: ^{1}H ($CDCl_3$): δ 3.52 [vt, *N*(PH) 10.6, 18 H, POMe], 3.05 [t, *J*(PH) 1.3, 6 H, ≡C-Me], 2.79 (br s, 2 H, cage-CH); ^{11}B-{^{1}H} (CD_2Cl_2): δ -0.7 (s, 1 B), -7.6 (s, 2 B), -9.8 (s, 3 B), -17.1 (s, 2 B), -20.1 (s, 1 B); ^{13}C-{^{1}H} (CD_2Cl_2): δ 222.0 (br s, ≡*C*Me), 53.2 (s, POMe), 46.8 (br s, cage-C), 21.3 (s, C-*Me*); ^{31}P-{^{1}H} (CD_2Cl_2): δ 180.6 (s).

3.18 Synthesis of the Complexes [*closo*-3-(η^2-RC_2R)-3-(η^2-$R'C_2R'$)-3-{$P(OMe)_3$}-3,1,2-$MoC_2B_9H_{11}$] 26, 27.

a) R=R'= Me; in a sealed Schlenk tube a mixture of complex **24** (0.04g, 0.075mmol) and but-2-yne (0.1 ml, 1.28mmol) in toluene (5ml) was heated to 90 °C. The colour changed immediately from blue to yellow. After 10 min the solution was cooled to room temperature, and the solvent removed *in vacuo*. Crystallisation of the residue from CH_2Cl_2/hexane afforded **26** as a bright yellow powder (0.032g, 93%). Anal. Found: C, 33.7; H, 7.2. $C_{13}H_{32}B_9MoO_3P$ requires C, 33.9; H, 7.0%.

NMR: ^{1}H (CD_2Cl_2): δ 4.36 [d, *J*(PH) 10.4, 9 H, POMe], 3.30 (s, 6 H, Me), 2.86 (s, 6 H, Me), 2.40 (br s, 2 H, cage-CH); ^{11}B-{^{1}H} (CD_2Cl_2): δ -2.2 (s, 1 B), -5.3 (s, 1 B), -9.4 (s, 2 B), -11.8 (s, 1 B), -12.4 (s, 1 B), -16.8 (s, 2 B), -21.4 (s, 1 B); ^{13}C-{^{1}H} (CD_2Cl_2): δ 180.7 [d, *J*(PC) 8.1, *C*≡C], 154.1 [d, *J*(PC) 29.8, C≡*C*], 53.8 (s, POMe), 51.3 (br s, cage-C), 17.1 (s, Me), 16.6 [d, *J*(PC) 6.1, Me]; ^{31}P-{^{1}H} (CD_2Cl_2): δ 167.6 (s).

b) R= Ph, R'= Me; similarly, the reaction of **22** (0.04g, 0.061mmol) with but-2-yne gave bright yellow crystals of **27** (0.032g, 90%). Anal. Found: C, 47.3; H, 6.2. $C_{23}H_{36}B_9MoO_3P$ requires C, 47.2; H, 6.2%.
NMR: ^{1}H (CD_2Cl_2): δ 7.47-6.89 (m, 10 H, Ph) 3.64 [d, *J*(PH) 10.4, 9 H, POMe], 3.10 (br s, 1 H, cage-CH), 2.85 (br s, 6 H, Me), 2.17 (br s, 1 H, cage-CH); ^{11}B-{^{1}H} (CD_2Cl_2), δ -2.0 (s, 1 B), -6.1 (s, 1 B), -8.3 (s, 1 B), -10.9 (s, 1 B), -12.6 (s, 1 B), -15.8 (s, 2 B), -16.9 (s, 2 B), -20.6 (s, 1 B); ^{13}C-{^{1}H} (CD_2Cl_2), δ 166.7 [d, *J*(PC) 8.1, ≡*C*-Ph], 146.7 [d, *J*(PC) 27.1, ≡*C*-Ph], 141.0 [d, *J*(PC) 10.8, ≡*C*-Me], 133.7-126.6 (Ph), 55.6 (br s, POMe), 52.1 (br s, cage-C), 49.6 (br s, cage-C), 19.1 (s, ≡C-*Me*); ^{31}P-{^{1}H} (CD_2Cl_2), δ 160.6 (s).

c) R= Ph, R'= Me; in an analogous reaction **24** (0.04g, 0.075mmol) and diphenylacetylene (0.025g, 0.14mmol) were heated in toluene (5ml) for 2 hrs. After cooling of the reaction mixture to room temperature, the solvent was removed *in vacuo*, and the residue recrystallised from CH_2Cl_2/hexane to give **27** (0.032g, 73%).

3.19 Synthesis of the Complex [*closo*-3-(η^2-PhC$_2$Ph)-3,3-{P(OMe)$_3$}$_2$-8-{σ-*trans*-C(Ph)=C(H)Ph}-3,1,2-MoC$_2$B$_9$H$_{10}$] 28.

A mixture of **22** (0.175g, 0.267mmol) and diphenylacetylene (0.25g, 1.4mmol) in toluene (5ml) was kept at 90°C for 12hrs with no apparent colour change. After removal of the solvent *in vacuo*, the residue was dissolved in toluene (1ml) and chromatographed on alumina (10cm). Elution with toluene gave a green fraction from which the solvent was removed *in vacuo*. Crystallisation from CH_2Cl_2/hexane yielded green *microcrystals* of **28** (0.169g, 76%). Anal. Found: C, 51.8; H, 6.0. $C_{36}H_{49}B_9MoO_6P_2$ requires C, 51.9; H, 5.9 %.

NMR: ^{1}H (CD_2Cl_2): δ 7.50-6.06 (m, 20 H, Ph), 5.88 (s, 1 H, =C-H), 3.43 (vt, *N*(PH) 10.6, 18 H, POMe), 2.73 (br s, 2 H, cage-CH); ^{11}B-{^{1}H} (CD_2Cl_2): δ 14.9 (s, 1 B), -4.6 (s, 1 B), -5.2 (s, 1 B), -9.5 (s, 2 B), -12.9 (s, 2 B), -17.8 (s, 2 B); ^{13}C-{^{1}H} (CD_2Cl_2): δ 227.2 [t, *J*(PC) 16.3, *C*≡*C*], 145.8-124.6 (Ph), 54.2 (s, POMe), 46.8 (br s, cage-C), vinyl signals are obscured; ^{31}P-{^{1}H} (CD_2Cl_2): δ 169.6 (s).

3.20 Reaction of 18 with Acetonitrile.

a) In the absence of PhC_2Ph; complex **18** (0.643g, 1.245mmol) was refluxed in NCMe for 15 hrs after which the colour of the solution had changed to green. The mixture was cooled to room temperature and yellow *crystals* precipitated. The supernatant liquid was decanted and the crystals washed with Et_2O. A ^{1}H NMR spectrum of the product showed peaks for **29** and **30** in a ratio of *ca.* 1:1. The *crystals* were dissolved in CH_2Cl_2 (1ml) and transferred to the top of a column (Al_2O_3/15cm). Elution with CH_2Cl_2/hexane (2:1) gave two not fully separated fractions. Both fractions were collected, the sovents were removed *in vacuo*, and the residues were recrystallised from CH_2Cl_2/hexane. The first fraction yielded yellow *microcrystals* of **29** (*ca.* 0.070g, 9%). The second fraction gave **30** in the form of yellow *microcrystals* (0.250g, 25%).

29: Anal. Found: C, 61.3; H, 5.5. $C_{32}H_{34}B_9MoN$ requires C, 61.4; H, 5.5%.
NMR: ^{1}H (CD_2Cl_2): δ 7.49-7.19 (m, 20 H, Ph), 2.74 (br s, 2 H, cage-CH), 2.01 (s, 3 H, Me); ^{13}C-{^{1}H} (CD_2Cl_2): δ 180.2 (s, *C*=*C*), 130.5-126.8 (s, Ph), 51.7 (br s, cage-C), 4.3 (s, Me); ^{11}B-{^{1}H} (CD_2Cl_2): δ -2.5 (s, 1 B), -3.6 (s, 1 B), -4.9 (s, 2 B), -7.8 (s, 2 B), -11.8 (s, 1 B), -16.7 (s, 2 B).

30: Anal. Found: C, 68.7, H,5.4. $C_{46}H_{44}B_9MoN$ requires C, 68.7; H, 5.5%.
NMR: ^{1}H (CD_2Cl_2), δ 7.45-6.74 (m, 30 H, Ph), 6.50 (s, 1 H, vinyl-H), 2.70 (br s, 2 H, cage-CH), 1.71 (s, 3 H, Me); ^{11}B-{^{1}H} (CD_2Cl_2): δ 8.7 (s, 1 B, B-C=), -3.6 (s, 2 B), -9.5 (s, 2 B), -10.8 (s, 2 B), -19.7 (s, 2 B); ^{13}C-{^{1}H} (CD_2Cl_2): δ 178.5 (s, *C*=*C*), 145.8-124.4 (s, Ph), 47.1 (br s, cage-C), 4.2 (s, Me); vinyl signals are obscured.

b) In the presence of PhC_2Ph; in an analogous experiment a mixture of **18** (0.568g, 1.10mmol) and PhC_2Ph (0.210g, 1.12mmol) was refluxed in NCMe (10ml) for 20 hrs. The reaction mixture was cooled to room temperature and left for 4 hrs, during which yellow *microcrystals* were formed. The ratio of **29** : **30** as detected by NMR was about 15 : 85. Column chromatography (Al_2O_3/ 15 cm) with CH_2Cl_2/hexane (1:1) afforded a first fraction containing **29** and some unidentified byproducts. The isolation of **29** could not be accomplished. After further elution with the same solvent mixture a second, yellow fraction was collected. The solvent was removed *in vacuo* and the remaining oil was recrystallised from CH_2Cl_2/hexane to yield a yellow powder of **30** (0.522g, 59%).

3.21 Preparation of [*closo*-3,3-$(CO)_2$-3-{η^4-$P_2C_2(Bu^t)_2$}-3,1,2-$MoC_2B_9H_{11}$] 31.

$HBF_4.Et_2O$ (0.051ml, 0.318mmol) was added to a solution of [NEt_4][*closo*-3,3-$(CO)_2$-3-(η^3-C_3H_5)-3,1,2-$MoC_2B_9H_{11}$] **XXXII** (0.145g, 0.318mmol) at -78°C. The solution was warmed to -20°C and after the colour had changed to red the mixture was recooled. $CBu^t{\equiv}P$ (0.102ml, 0.636mmol) was added and the reaction mixture warmed to room temperature. After the mixture was stirred for 5 min the volatiles were removed *in vacuo* and the residue recrystallised with CH_2Cl_2/hexane to give **31** in the form of bright yellow *microcrystals* (0.095g, 62%). Anal. Found: C, 34.3; H, 6.10. $C_{14}H_{29}B_9MoO_2P_2$ requires C, 34.7; H, 6.03 %.
NMR: ^1H ($CDCl_3$): δ 3.70 (br s, 2 H, cage-CH), 1.15 (s, 18 H, Bu^t); ^{11}B-{^1H} (CD_2Cl_2): δ -3.5 (s, 1 B), -4.6 (s, 1 B), -6.2 (s, 1 B), -9.5 (s, 2 B), -12.6 (s, 2 B), -18.8 (s, 2 B); ^{13}C-{^1H} ($CDCl_3$): δ 217.4 (s, CO), 110.3 [t, *J*(PC) 55.1, P=*C*], 42.7 (br s, cage-C), 37.1 [t, *J*(PC) 7.1, *C*$(Me)_3$], 33.2 [t, *J*(PC) 5.6, Me]; ^{31}P-{^1H} ($CDCl_3$): no resonance was detected. IR(CH_2Cl_2): 2049, 2012 cm^{-1}.

4. References

1 a) T. J. Katz, S. M. Haker, R. D. Kendrick, and C. S. Yannoni, *J. Am. Chem. Soc.*, 1985, **107**, 2182,
b) R. R. Schrock, *Acc. Chem. Res.*, 1986, **19**, 342,
c) M. I. Bruce and A. G. Swinger, *Adv. Organomet. Chem.*, 1983, **22**, 59.

2 J. L. Templeton, P. B. Winston and B. C. Ward, *J. Am. Chem. Soc.*, 1981, **103**, 7713.

3 a) M. J. S. Dewar, *Bull. Soc. Chim.*, 1951, **18**, C79;
b) J. Chatt and L. A. Duncanson, *J. Chem. Soc.* B, **1953**, 2939.

4 J. P. Collman and L. S. Hegedus, *Principles and Applications of Organotransition Metal Chemistry*, University Science Books, 1987.

5 J. M. Augl and D. P. Tate, *J. Am. Chem. Soc.*, 1963, **85**, 2174.

6 J. M. Augl, J.G. Grasselli, W. M. Ritchey, B. L. Ross and D. P. Tate, *J. Am. Chem. Soc.*, 1964, **86**, 3261.

7 R. M. Laine, R. F. Moriaty and R. Bau, *J. Am. Chem. Soc.*, 1972, **94**, 1402.

8 R. B. King, *Inorg. Chem.*, 1968, **6**, 1044.

9 J. L. Thomas, *Inorg. Chem.* 1973, **17**, 1507.

10 K. Sünkel, U. Nagel and W. Beck, *J. Organomet. Chem.* 1981, **222**, 251.

11 J. L. Templeton and B. C. Ward, *J. Am. Chem. Soc.*, 1980, **102**, 3288.

12 J. L. Templeton, *Adv. Organomet. Chem.*, 1989, **29**, 1.

13 J. L. Davidson and D. W. A. Sharp, *J. Chem. Soc., Dalton Trans.*, 1975, 2531.

14 P. L. Watson and R. G. Bergman, *J. Am. Chem. Soc.*, 1980, **102**, 2698.

15 S. R. Allen, P. K. Baker, S. G. Barnes, M. Green, L. Trollope, L. Manojlovic-Muir and K. W. Muir, *J. Chem. Soc., Dalton Trans.*, 1981, 873.

16 J. W. Faller and H. H. Murray, *J. Organomet. Chem.*, 1979, **172**, 171.

17 A. M. Kook, P. N. Nicklas, J. P. Selegue and S. L. Smith, *Organometallics*, 1984, **3**, 499.

18 K. R. Birdwhistell, T. L. Tonker and J. L. Templeton, *J. Am. Chem. Soc.*, 1987, **109**, 1401.

19 S. R. Allen, T. H. Glauert, M. Green, K. A. Mead, N. C. Norman, A. G. Orpen, C. J. Schaverien and P. Woodward, *J. Chem. Soc., Dalton Trans.*, 1984, 2747.

20 A. De Cian, J. Colin, M. Schappacher, L. Ricard and R. Weiss, *J. Am. Chem. Soc.*, 1981, **103**, 1850.

21 K. A. Mead, H. Morgan and P. Woodward, *J. Chem. Soc., Dalton Trans.*, 1983, 271.

22 L. Ricard, R. Weiss, W. E. Newton, G. J.-J. Chen and J. W. McDonald, *J. Am. Chem. Soc.*, 1978, **100**, 1318.

23 P. W. R. Corfield, L. M. Baltusis and S. J. Lippard, *Inorg. Chem.*, 1981, **20**, 2883.

24 J. R. Morrow, T. L. Tonker and J. L. Templeton, *J. Am. Chem. Soc.*, 1985, **107**, 6956.

25 J. A. K. Howard, R. F. D. Stansfield and P. Woodward, *J. Chem. Soc., Dalton Trans.*, 1976, 246.

26 J. L. Davidson, M. Green, D. W. A. Sharp, F. G. A. Stone and A. J. Welch, *J. Chem. Soc., Chem. Commun.*, 1974, 706.

27 D. L. Reger and P. J. McElligott, *J. Am. Chem. Soc.*,1980, **102**, 5923.

28 M. Bottrill and M. Green, *J. Am. Chem. Soc.*, 1977, **99**, 5795.

29 M. Green, N. C. Norman, and A. G. Orpen, *J. Am. Chem.Soc.*, 1981, **103**, 1267.

30 S. R. Allen, R. G. Beevor, M. Green, N.C. Norman, A. G. Orpen, and I. D. Williams, *J. Chem. Soc., Dalton Trans.*, 1985, 435.

31 S. R. Allen, P. K. Baker, S. G. Barnes, M. Bottrill, M. Green, A. G. Orpen, I. D. Williams and A. J. Welch, *J. Chem. Soc., Dalton Trans.*, 1983, 927.

32 M. R. Churchill and W. J. Youngs, *Inorg. Chem.*, 1979, **18**, 2454.

33 I.U.P.A.C., Nomenclature of Inorganic Chemistry, 1970, Section II.

34 M. Bottrill and M. Green, *J. Chem. Soc., Dalton Trans.*, 1977, 2365.

35 M. F. Hawthorne, D. C. Young and P. A. Wegner, *J. Am Chem. Soc.*, 1965, **87**, 1818.

36 M. F. Hawthorne and R. L. Pilling, *J. Am Chem. Soc.*, 1965, **87**, 3987.

37 R. B. King, *Organomet. Synth.*, 1965, **1**, 109.

38 R. B. King, *Can. J. Chem.*, 1969, **47**, 2959.

39 M. F. Hawthorne, D. C. Young, T. D. Andrews, D. V. Howe, R. L. Pilling, A. D. Pitts, M. Reintjes, L. F. Warren and P. A. Wegner, *J. Am Chem. Soc.*, 1968, **90**, 879.

40 R. N. Grimes in *Comprehensive Organometallic Chemistry*, ed. G. Wilkinson, F. G. A. Stone and E. W. Abel, Pergamon Press, 1982, Vol. 1, Chap 5.5., p. 515.

41 E. B. Moore, L. L. Lohr and W. N. Lipscomb, *J. Chem. Phys.*, 1961, **35**, 1329.

42 T. P. Hanusa, *Polyhedron*, 1982, **1**, 663.

43 D. M. P. Mingos, *Polyhedron*, 1984, **3**, 1289.

44 T. S. Piper, F. A. Cotton and G. Wilkinson, *J. Inorg. Nucl. Chem.* 1955, **1**, 165.

45 E. O. Fischer and K. Ulm, *Chem. Ber.*, 1962, **95**, 692.

46 M. F. Hawthorne and G. B. Dunks, *Science,* 1972, **178,** 462.

47 D. M. P. Mingos, M. I. Forsyth and A. J. Welch, *J. Chem. Soc., Dalton Trans.*, 1978, 1363.

48 L. F. Warren and M. F. Hawthorne, *J. Am. Chem. Soc.*, 1970, **92**, 1157.

49 H. M. Colquhoun, T. J. Greenhough and M. G. H. Wallbridge, *J. Chem. Soc., Dalton Trans.*, 1985, 761.

50 F. G. A. Stone, *Adv. Organomet. Chem.*, 1990, **31**, 53.

51 S. Brew and F. G. A. Stone, *Adv. Organomet. Chem.*, 1994, **35**, 135.

52 M. Green, J. A. K. Howard, A. P. James, C. M. Nunn and F. G. A. Stone, *J. Chem. Soc., Dalton Trans.*, 1987, 61.

53 F.-E. Baumann, J. A. K. Howard and F. G. A. Stone, *J. Chem. Soc., Dalton Trans.*, 1987, 2661.

54 D. D. Devore, C. Emmerich, J. A. K. Howard and F. G. A. Stone, *J. Chem. Soc., Dalton Trans.*, 1989, 797.

55 M. Green, J. A. K. Howard, A. N. de M. Jelfs, O. Johnson and F. G. A. Stone, *J. Chem. Soc., Dalton Trans.*, 1987, 73.

56 S. J. Dossett. S. Li and G. A. Stone, *J. Chem. Soc., Dalton Trans.*, 1993, 1585.

57 S. J. Dossett. S. Li, D. F. Mullica, E. L.Sappenfield and F. G. A. Stone, *J. Chem. Soc., Dalton Trans.*, 1993, 3551.

58 S. Li and F. G. A. Stone, *Polyhedron,* 1993, **12**, 1696.

59 F. J. Feher, M. Green and A. G. Orpen, *J. Chem. Soc., Chem. Commun.* 1986, 291.

60 S. R. Allen, M. Green, N. C. Norman, K. E. Paddick and A. G. Orpen, *J. Chem. Soc., Dalton Trans.*, 1983, 1625.

61 W. Hirpo and M. D. Curtis, *Organometallics,* 1994, **13**, 2706.

62 P. W. Jolly and G. Wilke in The Organic Chemistry of Nickel, (Academic Press) 1975, Vol 2, 94-107.

63 P. M. Maitlis, *Acc. Chem. Res.*, 1970, **9**, 93.

64 D. F. Pollock and P. M. Maitlis, *J. Organomet. Chem.*, 1971, **26**, 407.

65 J. A. Dean, *Lange's Handbook of Chemistry,* McGraw-Hill, 14th edition, 1992.

66 R. Hoffmann, *Angew. Chem., Int. Ed. Engl.*, 1982, **21**, 711.

67 R. Hoffmann and R. B. Woodward, *J. Am. Chem. Soc.*, 1965, **87**, 4389.

68 a) J. M. Brown, B. T. Golding and J. J. Stofko, *J. Chem. Soc., Chem. Commun.*, 1973, 319;

b) M. P. Schneider and J. Rebell, *J. Chem. Soc., Chem. Commun.*, 1975, 283.

69 F. Biasotto, M. Etienne and F. Dahan, *Organometallics,* 1995, **14**, 1870.

70 M. Etienne, F. Biasotto and R. Mathieu, *J. Chem. Soc., Chem. Commun.*, 1994, 1661.

71 F. Bertini, P. Grasselli, G. Zubiani and G. Cainelly, *Tetrahedron,* 1970, **26**, 1281.

72 F. Bickelhaupt, *Angew. Chem., Int. Engl. Ed.*, 1987, **26**, 990.

73 P. S. Pregosin and R. W. Kunz in, *31P and 13C NMR of Transition Metal Phosphine Complexes*, Springer, 1979, 67-8.

74 a) H. Werner and T. N. Khac, *Angew. Chem.*, 1977, **89**, 332.

b) H. Werner and T. N. Khac, *Z. Anorg. Allg. Chem.*, 1981, **475**, 241.

75 H. Werner and T. N. Khac, *Z. Anorg. Allg. Chem.*, 1981, **479**, 134.

76 S. G. Feng, P. S. White and J. L. Templeton, *J. Am. Chem. Soc.*, 1992, **114**, 2951.

77 a) S. Trofimenko, *Chem. Rev.*, 1993, **93**, 943;

b) H. Memmler, L. H. Gade and J. W. Lauher, *Inorg. Chem.*, 1994, **33**, 3064;

c) C. C. Cummins, R. R. Schrock and W. M. Davis, *Angew. Chem., Int Engl. Ed.*, 1993, **32**, 756.

78 U. Kölle, T. Rüther, N. Le Narvor, U. Englert and W. Kläui, *Angew. Chem., Int. Ed. Engl.* 1994, **33**, 991.

79 a) G. Becker, G. Gresser and W. Uhl, *Z. Naturforsch. B; Anorg. Chem. Org. Chem.*, 1981, **36**,16;

b) R. Appel and A. Westerhaus, *Tetrahedron Letters*, 1981, **22**, 2159.

80 J. F. Nixon, *Chem. Rev.*, 1988, **88**, 1327.

81 a) J. F. Nixon, *Endeavour*, 1991, **15**, 49;

b) J. F. Nixon, *Chem. and Ind.*, 1993, 404.

82 M. Regitz and P. Binger, *Angew. Chem., Int. Ed. Engl.* 1988, **27**, 1484.

83 P. Binger, B. Biedenbach, A. T. Herrmann, F. Langhauser, P. Betz, R. Goddard and C. Krüger, *Chem. Ber.*, 1990, **123**, 1617.

84 J. C. T. R. Burckett-St. Laurent, P. B. Hitchcock, H. W. Kroto and J. F. Nixon, *J. Chem. Soc., Chem. Commun.*, 1981, 1141.

85 S. I. Al-Resayes, P. B. Hitchcock, M. F. Meidine and J. F. Nixon, *J. Chem. Soc., Chem. Commun.*, 1984, 1080.

86 S. I. Al-Resayes, S. I. Klein, H. W. Kroto, M. F. Meidine and J. F. Nixon, *J. Chem. Soc.; Chem. Commun.*, 1983, 930.

87 K. K. Laali, B. Geissler, O. Wagner, J. Hoffmann, R. Armbrust, W. Eisfeld and M. Regitz, *J. Am. Chem. Soc.*, 1994, **116**, 9407.

88 J. Barrera, M. Sabat and W. Dean Harman, *J. Am. Chem. Soc.*, 1991, **113**, 8178

89 P. Binger, R. Milczarek, R. Mynott and M. Regitz, *J. Organomet. Chem.*, 1987, **323**, C35.

90 W. Malisch, R. Miasch, I. J. Colguhoum and W. MacFarbanc, *J. Organomet. Chem.*, 1981, **220**, C1.

91 W. E. Buhro, S. Georgiou, J. P. Hutchinson and J. A. Gladysz, *J. Am. Chem. Soc.*, 1985, **107**, 3346.

92 R. T. Baker, J. F. Whitney and S. S. Wreford, *Organometallics*, 1983, **2**, 1049.

93 R. T. Baker, J. C. Calabrese, R. L. Harlow and I. D. Williams, *Organometallics*, 1993, **12**, 830.

94 J. P. Collman and L. S. Hegedus in *Principles and Applications of Organotransition Metal Chemistry*,University Science Books, 1987.

95 M. Bottrill, M. Green, A. G. Orpen, D. R. Saunders and I. D. Williams, *J. Chem. Soc., Dalton Trans.*, 1989, 511

96 C. Carfagna, M. Green, K. R. Nagle, D. J. Williams and C. M. Woolhouse, *J. Chem. Soc., Dalton Trans.*, 1993, 1761; and references therein.

97 M. Green, *J. Organomet. Chem.*, 1986, **300**, 93.

98 A. P. James and F. G. A. Stone, *J. Organomet. Chem.*, 1986, **310**, 47.

99 P. E. Behnken, J. A. Belmont, D. C. Busby, M. S. Delaney, R. E. King III, C. W. Kreimendahl, T. B. Marder, J. J. Wilczynski and M. F. Hawthorne, *J. Am. Chem. Soc.*106, **1984**, 3011; and references therein.

100 M. Green, J. A. K. Howard, A. P. James, C. M. Nunn and F. G. A. Stone, *J. Chem. Soc., Dalton Trans.*, 1987, 81.

101 P. B. Hitchcock, M. J. Maah, J. F. Nixon and M. Green, *J. Organomet. Chem.*, 1994, **466**, 153.

102 M. Regitz and P. Binger, *Angew. Chem., Int. Engl. Ed.*, 1988, **27**, 1484.

103 H. F. Dare, J. A. K. Howard, M. U. Pilotti, F. G. A. Stone and J. Szameitat, *J. Chem. Soc., Dalton Trans.*, 1990, 2263.

104 D. D. Perrin, W. L. F. Armavego and D. R. Perrin, Purification of Laboratory Chemicals, 2nd edition, Pergamaon Press.

5. Appendix

5.1 Crystal data for 4

Empirical formula	$[MoC_{47}H_{35}][C_7H_8]$
Crystal System	monoclinic
Space Group	$P2_1/n$
Unit Cell Dimensions (Å): a	24.871 (6)
b	19.592 (11)
c	16.266 (2)
β	97.50 (2)°
Volume $Å^3$	7858.17
D_{calcd}	1.33 g/cm^{-3}
Z	8
F(000)	3277
T	173 K
R_F	0.046
R_W	0.049

Table 1: Fractional atomic coordinates ($*10^4$)

	x	y	z
Mo(1)	2081.6(2)	269.9(3)	2966.8(3)
C(11)	1635(2)	-522(2)	2055(3)
C(12)	2131(2)	-350(2)	1763(3)
C(13)	2113(2)	355(2)	1554(3)
C(14)	1605(2)	618(2)	1717(3)
C(15)	1310(2)	76(2)	2027(3)
C(16)	2060(3)	-7(3)	4306(4)
C(17)	2576(2)	-207(3)	4074(3)
C(18)	2908(2)	279(3)	3712(3)
C(19)	2721(2)	973(3)	3565(4)
C(110)	2208(2)	1184(3)	3806(3)
C(111)	1881(2)	695(3)	4173(4)
C(113)	1632(2)	-403(2)	5535(2)
C(114)	1361(2)	-895(2)	5946(2)
C(115)	1190(2)	-1501(2)	5543(2)
C(116)	1290(2)	-1615(2)	4730(2)
C(117)	1560(2)	-1124(2)	4319(2)
C(112)	1731(2)	-518(2)	4722(2)
C(119)	2948(2)	-1125(2)	5055(2)
C(120)	3221(2)	-1742(2)	5213(2)
C(121)	3337(2)	-2150(2)	4556(2)
C(122)	3179(2)	-1941(2)	3740(2)
C(123)	2905(2)	-1324(2)	3582(2)
C(118)	2790(2)	-916(2)	4239(2)
C(125)	3851(2)	-140(2)	4139(2)
C(126)	4350(2)	-380(2)	3957(2)
C(127)	4453(2)	-415(2)	3136(2)
C(128)	4057(2)	-211(2)	2496(2)
C(129)	3558(2)	29(2)	2678(2)

Table 1 (cont.): Fractional atomic coordinates ($*10^4$)

	x	y	z
C(124)	3455(2)	64(2)	3499(2)
C(131)	3593(2)	1613(2)	3514(2)
C(132)	3910(2)	2079(2)	3143(2)
C(133)	3697(2)	2415(2)	2416(2)
C(134)	3165(2)	2283(2)	2061(2)
C(135)	2848(2)	1817(2)	2431(2)
C(130)	3062(2)	1481(2)	3158(2)
C(137)	2370(1)	2420(2)	4107(2)
C(138)	2203(1)	3100(2)	4067(2)
C(139)	1699(1)	3275(2)	3641(2)
C(140)	1361(1)	2770(2)	3254(2)
C(141)	1527(1)	2089(2)	3294(2)
C(136)	2032(1)	1914(2)	3720(2)
C(143)	1396(1)	1375(2)	5138(2)
C(144)	929(1)	1577(2)	5462(2)
C(145)	425(1)	1317(2)	5128(2)
C(146)	389(1)	856(2)	4470(2)
C(147)	857(1)	654(2)	4146(2)
C(142)	1360(1)	914(2)	4480(2)
Mo(2)	3429.9(2)	1429.6(3)	7042.4(3)
C(21)	3827(2)	667(5)	6221(7)
C(22)	3551(2)	275(5)	6770(7)
C(23)	2989(2)	422(5)	6595(7)
C(24)	2917(2)	904(5)	5938(7)
C(25)	3435(2)	1056(5)	5707(7)
C(26)	4015(2)	1770(3)	8129(4)
C(27)	4006(2)	2272(3)	7482(4)
C(28)	3500(3)	2572(3)	7125(4)
C(29)	3004(2)	2372(3)	7420(4)
C(210)	3004(2)	1868(3)	8058(4)
C(211)	3513(3)	1571(3)	8422(4)
C(213)	4625(2)	786(2)	8617(2)
C(214)	5090(2)	533(2)	9091(2)
C(215)	5467(2)	983(2)	9507(2)
C(216)	5378(2)	1685(2)	9448(2)
C(217)	4913(2)	1938(2)	8974(2)
C(212)	4536(2)	1488(2)	8558(2)
C(219)	4805(2)	2043(2)	6708(3)
C(220)	5269(2)	2267(2)	6392(3)
C(221)	5453(2)	2934(2)	6539(3)
C(222)	5173(2)	3377(2)	7004(3)
C(223)	4709(2)	3153(2)	7320(3)
C(218)	4525(2)	2486(2)	7172(3)
C(225)	3638(2)	2965(2)	5684(3)
C(226)	3623(2)	3477(2)	5086(3)
C(227)	3462(2)	4136(2)	5268(3)
C(228)	3315(2)	4283(2)	6048(3)
C(229)	3330(2)	3770(2)	6646(3)

Table 1 (cont.): Fractional atomic coordinates ($*10^4$)

	x	y	z
C(224)	3491(2)	3111(2)	6464(3)
C(231)	2249(2)	2733(2)	6298(2)
C(232)	1777(2)	3103(2)	6053(2)
C(233)	1544(2)	3492(2)	6632(2)
C(234)	1784(2)	3511(2)	7457(2)
C(235)	2257(2)	3141(2)	7702(2)
C(230)	2490(2)	2752(2)	7122(2)
C(237)	2060(2)	1387(2)	7756(3)
C(238)	1582(2)	1155(2)	8025(3)
C(239)	1522(2)	1182(2)	8865(3)
C(240)	1939(2)	1442(2)	9436(3)
C(241)	2417(2)	1675(2)	9167(3)
C(236)	2477(2)	1647(2)	8327(3)
C(243)	3228(2)	434(2)	8966(2)
C(244)	3166(2)	6(2)	9633(2)
C(245)	3378(2)	199(2)	10436(2)
C(246)	3651(2)	819(2)	10572(2)
C(247)	3712(2)	1246(2)	9905(2)
C(242)	3501(2)	1054(2)	9102(2)
C(48)	515(6)	2802(7)	8206(15)
C(49)	445(5)	2567(7)	7470(12)
C(50)	159(5)	2891(7)	6567(8)
C(51)	50(5)	3474(7)	6725(10)
C(52)	92(4)	3830(6)	7502(8)
C(53)	314(5)	3534(9)	8153(10)
C(54)	378(5)	3789(9)	8922(8)
C(55)	328(4)	202(6)	8543(8)
C(56)	341(5)	64(6)	7724(10)
C(57)	77(5)	469(7)	7113(8)
C(58)	-214(5)	1003(6)	7329(9)
C(59)	-218(4)	1162(5)	8150(8)
C(60)	37(4)	783(6)	8750(7)
C(61)	36(6)	965(9)	9632(8)

Table 2: Bond lengths (Å)

C(11)-Mo(1)	2.326(6)	C(12)-Mo(1)	2.321(6)
C(13)-Mo(1)	2.316(7)	C(14)-Mo(1)	2.318(6)
C(15)-Mo(1)	2.323(7)	C(16)-Mo(1)	2.252(8)
C(17)-Mo(1)	2.247(7)	C(18)-Mo(1)	2.246(7)
C(19)-Mo(1)	2.230(8)	C(110)-Mo(1)	2.249(8)
C(111)-Mo(1)	2.246(8)	C(11)-C(12)	1.420(8)
C(12)-C(13)	1.420(7)	C(13)-C(14)	1.420(8)
C(14)-C(15)	1.420(7)	C(15)-C(11)	1.420(7)
C(16)-C(17)	1.439(10)	C(17)-C(18)	1.435(10)
C(17)-C(118)	1.499(8)	C(18)-C(19)	1.447(10)
C(18)-C(124)	1.505(9)	C(19)-C(110)	1.445(10)
C(19)-C(130)	1.515(9)	C(110)-C(111)	1.436(9)
C(110)-C(136)	1.497(8)	C(111)-C(16)	1.453(9)
C(111)-C(142)	1.510(9)	C(16)-C(112)	1.507(9)
C(21)-Mo(2)	2.311(12)	C(22)-Mo(2)	2.332(12)
C(23)-Mo(2)	2.329(11)	C(24)-Mo(2)	2.305(11)
C(25)-Mo(2)	2.294(13)	C(26)-Mo(2)	2.238(8)
C(27)-Mo(2)	2.241(8)	C(28)-Mo(2)	2.248(8)
C(29)-Mo(2)	2.253(8)	C(210)-Mo(2)	2.246(8)
C(211)-Mo(2)	2.244(8)	C(21)-C(22)	1.420(15)
C(22)-C(23)	1.420(10)	C(23)-C(24)	1.420(15)
C(24)-C(25)	1.420(11)	C(25)-C(21)	1.420(13)
C(26)-C(27)	1.439(9)	C(27)-C(28)	1.441(9)
C(27)-C(218)	1.505(10)	C(28)-C(29)	1.436(10)
C(28)-C(224)	1.505(9)	C(29)-C(210)	1.433(10)
C(29)-C(230)	1.504(9)	C(210)-C(211)	1.446(9)
C(210)-C(236)	1.498(9)	C(211)-C(26)	1.448(10)
C(211)-C(242)	1.502(9)	C(26)-C(212)	1.496(8)
C(48)-C(49)	1.272(30)	C(49)-C(50)	1.673(23)
C(50)-C(51)	1.208(20)	C(51)-C(52)	1.436(21)
C(52)-C(53)	1.269(20)	C(53)-C(54)	1.337(22)
C(53)-C(48)	1.518(24)		
C(55)-C(56)	1.363(22)	C(56)-C(57)	1.371(20)
C(57)-C(58)	1.346(19)	C(58)-C(59)	1.373(20)
C(59)-C(60)	1.320(16)	C(60)-C(61)	1.479(19)
C(60)-C(55)	1.412(17)		

Table 3: Bond angles (°)

C(12)-Mo(1)-C(11)	35.6(2)	C(13)-Mo(1)-C(11)	59.3(3)
C(13)-Mo(1)-C(12)	35.7(1)	C(14)-Mo(1)-C(11)	59.3(2)
C(14)-Mo(1)-C(12)	59.4(3)	C(14)-Mo(1)-C(13)	35.7(2)
C(15)-Mo(1)-C(11)	35.6(2)	C(15)-Mo(1)-C(12)	59.3(3)
C(15)-Mo(1)-C(13)	59.4(3)	C(15)-Mo(1)-C(14)	35.6(2)
C(16)-Mo(1)-C(11)	112.7(3)	C(16)-Mo(1)-C(12)	134.5(2)
C(16)-Mo(1)-C(13)	170.2(2)	C(16)-Mo(1)-C(14)	147.7(2)
C(16)-Mo(1)-C(15)	118.4(3)	C(17)-Mo(1)-C(11)	113.6(3)
C(17)-Mo(1)-C(12)	112.0(3)	C(17)-Mo(1)-C(13)	137.7(2)
C(17)-Mo(1)-C(14)	171.4(2)	C(17)-Mo(1)-C(15)	141.1(2)
C(17)-Mo(1)-C(16)	37.3(2)	C(18)-Mo(1)-C(11)	132.6(2)
C(18)-Mo(1)-C(12)	108.3(3)	C(18)-Mo(1)-C(13)	112.8(3)
C(18)-Mo(1)-C(14)	142.9(2)	C(18)-Mo(1)-C(15)	167.3(2)
C(18)-Mo(1)-C(16)	67.4(3)	C(18)-Mo(1)-C(17)	37.3(2)
C(19)-Mo(1)-C(11)	160.8(2)	C(19)-Mo(1)-C(12)	125.3(3)
C(19)-Mo(1)-C(13)	105.9(3)	C(19)-Mo(1)-C(14)	117.1(3)
C(19)-Mo(1)-C(15)	150.4(2)	C(19)-Mo(1)-C(16)	80.3(3)
C(19)-Mo(1)-C(17)	67.8(3)	C(19)-Mo(1)-C(18)	37.7(2)
C(110)-Mo(1)-C(11)	159.3(2)	C(110)-Mo(1)-C(12)	155.5(2)
C(110)-Mo(1)-C(13)	121.7(3)	C(110)-Mo(1)-C(14)	108.2(3)
C(110)-Mo(1)-C(15)	124.6(3)	C(110)-Mo(1)-C(16)	67.9(3)
C(110)-Mo(1)-C(17)	80.0(3)	C(110)-Mo(1)-C(18)	67.7(3)
C(110)-Mo(1)-C(19)	37.6(2)	C(111)-Mo(1)-C(11)	131.4(2)
C(111)-Mo(1)-C(12)	166.7(2)	C(111)-Mo(1)-C(13)	151.7(2)
C(111)-Mo(1)-C(14)	120.7(3)	C(111)-Mo(1)-C(15)	112.1(3)
C(111)-Mo(1)-C(16)	37.7(2)	C(111)-Mo(1)-C(17)	67.4(3)
C(111)-Mo(1)-C(18)	79.5(3)	C(111)-Mo(1)-C(19)	67.5(3)
C(111)-Mo(1)-C(110)	37.3(2)	C(12)-C(11)-Mo(1)	72.0(3)
C(15)-C(11)-Mo(1)	72.1(3)	C(15)-C(11)-C(12)	108.0(5)
C(11)-C(12)-Mo(1)	72.4(4)	C(13)-C(12)-Mo(1)	72.0(3)
C(13)-C(12)-C(11)	108.0(5)	C(12)-C(13)-Mo(1)	72.4(4)
C(14)-C(13)-Mo(1)	72.2(4)	C(14)-C(13)-C(12)	108.0(5)
C(13)-C(14)-Mo(1)	72.1(4)	C(15)-C(14)-Mo(1)	72.4(3)
C(15)-C(14)-C(13)	108.0(5)	C(11)-C(15)-Mo(1)	72.3(4)
C(14)-C(15)-Mo(1)	72.0(4)	C(14)-C(15)-C(11)	108.0(5)
C(17)-C(16)-Mo(1)	71.2(4)	C(111)-C(16)-Mo(1)	70.9(4)
C(111)-C(16)-C(17)	119.0(6)	C(112)-C(16)-Mo(1)	132.6(4)
C(112)-C(16)-C(17)	119.5(6)	C(112)-C(16)-C(111)	121.4(6)
C(16)-C(17)-Mo(1)	71.5(4)	C(18)-C(17)-Mo(1)	71.3(4)
C(18)-C(17)-C(16)	120.5(6)	C(118)-C(17)-Mo(1)	132.3(4)
C(118)-C(17)-C(16)	120.8(6)	C(118)-C(17)-C(18)	118.6(6)
C(17)-C(18)-Mo(1)	71.4(4)	C(19)-C(18)-Mo(1)	70.5(4)
C(19)-C(18)-C(17)	120.1(6)	C(124)-C(18)-Mo(1)	131.6(3)
C(124)-C(18)-C(17)	119.6(6)	C(124)-C(18)-C(19)	120.3(6)
C(18)-C(19)-Mo(1)	71.7(4)	C(110)-C(19)-Mo(1)	71.9(4)
C(110)-C(19)-C(18)	120.0(6)	C(130)-C(19)-Mo(1)	128.6(4)
C(130)-C(19)-C(18)	120.3(6)	C(130)-C(19)-C(110)	119.7(6)
C(19)-C(110)-Mo(1)	70.5(4)	C(111)-C(110)-Mo(1)	71.3(4)
C(111)-C(110)-C(19)	119.3(6)	C(136)-C(110)-Mo(1)	133.5(3)
C(136)-C(110)-C(19)	120.4(6)	C(136)-C(110)-C(111)	120.2(6)
C(16)-C(111)-Mo(1)	71.4(4)	C(110)-C(111)-Mo(1)	71.5(4)
C(110)-C(111)-C(16)	121.0(6)	C(142)-C(111)-Mo(1)	133.8(3)
C(142)-C(111)-C(16)	118.7(6)	C(142)-C(111)-C(110)	120.2(6)
C(113)-C(112)-C(16)	119.5(5)	C(117)-C(112)-C(16)	120.3(5)
C(119)-C(118)-C(17)	119.5(5)	C(123)-C(118)-C(17)	119.8(4)
C(125)-C(124)-C(18)	118.7(4)	C(129)-C(124)-C(18)	121.2(4)

Table 3 (cont.): Bond angles (°)

C(131)-C(130)-C(19)	119.5(4)	C(135)-C(130)-C(19)	120.5(5)
C(137)-C(136)-C(110)	119.0(4)	C(141)-C(136)-C(110)	120.9(5)
C(143)-C(142)-C(111)	117.8(4)	C(147)-C(142)-C(111)	122.1(5)
C(22)-Mo(2)-C(21)	35.6(3)	C(23)-Mo(2)-C(21)	59.4(4)
C(23)-Mo(2)-C(22)	35.5(2)	C(24)-Mo(2)-C(21)	59.7(4)
C(24)-Mo(2)-C(22)	59.4(4)	C(24)-Mo(2)-C(23)	35.7(3)
C(25)-Mo(2)-C(21)	35.9(3)	C(25)-Mo(2)-C(22)	59.5(5)
C(25)-Mo(2)-C(23)	59.6(4)	C(25)-Mo(2)-C(24)	36.0(3)
C(26)-Mo(2)-C(21)	111.5(3)	C(26)-Mo(2)-C(22)	110.6(4)
C(26)-Mo(2)-C(23)	136.9(3)	C(26)-Mo(2)-C(24)	169.9(3)
C(26)-Mo(2)-C(25)	139.4(2)	C(27)-Mo(2)-C(21)	110.9(3)
C(27)-Mo(2)-C(22)	133.0(2)	C(27)-Mo(2)-C(23)	168.5(2)
C(27)-Mo(2)-C(24)	147.5(3)	C(27)-Mo(2)-C(25)	117.1(4)
C(27)-Mo(2)-C(26)	37.5(2)	C(28)-Mo(2)-C(21)	130.0(4)
C(28)-Mo(2)-C(22)	165.1(3)	C(28)-Mo(2)-C(23)	153.2(2)
C(28)-Mo(2)-C(24)	121.4(4)	C(28)-Mo(2)-C(25)	111.4(4)
C(28)-Mo(2)-C(26)	67.6(3)	C(28)-Mo(2)-C(27)	37.4(2)
C(29)-Mo(2)-C(21)	159.9(3)	C(29)-Mo(2)-C(22)	157.4(2)
C(29)-Mo(2)-C(23)	124.1(3)	C(29)-Mo(2)-C(24)	110.2(3)
C(29)-Mo(2)-C(25)	125.5(4)	C(29)-Mo(2)-C(26)	79.7(3)
C(29)-Mo(2)-C(27)	67.3(3)	C(29)-Mo(2)-C(28)	37.2(2)
C(210)-Mo(2)-C(21)	161.9(3)	C(210)-Mo(2)-C(22)	126.5(4)
C(210)-Mo(2)-C(23)	107.8(4)	C(210)-Mo(2)-C(24)	118.5(3)
C(210)-Mo(2)-C(25)	151.7(2)	C(210)-Mo(2)-C(26)	68.0(3)
C(210)-Mo(2)-C(27)	80.0(3)	C(210)-Mo(2)-C(28)	67.4(3)
C(210)-Mo(2)-C(29)	37.2(2)	C(211)-Mo(2)-C(21)	131.9(3)
C(211)-Mo(2)-C(22)	108.2(4)	C(211)-Mo(2)-C(23)	113.3(4)
C(211)-Mo(2)-C(24)	143.5(3)	C(211)-Mo(2)-C(25)	167.2(3)
C(211)-Mo(2)-C(26)	37.7(2)	C(211)-Mo(2)-C(27)	67.6(3)
C(211)-Mo(2)-C(28)	79.7(3)	C(211)-Mo(2)-C(29)	67.2(3)
C(211)-Mo(2)-C(210)	37.6(2)	C(22)-C(21)-Mo(2)	73.0(7)
C(25)-C(21)-Mo(2)	71.4(6)	C(25)-C(21)-C(22)	108.0(7)
C(21)-C(22)-Mo(2)	71.4(6)	C(23)-C(22)-Mo(2)	72.1(6)
C(23)-C(22)-C(21)	108.0(9)	C(22)-C(23)-Mo(2)	72.4(6)
C(24)-C(23)-Mo(2)	71.2(6)	C(24)-C(23)-C(22)	108.0(8)
C(23)-C(24)-Mo(2)	73.1(6)	C(25)-C(24)-Mo(2)	71.6(6)
C(25)-C(24)-C(23)	108.0(7)	C(21)-C(25)-Mo(2)	72.7(7)
C(24)-C(25)-Mo(2)	72.5(7)	C(24)-C(25)-C(21)	108.0(9)
C(27)-C(26)-Mo(2)	71.4(4)	C(211)-C(26)-Mo(2)	71.4(4)
C(211)-C(26)-C(27)	119.6(6)	C(212)-C(26)-Mo(2)	133.9(4)
C(212)-C(26)-C(27)	121.6(6)	C(212)-C(26)-C(211)	118.6(6)
C(26)-C(27)-Mo(2)	71.2(4)	C(28)-C(27)-Mo(2)	71.6(4)
C(28)-C(27)-C(26)	120.2(7)	C(218)-C(27)-Mo(2)	129.7(5)
C(218)-C(27)-C(26)	120.2(6)	C(218)-C(27)-C(28)	119.5(6)
C(27)-C(28)-Mo(2)	71.0(4)	C(29)-C(28)-Mo(2)	71.6(4)
C(29)-C(28)-C(27)	119.8(6)	C(224)-C(28)-Mo(2)	131.5(4)
C(224)-C(28)-C(27)	120.3(6)	C(224)-C(28)-C(29)	119.9(6)
C(28)-C(29)-Mo(2)	71.2(4)	C(210)-C(29)-Mo(2)	71.2(4)
C(210)-C(29)-C(28)	120.7(6)	C(230)-C(29)-Mo(2)	136.8(4)
C(230)-C(29)-C(28)	119.3(6)	C(230)-C(29)-C(210)	119.6(6)
C(29)-C(210)-Mo(2)	71.7(5)	C(211)-C(210)-Mo(2)	71.1(4)
C(211)-C(210)-C(29)	119.5(7)	C(236)-C(210)-Mo(2)	128.2(5)
C(236)-C(210)-C(29)	119.5(6)	C(236)-C(210)-C(211)	121.1(6)
C(26)-C(211)-Mo(2)	70.9(4)	C(210)-C(211)-Mo(2)	71.3(4)
C(210)-C(211)-C(26)	120.1(6)	C(242)-C(211)-Mo(2)	130.2(4)
C(242)-C(211)-C(26)	121.7(6)	C(242)-C(211)-C(210)	118.2(6)
C(213)-C(212)-C(26)	121.0(5)	C(217)-C(212)-C(26)	118.6(5)

Table 3 (cont.): Bond angles (°)

C(219)-C(218)-C(27)	121.2(5)	C(223)-C(218)-C(27)	118.7(5)
C(225)-C(224)-C(28)	121.6(5)	C(229)-C(224)-C(28)	118.4(5)
C(231)-C(230)-C(29)	122.4(5)	C(235)-C(230)-C(29)	117.6(5)
C(237)-C(236)-C(210)	120.9(5)	C(241)-C(236)-C(210)	119.0(5)
C(243)-C(242)-C(211)	121.8(4)	C(247)-C(242)-C(211)	117.8(5)
C(53)-C(48)-C(49)	106.6(17)	C(50)-C(49)-C(48)	132.7(13)
C(51)-C(50)-C(49)	104.7(13)	C(52)-C(51)-C(50)	130.8(14)
C(53)-C(52)-C(51)	119.1(13)	C(52)-C(53)-C(48)	125.7(17)
C(54)-C(53)-C(48)	107.6(16)	C(54)-C(53)-C(52)	126.5(17)
C(60)-C(55)-C(56)	118.1(11)	C(57)-C(56)-C(55)	121.5(12)
C(58)-C(57)-C(56)	119.0(14)	C(59)-C(58)-C(57)	120.2(12)
C(60)-C(59)-C(58)	121.9(12)	C(59)-C(60)-C(55)	119.3(12)
C(61)-C(60)-C(55)	119.4(12)	C(61)-C(60)-C(59)	121.3(12)

5.2 Crystal data for 5

Empirical formula	$C_{28}H_{38}MoO_6P_2$
Crystal System	monoclinic
Space Group	$P2_1/n$ (no.14)
Unit Cell Dimensions (Å): a	15.103 (6)
b	10.681 (3)
c	18.437 (7)
α(°)	90
β	100.90(3)
γ	90
Volume $Å^3$	2921(2)
D_{calcd}	1.43 Mg/m^{-3}
Z	4
F(000)	1304
T	293 K
R_F	0.0400
R_W	0.0468

Table 1: Fractional atomic coordinates ($*10^4$)

	x	y	z
Mo(1)	623(1)	1544(1)	2021(1)
P(1)	1549(1)	2082(1)	1117(1)
P(2)	-537(1)	2912(1)	1365(1)
O(1)	1347(2)	3383(3)	693(2)
O(2)	1510(2)	1060(3)	469(2)
O(3)	2629(2)	2290(3)	1389(2)
O(4)	-637(2)	3289(3)	500(2)
O(5)	-641(2)	4323(3)	1651(2)
O(6)	-1515(2)	2362(3)	1382(2)
C(1)	1949(4)	4190(6)	423(4)
C(2)	2022(4)	1153(6)	-108(3)
C(3)	3187(3)	1274(5)	1715(3)
C(4)	-698(3)	2339(5)	-51(3)
C(5)	-152(4)	5349(5)	1437(3)
C(6)	-2331(3)	3039(6)	1084(3)
C(7)	1364(3)	3340(5)	2452(3)
C(8)	1755(3)	2302(5)	2866(2)
C(9)	1601(3)	2116(6)	3640(3)
C(10)	609(3)	2258(4)	3665(2)
C(11)	9(3)	2099(4)	3037(2)
C(12)	1070(3)	-494(4)	2466(3)
C(13)	1097(3)	-417(4)	1710(3)

Table 1 (cont.): Fractional atomic coordinates ($*10^4$)

	x	y	z
C(14)	208(3)	-175(4)	1312(2)
C(15)	-360(3)	-95(4)	1840(2)
C(16)	176(3)	-312(4)	2544(2)
C(31)	-971(3)	2276(4)	3057(2)
C(21)	407(3)	2517(5)	4418(2)
C(22)	-108(4)	1717(7)	4750(3)
C(23)	-259(5)	1940(10)	5463(4)
C(24)	119(6)	2946(12)	5841(4)
C(25)	606(6)	3747(9)	5527(4)
C(26)	758(4)	3553(6)	4814(3)
C(32)	-1298(3)	3468(4)	3125(2)
C(33)	-2197(3)	3693(4)	3148(3)
C(34)	-2803(3)	2711(5)	3094(3)
C(35)	-2490(3)	1509(5)	3034(3)
C(36)	-1591(3)	1293(4)	3017(3)

Table 2: Bond lengths (Å)

Mo(1)-P(1)	2.437 (2)	Mo(1)-P(2)	2.422 (1)	Mo(1)-C(7)	2.286 (5)
Mo(1)-C(8)	2.235 (4)	Mo(1)-C(11)	2.319 (4)	Mo(1)-C(12)	2.379 (4)
Mo(1)-C(13)	2.320 (5)	Mo(1)-C(14)	2.272 (4)	Mo(1)-C(15)	2.279 (4)
Mo(1)-C(16)	2.359 (4)	P(1)-O(1)	1.595 (3)	P(1)-O(2)	1.611 (3)
P(1)-O(3)	1.629 (3)	P(2)-O(4)	1.623 (3)	P(2)-O(5)	1.614 (3)
P(2)-O(6)	1.596 (3)	C(7)-C(8)	1.410 (7)	C(8)-C(9)	1.502 (7)
C(9)-C(10)	1.515 (7)	C(10)-C(11)	1.338 (5)	C(10)-C(21)	1.503 (6)
C(11)-C(31)	1.500 (6)				

Table 3: Bond angles (°)

P(1)-Mo(1)-P(2)	88.3(1)	P(1)-Mo(1)-C(7)	74.6(1)
P(2)-Mo(1)-C(7)	85.9(1)	P(1)-Mo(1)-C(8)	85.9(1)
P(2)-Mo(1)-C(8)	121.0(1)	C(7)-Mo(1)-C(8)	36.3(2)
P(1)-Mo(1)-C(11)	149.4(1)	P(2)-Mo(1)-C(11)	83.5(1)
C(7)-Mo(1)-C(11)	75.4(2)	C(8)-Mo(1)-C(11)	73.4(2)
Mo(1)-P(1)-O(1)	117.4(1)	Mo(1)-P(1)-O(2)	113.7(1)
O(1)-P(1)-O(2)	104.4(2)	Mo(1)-P(1)-O(3)	119.5(1)
O(1)-P(1)-O(3)	96.9(2)	O(2)-P(1)-O(3)	102.4(2)
Mo(1)-P(2)-O(4)	124.3(1)	Mo(1)-P(2)-O(5)	120.4(1)
O(4)-P(2)-O(5)	95.3(2)	Mo(1)-P(2)-O(6)	110.7(1)
O(4)-P(2)-O(6)	101.3(2)	O(5)-P(2)-O(6)	101.0(2)
Mo(1)-C(7)-C(8)	69.9(3)	Mo(1)-C(8)-C(7)	73.8(2)
Mo(1)-C(8)-C(9)	112.3(3)	C(7)-C(8)-C(9)	119.5(4)
C(8)-C(9)-C(10)	110.3(3)	C(9)-C(10)-C(11)	118.2(4)
C(9)-C(10)-C(21)	114.9(3)	C(11)-C(10)-C(21)	126.9(4)
Mo(1)-C(11)-C(10)	115.0(3)	Mo(1)-C(11)-C(31)	126.8(3)
C(10)-C(11)-C(31)	118.2(4)		

5.3 Crystal data for 6

Empirical formula	$C_{23}H_{27}BF_2MoO_6P_2$
Crystal System	Triclinic
Space Group	P $\bar{1}$ (no. 2)
Unit Cell Dimensions (Å): a	9.688 (4)
b	10.788 (6)
c	12.961 (6)
α(°)	98.13 (4)
β	96.17 (3)
γ	102.52 (4)
Volume $Å^3$	1295 (1)
D_{calcd}	1.53 Mg/m^{-3}
Z	2
F(000)	616
T	293 K
R_F	0.0273
R_W	0.0375

Table 1: Fractional atomic coordinates ($*10^4$)

	x	y	z
Mo	4830(1)	1620(1)	3518(1)
P(2)	7192(1)	2739(1)	4276(1)
P(1)	5181(1)	3078(1)	2284(1)
O(1)	8269(2)	3416(2)	3608(1)
O(4)	6709(2)	3659(2)	2091(1)
O(3)	7137(2)	3811(2)	5241(1)
O(2)	8066(2)	1836(2)	4784(2)
C(7)	5904(2)	483(2)	2674(2)
O(5)	4450(2)	4241(2)	2535(2)
O(6)	4588(2)	2455(2)	1089(2)
C(9)	3659(3)	-1751(3)	999(2)
C(14)	7160(2)	142(2)	2296(2)
C(6)	4548(2)	-94(2)	2576(2)
C(8)	3567(2)	-1290(2)	2039(2)
C(1)	3337(3)	971(3)	4728(2)
C(2)	2458(3)	1092(3)	3837(2)
C(3)	2781(3)	2377(3)	3700(3)
C(4)	3870(3)	3069(3)	4519(3)
C(5)	4215(3)	2186(3)	5151(2)
C(13)	2524(3)	-1965(2)	2533(2)
C(10)	2684(4)	-2837(3)	460(3)
C(12)	1565(3)	-3067(3)	1979(3)
C(19)	8059(3)	931(3)	1775(2)
C(16)	8641(3)	-1380(3)	2105(3)
C(15)	7456(3)	-1027(3)	2449(2)
C(11)	1655(4)	-3478(3)	948(3)
C(17)	9509(3)	-599(4)	1580(3)

Table 1 (cont.): Fractional atomic coordinates ($*10^4$)

	x	y	z
F(1)	9136(2)	4271(2)	2219(1)
F(2)	8034(2)	5434(2)	3299(2)
C(20)	8391(3)	4714(3)	5777(2)
C(18)	9221(3)	544(3)	1414(3)
C(21)	9517(3)	1832(3)	4754(3)
B	8047(3)	4228(3)	2814(3)
C(22)	3128(3)	1813(4)	782(3)
C(23)	4721(5)	5327(4)	1989(4)

Table 2: Bond lengths (Å)

Mo-P(2)	2.375(1)	Mo-P(1)	2.397(1)
Mo-C(7)	2.050(3)	Mo-C(6)	2.013(2)
Mo-C(1)	2.325(3)	Mo-C(2)	2.341(3)
Mo-C(3)	2.326(3)	Mo-C(4)	2.304(3)
Mo-C(5)	2.297(3)	P(2)-O(1)	1.553(2)
P(2)-O(3)	1.592(2)	P(2)-O(2)	1.587(2)
P(1)-O(4)	1.539(2)	P(1)-O(5)	1.581(3)
P(1)-O(6)	1.590(2)	O(1)-B	1.471(4)
O(4)-B	1.471(3)	O(3)-C(20)	1.421(3)
O(2)-C(21)	1.412(3)	C(7)-C(14)	1.458(4)
C(7)-C(6)	1.310(3)	O(5)-C(23)	1.443(5)
O(6)-C(22)	1.419(4)		

Table 3: Bond angles (°)

P(2)-Mo-P(1)	83.5(1)	P(2)-Mo-C(7)	82.0(1)
P(1)-Mo-C(7)	88.9(1)	P(2)-Mo-C(6)	118.4(1)
P(1)-Mo-C(6)	101.6(1)	C(7)-Mo-C(6)	37.6(1)
Mo-P(2)-O(1)	121.5(1)	Mo-P(2)-O(3)	109.6(1)
O(1)-P(2)-O(3)	106.0(1)	Mo-P(2)-O(2)	112.4(1)
O(1)-P(2)-O(2)	101.6(1)	O(3)-P(2)-O(2)	104.1(1)
Mo-P(1)-O(4)	119.2(1)	Mo-P(1)-O(5)	112.4(1)
O(4)-P(1)-O(5)	106.8(1)	Mo-P(1)-O(6)	115.2(1)
O(4)-P(1)-O(6)	95.8(1)	O(5)-P(1)-O(6)	105.7(1)
P(2)-O(1)-B	129.5(2)	P(1)-O(4)-B	132.2(2)
P(2)-O(3)-C(20)	121.8(2)	P(2)-O(2)-C(21)	127.6(2)
Mo-C(7)-C(14)	155.3(2)	Mo-C(7)-C(6)	69.7(2)
C(14)-C(7)-C(6)	135.0(2)	P(1)-O(5)-C(23)	120.9(3)
P(1)-O(6)-C(22)	120.7(2)	Mo-C(6)-C(7)	72.7(1)
Mo-C(6)-C(8)	148.0(2)	C(7)-C(6)-C(8)	139.3(2)
O(1)-B-F(1)	107.7(3)	O(1)-B-O(4)	111.2(2)
O(1)-B-F(2)	109.9(2)	O(4)-B-F(1)	106.8(2)
F(1)-B-F(2)	111.0(2)	O(4)-B-F(2)	110.2(3)

5.4 Crystal data for 28

Empirical formula	$C_{36}H_{49}O_{24}B_9P_2Mo$
Crystal System	monoclinic
Space Group	$P2_1/c$
Unit Cell Dimensions (Å): a	11.736 (2)
b	19.367 (3)
c	17.781 (3)
β	100.67 (2)°
Volume $Å^3$	3971.6
D_{calcd}	1.39 g/cm^{-3}
Z	4
F(000)	1720
T	170 K
R_F	0.0491
R_W	0.0458

Table 1: Fractional atomic coordinates ($*10^4$)

	x	y	z
Mo(1)	1064	1850	2959
P(1)	272(1)	2681(1)	3746(1)
P(2)	1810(1)	2851(1)	2422(1)
O(1)	-427(3)	3287(2)	3283(2)
O(2)	-702(3)	2426(2)	4211(2)
O(3)	1248(3)	2995(2)	4387(2)
O(4)	857(3)	3186(2)	1760(2)
O(5)	2231(3)	3454(2)	3010(2)
O(6)	2944(3)	2811(2)	2041(2)
B(1)	471(6)	1527(4)	1654(4)
B(2)	717(6)	762(3)	2261(4)
B(3)	-268(6)	862(4)	2920(4)
B(4)	-192(6)	715(3)	1327(4)
B(5)	-642(6)	308(4)	2109(4)
B(6)	-1716(6)	821(4)	2397(4)
B(7)	-1957(6)	1547(4)	1776(4)
B(8)	-998(6)	1484(4)	1130(4)

Table 1 (cont.): Fractional atomic coordinates ($*10^4$)

	x	y	z
B(9)	-1689(6)	736(4)	1401(4)
C(1)	-1233(6)	3728(3)	3597(4)
C(2)	-395(6)	1936(3)	4829(3)
C(3)	1334(6)	3716(3)	4612(4)
C(4)	1079(6)	3836(3)	1416(3)
C(5)	3162(5)	3937(3)	2991(3)
C(6)	3075(6)	2346(4)	1437(4)
C(7)	2698(5)	1961(3)	3591(3)
C(8)	2156(5)	1439(3)	3865(3)
C(21)	1847(5)	302(3)	2459(3)
C(22)	1882(5)	-210(3)	2988(3)
C(35)	-612(5)	1956(3)	1956(3)
C(36)	-1022(5)	1575(3)	2654(3)

Table 2: Bond lengths (Å)

P(1)-Mo(1)	2.427(4)	P(2)-Mo(1)	2.398(4)
B(1)-Mo(1)	2.380(8)	B(2)-Mo(1)	2.441(8)
B(3)-Mo(1)	2.464(9)	C(7)-Mo(1)	2.046(8)
C(8)-Mo(1)	2.026(8)	C(35)-Mo(1)	2.407(8)
C(36)-Mo(1)	2.466(8)	O(1)-P(1)	1.575(6)
O(2)-P(1)	1.608(6)	O(3)-P(1)	1.581(6)
O(4)-P(2)	1.602(6)	O(5)-P(2)	1.585(6)
O(6)-P(2)	1.602(6)	C(1)-O(1)	1.460(8)
C(2)-O(2)	1.446(7)	C(3)-O(3)	1.452(8)
C(4)-O(4)	1.445(7)	C(5)-O(5)	1.443(7)
C(6)-O(6)	1.430(8)	B(2)-B(1)	1.825(11)
B(4)-B(1)	1.802(11)	B(8)-B(1)	1.804(11)
C(35)-B(1)	1.688(11)	B(3)-B(2)	1.802(11)

Table 3 (cont.): Bond lengths (Å)

B(4)-B(2)	1.803(11)	B(5)-B(2)	1.796(11)
C(21)-B(2)	1.582(10)	B(5)-B(3)	1.786(11)
B(6)-B(3)	1.782(11)	C(36)-B(3)	1.662(11)
B(5)-B(4)	1.762(11)	B(8)-B(4)	1.765(11)
B(9)-B(4)	1.786(12)	B(6)-B(5)	1.753(12)
B(9)-B(5)	1.791(11)	B(7)-B(6)	1.780(12)
B(9)-B(6)	1.786(12)	C(36)-B(6)	1.694(11)
B(8)-B(7)	1.755(12)	B(9)-B(7)	1.759(12)
C(35)-B(7)	1.742(11)	C(36)-B(7)	1.735(11)
B(9)-B(8)	1.770(12)	C(35)-B(8)	1.717(11)
C(8)-C(7)	1.333(9)	C(9)-C(7)	1.480(9)
C(15)-C(8)	1.479(9)	C(10)-C(9)	1.396(9)
C(14)-C(9)	1.397(9)	C(11)-C(10)	1.392(9)
C(12)-C(11)	1.370(9)	C(13)-C(12)	1.391(10)
C(14)-C(13)	1.399(9)	C(16)-C(15)	1.398(9)
C(20)-C(15)	1.392(9)	C(17)-C(16)	1.404(10)
C(18)-C(17)	1.373(10)	C(19)-C(18)	1.385(9)
C(20)-C(19)	1.402(9)	C(22)-C(21)	1.362(9)
C(23)-C(21)	1.495(9)	C(29)-C(22)	1.474(9)
C(24)-C(23)	1.405(9)	C(28)-C(23)	1.396(9)
C(25)-C(24)	1.376(9)	C(26)-C(25)	1.356(10)
C(27)-C(26)	1.402(10)	C(28)-C(27)	1.386(9)
C(30)-C(29)	1.400(9)	C(34)-C(29)	1.404(9)
C(31)-C(30)	1.388(9)	C(32)-C(31)	1.371(9)
C(33)-C(32)	1.373(9)	C(34)-C(33)	1.379(9)
C(36)-C(35)	1.593(10)	H(1)-B(1)	1.095(64)
H(3)-B(3)	1.156(62)	H(4)-B(4)	1.098(64)
H(5)-B(5)	1.088(66)	H(6)-B(6)	1.035(64)
H(7)-B(7)	1.007(66)	H(8)-B(8)	1.123(63)

Table 3 (cont.): Bond lengths (Å)

H(9)-B(9)	1.064(65)	H(11)-C(1)	0.960
H(12)-C(1)	0.960	H(13)-C(1)	0.960
H(21)-C(2)	0.960	H(22)-C(2)	0.960
H(23)-C(2)	0.960	H(31)-C(3)	0.960
H(32)-C(3)	0.960	H(33)-C(3)	0.960
H(41)-C(4)	0.960	H(42)-C(4)	0.960
H(43)-C(4)	0.960	H(51)-C(5)	0.960
H(52)-C(5)	0.960	H(53)-C(5)	0.960
H(61)-C(6)	0.960	H(62)-C(6)	0.960
H(63)-C(6)	0.960	H(101)-C(10)	0.960
H(111)-C(11)	0.960	H(121)-C(12)	0.960
H(131)-C(13)	0.960	H(141)-C(14)	0.960
H(161)-C(16)	0.960	H(171)-C(17)	0.960
H(181)-C(18)	0.960	H(191)-C(19)	0.960
H(201)-C(20)	0.960	H(221)-C(22)	0.996(65)
H(241)-C(24)	0.960	H(251)-C(25)	0.960
H(261)-C(26)	0.960	H(271)-C(27)	0.960
H(281)-C(28)	0.960	H(301)-C(30)	0.960
H(311)-C(31)	0.960	H(321)-C(32)	0.960
H(331)-C(33)	0.960	H(341)-C(34)	0.960
H(351)-C(35)	1.005(69)	H(361)-C(36)	1.015(66)

Table 3: Bond angles (°)

P(2)-Mo(1)-P(1)	84.3(2)	B(1)-Mo(1)-P(1)	131.5(2)
B(1)-Mo(1)-P(2)	83.5(3)	B(2)-Mo(1)-P(1)	145.0(2)
B(2)-Mo(1)-P(2)	122.3(3)	B(2)-Mo(1)-B(1)	44.5(2)
B(3)-Mo(1)-P(1)	102.8(3)	B(3)-Mo(1)-P(2)	153.3(2)
B(3)-Mo(1)-B(1)	72.5(3)	B(3)-Mo(1)-B(2)	43.1(2)
C(7)-Mo(1)-P(1)	91.9(3)	C(7)-Mo(1)-P(2)	76.1(3)
C(7)-Mo(1)-B(1)	129.7(3)	C(7)-Mo(1)-B(2)	114.9(3)
C(7)-Mo(1)-B(3)	128.5(3)	C(8)-Mo(1)-P(1)	93.2(3)
C(8)-Mo(1)-P(2)	114.3(3)	C(8)-Mo(1)-B(1)	134.4(2)
C(8)-Mo(1)-B(2)	95.0(3)	C(8)-Mo(1)-B(3)	91.2(3)
C(8)-Mo(1)-C(7)	38.2(2)	C(35)-Mo(1)-P(1)	91.3(2)
C(35)-Mo(1)-P(2)	86.8(2)	C(35)-Mo(1)-B(1)	41.3(2)
C(35)-Mo(1)-B(2)	70.1(3)	C(35)-Mo(1)-B(3)	67.6(3)
C(35)-Mo(1)-C(7)	162.2(2)	C(35)-Mo(1)-C(8)	158.8(2)
C(36)-Mo(1)-P(1)	78.4(2)	C(36)-Mo(1)-P(2)	120.5(2)
C(36)-Mo(1)-B(1)	68.3(3)	C(36)-Mo(1)-B(2)	68.7(3)
C(36)-Mo(1)-B(3)	39.4(2)	C(36)-Mo(1)-C(7)	159.2(2)
C(36)-Mo(1)-C(8)	123.1(3)	C(36)-Mo(1)-C(35)	38.1(2)
O(1)-P(1)-Mo(1)	114.3(2)	O(2)-P(1)-Mo(1)	118.5(3)
O(2)-P(1)-O(1)	98.4(3)	O(3)-P(1)-Mo(1)	111.6(3)
O(3)-P(1)-O(1)	109.2(3)	O(3)-P(1)-O(2)	103.6(3)
O(4)-P(2)-Mo(1)	111.3(3)	O(5)-P(2)-Mo(1)	115.1(3)
O(5)-P(2)-O(4)	106.1(3)	O(6)-P(2)-Mo(1)	121.5(3)
O(6)-P(2)-O(4)	103.4(3)	O(6)-P(2)-O(5)	97.7(3)
C(1)-O(1)-P(1)	123.2(4)	C(2)-O(2)-P(1)	119.4(5)
C(3)-O(3)-P(1)	125.0(5)	C(4)-O(4)-P(2)	120.4(5)
C(5)-O(5)-P(2)	127.3(4)	C(6)-O(6)-P(2)	124.1(5)

Table 3 (cont.): Bond angles (°)

B(2)-B(1)-Mo(1)	69.5(4)	B(4)-B(1)-Mo(1)	125.1(5)
B(4)-B(1)-B(2)	59.6(4)	B(8)-B(1)-Mo(1)	126.4(5)
B(8)-B(1)-B(2)	107.4(6)	B(8)-B(1)-B(4)	58.6(5)
C(35)-B(1)-Mo(1)	70.2(4)	C(35)-B(1)-B(2)	104.9(6)
C(35)-B(1)-B(4)	103.1(6)	C(35)-B(1)-B(8)	58.8(5)
B(1)-B(2)-Mo(1)	66.0(4)	B(3)-B(2)-Mo(1)	69.1(4)
B(3)-B(2)-B(1)	104.4(5)	B(4)-B(2)-Mo(1)	121.8(5)
B(4)-B(2)-B(1)	59.6(4)	B(4)-B(2)-B(3)	105.3(6)
B(5)-B(2)-Mo(1)	124.0(5)	B(5)-B(2)-B(1)	105.6(5)
B(5)-B(2)-B(3)	59.5(5)	B(5)-B(2)-B(4)	58.6(4)
C(21)-B(2)-Mo(1)	108.6(5)	C(21)-B(2)-B(1)	128.5(6)
C(21)-B(2)-B(3)	121.9(6)	C(21)-B(2)-B(4)	120.3(6)
C(21)-B(2)-B(5)	116.3(6)	B(2)-B(3)-Mo(1)	67.8(4)
B(5)-B(3)-Mo(1)	123.3(5)	B(5)-B(3)-B(2)	60.1(5)
B(6)-B(3)-Mo(1)	126.0(5)	B(6)-B(3)-B(2)	108.7(6)
B(6)-B(3)-B(5)	58.9(5)	C(36)-B(3)-Mo(1)	70.4(4)
C(36)-B(3)-B(2)	106.0(6)	C(36)-B(3)-B(5)	103.3(6)
C(36)-B(3)-B(6)	58.8(5)	B(2)-B(4)-B(1)	60.8(4)
B(5)-B(4)-B(1)	108.0(6)	B(5)-B(4)-B(2)	60.5(4)
B(8)-B(4)-B(1)	60.7(5)	B(8)-B(4)-B(2)	110.1(6)
B(8)-B(4)-B(5)	107.8(6)	B(9)-B(4)-B(1)	109.2(6)
B(9)-B(4)-B(2)	110.7(6)	B(9)-B(4)-B(5)	60.6(5)
B(9)-B(4)-B(8)	59.8(5)	B(3)-B(5)-B(2)	60.4(4)
B(4)-B(5)-B(2)	60.9(5)	B(4)-B(5)-B(3)	107.8(6)
B(6)-B(5)-B(2)	110.2(6)	B(6)-B(5)-B(3)	60.5(5)
B(6)-B(5)-B(4)	108.4(6)	B(9)-B(5)-B(2)	110.8(6)
B(9)-B(5)-B(3)	109.0(6)	B(9)-B(5)-B(4)	60.4(5)
B(9)-B(5)-B(6)	60.5(5)	B(5)-B(6)-B(3)	60.7(5)
B(7)-B(6)-B(3)	108.4(6)	B(7)-B(6)-B(5)	107.8(6)
B(9)-B(6)-B(3)	109.4(6)	B(9)-B(6)-B(5)	60.8(5)
B(9)-B(6)-B(7)	59.1(5)	C(36)-B(6)-B(3)	57.1(5)
C(36)-B(6)-B(5)	103.4(6)	C(36)-B(6)-B(7)	59.9(5)

Table 3 (cont.): Bond angles (°)

C(36)-B(6)-B(9)	104.5(6)	B(8)-B(7)-B(6)	107.7(6)
B(9)-B(7)-B(6)	60.6(5)	B(9)-B(7)-B(8)	60.5(5)
C(35)-B(7)-B(6)	102.2(6)	C(35)-B(7)-B(8)	58.8(5)
C(35)-B(7)-B(9)	104.8(6)	C(36)-B(7)-B(6)	57.6(5)
C(36)-B(7)-B(8)	102.4(6)	C(36)-B(7)-B(9)	104.0(6)
C(36)-B(7)-C(35)	54.6(4)	B(4)-B(8)-B(1)	60.7(5)
B(7)-B(8)-B(1)	109.1(6)	B(7)-B(8)-B(4)	108.4(6)
B(9)-B(8)-B(1)	109.9(6)	B(9)-B(8)-B(4)	60.7(5)
B(9)-B(8)-B(7)	59.9(5)	C(35)-B(8)-B(1)	57.2(4)
C(35)-B(8)-B(4)	103.5(5)	C(35)-B(8)-B(7)	60.2(5)
C(35)-B(8)-B(9)	105.4(6)	B(5)-B(9)-B(4)	59.0(5)
B(6)-B(9)-B(4)	105.9(6)	B(6)-B(9)-B(5)	58.7(5)
B(7)-B(9)-B(4)	107.2(6)	B(7)-B(9)-B(5)	107.1(6)
B(7)-B(9)-B(6)	60.3(5)	B(8)-B(9)-B(4)	59.5(5)
B(8)-B(9)-B(5)	106.3(6)	B(8)-B(9)-B(6)	106.7(6)
B(8)-B(9)-B(7)	59.6(5)	C(8)-C(7)-Mo(1)	70.1(4)
C(9)-C(7)-Mo(1)	153.1(4)	C(9)-C(7)-C(8)	136.4(5)
C(7)-C(8)-Mo(1)	71.7(4)	C(15)-C(8)-Mo(1)	155.2(4)
C(15)-C(8)-C(7)	132.9(5)	C(10)-C(9)-C(7)	119.7(6)
C(14)-C(9)-C(7)	121.7(6)	C(14)-C(9)-C(10)	118.6(6)
C(11)-C(10)-C(9)	120.6(6)	C(12)-C(11)-C(10)	120.9(7)
C(13)-C(12)-C(11)	119.3(7)	C(14)-C(13)-C(12)	120.5(7)
C(13)-C(14)-C(9)	120.1(7)	C(16)-C(15)-C(8)	119.2(6)
C(20)-C(15)-C(8)	121.9(6)	C(20)-C(15)-C(16)	118.9(7)
C(17)-C(16)-C(15)	120.3(7)	C(18)-C(17)-C(16)	120.3(7)
C(19)-C(18)-C(17)	119.9(7)	C(20)-C(19)-C(18)	120.4(7)
C(19)-C(20)-C(15)	120.2(7)	C(22)-C(21)-B(2)	118.7(6)
C(23)-C(21)-B(2)	121.8(6)	C(23)-C(21)-C(22)	119.6(6)
C(29)-C(22)-C(21)	133.2(6)	C(24)-C(23)-C(21)	120.0(6)
C(28)-C(23)-C(21)	122.3(6)	C(28)-C(23)-C(24)	117.7(6)
C(25)-C(24)-C(23)	120.9(7)	C(26)-C(25)-C(24)	120.7(8)
C(27)-C(26)-C(25)	120.5(8)	C(28)-C(27)-C(26)	118.9(7)

Table 3 (cont.): Bond angles (°)

C(27)-C(28)-C(23)	121.2(7)	C(30)-C(29)-C(22)	126.5(6)
C(34)-C(29)-C(22)	116.5(6)	C(34)-C(29)-C(30)	116.9(6)
C(31)-C(30)-C(29)	120.7(6)	C(32)-C(31)-C(30)	120.8(7)
C(33)-C(32)-C(31)	119.9(7)	C(34)-C(33)-C(32)	119.9(7)
C(33)-C(34)-C(29)	121.7(7)	B(1)-C(35)-Mo(1)	68.5(4)
B(7)-C(35)-Mo(1)	133.3(4)	B(7)-C(35)-B(1)	115.4(6)
B(8)-C(35)-Mo(1)	129.7(5)	B(8)-C(35)-B(1)	64.0(5)
B(8)-C(35)-B(7)	61.0(5)	C(36)-C(35)-Mo(1)	72.9(4)
C(36)-C(35)-B(1)	112.0(6)	C(36)-C(35)-B(7)	62.5(5)
C(36)-C(35)-B(8)	110.5(6)	B(3)-C(36)-Mo(1)	70.2(4)
B(6)-C(36)-Mo(1)	130.8(4)	B(6)-C(36)-B(3)	64.1(5)
B(7)-C(36)-Mo(1)	129.9(5)	B(7)-C(36)-B(3)	116.4(6)
B(7)-C(36)-B(6)	62.5(5)	C(35)-C(36)-Mo(1)	68.9(4)
C(35)-C(36)-B(3)	112.6(6)	C(35)-C(36)-B(6)	112.8(6)
C(35)-C(36)-B(7)	62.9(5)	H(1)-B(1)-Mo(1)	107.9(34)
H(1)-B(1)-B(2)	129.1(34)	H(1)-B(1)-B(4)	119.3(34)
H(1)-B(1)-B(8)	112.2(34)	H(1)-B(1)-C(35)	122.4(34)
H(3)-B(3)-Mo(1)	105.3(32)	H(3)-B(3)-B(2)	128.4(32)
H(3)-B(3)-B(5)	123.6(32)	H(3)-B(3)-B(6)	114.4(33)
H(3)-B(3)-C(36)	119.9(32)	H(4)-B(4)-B(1)	119.1(34)
H(4)-B(4)-B(2)	118.7(34)	H(4)-B(4)-B(5)	123.5(34)
H(4)-B(4)-B(8)	121.2(34)	H(4)-B(4)-B(9)	122.6(34)
H(5)-B(5)-B(2)	112.5(35)	H(5)-B(5)-B(3)	117.0(34)
H(5)-B(5)-B(4)	121.8(34)	H(5)-B(5)-B(6)	125.1(34)
H(5)-B(5)-B(9)	127.8(35)	H(6)-B(6)-B(3)	120.9(36)
H(6)-B(6)-B(5)	128.7(37)	H(6)-B(6)-B(7)	117.2(36)
H(6)-B(6)-B(9)	125.3(36)	H(6)-B(6)-C(36)	119.5(36)
H(7)-B(7)-B(6)	125.0(38)	H(7)-B(7)-B(8)	126.4(38)
H(7)-B(7)-B(9)	137.7(37)	H(7)-B(7)-C(35)	113.1(38)
H(7)-B(7)-C(36)	112.9(38)	H(8)-B(8)-B(1)	116.7(33)
H(8)-B(8)-B(4)	126.7(33)	H(8)-B(8)-B(7)	120.1(33)
H(8)-B(8)-B(9)	127.9(34)	H(8)-B(8)-C(35)	118.5(33)

Table 3 (cont.): Bond angles (°)

H(9)-B(9)-B(4)	126.1(35)	H(9)-B(9)-B(5)	127.0(36)
H(9)-B(9)-B(6)	121.8(34)	H(9)-B(9)-B(7)	117.0(36)
H(9)-B(9)-B(8)	120.5(35)	H(11)-C(1)-O(1)	109.5(4)
H(12)-C(1)-O(1)	109.5(4)	H(12)-C(1)-H(11)	109.5
H(13)-C(1)-O(1)	109.4(4)	H(13)-C(1)-H(11)	109.5
H(13)-C(1)-H(12)	109.5	H(21)-C(2)-O(2)	109.5(4)
H(22)-C(2)-O(2)	109.4(4)	H(22)-C(2)-H(21)	109.5
H(23)-C(2)-O(2)	109.5(4)	H(23)-C(2)-H(21)	109.5
H(23)-C(2)-H(22)	109.5	H(31)-C(3)-O(3)	109.5(4)
H(32)-C(3)-O(3)	109.4(4)	H(32)-C(3)-H(31)	109.5
H(33)-C(3)-O(3)	109.4(4)	H(33)-C(3)-H(31)	109.5
H(33)-C(3)-H(32)	109.5	H(41)-C(4)-O(4)	109.4(4)
H(42)-C(4)-O(4)	109.6(4)	H(42)-C(4)-H(41)	109.5
H(43)-C(4)-O(4)	109.5(4)	H(43)-C(4)-H(41)	109.5
H(43)-C(4)-H(42)	109.5	H(51)-C(5)-O(5)	109.5(4)
H(52)-C(5)-O(5)	109.5(4)	H(52)-C(5)-H(51)	109.5
H(53)-C(5)-O(5)	109.4(4)	H(53)-C(5)-H(51)	109.5
H(53)-C(5)-H(52)	109.5	H(61)-C(6)-O(6)	109.5(4)
H(62)-C(6)-O(6)	109.5(5)	H(62)-C(6)-H(61)	109.5
H(63)-C(6)-O(6)	109.4(5)	H(63)-C(6)-H(61)	109.5
H(63)-C(6)-H(62)	109.5	H(101)-C(10)-C(9)	119.7(4)
C(11)-C(10)-H(101)	119.8(5)	H(111)-C(11)-C(10)	119.5(5)
C(12)-C(11)-H(111)	119.6(5)	H(121)-C(12)-C(11)	120.3(5)
C(13)-C(12)-H(121)	120.4(5)	H(131)-C(13)-C(12)	119.7(5)
C(14)-C(13)-H(131)	119.8(5)	H(141)-C(14)-C(9)	119.9(4)
H(141)-C(14)-C(13)	119.9(5)	H(161)-C(16)-C(15)	119.9(5)
C(17)-C(16)-H(161)	119.8(5)	H(171)-C(17)-C(16)	119.8(5)
C(18)-C(17)-H(171)	119.9(5)	H(181)-C(18)-C(17)	120.0(5)
C(19)-C(18)-H(181)	120.1(5)	H(191)-C(19)-C(18)	119.9(5)
C(20)-C(19)-H(191)	119.7(5)	H(201)-C(20)-C(15)	120.0(4)
H(201)-C(20)-C(19)	119.9(5)	H(221)-C(22)-C(21)	117.9(39)
C(29)-C(22)-H(221)	108.9(39)	H(241)-C(24)-C(23)	119.5(4)

Table 3 (cont.): Bond angles (°)

C(25)-C(24)-H(241)	119.6(5)	H(251)-C(25)-C(24)	119.7(5)
C(26)-C(25)-H(251)	119.7(5)	H(261)-C(26)-C(25)	119.8(5)
C(27)-C(26)-H(261)	119.7(5)	H(271)-C(27)-C(26)	120.5(5)
C(28)-C(27)-H(271)	120.6(5)	H(281)-C(28)-C(23)	119.4(4)
H(281)-C(28)-C(27)	119.4(5)	H(301)-C(30)-C(29)	119.7(4)
C(31)-C(30)-H(301)	119.6(4)	H(311)-C(31)-C(30)	119.6(4)
C(32)-C(31)-H(311)	119.7(5)	H(321)-C(32)-C(31)	120.1(5)
C(33)-C(32)-H(321)	120.0(5)	H(331)-C(33)-C(32)	120.1(5)
C(34)-C(33)-H(331)	120.0(5)	H(341)-C(34)-C(29)	119.1(4)
H(341)-C(34)-C(33)	119.1(5)	H(351)-C(35)-Mo(1)	101.8(38)
H(351)-C(35)-B(1)	119.1(37)	H(351)-C(35)-B(7)	112.8(38)
H(351)-C(35)-B(8)	114.8(37)	C(36)-C(35)-H(351)	122.2(37)
H(361)-C(36)-Mo(1)	92.8(37)	H(361)-C(36)-B(3)	114.5(37)
H(361)-C(36)-B(6)	121.9(37)	H(361)-C(36)-B(7)	121.6(38)
H(361)-C(36)-C(35)	118.6(37)		

5.5 Crystal data for 30

Empirical formula	$C_{46}H_{44}B_9NMo$
Crystal system	orthorhombic
Space group	$Pn2_1c$
Unit Cell Dimensions (Å): a	9.940 (1)
b	20.258 (4)
c	21.032 (3)
Volume $Å^3$	4235.1
D_{calcd}	1.26 g/cm^{-3}
Z	4
F(000)	1656
T	293 K
R_F	0.0493
R_W	0.0406

Table 1: Fractional atomic coordinates ($*10^4$)

	x	y	z
Mo(1)	1117(1)	0	2302
N(1)	-852(8)	280(6)	2596(4)
B(1)	4133(12)	-792(8)	3074(7)
B(2)	3119(16)	-1511(10)	2933(7)
B(3)	1689(15)	-1433(10)	3449(7)
B(4)	1870(13)	-697(11)	3925(6)
B(5)	3336(15)	-1168(15)	3712(9)
B(6)	3247(13)	-97(12)	2888(5)
B(7)	841(14)	-715(10)	3226(7)
B(8)	1811(11)	5(13)	3417(5)
B(9)	3405(15)	-319(10)	3690(7)
C(1')	2967(10)	-783(8)	2479(5)
C(2')	1636(11)	-1136(7)	2688(6)
C(1)	1116(12)	-501(7)	1430(4)
C(2)	-82(11)	-527(7)	1645(5)
C(3)	2166(11)	729(7)	1827(5)
C(4)	1013(12)	948(8)	2018(6)
C(5)	1410(11)	681(9)	3723(6)
C(6)	148(13)	757(8)	3980(6)
C(7)	-3158(11)	704(10)	2975(7)
C(8)	-1866(12)	450(8)	2746(6)

Table 1 (cont.): Fractional atomic coordinates ($*10^4$)

	x	y	z
C(10)	2018(10)	-1428(6)	807(5)
C(11)	2703(10)	-1679(6)	281(5)
C(12)	3331(10)	-1250(6)	-144(5)
C(13)	3273(10)	-570(6)	-44(5)
C(14)	2587(10)	-319(6)	482(5)
C(9)	1960(10)	-748(6)	907(5)
C(16)	-2284(7)	-1007(5)	1921(3)
C(17)	-3540(7)	-1244(5)	1733(3)
C(18)	-3931(7)	-1202(5)	1097(3)
C(19)	-3064(7)	-924(5)	649(3)
C(20)	-1808(7)	-688(5)	837(3)
C(15)	-1418(7)	-729(5)	1473(3)
C(22)	4502(10)	516(5)	1464(4)
C(23)	5746(10)	745(5)	1251(4)
C(24)	5983(10)	1422(5)	1203(4)
C(25)	4976(10)	1870(5)	1367(4)
C(26)	3731(10)	1641(5)	1580(4)
C(21)	3494(10)	964(5)	1628(4)
C(28)	-168(10)	1775(6)	1368(4)
C(29)	-1020(10)	2319(6)	1308(4)
C(30)	-1545(10)	2621(6)	1850(4)
C(31)	-1218(10)	2380(6)	2451(4)
C(32)	-366(10)	1836(6)	2511(4)
C(27)	159(10)	1534(6)	1970(4)
C(34)	3101(10)	1242(5)	4422(4)
C(35)	4215(10)	1650(5)	4516(4)
C(36)	4727(10)	2020(5)	4012(4)
C(37)	4125(10)	1982(5)	3414(4)
C(38)	3011(10)	1575(5)	3320(4)
C(33)	2499(10)	1205(5)	3824(4)
C(40)	-1628(10)	1176(6)	4665(5)

Table 1 (cont.): Fractional atomic coordinates ($*10^4$)

	x	y	z
C(41)	-2344(10)	1664(6)	4989(5)
C(42)	-1909(10)	2318(6)	4969(5)
C(43)	-758(10)	2485(6)	4625(5)
C(44)	-42(10)	1998(6)	4301(5)
C(39)	-477(10)	1343(6)	4321(5)

Table 2: Bond lengths (Å)

N(1)-Mo(1)	2.130(10)	B(6)-Mo(1)	2.458(14)
B(7)-Mo(1)	2.439(18)	B(8)-Mo(1)	2.443(12)
C(1')-Mo(1)	2.456(15)	C(2')-Mo(1)	2.494(16)
C(1)-Mo(1)	2.096(12)	C(2)-Mo(1)	2.116(14)
C(3)-Mo(1)	2.017(14)	C(4)-Mo(1)	2.014(18)
Mo(1)-N(1)	2.130(10)	C(8)-N(1)	1.111(16)
B(2)-B(1)	1.796(26)	B(5)-B(1)	1.734(27)
B(6)-B(1)	1.707(28)	B(9)-B(1)	1.766(24)
C(1')-B(1)	1.707(19)	B(1)-B(2)	1.796(26)
B(3)-B(2)	1.796(24)	B(5)-B(2)	1.794(28)
C(1')-B(2)	1.765(25)	C(2')-B(2)	1.736(22)
B(2)-B(3)	1.796(24)	B(4)-B(3)	1.804(30)
B(5)-B(3)	1.810(25)	B(7)-B(3)	1.746(28)
C(2')-B(3)	1.711(22)	B(3)-B(4)	1.804(30)
B(5)-B(4)	1.798(29)	B(7)-B(4)	1.790(21)
B(8)-B(4)	1.779(31)	B(9)-B(4)	1.777(24)
B(1)-B(5)	1.734(27)	B(2)-B(5)	1.794(28)
B(3)-B(5)	1.810(25)	B(4)-B(5)	1.798(29)
B(9)-B(5)	1.722(39)	Mo(1)-B(6)	2.458(14)
B(1)-B(6)	1.707(28)	B(8)-B(6)	1.821(19)
B(9)-B(6)	1.752(21)	C(1')-B(6)	1.658(28)
Mo(1)-B(7)	2.439(18)	B(3)-B(7)	1.746(28)
B(4)-B(7)	1.790(21)	B(8)-B(7)	1.792(31)
C(2')-B(7)	1.622(22)	Mo(1)-B(8)	2.443(12)
B(4)-B(8)	1.779(31)	B(6)-B(8)	1.821(19)
B(7)-B(8)	1.792(31)	B(9)-B(8)	1.808(23)
C(5)-B(8)	1.566(31)	B(1)-B(9)	1.766(24)

Table 2 (cont.): Bond lengths (Å)

B(4)-B(9)	1.777(24)	B(5)-B(9)	1.722(39)
B(6)-B(9)	1.752(21)	B(8)-B(9)	1.808(23)
Mo(1)-C(1')	2.456(15)	B(1)-C(1')	1.707(19)
B(2)-C(1')	1.765(25)	B(6)-C(1')	1.658(28)
C(2')-C(1')	1.568(19)	Mo(1)-C(2')	2.494(16)
B(2)-C(2')	1.736(22)	B(3)-C(2')	1.711(22)
B(7)-C(2')	1.622(22)	C(1')-C(2')	1.568(19)
Mo(1)-C(1)	2.096(12)	C(2)-C(1)	1.275(17)
C(9)-C(1)	1.471(16)	Mo(1)-C(2)	2.116(14)
C(1)-C(2)	1.275(17)	C(15)-C(2)	1.435(15)
Mo(1)-C(3)	2.017(14)	C(4)-C(3)	1.264(18)
C(21)-C(3)	1.498(16)	Mo(1)-C(4)	2.014(18)
C(3)-C(4)	1.264(18)	C(27)-C(4)	1.462(19)
B(8)-C(5)	1.566(31)	C(6)-C(5)	1.374(18)
C(33)-C(5)	1.531(20)	C(5)-C(6)	1.374(18)
C(39)-C(6)	1.521(20)	C(8)-C(7)	1.464(19)
N(1)-C(8)	1.111(16)	C(7)-C(8)	1.464(19)
C(11)-C(10)	1.395(15)	C(9)-C(10)	1.395(18)
C(10)-C(11)	1.395(15)	C(12)-C(11)	1.395(16)
C(11)-C(12)	1.395(16)	C(13)-C(12)	1.395(18)
C(12)-C(13)	1.395(18)	C(14)-C(13)	1.395(15)
C(13)-C(14)	1.395(15)	C(9)-C(14)	1.395(16)
C(1)-C(9)	1.471(16)	C(10)-C(9)	1.395(18)
C(14)-C(9)	1.395(16)	C(17)-C(16)	1.395(11)
C(15)-C(16)	1.395(11)	C(16)-C(17)	1.395(11)
C(18)-C(17)	1.395(9)	C(17)-C(18)	1.395(9)
C(19)-C(18)	1.395(11)	C(18)-C(19)	1.395(11)
C(20)-C(19)	1.395(11)	C(19)-C(20)	1.395(11)
C(15)-C(20)	1.395(9)	C(2)-C(15)	1.435(15)
C(16)-C(15)	1.395(11)	C(20)-C(15)	1.395(9)
C(23)-C(22)	1.395(15)	C(21)-C(22)	1.395(15)
C(22)-C(23)	1.395(15)	C(24)-C(23)	1.395(16)

Table 2 (cont.): Bond lengths (Å)

C(23)-C(24)	1.395(16)	C(25)-C(24)	1.395(15)
C(24)-C(25)	1.395(15)	C(26)-C(25)	1.395(15)
C(25)-C(26)	1.395(15)	C(21)-C(26)	1.395(16)
C(3)-C(21)	1.498(16)	C(22)-C(21)	1.395(15)
C(26)-C(21)	1.395(16)	C(29)-C(28)	1.395(17)
C(27)-C(28)	1.395(14)	C(28)-C(29)	1.395(17)
C(30)-C(29)	1.395(14)	C(29)-C(30)	1.395(14)
C(31)-C(30)	1.395(14)	C(30)-C(31)	1.395(14)
C(32)-C(31)	1.395(17)	C(31)-C(32)	1.395(17)
C(27)-C(32)	1.395(14)	C(4)-C(27)	1.462(19)
C(28)-C(27)	1.395(14)	C(32)-C(27)	1.395(14)
C(35)-C(34)	1.395(15)	C(33)-C(34)	1.395(13)
C(34)-C(35)	1.395(15)	C(36)-C(35)	1.395(14)
C(35)-C(36)	1.395(14)	C(37)-C(36)	1.395(13)
C(36)-C(37)	1.395(13)	C(38)-C(37)	1.395(15)
C(37)-C(38)	1.395(15)	C(33)-C(38)	1.395(14)
C(5)-C(33)	1.531(20)	C(34)-C(33)	1.395(13)
C(38)-C(33)	1.395(14)	C(41)-C(40)	1.395(16)
C(39)-C(40)	1.395(15)	C(40)-C(41)	1.395(16)
C(42)-C(41)	1.395(17)	C(41)-C(42)	1.395(17)
C(43)-C(42)	1.395(15)	C(42)-C(43)	1.395(15)
C(44)-C(43)	1.395(16)	C(43)-C(44)	1.395(16)
C(39)-C(44)	1.395(17)	C(6)-C(39)	1.521(20)
C(40)-C(39)	1.395(15)	C(44)-C(39)	1.395(17)

Table 3: Bond angles (°)

B(6)-Mo(1)-N(1)	131.9(4)	B(7)-Mo(1)-N(1)	79.9(5)
B(7)-Mo(1)-B(6)	69.5(6)	B(8)-Mo(1)-N(1)	88.9(5)
B(8)-Mo(1)-B(6)	43.6(4)	B(8)-Mo(1)-B(7)	43.1(7)
C(1')-Mo(1)-N(1)	144.8(4)	C(1')-Mo(1)-B(6)	39.4(6)
C(1')-Mo(1)-B(7)	65.2(5)	C(1')-Mo(1)-B(8)	69.3(6)
C(2')-Mo(1)-N(1)	110.0(5)	C(2')-Mo(1)-B(6)	65.5(7)
C(2')-Mo(1)-B(7)	38.4(5)	C(2')-Mo(1)-B(8)	68.4(8)
C(2')-Mo(1)-C(1')	36.9(4)	C(1)-Mo(1)-N(1)	112.5(5)
C(1)-Mo(1)-B(6)	113.6(6)	C(1)-Mo(1)-B(7)	114.2(6)
C(1)-Mo(1)-B(8)	147.3(7)	C(1)-Mo(1)-C(1')	79.6(5)
C(1)-Mo(1)-C(2')	80.7(6)	C(2)-Mo(1)-N(1)	78.8(5)
C(2)-Mo(1)-B(6)	140.6(6)	C(2)-Mo(1)-B(7)	99.1(6)
C(2)-Mo(1)-B(8)	142.0(6)	C(2)-Mo(1)-C(1')	101.2(6)
C(2)-Mo(1)-C(2')	82.2(6)	C(2)-Mo(1)-C(1)	35.2(4)
C(3)-Mo(1)-N(1)	114.1(6)	C(3)-Mo(1)-B(6)	80.5(7)
C(3)-Mo(1)-B(7)	147.8(5)	C(3)-Mo(1)-B(8)	106.1(7)
C(3)-Mo(1)-C(1')	98.8(6)	C(3)-Mo(1)-C(2')	135.5(4)
C(3)-Mo(1)-C(1)	88.1(6)	C(3)-Mo(1)-C(2)	111.8(6)
C(4)-Mo(1)-N(1)	77.6(6)	C(4)-Mo(1)-B(6)	105.6(8)
C(4)-Mo(1)-B(7)	142.8(5)	C(4)-Mo(1)-B(8)	107.2(8)
C(4)-Mo(1)-C(1')	134.3(5)	C(4)-Mo(1)-C(2')	170.8(4)
C(4)-Mo(1)-C(1)	101.7(6)	C(4)-Mo(1)-C(2)	105.0(6)
C(4)-Mo(1)-C(3)	36.5(5)	C(8)-N(1)-Mo(1)	177.4(12)
B(5)-B(1)-B(2)	61.0(12)	B(6)-B(1)-B(2)	110.0(11)
B(6)-B(1)-B(5)	107.7(13)	B(9)-B(1)-B(2)	109.4(11)
B(9)-B(1)-B(5)	58.9(13)	B(9)-B(1)-B(6)	60.6(9)
C(1')-B(1)-B(2)	60.4(10)	C(1')-B(1)-B(5)	105.2(11)

Table 3 (cont.): Bond angles (°)

B(6)-B(8)-B(4)	104.5(14)	B(7)-B(8)-Mo(1)	68.3(7)
B(7)-B(8)-B(4)	60.2(12)	B(7)-B(8)-B(6)	101.2(14)
B(9)-B(8)-Mo(1)	123.4(9)	B(9)-B(8)-B(4)	59.4(10)
B(9)-B(8)-B(6)	57.7(8)	B(9)-B(8)-B(7)	104.4(16)
C(5)-B(8)-Mo(1)	109.0(12)	C(5)-B(8)-B(4)	117.4(10)
C(5)-B(8)-B(6)	123.3(17)	C(5)-B(8)-B(7)	131.8(10)
C(5)-B(8)-B(9)	114.2(12)	B(4)-B(9)-B(1)	108.7(13)
B(5)-B(9)-B(1)	59.6(11)	B(5)-B(9)-B(4)	61.8(12)
B(6)-B(9)-B(1)	58.1(11)	B(6)-B(9)-B(4)	107.5(11)
B(6)-B(9)-B(5)	106.2(14)	B(8)-B(9)-B(1)	108.9(11)
B(8)-B(9)-B(4)	59.5(11)	B(8)-B(9)-B(5)	109.6(14)
B(8)-B(9)-B(6)	61.5(9)	B(1)-C(1')-Mo(1)	128.8(10)
B(2)-C(1')-Mo(1)	133.3(8)	B(2)-C(1')-B(1)	62.3(10)
B(6)-C(1')-Mo(1)	70.3(8)	B(6)-C(1')-B(1)	61.0(10)
B(6)-C(1')-B(2)	113.9(11)	C(2')-C(1')-Mo(1)	72.8(7)
C(2')-C(1')-B(1)	111.2(10)	C(2')-C(1')-B(2)	62.5(10)
C(2')-C(1')-B(6)	112.2(10)	B(2)-C(2')-Mo(1)	132.5(9)
B(3)-C(2')-Mo(1)	129.5(10)	B(3)-C(2')-B(2)	62.8(9)
B(7)-C(2')-Mo(1)	69.0(9)	B(7)-C(2')-B(2)	115.9(11)
B(7)-C(2')-B(3)	63.1(11)	C(1')-C(2')-Mo(1)	70.2(8)
C(1')-C(2')-B(2)	64.3(10)	C(1')-C(2')-B(3)	113.5(10)
C(1')-C(2')-B(7)	111.6(12)	C(2)-C(1)-Mo(1)	73.2(8)
C(9)-C(1)-Mo(1)	144.9(8)	C(9)-C(1)-C(2)	141.6(11)
C(1)-C(2)-Mo(1)	71.6(8)	C(15)-C(2)-Mo(1)	146.0(8)
C(15)-C(2)-C(1)	141.9(10)	C(4)-C(3)-Mo(1)	71.6(10)
C(21)-C(3)-Mo(1)	147.5(9)	C(21)-C(3)-C(4)	140.3(13)
C(3)-C(4)-Mo(1)	71.8(10)	C(27)-C(4)-Mo(1)	145.5(9)
C(27)-C(4)-C(3)	142.6(13)	C(6)-C(5)-B(8)	119.5(14)
C(33)-C(5)-B(8)	118.9(11)	C(33)-C(5)-C(6)	120.9(14)
C(39)-C(6)-C(5)	130.2(13)	C(7)-C(8)-N(1)	176.1(14)
C(9)-C(10)-C(11)	120.0(11)	C(12)-C(11)-C(10)	120.0(12)
C(13)-C(12)-C(11)	120.0(10)	C(14)-C(13)-C(12)	120.0(11)

Table 3 (cont.): Bond angles (°)

C(1')-B(1)-B(6)	58.1(10)	C(1')-B(1)-B(9)	104.7(10)
B(3)-B(2)-B(1)	105.8(13)	B(5)-B(2)-B(1)	57.8(12)
B(5)-B(2)-B(3)	60.5(10)	C(1')-B(2)-B(1)	57.3(9)
C(1')-B(2)-B(3)	100.7(12)	C(1')-B(2)-B(5)	100.4(15)
C(2')-B(2)-B(1)	99.8(12)	C(2')-B(2)-B(3)	57.9(9)
C(2')-B(2)-B(5)	101.7(13)	C(2')-B(2)-C(1')	53.2(9)
B(4)-B(3)-B(2)	109.2(13)	B(5)-B(3)-B(2)	59.7(10)
B(5)-B(3)-B(4)	59.7(12)	B(7)-B(3)-B(2)	107.0(13)
B(7)-B(3)-B(4)	60.5(11)	B(7)-B(3)-B(5)	105.7(16)
C(2')-B(3)-B(2)	59.3(9)	C(2')-B(3)-B(4)	103.3(14)
C(2')-B(3)-B(5)	102.1(12)	C(2')-B(3)-B(7)	56.0(9)
B(5)-B(4)-B(3)	60.3(12)	B(7)-B(4)-B(3)	58.1(11)
B(7)-B(4)-B(5)	104.4(12)	B(8)-B(4)-B(3)	108.9(12)
B(8)-B(4)-B(5)	107.5(12)	B(8)-B(4)-B(7)	60.3(10)
B(9)-B(4)-B(3)	106.7(12)	B(9)-B(4)-B(5)	57.6(12)
B(9)-B(4)-B(7)	105.7(11)	B(9)-B(4)-B(8)	61.1(10)
B(2)-B(5)-B(1)	61.2(11)	B(3)-B(5)-B(1)	107.9(12)
B(3)-B(5)-B(2)	59.8(10)	B(4)-B(5)-B(1)	109.3(17)
B(4)-B(5)-B(2)	109.6(12)	B(4)-B(5)-B(3)	60.0(11)
B(9)-B(5)-B(1)	61.5(13)	B(9)-B(5)-B(2)	111.5(15)
B(9)-B(5)-B(3)	108.9(15)	B(9)-B(5)-B(4)	60.6(13)
B(1)-B(6)-Mo(1)	128.7(13)	B(8)-B(6)-Mo(1)	67.8(6)
B(8)-B(6)-B(1)	110.9(14)	B(9)-B(6)-Mo(1)	125.4(9)
B(9)-B(6)-B(1)	61.4(11)	B(9)-B(6)-B(8)	60.8(9)
C(1')-B(6)-Mo(1)	70.2(7)	C(1')-B(6)-B(1)	60.9(11)
C(1')-B(6)-B(8)	106.2(13)	C(1')-B(6)-B(9)	107.4(16)
B(3)-B(7)-Mo(1)	130.9(9)	B(4)-B(7)-Mo(1)	125.3(11)
B(4)-B(7)-B(3)	61.4(11)	B(8)-B(7)-Mo(1)	68.6(8)
B(8)-B(7)-B(3)	111.0(12)	B(8)-B(7)-B(4)	59.5(11)
C(2')-B(7)-Mo(1)	72.6(8)	C(2')-B(7)-B(3)	60.9(10)
C(2')-B(7)-B(4)	107.7(12)	C(2')-B(7)-B(8)	108.7(11)
B(4)-B(8)-Mo(1)	125.6(14)	B(6)-B(8)-Mo(1)	68.6(6)

Table 3 (cont.): Bond angles (°)

C(9)-C(14)-C(13)	120.0(12)	C(10)-C(9)-C(1)	118.1(11)
C(14)-C(9)-C(1)	121.6(12)	C(14)-C(9)-C(10)	120.0(10)
C(15)-C(16)-C(17)	120.0(7)	C(18)-C(17)-C(16)	120.0(7)
C(19)-C(18)-C(17)	120.0(8)	C(20)-C(19)-C(18)	120.0(7)
C(15)-C(20)-C(19)	120.0(7)	C(16)-C(15)-C(2)	121.1(8)
C(20)-C(15)-C(2)	118.8(8)	C(20)-C(15)-C(16)	120.0(8)
C(21)-C(22)-C(23)	120.0(10)	C(24)-C(23)-C(22)	120.0(10)
C(25)-C(24)-C(23)	120.0(10)	C(26)-C(25)-C(24)	120.0(10)
C(21)-C(26)-C(25)	120.0(10)	C(22)-C(21)-C(3)	120.8(11)
C(26)-C(21)-C(3)	119.1(10)	C(26)-C(21)-C(22)	120.0(10)
C(27)-C(28)-C(29)	120.0(10)	C(30)-C(29)-C(28)	120.0(9)
C(31)-C(30)-C(29)	120.0(11)	C(32)-C(31)-C(30)	120.0(10)
C(27)-C(32)-C(31)	120.0(9)	C(28)-C(27)-C(4)	118.8(10)
C(32)-C(27)-C(4)	121.1(10)	C(32)-C(27)-C(28)	120.0(11)
C(33)-C(34)-C(35)	120.0(9)	C(36)-C(35)-C(34)	120.0(9)
C(37)-C(36)-C(35)	120.0(10)	C(38)-C(37)-C(36)	120.0(9)
C(33)-C(38)-C(37)	120.0(9)	C(34)-C(33)-C(5)	117.8(10)
C(38)-C(33)-C(5)	121.7(9)	C(38)-C(33)-C(34)	120.0(10)
C(39)-C(40)-C(41)	120.0(11)	C(42)-C(41)-C(40)	120.0(10)
C(43)-C(42)-C(41)	120.0(11)	C(44)-C(43)-C(42)	120.0(11)
C(39)-C(44)-C(43)	120.0(10)	C(40)-C(39)-C(6)	112.9(11)
C(44)-C(39)-C(6)	127.0(10)	C(44)-C(39)-C(40)	120.0(11)

5.6 Crystal data for 31

Empirical formula	$C_{14}H_{29}MoO_2P_2$
crystal system	triclinic
space group	$P\bar{1}$ (no.2)
Unit Cell Dimensions (Å): a	9.710 (1)
b	13.803 (4)
c	17.696 (3)
α(°)	86.06 (2)
β	88.63 (1)
γ	78.12 (1)
Volume $Å^3$	2315.4 (7)
D_{calcd}	1.39 g/cm^{-3}
Z	4
F(000)	984
T	293 K
R_F	0.052
R_W	0.057

Table 1: Fractional atomic coordinates ($*10^4$)

	x	y	z
Molecule a			
Mo	0.15302(6)	0.64686(4)	0.36953(3)
P1	0.1132(2)	0.8262(1)	0.4085(1)
P2	0.0099(2)	0.6881(1)	0.4886(1)
O1	0.2725(6)	0.4620(4)	0.4784(3)
O2	-0.0797(6)	0.5223(4)	0.3615(3)
C1	0.2304(8)	0.5317(5)	0.4413(4)
C2	-0.0021(7)	0.5726(5)	0.3655(4)
C3	-0.0361(6)	0.7716(5)	0.4059(3)
C4	0.1729(6)	0.7317(5)	0.4792(4)
C5	-0.1782(7)	0.8186(5)	0.3721(4)
C6	-0.2668(9)	0.7424(8)	0.3617(7)
C7	-0.1615(10)	0.8685(8)	0.2967(5)
C8	-0.2524(11)	0.8908(8)	0.4264(6)
C9	0.2883(7)	0.7286(5)	0.5365(4)
C10	0.2460(9)	0.8199(7)	0.5813(5)
C11	0.4257(8)	0.7347(8)	0.4963(5)
C12	0.3044(12)	0.6395(8)	0.5912(6)

Table 1 (cont.): Fractional atomic coordinates ($*10^4$)

	x	y	z
C13	0.1944(7)	0.7284(5)	0.2499(4)
C14	0.3407(7)	0.6992(5)	0.2971(4)
B1	0.3845(9)	0.5778(6)	0.3232(5)
B2	0.2463(9)	0.5237(6)	0.2837(5)
B3	0.1214(10)	0.6301(6)	0.2376(5)
B4	0.4751(10)	0.6304(7)	0.2450(5)
B5	0.3492(10)	0.7326(7)	0.2000(5)
B6	0.2127(10)	0.6810(7)	0.1611(5)
B7	0.2518(11)	0.5517(7)	0.1811(5)
B8	0.4126(11)	0.5188(7)	0.2329(5)
B9	0.3917(10)	0.6144(7)	0.1596(5)
Molecule b			
Mob	0.13149(6)	0.15511(4)	0.14951(3)
P1b	0.1514(2)	0.3139(1)	0.0720(1)
P2b	-0.0120(2)	0.1953(1)	0.0296(1)
O1b	-0.1552(6)	0.1036(6)	0.2029(4)
O2b	0.1569(8)	-0.0517(4)	0.0842(4)
C1b	-0.0545(8)	0.1268(7)	0.1818(5)
C2b	0.1509(9)	0.0248(5)	0.1038(4)
C3b	0.1674(7)	0.2064(5)	0.0216(4)
C4b	-0.0208(7)	0.2954(5)	0.0904(4)
C5b	0.2797(8)	0.1690(6)	-0.0377(4)
C6b	0.2652(12)	0.0688(8)	-0.0637(6)
C7b	0.4251(9)	0.1628(9)	-0.0082(5)
C8b	0.2559(10)	0.2448(8)	-0.1049(5)
C9b	-0.1497(8)	0.3690(6)	0.1164(4)
C10b	-0.1771(12)	0.4549(8)	0.0574(6)
C11b	-0.1237(11)	0.4096(7)	0.1906(5)
C12b	-0.2776(11)	0.3244(9)	0.1217(9)
C13b	0.3538(7)	0.1710(5)	0.1958(4)
C14b	0.2283(7)	0.2366(5)	0.2440(4)
B1b	0.1186(9)	0.1669(7)	0.2842(5)
B2b	0.1899(8)	0.0400(6)	0.2572(4)
B3b	0.3438(8)	0.0512(6)	0.1975(5)

Table 1 (cont.): Fractional atomic coordinates ($*10^4$)

	x	y	z
B4b	0.2484(10)	0.2054(7)	0.3391(5)
B5b	0.3974(9)	0.2113(6)	0.2819(5)
B6b	0.4706(9)	0.0907(6)	0.2543(5)
B7b	0.3667(9)	0.0079(6)	0.2958(5)
B8b	0.2253(9)	0.0798(6)	0.3495(5)
B9b	0.3979(10)	0.1069(6)	0.3484(5)

Table 2: Bond lengths (Å)

Mo-CBa	1.887(1)	Mo-CPa	2.107(1)
Mob-CBb	1.885(1)	Mob-CPb	2.112(1)
Mo-P1	2.565(2)	Mo-P2	2.529(2)
Mo-C1	1.995(7)	Mo-C2	1.994(8)
Mo-C3	2.355(6)	Mo-C4	2.366(7)
Mo-C13	2.393(7)	Mo-C14	2.406(7)
Mo-B1	2.403(8)	Mo-B2	2.381(8)
Mo-B3	2.395(8)	P1-C3	1.769(7)
P1-C4	1.761(6)	P2-C3	1.805(6)
P2-C4	1.806(7)	O1-C1	1.135(8)
O2-C2	1.132(10)	C3-C5	1.517(9)
C4-C9	1.520(10)	C5-C6	1.512(14)
C5-C7	1.480(12)	C5-C8	1.497(13)
C9-C10	1.515(12)	C9-C11	1.512(11)
C9-C12	1.496(13)	C13-C14	1.629(9)
C13-B3	1.684(12)	C13-B5	1.735(12)
C13-B6	1.736(11)	C14-B1	1.677(11)
C14-B4	1.735(11)	C14-B5	1.753(11)
B1-B2	1.838(13)	B1-B4	1.812(13)
B1-B8	1.832(13)	B2-B3	1.855(11)
B2-B7	1.832(13)	B2-B8	1.821(14)
B3-B6	1.784(13)	B3-B7	1.815(12)

Table 2 (cont.): Bond lengths (Å)

B4-B5	1.816(12)	B4-B8	1.79(2)
B4-B9	1.779(14)	B5-B6	1.800(15)
B5-B9	1.793(14)	B6-B7	1.759(13)
B6-B9	1.792(13)	B7-B8	1.789(14)
B7-B9	1.78(2)	B8-B9	1.769(13)
Mob-P1b	2.544(2)	Mob-P2b	2.533(2)
Mob-C1b	1.987(9)	Mob-C2b	1.995(8)
Mob-C3b	2.365(6)	Mob-C4b	2.377(6)
Mob-C13b	2.383(7)	Mob-C14b	2.390(7)
Mob-B1b	2.399(8)	Mob-B2b	2.397(8)
Mob-B3b	2.394(7)	P1b-C3b	1.763(7)
P1b-C4b	1.762(8)	P2b-C3b	1.781(7)
P2b-C4b	1.796(7)	O1b-C1b	1.138(11)
O2b-C2b	1.124(10)	C3b-C5b	1.530(10)
C4b-C9b	1.524(10)	C5b-C6b	1.521(14)
C5b-C7b	1.500(12)	C5b-C8b	1.519(12)
C9b-C10b	1.511(13)	C9b-C11b	1.509(13)
C9b-C12b	1.49(2)	C13b-C14b	1.623(9)
C13b-B3b	1.674(11)	C13b-B5b	1.749(11)
C13b-B6b	1.724(10)	C14b-B1b	1.691(12)
C14b-B4b	1.714(10)	C14b-B5b	1.747(11)
B1b-B2b	1.837(12)	B1b-B4b	1.794(14)
B1b-B8b	1.791(11)	B2b-B3b	1.836(12)
B2b-B7b	1.820(12)	B2b-B8b	1.820(12)
B3b-B6b	1.798(13)	B3b-B7b	1.804(12)
B4b-B5b	1.758(13)	B4b-B8b	1.790(13)
B4b-B9b	1.775(12)	B5b-B6b	1.768(12)
B5b-B9b	1.796(12)	B6b-B7b	1.785(13)
B6b-B9b	1.803(13)	B7b-B8b	1.811(12)
B7b-B9b	1.785(13)	B8b-B9b	1.790(14)

Table 3: Bond angles (°)

P1-Mo-P2	62.57(6)	P1-Mo-C1	121.8(2)
P1-Mo-C2	122.9(2)	P1-Mo-C3	41.9(2)
P1-Mo-C4	41.6(2)	P1-Mo-C13	80.6(2)
P1-Mo-C14	81.3(2)	P1-Mo-B1	116.1(2)
P1-Mo-B2	150.5(2)	P1-Mo-B3	115.0(2)
P2-Mo-C1	77.6(2)	P2-Mo-C2	75.6(2)
P2-Mo-C3	43.2(1)	P2-Mo-C4	43.1(2)
P2-Mo-C13	137.8(2)	P2-Mo-C14	139.5(2)
P2-Mo-B1	143.6(2)	P2-Mo-B2	146.9(2)
P2-Mo-B3	140.3(2)	C1-Mo-C2	81.1(3)
C1-Mo-C3	120.6(2)	C1-Mo-C4	80.3(3)
C1-Mo-C13	143.3(3)	C1-Mo-C14	110.2(3)
C1-Mo-B1	73.8(3)	C1-Mo-B2	78.9(3)
C1-Mo-B3	122.7(3)	C2-Mo-C3	81.0(2)
C2-Mo-C4	118.4(3)	C2-Mo-C13	112.5(3)
C2-Mo-C14	143.8(3)	C2-Mo-B1	120.6(3)
C2-Mo-B2	77.9(3)	C2-Mo-B3	74.8(3)
C3-Mo-C4	60.6(2)	C3-Mo-C13	95.6(2)
C3-Mo-C14	117.2(2)	C3-Mo-B1	157.0(3)
C3-Mo-B2	148.4(3)	C3-Mo-B3	105.9(2)
C4-Mo-C13	117.1(2)	C4-Mo-C14	97.6(2)
C4-Mo-B1	109.1(3)	C4-Mo-B2	151.0(3)
C4-Mo-B3	156.3(3)	C13-Mo-C14	39.7(2)
C13-Mo-B1	70.0(3)	C13-Mo-B2	71.6(3)
C13-Mo-B3	41.2(3)	C14-Mo-B1	40.8(3)
C14-Mo-B2	71.2(3)	C14-Mo-B3	70.3(3)
B1-Mo-B2	45.2(3)	B1-Mo-B3	75.4(3)
B2-Mo-B3	45.7(3)	Mo-P1-C3	62.7(2)
Mo-P1-C4	63.1(2)	C3-P1-C4	84.8(3)
Mo-P2-C3	63.3(2)	Mo-P2-C4	63.6(2)
C3-P2-C4	82.5(3)	Mo-C1-O1	175.1(7)
Mo-C2-O2	172.9(6)	Mo-C3-P1	75.4(2)
Mo-C3-P2	73.6(2)	Mo-C3-C5	134.3(5)

Table 3 (cont.): Bond angles (°)

P1-C3-P2	95.5(3)	P1-C3-C5	126.9(5)
P2-C3-C5	131.0(5)	Mo-C4-P1	75.3(2)
Mo-C4-P2	73.2(2)	Mo-C4-C9	134.7(4)
P1-C4-P2	95.7(3)	P1-C4-C9	127.2(5)
P2-C4-C9	130.4(5)	C3-C5-C6	111.8(6)
C3-C5-C7	110.9(6)	C3-C5-C8	107.1(6)
C6-C5-C7	107.2(8)	C6-C5-C8	108.6(7)
C7-C5-C8	111.2(7)	C4-C9-C10	107.2(5)
C4-C9-C11	110.4(6)	C4-C9-C12	112.4(7)
C10-C9-C11	107.5(7)	C10-C9-C12	107.8(7)
C11-C9-C12	111.4(7)	Mo-C13-C14	70.6(3)
Mo-C13-B3	69.5(4)	Mo-C13-B5	131.1(4)
Mo-C13-B6	128.7(5)	C14-C13-B3	113.0(5)
C14-C13-B5	62.7(4)	C14-C13-B6	111.7(5)
B3-C13-B5	116.2(6)	B3-C13-B6	62.9(5)
B5-C13-B6	62.5(5)	Mo-C14-C13	69.7(3)
Mo-C14-B1	69.5(4)	Mo-C14-B4	129.8(5)
Mo-C14-B5	129.2(5)	C13-C14-B1	112.7(6)
C13-C14-B4	111.7(5)	C13-C14-B5	61.6(4)
B1-C14-B4	64.1(5)	B1-C14-B5	116.7(6)
B4-C14-B5	62.8(5)	Mo-B1-C14	69.7(3)
Mo-B1-B2	66.8(4)	Mo-B1-B4	125.7(5)
Mo-B1-B8	121.9(5)	C14-B1-B2	104.9(5)
C14-B1-B4	59.5(5)	C14-B1-B8	103.6(6)
B2-B1-B4	108.0(6)	B2-B1-B8	59.5(5)
B4-B1-B8	59.0(5)	Mo-B2-B1	68.0(4)
Mo-B2-B3	67.5(4)	Mo-B2-B7	122.3(5)
Mo-B2-B8	123.6(6)	B1-B2-B3	105.3(6)
B1-B2-B7	105.9(6)	B1-B2-B8	60.1(5)
B3-B2-B7	59.0(5)	B3-B2-B8	105.6(6)
B7-B2-B8	58.7(5)	Mo-B3-C13	69.3(4)
Mo-B3-B2	66.8(4)	Mo-B3-B6	126.0(6)
Mo-B3-B7	122.4(5)	C13-B3-B2	104.0(6)
C13-B3-B6	60.0(5)	C13-B3-B7	103.5(6)
B2-B3-B6	107.6(6)	B2-B3-B7	59.9(5)

Table 3 (cont.): Bond angles (°)

B6-B3-B7	58.5(5)	C14-B4-B1	56.4(4)
C14-B4-B5	59.1(4)	C14-B4-B8	102.8(6)
C14-B4-B9	103.7(6)	B1-B4-B5	107.2(6)
B1-B4-B8	61.1(5)	B1-B4-B9	108.0(7)
B5-B4-B8	107.3(7)	B5-B4-B9	59.8(5)
B8-B4-B9	59.3(6)	C13-B5-C14	55.7(4)
C13-B5-B4	103.3(6)	C13-B5-B6	58.8(5)
C13-B5-B9	103.4(7)	C14-B5-B4	58.1(4)
C14-B5-B6	103.3(6)	C14-B5-B9	102.4(6)
B4-B5-B6	107.4(7)	B4-B5-B9	59.1(5)
B6-B5-B9	59.9(5)	C13-B6-B3	57.1(5)
C13-B6-B5	58.7(5)	C13-B6-B7	103.7(6)
C13-B6-B9	103.4(6)	B3-B6-B5	108.2(6)
B3-B6-B7	61.6(5)	B3-B6-B9	109.0(6)
B5-B6-B7	108.5(6)	B5-B6-B9	59.9(5)
B7-B6-B9	60.0(6)	B2-B7-B3	61.1(5)
B2-B7-B6	109.7(6)	B2-B7-B8	60.4(5)
B2-B7-B9	108.6(7)	B3-B7-B6	59.8(5)
B3-B7-B8	108.7(7)	B3-B7-B9	108.3(7)
B6-B7-B8	108.9(8)	B6-B7-B9	60.9(6)
B8-B7-B9	59.5(6)	B1-B8-B2	60.4(5)
B1-B8-B4	59.9(5)	B1-B8-B7	107.9(6)
B1-B8-B9	107.6(7)	B2-B8-B4	109.4(6)
B2-B8-B7	61.0(5)	B2-B8-B9	109.4(6)
B4-B8-B7	108.0(6)	B4-B8-B9	59.9(6)
B7-B8-B9	59.9(6)	B4-B9-B5	61.1(5)
B4-B9-B6	109.4(6)	B4-B9-B7	109.4(7)
B4-B9-B8	60.8(6)	B5-B9-B6	60.3(5)
B5-B9-B7	108.1(7)	B5-B9-B8	109.5(7)
B6-B9-B7	59.1(5)	B6-B9-B8	108.3(7)
B7-B9-B8	60.6(6)	P1b-Mob-P2b	63.09(7)
P1b-Mob-C1b	121.4(2)	P1b-Mob-C2b	122.8(2)
P1b-Mob-C3b	41.9(2)	P1b-Mob-C4b	41.8(2)
P1b-Mob-C13b	82.5(2)	P1b-Mob-C14b	81.0(2)
P1b-Mob-B1b	115.5(2)	P1b-Mob-B2b	151.7(2)

Table 3 (cont.): Bond angles (°)

P1b-Mob-B3b	117.8(2)	P2b-Mob-C1b	76.9(2)
P2b-Mob-C2b	75.8(2)	P2b-Mob-C3b	42.5(2)
P2b-Mob-C4b	42.8(2)	P2b-Mob-C13b	139.3(2)
P2b-Mob-C14b	140.2(2)	P2b-Mob-B1b	143.1(2)
P2b-Mob-B2b	145.2(2)	P2b-Mob-B3b	141.1(2)
C1b-Mob-C2b	82.1(4)	C1b-Mob-C3b	119.3(3)
C1b-Mob-C4b	79.7(3)	C1b-Mob-C13b	143.1(3)
C1b-Mob-C14b	111.4(3)	C1b-Mob-B1b	74.0(3)
C1b-Mob-B2b	77.4(3)	C1b-Mob-B3b	120.3(3)
C2b-Mob-C3b	80.9(3)	C2b-Mob-C4b	118.3(3)
C2b-Mob-C13b	109.6(3)	C2b-Mob-C14b	142.5(3)
C2b-Mob-B1b	121.3(3)	C2b-Mob-B2b	77.9(3)
C2b-Mob-B3b	72.9(3)	C3b-Mob-C4b	59.3(2)
C3b-Mob-C13b	97.3(2)	C3b-Mob-C14b	117.1(2)
C3b-Mob-B1b	156.8(3)	C3b-Mob-B2b	150.8(2)
C3b-Mob-B3b	109.2(3)	C4b-Mob-C13b	119.8(2)
C4b-Mob-C14b	98.8(2)	C4b-Mob-B1b	109.1(3)
C4b-Mob-B2b	149.6(2)	C4b-Mob-B3b	159.3(3)
C13b-Mob-C14b	39.8(2)	C13b-Mob-B1b	70.1(3)
C13b-Mob-B2b	71.6(3)	C13b-Mob-B3b	41.0(3)
C14b-Mob-B1b	41.4(3)	C14b-Mob-B2b	71.8(3)
C14b-Mob-B3b	70.1(3)	B1b-Mob-B2b	45.0(3)
B1b-Mob-B3b	74.6(3)	B2b-Mob-B3b	45.1(3)
Mob-P1b-C3b	63.6(2)	Mob-P1b-C4b	64.0(2)
C3b-P1b-C4b	83.5(3)	Mob-P2b-C3b	63.7(2)
Mob-P2b-C4b	64.0(2)	C3b-P2b-C4b	82.0(3)
Mob-C1b-O1b	174.5(7)	Mob-C2b-O2b	173.5(7)
Mob-C3b-P1b	74.5(2)	Mob-C3b-P2b	73.8(2)
Mob-C3b-C5b	133.1(4)	P1b-C3b-P2b	97.1(3)
P1b-C3b-C5b	127.3(6)	P2b-C3b-C5b	130.4(6)
Mob-C4b-P1b	74.2(2)	Mob-C4b-P2b	73.3(2)
Mob-C4b-C9b	134.3(5)	P1b-C4b-P2b	96.6(3)
P1b-C4b-C9b	128.9(6)	P2b-C4b-C9b	128.8(6)
C3b-C5b-C6b	111.5(7)	C3b-C5b-C7b	111.3(6)
C3b-C5b-C8b	106.4(6)	C6b-C5b-C7b	110.1(8)

Table 3 (cont.): Bond angles (°)

C6b-C5b-C8b	108.8(7)	C7b-C5b-C8b	108.6(8)
C4b-C9b-C10b	107.4(7)	C4b-C9b-C11b	111.4(7)
C4b-C9b-C12b	111.7(8)	C10b-C9b-C11b	107.6(8)
C10b-C9b-C12b	107.7(8)	C11b-C9b-C12b	110.8(9)
Mob-C13b-C14b	70.3(3)	Mob-C13b-B3b	69.8(4)
Mob-C13b-B5b	130.2(4)	Mob-C13b-B6b	130.0(5)
C14b-C13b-B3b	112.8(5)	C14b-C13b-B5b	62.3(4)
C14b-C13b-B6b	111.4(5)	B3b-C13b-B5b	115.1(5)
B3b-C13b-B6b	63.9(5)	B5b-C13b-B6b	61.2(5)
Mob-C14b-C13b	69.9(3)	Mob-C14b-B1b	69.6(4)
Mob-C14b-B4b	129.4(5)	Mob-C14b-B5b	129.9(4)
C13b-C14b-B1b	111.9(5)	C13b-C14b-B4b	110.8(5)
C13b-C14b-B5b	62.4(4)	B1b-C14b-B4b	63.6(5)
B1b-C14b-B5b	114.7(5)	B4b-C14b-B5b	61.0(5)
Mob-B1b-C14b	69.0(4)	Mob-B1b-B2b	67.4(4)
Mob-B1b-B4b	124.5(5)	Mob-B1b-B8b	123.4(5)
C14b-B1b-B2b	105.4(6)	C14b-B1b-B4b	58.8(5)
C14b-B1b-B8b	105.1(6)	B2b-B1b-B4b	108.3(6)
B2b-B1b-B8b	60.2(5)	B4b-B1b-B8b	59.9(5)
Mob-B2b-B1b	67.5(4)	Mob-B2b-B3b	67.4(3)
Mob-B2b-B7b	122.2(5)	Mob-B2b-B8b	122.1(5)
B1b-B2b-B3b	104.4(6)	B1b-B2b-B7b	105.3(6)
B1b-B2b-B8b	58.6(4)	B3b-B2b-B7b	59.1(4)
B3b-B2b-B8b	106.0(6)	B7b-B2b-B8b	59.7(5)
Mob-B3b-C13b	69.2(3)	Mob-B3b-B2b	67.5(3)
Mob-B3b-B6b	125.3(5)	Mob-B3b-B7b	123.1(5)
C13b-B3b-B2b	105.5(5)	C13b-B3b-B6b	59.4(5)
C13b-B3b-B7b	104.5(6)	B2b-B3b-B6b	108.5(6)
B2b-B3b-B7b	60.0(5)	B6b-B3b-B7b	59.4(5)
C14b-B4b-B1b	57.6(5)	C14b-B4b-B5b	60.4(5)
C14b-B4b-B8b	104.1(6)	C14b-B4b-B9b	106.4(6)
B1b-B4b-B5b	109.2(6)	B1b-B4b-B8b	60.0(5)
B1b-B4b-B9b	108.8(6)	B5b-B4b-B8b	109.3(6)
B5b-B4b-B9b	61.1(5)	B8b-B4b-B9b	60.3(5)
C13b-B5b-C14b	55.3(4)	C13b-B5b-B4b	103.1(6)

Table 3 (cont.): Bond angles (°)

C13b-B5b-B6b	58.7(5)	C13b-B5b-B9b	104.3(6)
C14b-B5b-B4b	58.5(4)	C14b-B5b-B6b	103.8(6)
C14b-B5b-B9b	104.1(6)	B4b-B5b-B6b	108.4(7)
B4b-B5b-B9b	59.9(5)	B6b-B5b-B9b	60.8(5)
C13b-B6b-B3b	56.7(4)	C13b-B6b-B5b	60.1(4)
C13b-B6b-B7b	103.2(6)	C13b-B6b-B9b	105.0(5)
B3b-B6b-B5b	108.3(6)	B3b-B6b-B7b	60.4(5)
B3b-B6b-B9b	108.2(6)	B5b-B6b-B7b	108.2(6)
B5b-B6b-B9b	60.4(5)	B7b-B6b-B9b	59.7(5)
B2b-B7b-B3b	60.9(5)	B2b-B7b-B6b	109.7(6)
B2b-B7b-B8b	60.2(5)	B2b-B7b-B9b	109.5(6)
B3b-B7b-B6b	60.1(5)	B3b-B7b-B8b	107.7(5)
B3b-B7b-B9b	108.8(6)	B6b-B7b-B8b	107.9(6)
B6b-B7b-B9b	60.7(5)	B8b-B7b-B9b	59.7(5)
B1b-B8b-B2b	61.2(5)	B1b-B8b-B4b	60.1(5)
B1b-B8b-B7b	107.6(6)	B1b-B8b-B9b	108.3(6)
B2b-B8b-B4b	109.2(6)	B2b-B8b-B7b	60.2(5)
B2b-B8b-B9b	109.2(6)	B4b-B8b-B7b	106.3(6)
B4b-B8b-B9b	59.5(5)	B7b-B8b-B9b	59.4(5)
B4b-B9b-B5b	59.0(5)	B4b-B9b-B6b	106.1(6)
B4b-B9b-B7b	108.0(7)	B4b-B9b-B8b	60.3(5)
B5b-B9b-B6b	58.8(5)	B5b-B9b-B7b	107.0(6)
B5b-B9b-B8b	107.6(6)	B6b-B9b-B7b	59.7(5)
B6b-B9b-B8b	108.0(7)	B7b-B9b-B8b	60.9(5)
C1-Mo-CBa	108.0(2)	C1-Mo-CPa	101.0(2)
C2-Mo-CBa	108.3(2)	C2-Mo-CPa	100.4(2)
CBa-Mo-CPa	141.67(3)	C1b-Mob-CBb	107.3(2)
C1b-Mob-CPb	100.1(2)	C2b-Mob-CBb	106.9(2)
C2b-Mob-CPb	100.3(2)	CBb-Mob-CPb	143.46(3)

CB and CP are the centroids of the C2B3 face of the carborane and the P2C2 ring respectively in molecules a and b.

Summary

The reaction of $[Mo(\eta^2\text{-}PhC_2Ph)\{P(OMe)_3\}_2(\eta\text{-}C_5H_5)][BF_4]$ **XI** with RMgX (R = Et, CH_2Ph) gives complexes $[Mo(\eta^2\text{-}PhC_2Ph)(R)\{P(OMe)_3\}(\eta\text{-}C_5H_5)]$ (R= Et **1**, CH_2Ph **2**). Compound **1** reacts with CO to form $[Mo\{\eta^2\text{=}C(Ph)C(Ph)C(Et)O\}(CO)\text{-}\{P(OMe)_3\}(\eta\text{-}C_5H_5)]$ **3** containing an oxametallacycle. Heating a solution of complex **2** in presence of diphenylacetylene affords the paramagnetic 17 electron complex $[Mo(\eta^6\text{-}C_6Ph_6)(\eta\text{-}C_5H_5)]$ **4**, whose structure was determined by X-ray crystallography. For the formation of **4** a radical mechanism is proposed.

On addition of allyl magnesium bromide to **XI** a complex with a σ-bonded allyl group is formed, which could not be isolated. However, after addition of trimethylphosphite to the reaction mixture the complex $[Mo\{\eta^2\text{-}C(Ph)\text{=}C(Ph)CH_2CH\text{=}CH_2\}\{P(OMe)_3\}_2\text{-}(\eta\text{-}C_5H_5)]$ **5** is formed, the structure of which was resolved by X-ray diffraction. The mechanism of this reaction probably involves a [3,3]-sigmatropic rearrangement.

Unexpectedly, the reaction of **XI** with $CH_2(MgI)_2$ affords the zwitterionic complex $[Mo(\eta^2\text{-}PhC_2Ph)\{\eta^2\text{-}P(OMe)_2OBF_2OP(OMe)_2\}(\eta\text{-}C_5H_5)]$ **6**. The structure of **6** was established by an X-ray diffraction study. Treatment of **6** with $K[HBBu^s_3]$ yields the anionic η^2-vinyl complexes $K[Mo(\eta^2\text{=}C(Ph)C(H)Ph)\{\eta^2\text{-}P(OMe)_2OBF_2OP(OMe)_2\}\text{-}(\eta\text{-}C_5H_5)]$ **9**. Protonation of **9** generates an unsaturated *trans*-stilbene complex $[Mo(\textit{trans}\text{-}PhHC_2PhH)\{\eta^2\text{-}P(OMe)_2OBF_2OP(OMe)_2\}(\eta\text{-}C_5H_5)]$ **A**, which was treated *in situ* with CO or trimethylphosphite to give $[Mo(L)_2\{\eta^2\text{-}P(OMe)_2OBF_2OP(OMe)_2\}\text{-}(\eta\text{-}C_5H_5)]$ (L= CO **11**, $P(OMe)_3$ **12**).

Addition of phosphaalkyne to **A** affords $[Mo\{\eta^2\text{-}P(OMe)_2OBF_2OP(OMe)_2\}(\eta^2\text{-}P\equiv CBu^t)(\eta\text{-}C_5H_5)]$ **14**, the first complex in which a phosphaalkyne adopts an η^2(4e) bonding mode. **14** reacts with a second molecule of phosphaalkyne to give the diphosphacyclobutadienyl complex $[Mo\{\eta^2\text{-}P(OMe)_2OBF_2OP(OMe)_2\}\{\eta^4\text{-}P_2C_2(Bu^t)_2\}(\eta\text{-}C_5H_5)]$ **15**.

Addition of two equivalents of diphenylphosphine to $[Mo(NCMe)(\eta^2\text{-}PhC_2Ph)_2(\eta\text{-}C_5H_5)][BF_4]$ **LXIX** gives the complex $[Mo(PPh_2H)_2(\eta^2\text{-}PhC_2Ph)(\eta\text{-}C_5H_5)][BF_4]$ **16**,

which can be deprotonated with $Li[N(SiMe_3)_2]$ or $K[BHBu^s_3]$ to afford the phosphide complex $[Mo(PPh_2)(PPh_2H)(\eta^2\text{-}PhC_2Ph)(\eta\text{-}C_5H_5)]$ **17**.

The carbaborane complexes [*closo*-3,3-$(\eta^2\text{-}PhC_2R)_2$-3-CO-3,1,2-$MoC_2B_9H_{11}$] (R= Ph **18**, R= Me **19**) were synthesised by protonation of $[NEt_4]$[*closo*-3,3-$(CO)_2$-3-$(\eta^3\text{-}C_3H_5)$-3,1,2-$MoC_2B_9H_{11}$] **XXXII** in the presence of the respective acetylene. Addition of trimethylphosphite to **18**, **19** and [*closo*-3,3-$(\eta^2\text{-}MeC_2Me)_2$-3-CO-3,1,2-$MoC_2B_9H_{11}$] **XXXIV** yields the *bis*-phosphite complexes [*closo*-3-$(\eta^2\text{-}RC_2R')$-3,3-$\{P(OMe)_3\}_2$-3,1,2-$MoC_2B_9H_{11}$] (R= R'= Ph **22**; R= Ph, R'= Me **23**; R= R'= Me **24**).

Treatment of **24** with but-2-yne at 90°C gives the complex [*closo*-3,3-$(\eta^2\text{-}MeC_2Me)_2$-3-$\{P(OMe)_3\}$-3,1,2-$MoC_2B_9H_{11}$] **26**, while treatment with diphenylacetylene yields [*closo*-3-$(\eta^2\text{-}MeC_2Me)$-3-$(\eta^2\text{-}PhC_2Ph)$-3-$\{P(OMe)_3\}$-3,1,2-$MoC_2B_9H_{11}$] **27**, which is also obtained when **22** is treated with but-2-yne. However, under the same conditions, **22** reacts with diphenylacetylene to give [*closo*-3-$(\eta^2\text{-}PhC_2Ph)$-3,3-$\{P(OMe)_3\}_2$-8-{σ-*trans*-C(Ph)=C(H)Ph}-3,1,2-$MoC_2B_9H_{10}$] **28**, whose structure was confirmed by X-ray crystallography. **28** is the product of an *exo*-polyhedral rearrangement, for which a mechanism involving two metal centres is proposed. A similar *exo*-polyhedral rearrangement reaction is observed when **18** is refluxed in acetonitrile yielding [*closo*-3,3-$(\eta^2\text{-}PhC_2Ph)_2$-3-(NCMe)-8-{σ-*trans*-C(Ph)=C(H)Ph}-3,1,2-$MoC_2B_9H_{10}$] **30**.

Protonation of **XXXII** followed by addition of $P{\equiv}CBu^t$ gives the diphosphacyclobutadienyl complex [*closo*-3,3-$(CO)_2$-3-$\{\eta^4\text{-}P_2C_2(Bu^t)_2\}$-3,1,2-$MoC_2B_9H_{11}$] **31**.